DOCTOR OF PHILOSOPHY

Seasonal and tidal cycles of suspended particulates in the Irish Sea

Weeks, Alison

Award date:
1989

Awarding institution:
Bangor University

DOCTOR OF PHILOSOPHY

Seasonal and tidal cycles of suspended particulates in the Irish Sea

Weeks, Alison

Award date:
1989

Awarding institution:
Bangor University

SEASONAL AND TIDAL CYCLES OF SUSPENDED PARTICULATES IN THE IRISH SEA

A thesis submitted in accordance with the requirements of the University of Wales for the Degree of Doctor of Philosophy by

Alison Weeks

School of Ocean Sciences

University College of North Wales,

Menai Bridge,

Anglesey,

Gwynedd LL59 2EY

July 1989

ABSTRACT

In spite of the widely perceived importance of suspended particulate material (SPM) , its distribution in the shelf seas and the processes controlling its variation are little known. This thesis reports an exploratory study of the spatial and time dependant variability of SPM in an area of the northern Irish Sea.SPM was determined both directly by gravimetric methods and via measurements of beam attenuation (c). Spatial distributions were determined from grid surveys using a profiling transmissometer.In addition a six month record of beam attenuation and current velocity was obtained from a site off the north coast of Anglesey.

A clear spatial pattern in the surface distribution of c was observed which was similar to the distribution of h/u^3, suggesting that concentrations of SPM are determined by the availability of TKE from tidal stirring.

A strong seasonal cycle of c was observed in mixed water, with values decreasing in June, July and August which suggested a reduction in the supply of SPM during summer. In stratified water, high concentrations of SPM remained confined to the dense layer below the thermocline.

The seasonal cycle was observed in the time series from the mooring, but in addition there was a marked response to tidal currents in the spring and in autumn. Close analysis of the record in April and May showed signals at M_2 and M_4 frequencies. These variations in c were attributed to a local response to tidal currents causing erosion of the sea-bed and to the oscillation of a horizontal gradient in c in the region. A regression model was found to explain 35% of the variance in data from a 5 week time series. 70% of the variance was explained for four day time series, near spring tides. The relationship between c and tidal flows was more marked at spring tides than at neaps.

ACKNOWLEDGEMENTS

I would like to thank all those whose interest in the work and whose encouragement gave me the confidence to carry out the study. I thank those who participated in the practical work.

In particular I am grateful to Ray Wilton whose help and optimism were vital to the success of the project in the early stages. I also thank Dave Boon for his ability to provide the transmissometers against all odds. I also thank Captain Hughes, and Captain Donovan and the officers and crew of the Prince Madog for their help. I am grateful to all those who were persuaded to join me on the cruises.

I am grateful to John Simpson for his guidance and support while supervising the project. I thank Paul Tett for many helpful discussions. In addition Toby Sherwin, Ed Hill and Dave Bowers provided valued advice at important stages. I thank Alan Davies for his helpful comments after reading the first draft of the thesis.

I gratefully acknowledge the receipt of a NERC studentship during the study. I thank Professor Denzil Taylor-Smith for the use of the facilities at the School of Ocean Sciences. I thank my family and friends for their loyal support.

TABLE OF CONTENTS

FIGURES

TABLES

CHAPTER 1. SUSPENDED PARTICULATE MATERIAL IN THE SHELF SEAS : INTRODUCTION

The shelf seas are characterised by shallow water depths (typically less than 200m) and frequently by vigorous mechanical stirring by winds and tides. The sea-bed is generally composed of unconsolidated sediments which are continuously reworked and may be repeatedly suspended and deposited.

In addition,the shelf seas are areas where there are high rates of primary production since nutrients released from organic material are rapidly mixed into the upper layers of the sea where photosynthesis takes place in the phytoplankton. Secondary production rates can be high. Organic material, both live and detrital, composes part of the suspended particulate material (SPM). Because of the abundance of the plankton there are in many cases rich fisheries which are an important natural resource.

Waste products from land are discharged into the shelf seas on the assumption that dispersion by diffusion and advection is rapid. Much of our domestic and agricultural sewage, as well as chemical and radio-active wastes from industry are discharged into the shelf seas around the U.K.

The soluble fraction of these pollutants are transported with the residual currents and eventually become so diluted that they cannot be measured. Heavy particles may be rapidly deposited after discharge onto the sea-bed. Fine-grained particles tend to remain permanently in suspension. Particles may become combined as aggregates, which may increase the settling rates of the SPM. Contaminants interact with material suspended in the water, or on the sea-bed, becoming adsorbed onto the particle surfaces (Duursma and Eisma,1973). Different elements vary in their capacity to become adsorbed onto particle surfaces, and there may be repeated adsorption and desorption by elements in aqueous and particulate form. Small particles have a large ratio of surface area to mass and so have more potential exchange sites than larger particles per unit volume of material. Suspended particles have a greater surface area exposed to the water than particles on the sea-bed and so exchange rates can be high.

The shelf seas are both a source of food and a sink for waste products. Suspended particles may intercept the safe disposal of these contaminants, causing them to remain close to the shore. Therefore the study of the distribution and transport of particles is essential in furthering our understanding of water

quality in the shelf seas.

However there is a marked paucity of knowledge of both the distribution and the processes important to the distribution of SPM in the shelf seas. This is partly because the subject is interdisciplinary, but also due to the limitations of present technology.

A principal difficulty is that the transport mechanisms for SPM movement in the shelf seas are not well understood. Significantly more work has been carried out on the transport of sands in the estuarine environment partly because transport mechanisms for particles increase in complexity as the size of the particle decreases. Whereas the transport mechanisms for sands and silts are generally physical, both biological and chemical processes become important for fine particles. Small particles may stay in suspension almost indefinitely, while larger ones are repeatedly deposited and resuspended.

The physical transport mechanisms for particles are erosion of the sea bed, particle settling and advective transport. Erosion of the sea bed is caused by shear stress induced mainly by surface waves and tidal flows. The settling velocity of particles is determined by their individual size and density and whether they are

combined in an aggregate. Aggregates may be composed of organic or inorganic material, but are often a combination of the two. Floccules are aggregates formed by chemical bonding and their formation depends on particle surface chemistry and the proximity of neighbouring particles. Aggregates have a greater settling velocity than the individual particles they are composed of. Particles in suspension may be transported by residual currents determined by horizontal density and pressure gradients , or by asymmetries in the tidal flows.

The stability of the sediment and its erodability are determined by the size and cohesive properties of the sedimentary particles, by bedforms and by compaction. Clay particles are generally shaped like laths whereas sands are more rounded. Because of this clays tend to be more closely packed than sands and are less easily eroded. In addition clay particle surfaces are more chemically reactive and so are more cohesive than sands and silts. Cohesion by binding from mucal films produced by plants,animals and bacteria varies seasonally, and is more common in fine grained sediments.

Understanding the behaviour of SPM in the shelf seas has been hindered by the lack of a theoretical framework for

the transport processes for the ensemble of particles described. The subject crosses the boundaries of physics,biology, geology and chemistry and hitherto only small sections of the mechanisms have been studied. Partly because of this, there is a lack of observational data from the shelf seas.

One of the reasons for the scarcity of observational data is the difficulty of making measurements of SPM concentrations. In rivers and estuaries, where concentrations are high, gravimetric measurements can be made with confidence, although the method can be tedious when taking a large number of samples. In the shelf seas large quantities of water must be filtered in order to obtain a measurable sample. New techniques are required to make routine measurements of SPM concentrations.

The beam transmissometer has been used with success in the shelf seas (Joseph,1955; Heathershaw and Simpson,1974). The attenuation of a collimated light beam through a fixed water pathlength is proportional to the concentration of the particles in the light beam. The instrument can be either interfaced with a data logger or a large amount of spatial or time series data can be obtained by interfacing the instrument with a CTD or a current meter. However to convert the electronic measurements to meaningful units of SPM

requires careful analysis of the particle size distribution, the organic fraction of the SPM, absorption of the light beam by chlorophyll, as well as standard gravimetric analysis.

The behaviour of SPM in the shelf seas requires a holistic approach, both in the acquisition of observational data and in the development of the theory of transport mechanisms. The work in this thesis is such an approach to the problem.

The thesis describes new results from observational studies of SPM distributions and attempts to interpret them in terms of the dominant physical and biological processes.

In Chapter 2 I shall review the present state of published knowledge of SPM in shallow seas and the mechanisms that control its distribution. From this will emerge a clear picture of the principal gaps in our knowledge and a formulation of the experimental strategy to rectify some of those omissions.

In chapter 3 there will be a discussion of the case for using optical instruments and an account of the optical theory required to interpret beam transmissometer measurements in terms of SPM concentrations. Chapter 4 will describe the development

of the beam transmissometers that I have used, the methods used to calibrate the transmissometers, and the strategy to assess the variability in the observations caused by the characteristics of the SPM. A description will be included of additional instrumentation used in the study.

In chapter 5 there will be a presentation of the results of the spatial surveys and their synthesis into a seasonal cycle, while Chapter 6 comprises the main body of time series data. The thesis concludes with a discussion in Chapter 7.

CHAPTER 2. BACKGROUND AND OBJECTIVES

2.1. Composition and origin of SPM in the shelf seas.

SPM in the shelf seas is composed of various substances and is frequently a combination of several of these. Inorganic SPM may be composed of lithogenous solids produced by the weathering of rocks or of hydrogenous solids formed by inorganic reactions. Sources of input to the sea are from coastal erosion, river runoff and erosion of the sea-bed.

Organic SPM may be composed of living material such as phytoplankton, zooplankton, bacteria, yeasts and fungi. It may comprise faecal pellets, detritus, inorganic shelf material and faecal tests (Lewis and Syvetski, 1983). Organic material may grow in suspension, on the sea-bed or coastal margins, or it may be carried into the sea from land.

Anthropogenic SPM is derived from discharges into the sea and may be composed of sewage, and industrial wastes including nuclear materials, hydrocarbons, or synthetic chemicals (Chester,1982).

The SPM may be combined in an aggregate from pelletisation or by adhesion by mucus produced by diatoms and bacteria (Rhoads and Boyer,1982). Aggregates may be formed by the flocculation of particles and

depends on the electrochemical charges on the surfaces of particles and on their close proximity in the water (Kranck,1974).

Sediments in suspension in the shelf seas range from clays to sands, from <1μm to 125μm (Dyer,1986). Single phytoplankton cells typically range from <1 to 100μm and frequently remain buoyant while they are alive.

2.2. Physical transport processes.

2.2.1. Introduction.

Observations in the near coastal zone suggest that small particles remain in suspension more or less permanently, whereas large particles are alternately resuspended from and deposited to the sea-bed. Schubel et al (1978), in their study in Chesapeake Bay, noted that particles with Stokes diameters of <2 μm remained in suspension, whereas those in the range from 2 to 63 μm were alternately deposited and resuspended in the tidal flow. Chester (1982) noted that particles smaller than 5 μm were influenced by large scale horizontal movements whereas those greater than 50 μm, mainly aggregates, were alternately deposited and resuspended in response to tidal flow and wave action.

Sands and silts are generally rounded or sub-rounded, having a mass sufficient to ensure that grain inertia is

important in their movement and they are transported as separate particles. However the transport of clays, which comprise much of the SPM in shelf seas, is strongly influenced by their interaction .It is, therefore, necessary to review the physical transport processes for non-cohesive and cohesive sediments separately.

To date there has been extensive work carried out on the deposition and erosion of non-cohesive sediments, but there has been less progress on the subject for cohesive sediments. A brief account of the parameters important in non-cohesive sediment transport follows. A fuller discussion will follow to identify important parameters for cohesive sediment transport.

2.2.2. Deposition and erosion of non-cohesive sediments.

The settling velocity of non-cohesive particles in water can be described by Stokes Law where

$$\omega_s = \frac{gD^2(\sigma - \rho)}{18\mu} = \epsilon D^2$$

σ = particles' density, ρ = water density, μ = molecular viscosity, g = acceleration due to gravity, D = diameter of a spherical particle, ϵ = a constant. (Dyer, 1986)

The settling velocity for natural sands and silts may be less than for equivalent spheres because the grains spin and oscillate as they fall.

Suspension of non-cohesive particles occurs when the upward directed component of velocity fluctuations exceeds the downward directed velocity gradient of the grains (Bagnold,1956).

$$\frac{u_*}{u_{*c}} = \frac{0{\cdot}8\,\omega_s}{u_{*c}}$$

u_* = friction velocity $(\tau/\rho)^{\frac{1}{2}}$, τ = shear stress$_{bed}$, ρ = density of water, u_{*c} = threshold friction velocity.

2.2.3. Deposition and erosion of cohesive sediments.

When particles become incorporated into a floccule they are more likely to become deposited on the sea-bed since the floccule settling velocity is greater than that for the individual particles.

Flocculation depends on the electrostatic charge of the particle, the molecular attractive forces and the ionic concentration of the fluid medium (Dyer,1986). Flocculation reaches an equilibrium situation when the particle population and the fluid medium remain stable. Flocculation is less effective as temperature rises. Organic binding makes floccules harder to break up.

Flocculation is principally controlled by the close

proximity of particles. Any mechanism which increases the likelihood of particle collisions enhances the rate of flocculation. Brownian motion, caused by thermally agitated water, is only effective at high concentrations for particles less than 0.5μm and can be discounted in the shelf seas as concentrations are typically low.

Particles may collide when there is a velocity gradient in the water column. The collision frequency is given by

$$K_v = 4/3 \, n \, R^3 \frac{du}{dz}$$

where du/dz is the local velocity gradient, n= the number of particles, R = the sum of the radii of colliding particles.

Inertial collisions are caused by the difference in response to local accelerations by small and large particles, and so may be important when there is a mixture of large and small particles. A collision frequency per unit volume (Saffman and Turner, 1956) is given by

$$K_i = 1.244 \, R^3 \, (\varepsilon/\nu)^{\frac{1}{2}} \, n_1 n_2$$

ε = energy dissipation rate, n_1, n_2 = number concentrations of the two sizes of spheres, R = the sum of the radii of colliding particles.

Another cause of particle collision is differential settling by the larger particles in relation to the smaller fraction. The collision frequency is given by

$$K_s \propto \pi R^2 \sigma_\omega n$$

σ_ω = relative settling frequency, R = the sum of the radii of colliding particles. (Dyer,1986).
This will occur in low velocity conditions when there are large particles, but will result in poorly bonded flocs.

Although the settling rate of clays is controlled by the collision frequency, deposition appears to be controlled by near-bed turbulence (Mehta and Partheniades,1975). Only a floc that can withstand the turbulent shear near the bed can finally settle.

Some experimental work indicates that the erosion of mud varies with the density of the bed and with salinity. Owen (1975) found that increasing bed density was closely related to a decrease in bed erosion.

Erosion of muddy sediments is not well understood at the present time. Several types of muddy sediment have been distinguished (Parker and Kirby, 1981; Parker and Kirby ,1982). These are mobile suspensions of freely moving material, stationary suspensions which may be gradually settling, and settled mud which resists

erosion. Functions for erosion rates will vary for these categories of sediments.

2.2.4. Concentrations of suspended particles.

Under steady state conditions the flux of settling particles is equal to the vertical turbulent flux of settling particles. This can be expressed by

$$C\,\omega_s = -\overline{\omega' C'}$$

(Dyer,1986)

where C and C' are the time-mean and turbulent components of the sediment concentration, respectively. The turbulent flux $\overline{\omega' C'}$ is commonly related to the mean gradient via and eddy diffusivity K_s such that

$$-\overline{\omega' C'} = K_s \frac{dC}{dz}$$

In an unsteady flow the concentration of SPM $C(z,t)$ may be described by a particle continuity equation

$$\frac{dC}{dt} = \omega_s \frac{dC}{dz} + \frac{d}{dz}\left(K_s \frac{dC}{dz}\right)$$

Boundary conditions are

1. At the surface there is no particle flux

i.e. $K_s \frac{dC}{dz} + \omega_s C = 0$ when z = h.

2.At the sea-bed there is either

a) a 'reference concentration' must be prescribed:

$$C_a(z_0, t) = F(t)$$

where z_0 = bed roughness length

or b) a 'pickup function' must be prescribed:

$$K\left(\frac{dC}{dz}\right)_{z_0} = P(t)$$

Although these approaches represent the only plausible boundary conditions, neither have been used successfully in the case of fine-grained sediments because both are generally unknown functions of the applied shear stress. Therefore, it is difficult to calculate the pick-up function.

Since the extent to which SPM may be mixed upwards depends largely on the vertical turbulent flux, it is related to the distribution of turbulent kinetic energy (TKE) in the water column. In winter the European shelf seas remain vertically well mixed due to convection induced by surface cooling. Soon after the spring equinox, however, the ocean starts to experience a net heat gain which is mixed down through the water column to an extent which depends on the amount of turbulent TKE present.

The TKE is principally determined by the magnitude of tidal dissipation which is the net rate of energy loss from the tidal motion due to frictional stresses. This dissipation is proportional to u^3, where u is the mean tidal amplitude, and varies in the shelf seas.

The competition between stirring by a tidal stream of

amplitude u and the stratifying effect of heat input at a rate $\dot{Q}$ to a water column of depth h can be expressed in terms of the parameter

$$\frac{A\dot{Q}h}{u^3}$$

where A is a constant. When $\frac{A\dot{Q}h}{u^3} > 1$ the water column is stratified and for values <1 it is vertically mixed (Simpson and Hunter,1974) .As an example of this the distribution of log h/u^3 is shown for the Irish Sea in figure 2.1. where h is the depth of water. The water is stratified for values log $h/u^3 > 2.7$.

In order to compare the distribution of h/u^3 with the stratification present in the water column, Simpson et al. (1977) developed the concept of the potential energy anomaly, which is the amount of TKE required to mix the water column. This is defined by

$$\phi = \frac{1}{h}\int_{-h}^{0} g z (\bar{\rho} - \rho(z))\, dz$$

$$\text{where} \quad \bar{\rho} = \frac{1}{h}\int_{-h}^{0} \rho(z)\, dz$$

g = gravitational acceleration, $\rho(z)$= density profile, h=total water depth.

ϕ can be shown to be $-\frac{1}{h}\int_{-h}^{0} g\, \rho(z)\left(z + \frac{h}{2}\right) dz$

Values of ϕ are 0 in mixed water and > 0 in stably stratified water. Thus when $\phi = 0$, in strongly mixed water , fine SPM concentrations gradients should be small, and should increase with ϕ in stratified water.

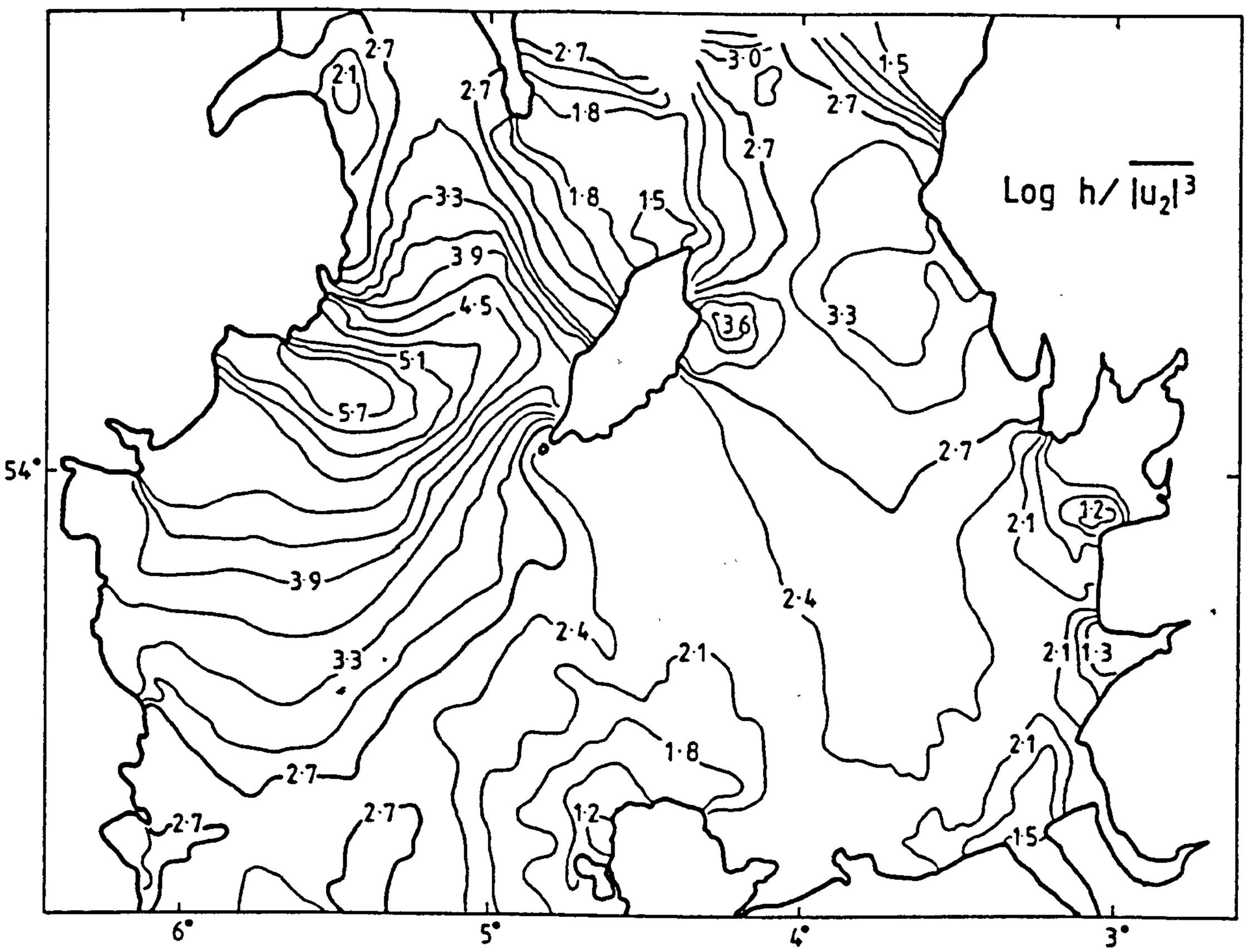

Figure 2.1. Log h/u^3, drawn by Czitrom (1982) from the digital data from the model, of Proctor (1982). Mesh size is 2.5' latitude, about 4.6 km.

2.2.5. Observations

There are several studies showing the influence of tidal and wind mixing to SPM concentrations, but they are mostly confined to estuaries or near the coast.

Concentrations of SPM were positively correlated with current speed in estuarine studies by Thorn (1975), Kirby and Parker (1983), Officer (1980), Nichols (1985) and Pejrup (1986). In addition Assinder et al (1985) noted in their study of the Esk estuary, that at slack water a higher proportion of fine-grained sediment remained in suspension than at mid-tide. This was attributed to the deposition of the coarse fraction when the current relaxed. Good agreement was found between resuspension of faecal pellets and tidal velocities in a 24 hour sampling period in the St. James River, Virginia (Haven and Morales-Alamo,1986). Robinson and Srisaengthong (1981) found coherence between patterns of reflectance from remotely sensed images (Landsat) and the semi-diurnal tidal cycle in a study of the Solent estuary.

The relationship between the spring to neap tidal cycle and SPM concentrations is well established in estuaries (Allen et al,1977), straits (Buchan et al,1967; Thompson, 1974) and the sub-tidal environment

Topliss,(1977). Newton (1986) using Secchi disc measurements to measure the diffuse attenuation of light in the water column in the Menai Straits, found higher attenuation during spring tides than during neaps.

Jago (1981) found that grain size and sediment concentration were closely related to current velocities over a spring tide in his study of the near-shore environment off the Northumbrian coast. The mean grain size, measured with a Coulter Counter, increased with current velocity. The response was greater near the sea-bed.

In some circumstances such as shallow micro-tidal estuaries, wind speed is closely related to variations in suspended sediment concentration. Pejrup (1986) found that SPM concentrations varied with wind speed and current in his study of an estuary, Ho Bugt, in Denmark.

There are few observations away from the coasts in the shelf seas. One of these examples is in the work of Joseph (1955), who used a beam transmissometer to measure the attenuation of a light beam . He found a consistent dependance between current velocity and beam attenuation over a tidal cycle in water 29 m

in depth at a site in the North Sea. Calibration of the transmissometer showed that it was a convincing measure of SPM concentrations.

Annual variations in temperature have significant consequences for the measurement of SPM concentrations. Nichols (1985) found that temperature variations of 20°C could alter the viscosity of water by a factor of 1.4. Since a seasonal range of 10°C is typical in European shelf seas, there may be a small seasonal variation in SPM settling velocity rates.

There is some evidence that variations in water density may cause the settling of SPM to vary. Duursma and Smies(1982) noted that the fallout of fine material is greater in water of low density, where velocities are less than 0.1 -0.2 m/s. This observation is consistant with Stokes Law which is discussed on page 10 of this chapter. Seasonal warming of the sea by solar radiation commences in mid-March in the shelf seas, causing the onset of stratification. This intensifies during the summer, finally breaking down as the surface waters cool and winds intensify in the autumn (Simpson and Hunter,1974).

There is evidence to suggest that SPM concentrations are higher at the surface in well-mixed waters than in stratified waters in the Irish Sea, and that there are

high concentrations below the pycnocline in stratified regions (Mitchelson,1984). Heathershaw and Simpson (1974) found that a change of 0.1°C was associated with a change in beam attenuation, in their study in the western Irish Sea. They noted that attenuation minima were associated with high temperature and with sharp density gradients.

This discussion presents convincing evidence that SPM concentrations vary with wind velocities, lunar and semi-diurnal tidal velocities and physical seasonal processes near the coasts. There is some indication of these relationships in the shelf seas, despite the limitations in the observations.

2.3. Biological processes which cause variations in the supply of SPM to the shelf seas.

The annual increase in sea-water temperature, in light intensity and in the duration of daylight which commences in the spring stimulates the growth of phytoplankton in the shelf seas. Secondary producers take advantage of the increase in food supply and the proportion of organic material, both living and detrital, increases.

The onset of the spring bloom is partly caused by the onset of stratification (Pingree at al.,1975, Simpson et

al.,1979). The phytoplankton remain in or above the pycnocline, which is sufficiently illuminated for photosynthesis to take place. At the end of the winter nutrient levels are high and uniform throughout the water column. The physical and chemical conditions for growth are optimal during the spring.

Following the spring bloom there is an increase in the amount of decaying organic material sinking to the sea-bed, which may trap small inorganic particles as it sinks, removing them from the water column. Water clarity is observed to increase at this time. The organic material on the sea-bed is rich material for microbial decomposers, and the organic films they produce increase the binding properties of the sea-bed (Meir-Reil et al.,1980).

The erodability of the sea-bed can be reduced by the growth of benthic diatoms (Holland et al.,1974). Frostick and McCave (1979) found that erosion rates of mud on tidal flats along the Deben estuary were significantly reduced from April to September, 1971. Benthic diatoms are capable of carrying out photosynthesis at low light levels (Round,1965). Mare (1942) noted concentrations of diatoms of 5.9×10^4 per cm^3 in the top 5mm of sediment in the Bristol Channel. Their growth depends on light intensity, and thus partly on water clarity. Highly turbid water

has been found to reduce primary production rates. Joint and Pomeroy (1981) noted a reduction in the expected seasonal variation of primary production in the inner part of the English Channel, which they associated with severe light limitation caused by highly turbid water.

An increase in temperature from spring onwards may stimulate the metabolic rate in animals living in the sediment. This causes an increase in pelletisation of the sediment and consequently enlarges the mean grain size so that greater shear stress is required to erode the sediment (Webb et al.,1976). Pelletisation and tracking by animals may roughen the surface and increase the critical entrainment velocity (Nowel et al,1981). Destabilisation, caused by bioturbation from filter feeders, may increase the erodability of the sediment, but the flux of nutrients produced by burrowing can stimulate the growth of micro-organisms and meio-fauna and increase binding (Rhoads and Boyer,1982).

Most marine plants, animals, and micro-organisms secrete mucus which is an organic compound consisting of high molecular weight polysaccharides or micro-protein. The mucus coats all surfaces, increasing the binding properties of the sediment (Probert,1984). This process reduces the erodability of the sea-bed by increasing the stickiness of the sediment, and increasing the size of

the particles due to their aggregation.

2.4. Observations of seasonal variations in SPM concentrations in the shelf seas.

There is a marked seasonal cycle of SPM concentrations in the shelf seas. Buchan et al (1967) found high SPM values during winter and low values during summer in their study of the Menai Straits in 1962 and 1963. They noted that high temperatures were associated with low log ash weight of SPM. Newton (1986) found a decrease in attenuation in the late spring and early summer in her experiment in the Menai Straits, using Secchi disc measurements.

Seasonal studies in the Irish Sea indicated that values of SPM in mixed and frontal water decreased by as much as 50% from late May to August, 1982 (Mitchelson (1984), Agnew (1983)).

The composite annual time series of satellite images from the CZCS (Coastal Zone Colour Scanner) , in figure 2.2. show high values of sea-surface reflectance in April and May in the region north of Anglesey. In June this has substantially decreased. Reflectance is proportional to backscatter by particles (Morel and Prieur, 1977) in the water, and so a seasonal cycle of variations in particle concentration is inferred with lower summer values. This is discussed more fully in Chapter 3.

Figure 2.2. Sequence of CZCS (Coastal Zone Colour Scanner) images of the Irish Sea, Channels 1,2 and 3 (443,520 and 550 nm).These are corrected for geometric distortion and Rayleigh scattering.(processed by S.Groom,Plymouth Polytechnic). Dark areas represent low reflectance, and light areas high represent reflectance.

a) 4/4/80
b) 16/4/81
c) 16/5/80
d) 2/6/85

a

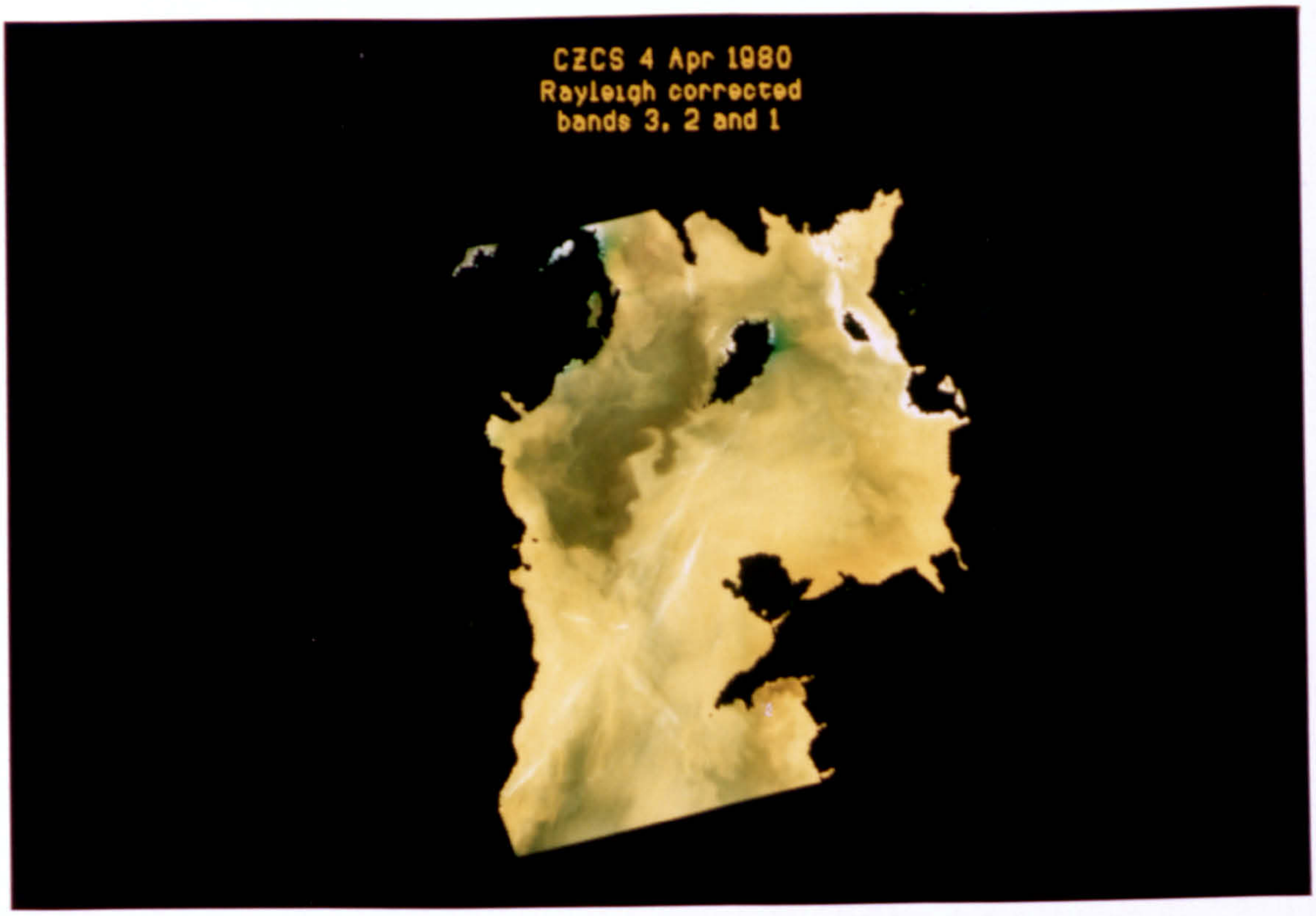
CZCS 4 Apr 1980
Rayleigh corrected
bands 3, 2 and 1

b

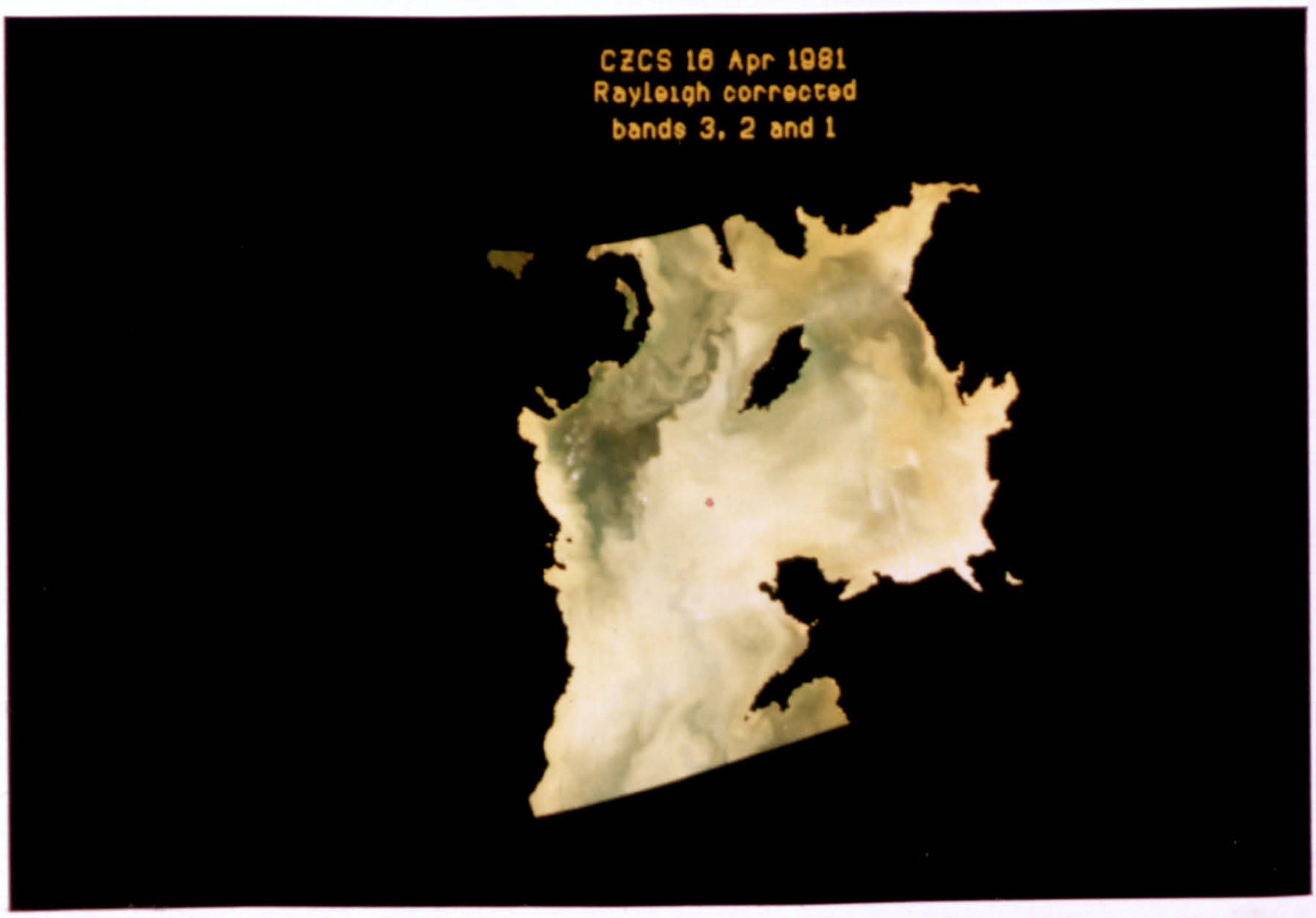
CZCS 16 Apr 1981
Rayleigh corrected
bands 3, 2 and 1

c

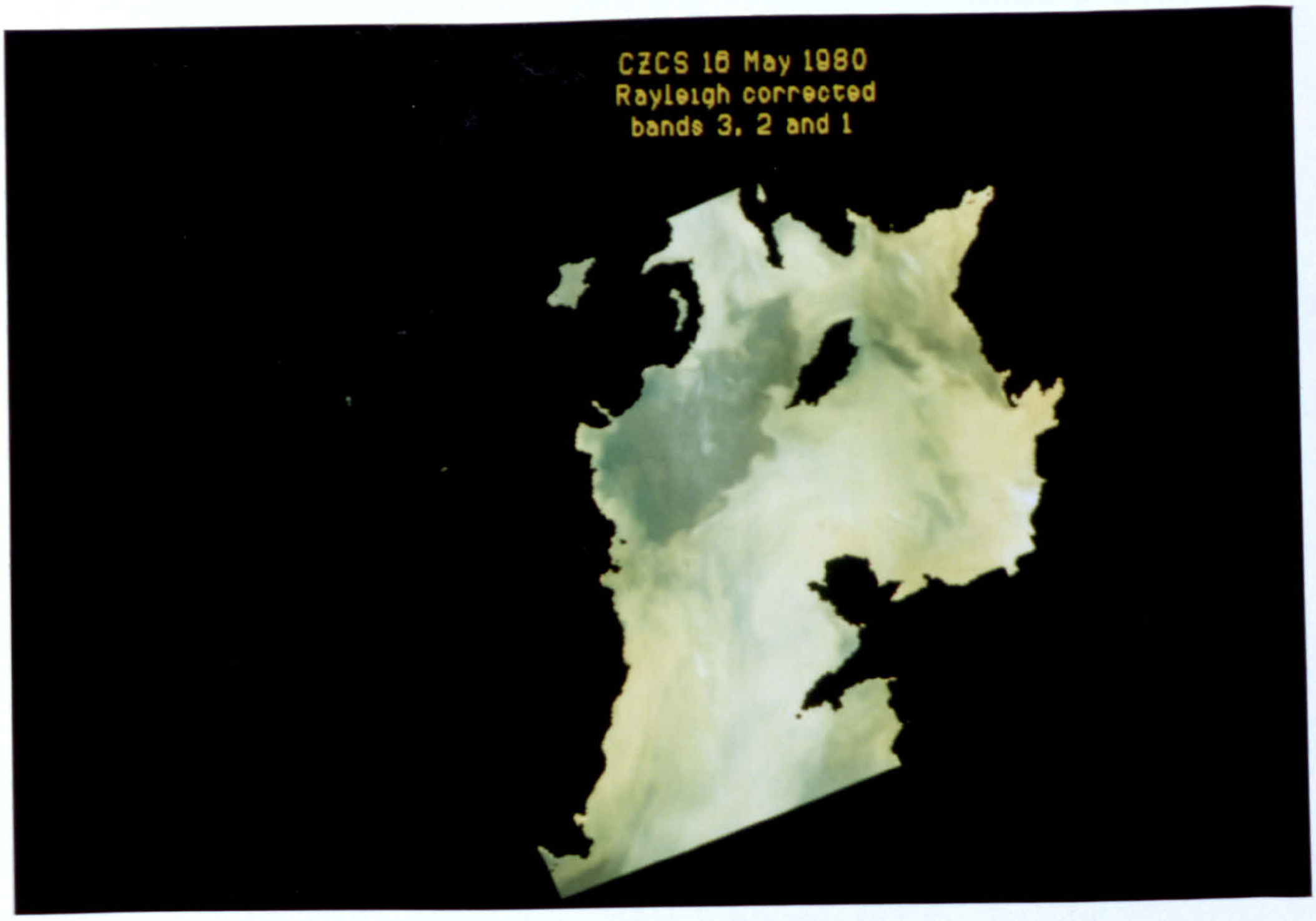
CZCS 16 May 1980
Rayleigh corrected
bands 3, 2 and 1

d

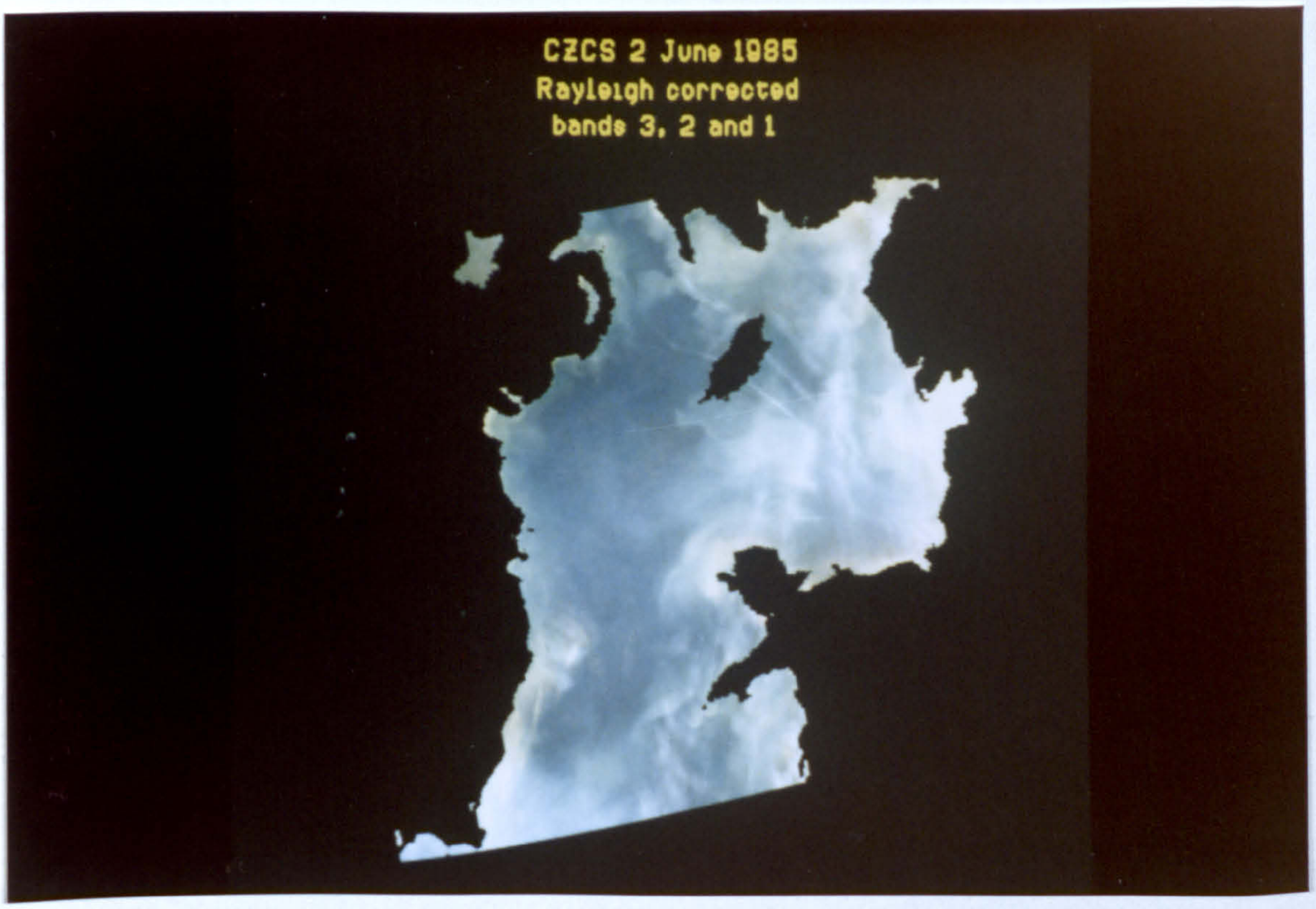
CZCS 2 June 1985
Rayleigh corrected
bands 3, 2 and 1

2.5. Chemical interactions with SPM.

A short review follows of published work on the interaction between suspended particles and of contaminants discharged into the sea.

The surface area of suspended particulates are relatively more exposed to the water than those on the sea-bed and so are effective scavengers of contaminants discharged into the sea. Duursma and Eisma (1973) found that 20 to 30% of radioisotopes discharged into the sea were adsorbed by SPM when concentrations were between 50 and 100mgl^{-1} . Any resuspension of uncontaminated sediment would be expected to increase the percentage uptake by SPM.

Several mechanisms operate in the sorption of contaminants onto sediments (Parker and Kirby,1982). These include direct retention by ion exchange, and indirect retention in thin films of water, hydrated oxide and humus on the particle surface.

Different elements have a characteristic equilibrium status for the proportion in solution and incorporated in a solid. This is expressed as the Kd ratio where

$$Kd = \frac{\text{concentration per gram of particulate}}{\text{concentration per gram of soluble fraction}} = \frac{ml^{-1}}{ml^{-1}}$$

An element with a high Kd value has a higher affinity to be adsorbed onto the surface of a solid than one with a low Kd value. Table 1 shows some Kd values for radioisotopes commonly present in the Irish Sea (Assinder,1982).

Small particles, with a large surface to mass ratio, provide more surface sites for the adsorption of contaminants than larger particles. Jones (1960) found that the uptake of Ruthenium-106 depended on the size of suspended particles. Assinder *et al* (1985) noted higher radioactivities in the fine-grained fraction of suspended sediments in his study in the Esk estuary. The mineralogy of the particles may also be important. Duursma and Eisma (1973) found that the specific surface and base exchange capacity of a solid was more important than the ratio of surface area to mass.

Kershaw and Young (1988) noted, in their study of Thorium-234 in the eastern Irish Sea, that the scavenging rate from solution was determined by the concentration of the particles suspended in sea-water. Where there was strong mixing, adsorption rates were

TABLE 1 KD RATIOS FOR RADIONUCLIDES.

Element	Range of Kd values	oxidation state
Tc	$2.5x10^{2}$ - $1.9x10^{3}$	
Np	$2.4x10^{3}$ - $3.3x10^{4}$	
Pu	$6.0x10^{3}$ - $1.4x10^{4}$	Pu (V + VI)
	$4.0x10^{5}$ - $6.0x10^{6}$	Pu (III + IV)
Am	$2.2x10^{6}$ - $2.4x10^{6}$	
Cm	$1.2x10^{6}$ -$1.6x10^{6}$	

high and residence times were short. Mean residence times were from 6 to 27 days, and settling velocities were calculated as between 1.8 to 7.4 m day^{-1}. Kershaw et al. (in press) developed a multi-compartmental box model incorporating water circulation, suspended particulate scavenging, particle mixing by bioturbation, pore water diffusion and advection, and particle resuspension and deposition. Problems identified were the variation of the circulation with depth, grain size variation, and regional and time dependant variations in circulation.

In order to model the pathways of contaminants adsorbed onto particles after discharge into the sea, it is necessary to know the mean particle size, density, and the Kd value of the contaminants involved, in addition to the physical processes to which the particles will be subjected.

2.6. The Irish Sea .

2.6.1. Sources and sinks of fine sediments.

The Irish Sea was the area chosen in which to make a study of the subject, partly due to its convenient access to workers at UCNW, but also because its bathymetry and physical characteristics are suitable for the study. The bathymetry , shown in figure 2.3.

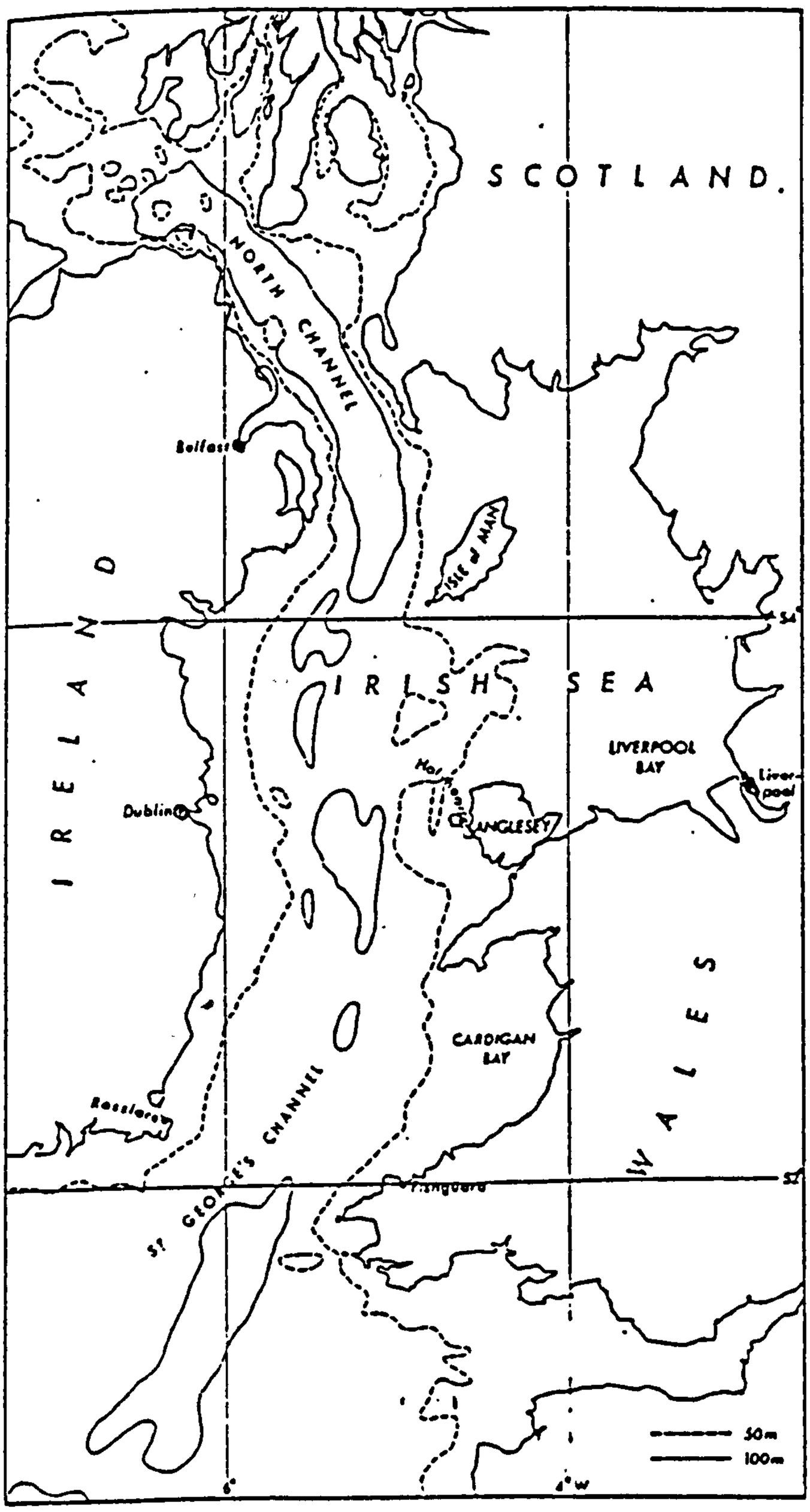

Figure 2.3. Bathymetry of the Irish Sea.

comprises a deep channel running from north to south along the Irish coast, with a shelf of 50m in depth running to the east.

The sediments on the sea-floor of the Irish Sea are mainly unconsolidated and were deposited during the Quaternary period. Mud deposition commenced in the Holocene, about 10,000 years ago (Belderson,1964). Figure 2.4. shows the distribution of sea-bed sediments (MAFF, 1987). There are two main areas of mud, one in the western Irish Sea and one off the Cumbrian coast. Bedload sand transport is observed, from features on the sea-bed in the southern Irish Sea (Stride,1973). Stride described the pathway of sand transport in the area from north Wales to the northern Irish Sea to be in a northerly and north-easterly direction. This is illustrated by the diagram in figure 2.5.

The distribution of sea-bed sediments may have been determined by the asymmetry of the tidal flows in the Irish Sea (Dobson and Evans, 1970). Figure 2.6. shows the maximum M2 current speeds (Robinson, 1979).When a comparison is made with figure 2.5., higher flows are generally associated with coarse sediments. The areas where there are weak flows correspond to areas of muddy deposits.

Third Party material excluded from digitised copy.
Please refer to original text to see this material.

Figure 2.4. Simplified distribution of surficial sediment types in the Irish Sea. From Ministry of Agriculture,Fisheries and Foods Aquatic Environmental Monitoring Report. No. 17.1987.

Figure 2.5. Sand transport paths around the British Isles (from Stride,1973).

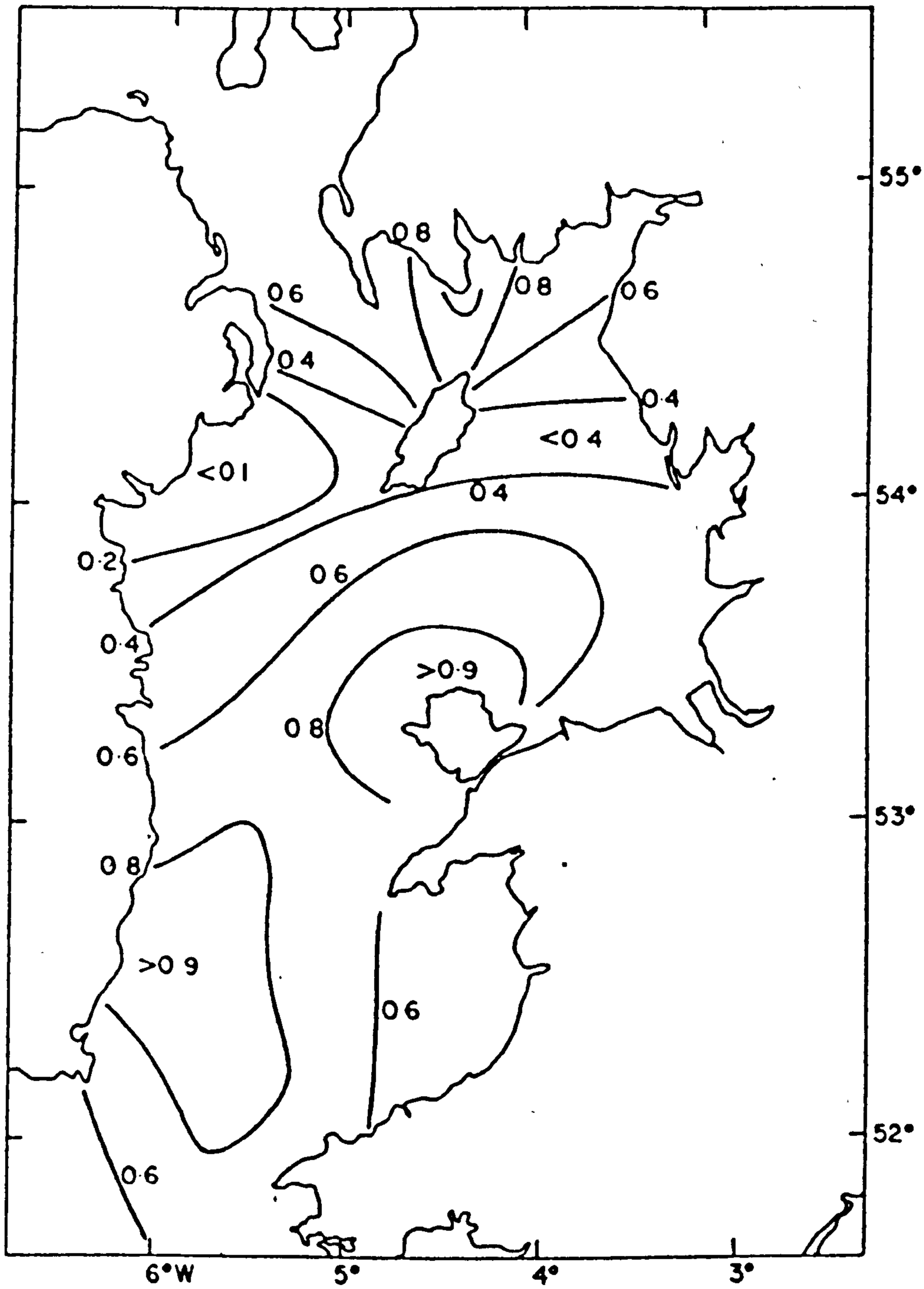

Figure 2.6 Magnitude of M_2 tidal currents around the U.K. from a model by Robinson (1979). (ms^{-1}).

Pingree and Griffiths (1979) showed that it was possible to derive the direction of bedload sand transport and the associated asymmetry of sand wave profiles, shown by Stride (figure 2.5.) from a non-linear model of the M2 tide in the Irish Sea. The combination of the M2 and the M4 tide produced an asymmetry in the bottom stress. The magnitude of the bottom stress from M2 and M4 tidal currents and the maximum bottom stress are shown in figure 2.7.

Until recently, mud deposition has been regarded as a continuing process. A source region for the western Irish sea (WIS) mud patch was identified at the north of St. Georges Channel (Belderson,1964). The Cumbrian mud patch was considered to be depositional (Belderson,1964; Pantin,1977,1978; Heatherington,1976). The Solway Firth and Wigtown areas were considered to be possible sources of fine material offshore (Williams et al.,1981).

Kirby (1987) argued that there was little evidence of riverine and coastal fine sediment supply to the Irish Sea. Buchan et al. (1967) found no evidence that SPM concentration was related to freshwater runoff in their study in the Menai Straits in 1962 and 1963.

Kirby (1987) suggested that fine sediment transport

Third Party Material excluded from digitised copy.
Please refer to original text to see this material.

Figure 2.7. a) Magnitude of the maximum bottom stress due to M_2 and M_4 tidal currents (Pingree 1979)
b) Maximum bottom stress vectors due to M_2 and M_4 tidal interactions.(Pingree, 1979)

was more likely to be toward the Cumbian coast than away from it. Figure 2.8. shows his hypothesis, which was supported by observations from sea-bed drifter In support of this, bedform analysis suggests easterly transport of coarse sediment at the north and the south of the Isle of Man (Williams et al.,1981). Other evidence of easterly transport in the eastern Irish Sea is given by Hamilton (1981) and Eakins et al., (1982) who noted that sediments contaminated by actinides were transported to the Cumbrian coast from the Irish Sea.

Little is known about the transport rate and magnitude of fine sediment from its source region, but Kirby (1987) suggested that this may be small. Consequently changes in the net budget may be small.

From this discussion it is evident that there is no clear consensus about sources and sinks of fine sediments in the Irish Sea.

2.6.2. Visible band satellite imagery in the Irish Sea.

Information about the upwelling irradiance from the sea surface, from sensors carried by satellites and aircraft, can be interpreted in terms of the suspended particulates in the surface layers of the sea. The

Figure 2.8. Postulated net sediment transport pathways in the coastal margin of the eastern Irish Sea . Size of arrow head indicates relative scale of exchange. (from Kirby,1987).

upwelling irradiance is influenced by the scatterance and absorbance of incident light ,the constituents in the water, and by the water itself. Therefore although the data cannot be used to give accurate measurements of SPM at the moment, it gives a broad synoptic view of SPM distributions.

The sequence of photographs in figure 2.2. are from three wavebands on the Coastal Zone Colour Scanner (CZCS) and shows variations in the sea surface radiance in the Irish Sea. The sharp gradient to the south west of the Isle of Man is closely associated with the position of a thermally induced density front (Mitchelson, 1984). The seasonal progression of the light absorbing water can be observed in this sequence of photographs. There is further discussion of application of remotely sensed optical data for the measurement of SPM concentrations in Chapter 3.

2.7. Discussion.

SPM in the shelf seas is a combination of organic and inorganic particles, ranging in size from <1 to 125μm. Particles in the size category below 20 μm become aggregated and do not conform to the same depositional and erosional processes as coarser sediments. These small particles may be semi-permanently in suspension.

Observations of the variations in SPM concentrations near the coast suggest that important processes are tidal, wind driven or seasonal. Seasonal variation may be caused by physical processes, such as stratification, or by biological processes such as an increase in the binding of the sediment by benthic organisms. There is little observational data away from the coasts.

The distribution of sea-bed sediments indicate that sediment size is related to the strength of tidal shear on the sea-bed. Satellite images also indicate that sea-surface radiance is related to the strength of tidal shear.

In order to model the transport pathways of contaminants discharged into the shelf seas, particle size distributions, particle density and the Kd values of the contaminants must be known, as well as the important physical and biological processes.

These are summarised in figure 2.9., which illustrates the interdisciplinary nature of the subject. The first three processes apply to both the inorganic and organic SPM, the last two are purely for organic SPM. The object of this diagram is to identify the important parameters that need to be assessed in order to understand the causes of SPM variation in the shelf seas.

processes	controls: physical	biological	geological	chemical	spm
deposition	water: viscosity density. turbulence	bloom settling	particle density	flocculation	→ fine
		pelletisation			→ coarse
erosion	water: viscosity density. shear stress	sea-bed binding	particle density, compaction	bonding	→ fine
			bedforms roughness		→ coarse
advection	residual flow		particle density		fine
					→ coarse
growth grazing	illumination, heat			nutrients	→ fine
					→ coarse
decay	illumination, heat	remineralisation			fine
					→ coarse

Figure 2.9. Processes controlling SPM concentrations in the shelf seas. The physical processes which determine the concentration of SPM in any one region are deposition, erosion and advection; biological processes are growth ,grazing and decay. The controls for these processes can be physical, biologicalal ,geological or chemical and are summarised in the figure.

There are two ways in which solutions to the problem may be approached. The first is by extending the theory of cohesive sediment transport to include the chemical and biological processes discussed , and by undertaking a programme of laboratory experiments to examine erosion and deposition of fine sediments.

The second approach is to undertake a programme of observations in a shelf sea with a view to identifying the important processes which control the spatial and time dependant variations in SPM concentrations.

The second approach was adopted partly because the aquisition of a useful data set was an attainable goal within the time limits of a Ph.D. project. However, the principal reason for adopting this approach was to explore the subject which had been hitherto neglected, and to attempt to identify the dominant controls on SPM transport in the shelf seas.

2.8. Objectives

The general aim of the study was to determine whether there were spatial variations in SPM concentrations in an area of the Irish Sea where the satellite imagery displayed strong variations in upwelling irradiance (shown in figure 2.2.). It was

also necessary to establish whether there was a seasonal cycle in SPM concentrations, as observed in the satellite images. A short sequence is shown in figure 2.2. Since high frequency variations in SPM concentrations may be of the same order as spatial and seasonal variations, it was important to establish the range of these. It was proposed that this could be partly accomplished by examining the semi-diurnal variation in SPM concentrations. In addition, to determine the cause of variations in SPM, parallel measurement of temperature, conductivity, depth and surface velocity were to be obtained.

In order to make routine measurements of SPM concentrations it was proposed that an optical instrument ,such as a transmissometer should be designed at UCNW and built there. It was to be interfaced with a CTD to give vertical profiles of measurements of beam attenuation. These measurement were to be calibrated by water samples analysed for SPM concentration by weight. A discussion of the case for using a transmissometer is presented in Chapter 3.

After the first year, when it was confirmed that there were significant spatial and seasonal variations in SPM concentrations , the objectives were partly redefined.

A fundamental question to be addressed was whether the erosion of the sea-bed by varying tidal flows was closely related to the spatial distribution of SPM. The second question was whether the seasonal variations were caused by physical or biological processes.

This was to be accomplished by obtaining a parallel annual time series of beam attenuation ,current velocity and wind speed in order to determine whether beam attenuation was controlled by current flows or by meteorological events. In addition the analysis of the relationship between SPM concentrations and the seasonal variation of the organic proportion of SPM would give an indication of the importance of biological processes.

At this stage , it was neccessary that the transmissometer should be upgraded to interface with a logger on a mooring. Recording current meters were to be mounted on the mooring so that an assessment could be made of the covariance of SPM concentrations and tidal flows.

CHAPTER THREE - OPTICAL OBSERVATION TECHNIQUES.

3.1. The Case for Optics.

3.1.1. Introduction.

A routine method to measure SPM concentrations was required in order to make a large number of measurements. This measurement, logged electronically, would give the detail of coverage that is now accepted as a routine requirement for physical oceanographic measurements.

Soulsby (1977) reviewed the subject of suspended sediment measurements (<63μm) and concluded that the beam transmissometer was an accurate instrument providing the particle size distribution was constant. He rejected the use of acoustic pressure sensors, optical occultation and impact sensors for the measurement of fine particle concentrations. Measurement methods using conductivity or gamma ray absorption are more suitable to higher concentrations of sediments than those typically found in the shelf seas (McCave,1979).

Optical instruments such as the transmissometer and the nephelometer can be used to measure particle concentration, but should not be calibrated in terms of

artificial turbidity standards (McCave,1979). Instead the relationship should be defined between the optical measurement and parallel weighed concentrations taken from water samples. Calibration of nephelometers has proved to be difficult and to date transmissometers have been used with more success (McCave,1979).

The transmissometer was chosen for the present study since its use and calibration have been widely documented. In addition , it requires low power and is a relatively inexpensive instrument to build. Beam attenuation is a function of the absorbance and scatterance of particles in the water as well as dissolved components and the water itself. Although it depends on the concentration of the particles, it also depends on the pigments present, and on the size, shape and refractive index of the particles. An account of the theory of beam attenuation follows, and the parameters which determine the scatterance and absorbance of light. From this a strategy for the calibration of the transmissometer will emerge.

3.1.2. The theory of beam attenuation.

The attenuation of light in water is caused by the scattering and absorbance by the water and by components

in the water. It is an inherent property because it does not depend on the natural light field but solely on the composition of the medium, (Priesendorfer,1961). Simply it is described by

$$c = a + b \qquad (1)$$

where c = attenuation, a = absorbance and b = scatterance.

The attenuation of light over a pathlength Δr is given by $$\Delta I = -(a+b) I \Delta r = -cI\Delta r \qquad (2)$$

where I is the radiant flux

and $$\Delta I / I = -c \Delta r \qquad (3)$$

where r = the pathlength through the water.

Integrating between o and r gives us

$$\ln \frac{I}{I_o} = -c\, r \qquad (4)$$

where I_o = the incident radiant flux.

and from (4)

$$c = \frac{1}{r} \ln \frac{I_o}{I} \qquad (5)$$

The beam transmittance (M) is equal to I / I_o and is normally expressed as a percentage .

3.1.3. Light scattering.

Light is scattered by seawater and by the particles suspended in it. In pure water scatterance increases toward shorter wavelengths. Figure 3.1.shows the spectral shift in light scattering by pure water.

Light scattering by particles is caused by diffraction, refraction and by external and internal reflection (Kirk,1983). Diffraction depends on the size and shape of the particle. Refraction and reflection depend on the refractive index of the particle. Diffraction by irregular, non-absorbing particles is similar to that of spherical particles of the same size. External reflection does not vary with size since the probability of reflection for all angles remains constant.

Mie (1908) developed a theoretical basis to predict the angular distribution of light scattering from particles of any size which was based on electromagnetic theory. Figure 3.2. shows the angular dependance of light scatterance predicted from Mie's theory, by particles with a known refractive index, and shows that light scatterance is predominantly in a forward direction.

Burt (1953) used Mie's theory to show that the maximum scattering efficiency of a particle is in the size range from 0.3 to 3 μm ,when the refractive index is

Figure 3.1. Spectral absorbance (a) and scatterance (b) of pure sea water (Robinson ,1983)

Figure 3.2. Angular distribution of scattered intensity from transparent spheres calculated from Mie theory or on the basis of transmission and reflection, or diffraction, transmission and reflection. The particles have a refractive index of 1.2(relative to the surrounding medium), and have diameters 5-12 times the wavelength of light.(from Kirk,1983)

high (1.4). The scattering efficiency remains constant for particles greater than 3 μm. The efficiency of scatterance by particle size is shown in Figure 3.3.

If particles are larger than a few wavelengths of light, scatterance can be described on the basis of refraction and geometrical optics. For example, considering light of wavelength 660 nm, the particle under consideration must be greater than 0.6 μm for this to apply. Van den Hulst (1957) developed a theory to calculate the scattering efficiency of particles with a refractive index up to twice that of the surrounding medium (in figure 3.4.) The diagram shows that scatterance is greatest for particles from 0.3 to 3.09 μm, where the refractive index is 1.7). However, SPM is frequently a combination of organic, inorganic material and water and has typical refractive indices of 1.0 to 1.2 .

Particle scattering does not vary much with wavelength. Pak et al (1971) found that scattering by clays was not wavelength dependant and that non-chlorophyllous particles were predominately forward scattering. However there is some evidence from experiments in natural waters that the particle scattering efficiency varies with shorter wavelengths scattered more intensly (Kirk,1980).

It should be noted that the shape of a particle, or its

Third Party Material excluded from digitised copy.
Please refer to original text to see this material.

Figure 3.3. Diagram showing scattering efficiency, Q_{scat} (effective area coefficient) on the basis of Rayleigh's equation and the Mie theory for non-absorbing spheres(Burt,1956) (From Jerlov,1968)

Third Party Material excluded from digitised copy.
Please refer to original text to see this material.

Figure 3.4. Scattering efficiency of a non-absorbing spherical particle as a function of size. Calculated using the equation of van de Hulst (1957).Particle has a refractive index of 1.17 relative to surrounding medium. λ = 550nm. (from Kirk 1983).

non-sphericity , can cause the underestimation of particle areas from equivalent spherical values calculated by volume sensitive particle counters like the Coulter Counter (Jonasz,1987).

3.1.4. Light absorption

The spectral absorption of pure sea water is well known. It is shown in figure 3.1. Absorption increases with wavelength (Robinson,1983).

Light is absorbed by pigments in particles suspended in the water such as photosynthetic and non-photosynthetic organisms, detritus, sediments. It is also absorbed by dissolved organic materials, or 'gelbstoff'. 'Gelbstoff' is derived by means of the bacterial decay process which causes the leaching of biogenic material into the water. Light absorption by 'gelbstoff' is strongly wavelength dependant, as figure 3.5. shows, with absorption inversely proportional to wavelength.

The photosynthetic pigments in phytoplankton absorb light strongly at particular wavelengths. The absorption maxima for chlorophyll-a are at 443 and 670 nm. Figure 3.6. shows the specific absorption coefficient corresponding to 1 mg chlorophyll-a m^{-3} ,(Kirk,1983).

Absorbance by organic and inorganic particles

Third Party Material excluded from digitised copy.
Please refer to original text to see this material.

Figure 3.5. Absorption spectrum for 'gelbstoff' .(from Robinson,1983)

Third Party Material excluded from digitised copy.
Please refer to original text to see this material.

Figure 3.6. Specific absorption coefficient (in situ), corresponding to 1 mg chlorophyll a m^{-3}, for oceanic phytoplankton (after Morel and Prieur,1977).

can be difficult to measure when light scattering is intense and masks the attenuation of the light by absorbance. The spectral variation in light attenuation is generally measured in a spectrophotometer. Kirk (1980) developed a method to measure the light absorbance by concentrated samples of particulate material from Australian inland waters. He used a spectrophotometer fitted with an integrating sphere which collected the light scattered out of the light path and scattered it back so that it was detected by the photocell. The reduction in light intensity was thus solely due to absorbance. His results showed an increase in absorbance with decreasing wavelengths.

Prieur and Sathyendranath (1981) also noted high absorbance at low wavelengths in their study of non-chlorophyllous suspended particles. They found an absorbance minimum in the green part of the spectrum. This is shown in figure 3.7.

3.1.5. Summary

Since beam attenuation increases with the concentration of absorbing and scattering components in the sea water in the light beam, it can in principle be used to

Figure 3.7. Normalised specific absorption curves for a) chlorophyllous pigments, b) non-chlorophyllous particles in suspension, c) yellow substance (from Mitchelson, 1984 (after Prieur and Sathyendranath, 1981).

quantify the concentration of these constituents. Scatterance and absorbance by pure water are, however, strongly wavelength dependant. Scatterance does not vary much with particle size for particles > 3 μm, although it varies for smaller particles. The refractive index of a particle may determine its scattering efficiency, as can variations in particle shape. Different pigments in the water or associated with the particles can cause a spectral shift in absorbance.

It is necessary, therefore, when using a transmissometer to make measurements of SPM concentrations and to assess the uniformity of these parameters associated with the particles in the study area. The necessary additional measurements are the particle size distribution, the organic to inorganic ratio, to estimate the change in the particle refractive indices, the variation in the dominant pigment concentrations and an indication of the uniformity in particle shapes.

The problems of interpreting beam transmissometer measurements are widely documented and a discussion of the conclusions follows.

3.2. Beam attenuation measurements : a review.

Joseph (1955) found a good relationship between beam attenuation and suspended particulate concentrations in his work in the Kattegat. He also noted that the attenuation of light was strongly wavelength dependant, due to the presence of 'gelbstoff' in the water. This observation resulted in the use of a red light source in transmissometers. Bartz et al (1978) designed the Sea-Tech transmissometer, which is now in widespread use, with a light source centred at 660nm ($\pm$11nm), over a 25cm pathlength.

Jones and Wills (1956) found high correlations between attenuation and concentrations of kaolin and Thames mud. They used an Admiralty laboratory hydrophotometer using a parallel beam of light from a tungsten filament. The suspended sediment was uniform in size and in its composition.

Lee and Foulkard (1969) used the same instrument, and noted that attenuation varied not only with concentration but with the size of the suspended particles.The size distribution was measured with a Coulter Counter.

Burt (1953) utilised the dependance of attenuation on particle size to measure the grain size of sediments. He used a spectrophotometer to measure attenuation. The dependance of attenuation on the grain size of the

particles has been the subject of several studies by Postma(1961), Smith (1980), Spinrad et al (1983) and Kitchen et al. (1982).

Baker and Lavelle (1984) fractionated their particulate samples into size categories and made measurements of attenuation in the laboratory using a Sea-Tech transmissometer in suspensions of increasing concentrations in each size class. The size classes ranged from 1 to 100 μm. They found different calibration curves for each size class, which are shown in figure 3.8. They concluded that attenuation increased as the volume of small particles in a sample increased and that beam attenuation measurements are acutely sensitive to particle size distributions. However the slopes of the curves for the size classes 1 to 3 (1 - 30 μm) are similar and indicate that the use of the transmissometer is acceptable for particles in this size range.

Spinrad (1986) described the response of beam attenuation per unit volume of SPM to changes in the particle size distribution by means of a calibration diagram. Most marine suspended loads can be described by a hyperbolic particle size distribution (Bader,1970) where the differential slope of the particle size distribution ranges from 3 to 6 for particles from 1 to 80 μm. Beam attenuation of a suspension of particles varies in relation to the diameter.

Figure 3.8. Calibration curves for the Sea-Tech transmissometer for particles of increasing concentrations in a series of size classes (from 1 to 9, which correspond to a range from 1 to 100 μm). (from Baker and Lavelle, 1984).

Figure 3.9 shows the beam attenuation coefficient per unit suspended volume as a function of the relative refractive index for varying differential slopes of the particle size distribution. This shows that as the relative refractive index increases, so does light attenuation. It also shows, since a large slope represents a greater volume of small particles, that attenuation increases as the proportion of small particles increases.

Moody et al (1986) calibrated the Sea-Tech transmissometer for particle size distribution with glass beads and natural sediments assuming

$$c = \frac{N\, Q\, \pi\, D^2}{4}$$

c = the attenuation coefficient for a given particle size of diameter D; N = the number of particles per unit volume; Q = the efficiency of attenuation, based on a relative refractive index.

Suspended material concentration is given by

$$SPM = \frac{2\rho_s}{3\,Q} \cdot D \; c_p$$

where ρ_s = particle density.

Figure 3.9. Specific beam attenuation coefficient (measured particulate beam attenuation coefficient, in m^{-1}, per unit suspended volume, in parts per million) as a function of the relative refractive index for a varying particle size distribution (on a scale of 3 to 6, corresponding to 1 to 80 μm). (from Spinrad et al. 1983)

The calibration slope as a function of particle diameter (in figure 3.10) is linear in the case of glass beads. The scatter of the regression for natural sediments is probably due to particle irregularity and roughness.

Campbell and Spinrad (1987) examined the relationship between c and particle characteristics in a turbid estuarine environment. They included environmental factors in their analysis and found in a multiple regression analysis of the data that wind speed and particle size distribution accounted for 94.7% of the variance in c. Particle size was determined by Coulter Counter and light microscope measurements.

Bishop (1986) found disturbing offsets in upward and downward transmissometer casts in warm core rings in the north west Atlantic, where there were strong vertical temperature gradients of up to 10° C. This was caused by the temperature sensitivity of the transmissometer and a correction was introduced into the transmissometer software to compensate from this.

This discussion indicates that although the concentration of SPM can be determined by beam attenuation measurements, it is important to determine the effect on the quality of the measurements by the particle size distribution, variations in the

Third Party Material excluded from digitised copy.
Please refer to original text to see this material.

Figure 3.10. Calibration curve for a Montedoro-Witney transmissometer as a function of particle size.
● = natural sediment, o = glass beads, △ =diatom culture.
Data from Baker and Lavelle (1984) are plotted using the symbols: ■ = natural sediment, □ = glass beads. The error bars are 1 s.d. of particle diameter or calibration slope. The results for a LED transmissometer are almost identical. (from Moody et al. 1986)

particle refractive indices and pigments associated with the particles or dissolved in the water.

Measurement of solar irradiance has been used to determine the concentration of suspended material, and is, of course, subject to the same inherent optical responses as measurements of beam attenuation. This is discussed in the following section.

3.3. The diffuse light field.

A brief description of the way in which natural light is absorbed and scattered by constituents in the sea is included in this chapter since irradiance can be used as a measure of material suspended in sea-water. Beam attenuation is an inherent optical property, depending only on the absorption and scatterance of the light beam by the water and its components. Irradiance depends, in addition, on the natural light field and so is an apparent optical property. Trends in the response of passive optical sensors can give useful information about the constituents of the water.

Observations can be made from satellite or aircraft mounted sensors. The ratio of upwardly scattered

light to downwelling light in the water can be used in the same way. The two parameters measure the same apparent properties of the constituents in the water.

Downwelling and upwelling irradiance are a function of the initial light intensity and the attenuation coefficient of the water. The theory is discussed fully in Kirk (1983).

The reflectance ratio is a measure of the intensity of the backscattered light and is given by

$$R = Eu(\lambda) / Ed(\lambda)$$

where $Eu(\lambda)$ is the upwelling irradiance and $Ed(\lambda)$ is the downwelling irradiance. Variations in $R(\lambda)$ depend on the concentrations of the constituents in the water . The wavelength dependance of R depends on the wavelength dependance of the absorption and scatterance of constituents in the water.

Satellite imagery gives us the water leaving radiance (Lw) which is influenced as much by incoming radiance as by the optical properties of the sea. Robinson (1983) describes the relationship between R and Lw by

$$\frac{R(\lambda_1)}{R(\lambda_2)} = \frac{Lw(\lambda_1)\, n(\lambda_1)\, [\,1 - q(\lambda_1)\,]}{Lw(\lambda_2)\, n(\lambda_2)\, [\,1 - q(\lambda_2)\,]}$$

where n = refractive index of water, q = Fresnel reflectivity of the water-air interface causing some Eu to be scattered downwards.

There is advantage in comparing ratios at different wavebands of the ratio of upwelling to downwelling irradiance as it is possible to quantify properties in the water which have differing spectral responses. For example ,the use of the blue/green reflectance ratio gives a measure of the amount of blue light absorbed by phytoplankton in the water and so can be used to quantify phytoplankton biomass.

Robinson (1983) noted that as suspended sediment concentration increased, reflectance became less wavelength dependant (figure 3.11.). The figure also shows an increase in absorption at small wavelengths when concentrations are low. Ritchie (1976) found increasing reflectance toward the longer wavelengths as suspended load increased. Topliss (1986) using upwelling quantum spectral irradiance measurements found similar trends.

Clarke et al (1980) had some success in predicting suspended loads from the ratio of different wavebands of upwelling water leaving radiance in their work in the Gulf of Mexico. Values of r^2 for L440:L550 were - 0.96

Third Party Material excluded from digitised copy.
Please refer to original text to see this material.

Figure 3.11. Typical reflectance spectra for a)Case 1 waters, b) Case 2 waters dominated by suspended sediment, c) Case 2 waters dominated by yellow substance. The dotted curve represents the reflectance spectra for clear blue water. (from Robinson,1983)

Third Party Material excluded from digitised copy.
Please refer to original text to see this material.

Figure 3.12. Variation of $d\Sigma/dR(550nm)\%$ with Σ_o, where Σ is SPM concentration, R is irradiance (550nm), Σ_o is organic SPM concentration (mgl^{-1}). Samples are from west coast waters of the U.K.(X),Meditteranean waters (o). Vertical bars represent standard errors, with the number of points and coefficients of determination (r^2) given by upper and lower bracketed numbers, respectively.(from Simpson and Brown (1987).

(s.d.=0.20 log units mg/l,d.f.=137); for L440:L520 r^2 was -0.97 (s.d.=0.17 log units mg/l,d.f.=137).

Landsat images have been used with success to predict suspended sediment concentrations, where the suspended load is high (Bukata,(1981), Ritchie et al (1976)). Landsat has a coarse spectral bandwidth of 100 nm. This means that it cannot be used in the analysis of spectrally varying constituents in the sea using colour ratios (Robinson,(1983).

Amos and Topliss (1985) found that reflectance ratios from Landsat imagery were not satisfactory in predicting concentrations of suspended sediment due to the spectral shift in spectral response with increasing loads. They found the CZCS sensor, with bandwidths of 20 nm to give high coefficients of determination (r^2 = 0.92;n=10) for suspended sediment concentrations from the ratios of 560nm:750 nm. They found that as the concentration of chlorophyll increased in the water, the relationship between reflectance ratios and suspended sediment deteriorated.

Simpson and Brown (1987) in their study in the Irish Sea , found generally a poor fit between SPM and reflectance (550nm). They used a multispectral irradiance meter, with sensors of similar

bandwidth as the CZCS. They noted a linear relationship between the ratio of SPM concentration and reflectance plotted against organic SPM. This suggested that as the organic load increased, reflectance decreased, with the increase in absorption by the organic material. This is shown in figure 3.12.

A universal algorithm for predicting SPM concentrations from airborne visible band sensors has not yet emerged. The difficulty may be due to the differences in the absorbance and scatterance of the different components of the SPM. The problem of interpreting remotely sensed imagery is further hampered by the absorption and scatterance of aerosols in the atmosphere. These may vary spatially and seasonally.

3.4. Conclusion

The discussion in this chapter indicates that the beam transmissometer can be used effectively to quantify SPM concentrations, but that the accuracy of the measurement may be modified by variations in the composition of the SPM. Passive optical measurements have provided a quantitative measure of chlorophyll concentrations but so far have had limited success in Case 2 waters. Case 2 waters are those with gelbstoff or with sediments which do not contain chlorophyll. Case 1 waters are dominated by phytoplankton and their degradation products.

The waters of the Irish Sea can be described as Case 2 water (Robinson, 1983) in which suspended sediment is the dominant optical component. The transmissometer is a suitable instrument for the determination of SPM concentrations. However the optical characteristics of the dissolved organic material and the SPM must be considered.

In order to minimise the absorption of light by 'gelbstoff' a transmissometer with a red light source (660 nm ± 11nm) can be used to make routine measurements of attenuation solely by particles in the light path of the instrument.

However, it will be necessary to assess the particle size distribution, relative refractive indices and pigment composition. Therefore, in addition to taking water samples for gravimetric analysis to measure the concentration of the SPM, measurements of the size distribution, the change in the ratio between the organic and inorganic fraction, and the change in the concentration of red light absorbing pigments should be made. It would also be useful to determine the variability in the shapes of the particles.

CHAPTER 4 INSTRUMENTATION AND LABORATORY MEASUREMENTS

4.1. Introduction

This chapter describes the UCNW profiling transmissometer, its stability and its deployment while interfaced with the profiling CTD. An account of the mooring design follows and of the deployment of the transmissometers and the recording current meters.

The methods for the measurements required to calibrate the transmissometer in terms of SPM concentration are described and an assessment of this relationship follows. The main causes of the variance in the relationship is examined from an analysis of the measurements of the proportion of organic material in the SPM, the chlorophyll concentration and the particle size distribution.

4.2. The Beam Transmissometer.

4.2.1. The design of the instrument.

The beam transmissometer measures the attenuation of a collimated beam of light through a fixed pathlength of water. The light from the source,Io, passes through the water and after scattering and absorbance by the water and its components, the attenuated light,I, is detected by the photocell. As in equation (5) in Chapter 3.1.2,

beam attenuation is given by

$$c = \frac{1}{r} \ln \frac{Io}{I}$$

It is important that the beam of light is collimated, so that the only loss in intensity from the light source to the detector is that caused by the scattering and absorbance of the water and its constituents.

Two versions of the transmissometers were designed and built at UCNW. The first,which was interfaced with the Plessey 9400 CTD, was constructed of anodised aluminium, and had a pathlength through the water of 0.3m. The second design, which was interfaced with Aanderaa thermistor loggers , had a pressure housing made of black acetyl, with rods connecting the light source and detector units made from the same material. Plastic was used where possible, to minimise corrosion. The facing plates were made of stainless steel to increase rigidity. The beam pathlength was 0.25m. The detector and light source units were constructed from black anodised aluminium. The surfaces exposed to sea water, close to the light beam, were painted with anti-fouling paint to minimise algal growth on or near the windows, which could obscure the light path. The remotely operated instrument is shown in Figure 4.1.

Figure 4.1. The UCNW transmissometer interfaced with an Aanderaa thermistor logger.


169

The detector and optical assembly units were of the same design for both instruments. This is shown in Figure 4.2. Lenses were used to focus the light. Threaded lens holders were made to fit inside the detector and light source units so that the relative position of the lenses and the detector and the light source could be adjusted. The width of the light beam was 20mm.

The light source was a red light emmitting diode (RS,Sweet-spot,301-915). The spectral peak was 665 ±11nm. This was chosen to minimise the signal from the absorbance of dissolved organic substances in the sea water.

The photocell was a silicon diode (RS,308-067) with an integrated amplifier and an active area of 5mm , and a spectral range of 300-1100nm.

The function of the beam transmissometer is to measure absorbed and scattered light.Because most scattering by natural waters is at small angles to the light beam, it is necessary to minimise the acceptance angle of the detector to avoid significant scattering remaining within the light beam. Failure to reduce the acceptance angle of the light beam would result in the underestimation of attenuation.

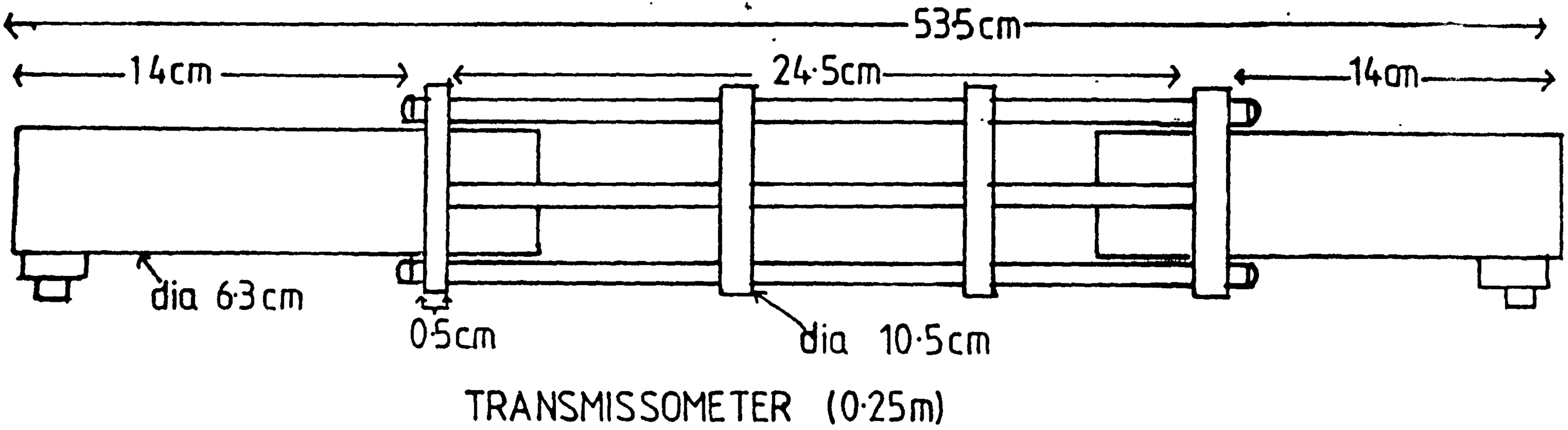

Figure 4.2. Drawing of UCNW transmissometer, showing the dimensions.

The half angle of acceptance, θ, is defined by

$$\tan\theta = r / f$$

where r=aperture radius, f=focal length. Figure 4.3. shows the acceptance angle. As r= 0.325mm, and f= 46.5mm, the half angle of acceptance is = 0.40^{o} . For ocean water, about 5% total scattering occurs in the interval $0^{o} - 1^{o}$. This gives a positive error of 3% for attenuation (Jerlov,1968).

The light beam was optically aligned after the instrument was assembled. The collimation of the light beam was checked throughout the experimental work. It was found unneccessary to readjust the alignment of the light beam.

4.2.2. Setting up procedure.

The windows of the transmissometer were cleaned using optical cleaner and lens cleaning tissues. The windows of the instrument interfaced with the CTD was cleaned daily, whereas those of the self-logging instrument were cleaned before the deployment. A cover was placed around the instrument to prevent ambient light entering the detector unit. A reading was taken of the frequency of the output,(A). The light source was then covered and another reading was taken,(B). This was the lower limit frequency, otherwise known as the dark reading.

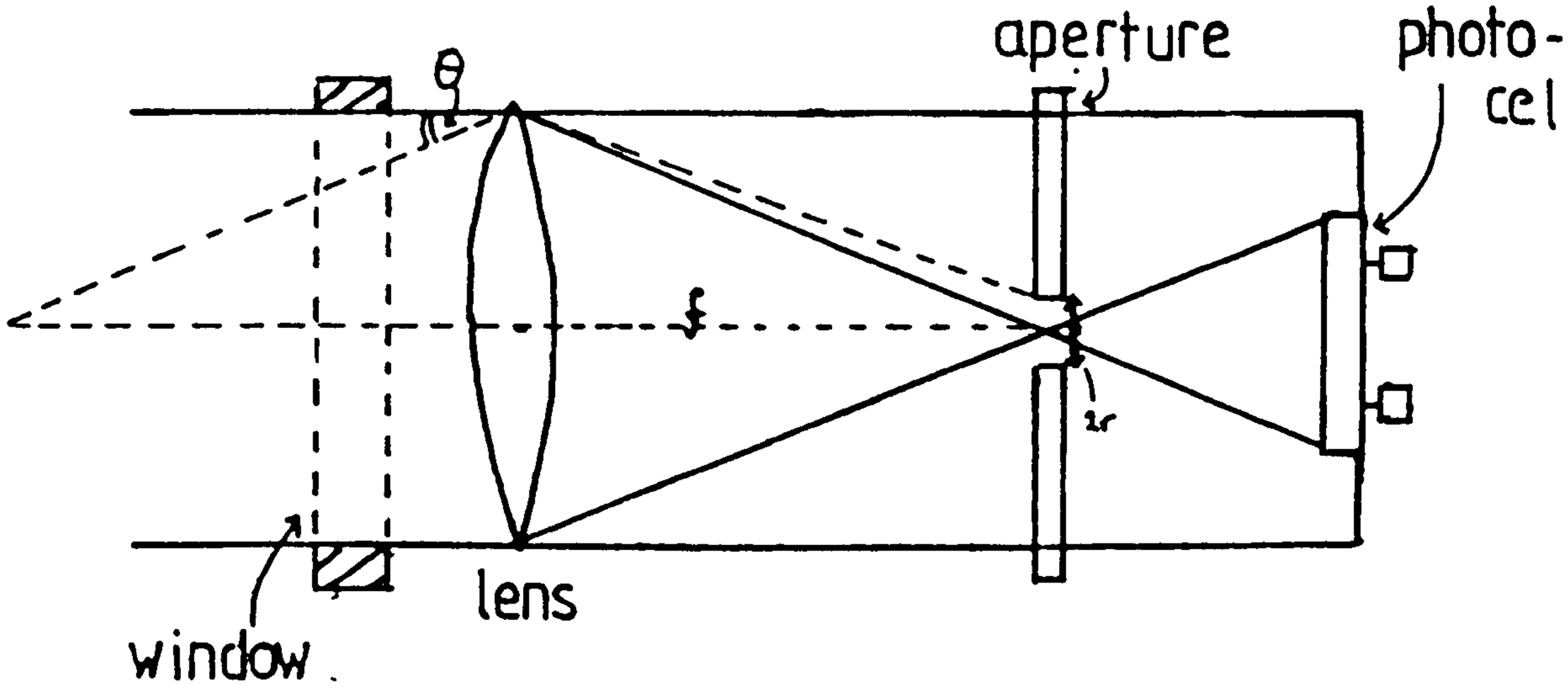

Figure 4.3. The angle of acceptance (2θ) is given by $\tan\theta = r/f$.
For the UCNW transmissometer 2r is 0.75mm, f is 46.5mm, therefore 2θ is 0.8°.

The incident light was given by

$$Io = A - B.$$

Io was entered into the CTD software, and noted for the self-logging instruments. Attenuation was calculated by

$$c = \frac{1}{r} \ln \frac{A-B}{M}$$

where M is the measured transmisttance, r = 0.3m.

4.2.3. Stability of the transmissometer.

1. Temperature stability.

Bishop (1986) noted that transmissometers are sensitive to changes in temperature, due to the time lag in response by the detector and electronic circuitry to the ambient temperature of the water. A temperature calibration was carried out for the two transmissometer designs. Figure 4.4.shows transmittance (%) plotted against T(^{o}C) for both designs.

A regression analysis showed that a difference of 1^{o} C caused a variation of transmittance of 0.5%. Surface to bottom temperature differences were 3^{o}C . The maximum error in transmittance was 1.5% .The calibration for temperature stability is shown in Table 2.

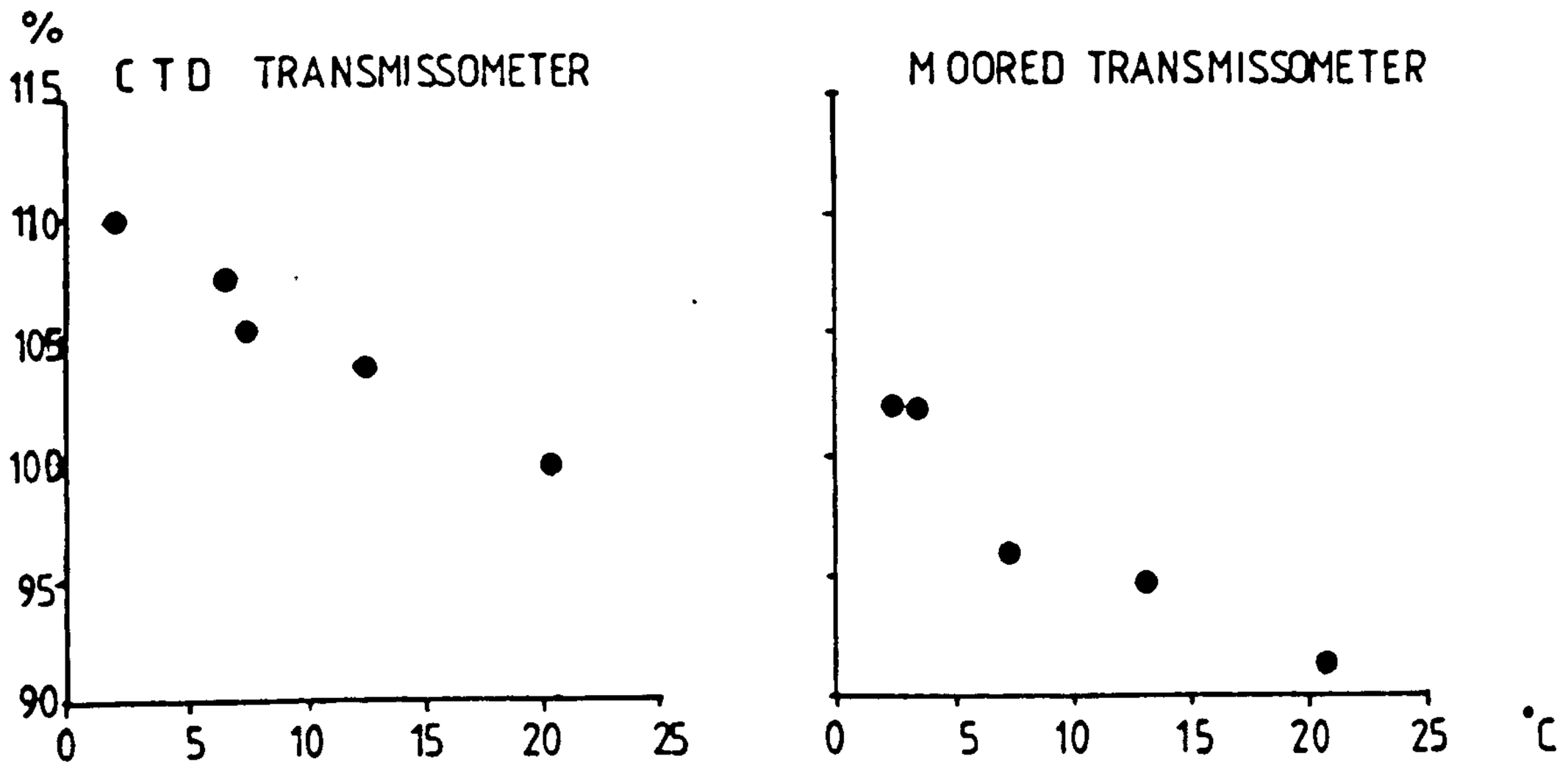

Figure 4.4., Temperature calibration curves for a) the transmissometer interfaced to the CTD, and b) the transmissometer interfaced to the Aanderaa loggers. Transmittance (%) in air is plotted against temperature (°C).

TABLE 2 - TEMPERATURE STABILITY

The regression is of the form

Transmittance(%)= n + Temperature (^{o}C) * p.

Instrument	constant(n)	slope(p)	r^2(%)	d.f.
Transmiss. CTD	111.0	0.531	95.1	4
Trans. Self logging	103.0	0.585	83.5	4

Therefore a change of 1^{o} C = a change of 0.5% transmittance.

2. Long Term Stability.

The transmissometer was set up in self-logging mode in a temperature controlled room (9°C) from 18th April to 19th May 1988,logging transmittance at 30 minute intervals.

Small fluctuations were noted in the readings and an assessment of the variance from the mean was calculated. This was 0.6% of the full beam measurement of transmittance in air, and 0.4% of the dark reading in one month. The results are tabulated in Table 3.

4.3. The CTD.

A CTD manufactured by Plessey Environmental Systems, model 9400, was used for measuring vertical profiles of measurements of depth, temperature,conductivity and transmittance. The CTD consists of a sea unit ,in which the properties are converted into electrical signals. The transmissometer, made at UCNW, was interfaced with the CTD, using the free channel, usually occupied by an oxygen sensor. Data were logged onto floppy discs by a BBC micro computer, using software developed at UCNW.

Temperature was measured by a platinum resistance sensor, conductivity by an inductively coupled toroidal sensor and pressure by a bonded strain

TABLE 3 INSTRUMENT DRIFT OVER 1 MONTH

Light beam	average reading	reading drift	% Transm.
on (100%)	1002.0	6.20	0.6
off (0%)	24.9	4.48	0.4

gauge transducer. Table 4 shows the specifications of the pressure, temperature and conductivity sensors. Each sensor is incorporated in a wheatsone bridge . Changes in the properties of the sea cause variations in the bridge output voltages, which are proportional to physical change.

The transmissometer has been described in section 2. The alterations to enable transmittance measurements to be made required that a DC to DC converter should produce a regulated current of 10 milliamperes to the LED from the 24V CTD supply. The 12V supply to the photodiode amplifier was taken from the input voltage. The voltage from the photocell was passed through a voltage to frequency converter along with the voltages from the pressure, temperature and conductivity sensors, in a mixer unit in the sea unit. Each channel was allotted a different frequency range and the resulting F.M. signals were transmitted to a deck unit on board the ship by a single conductor cable, which also supplied power to the probe. In the deck unit, the four signals were separated into their original constituents, converted to voltages and digitised.

At each station the bottom depth was recorded from the ship board sonar. A downward and upward profile was

TABLE 4 SPECIFICATIONS OF CTD SENSORS

	Conductivity	Temperature	Depth
Range	0 to 60 mmho/cm	-2 to 35°C	600m
Accuracy	0.03 mmho/cm	0.02 °C	0.25% or 1.5m
Resolution	0.0001mmho/cm	0.0001 °C	0.0002% or 0.0012m
Time constant	0.1 sec	0.35 sec	0.1 sec

The accuracies in the table are the manufacturer's claimed accuracies. Sea calibrations from this study conform with these claims.(see table 5)

logged and a real time profile of the physical properties was displayed on the VDU. Water samples were taken on the upward cast to calibrate the CTD. Water samples were also taken to calibrate the transmissometer by converting attenuation units to SPM units.

A rosette multisampler was attached to the cable,0.5m above the CTD. It was triggered from the deck unit. On alternate casts a calibration water bottle was mounted on the multisampler. This had two reversing thermometers attached to it. The calibration cast was made alternately near surface and near bottom in order to obtain as wide a range as possible in temperature and conductivity values. The surface depth reading was checked regularly for any drift.

Calibration procedure.

When the calibration bottle was triggered, the CTD depth, conductivity and temperature were noted in the cruise log. The in-situ temperature was calculated from the reversing thermometer measurements, and the conductivity ratio of the water samples were measured after the cruise using a Plessey bench salinometer. Conductivity was calculated from the formula in Unesco (1981).

The calibration constants for temperature,To, and conductivity,Ko, were calculated.

$$To = \overline{Tb - Tc}$$

$$\text{and} \quad K = \overline{Cb / Cc}$$

where Tc,Cc are the CTD values of temperature and conductivity; and Tb,Cb are the calibration water bottle values of temperature and conductivity. $\overline{Tb-Tc}$ is the mean of the differences between Tb and Tc; $\overline{Cb/Cc}$ is the mean of the ratios of Cb and Cc.

Table 5 shows the calibration constants To and K for the cruises made during this study.

Data processing.

The CTD data was transferred to the VAX mainframe computer at Bangor. The temperature and conductivity constants were calculated for each cruise.The CTD analysis program consisted of the following procedures.

1. CTD temperature and conductivity were calibrated.
2. Practical salinity was determined using corrected CTD temperature and conductivity.
3. Density (σt) was calculated according to the

TABLE 5 CTD CALIBRATION CONSTANTS

Cruise	Date	To	s.d.	K	s.d.	N
48	30.6.-4.7.86	-0.0355	0.0794	1.0021	0.0065	16
50	4-6.8.86	0.0185	0.0021	1.0021	0.0065	3*
51	22-25.9.86	0.047	0.035	0.9966	0.0044	14
52	11-22.11.86	0.042	0.013	0.9966	0.0044	5*
53	30.3-4.4.87	0.1247+	0.172	0.9955	0.0089	20
55	11-15.5.87	0.0522	0.0231	0.9980	0.0010	12
56	29.6-3.7.87	0.0823	0.048	0.9984	0.0047	14
57	3-7.8.87	0.037	0.017	0.9961	0.0061	12
58	7-11.9.87	0.030	0.005	0.9987	0.0018	7
59	12-16.10.87	0.0261	0.031	0.9974	0.0061	7

* = There was not enough data taken during this cruise to calibrate the CTD, therefore the constants from the previous cruise were used.

+ = There were large errors in the replicate readings from the thermometers, therefore the constants from the previous cruise were used.

international equation of the state of sea-water (Unesco,1981).

4. Beam attenuation was calculated.

5. The data were averaged to give mean values of the parameters for each metre of depth. The data were edited to remove erroneous values, such as measurements made during the triggering of the multi-sampler.

4.4. The Mooring.

4.4.1. Introduction.

The mooring was deployed in mixed water, 75m in depth, off the north west coast of Anglesey. Figure 4.5. shows the location (point X). Table 6 shows the details of the deployments which were at approximately the same positions (± 2km).

The design of the mooring is shown in Figure 4.6. A transmissometer and a recording current meter were attached within 0.5m of each other at two depths, one at 20m below the surface and one at 1.0 m above the sea-bed.

The parameters that were logged were transmittance, current speed and direction, and pressure. The logging interval was 30 minutes.

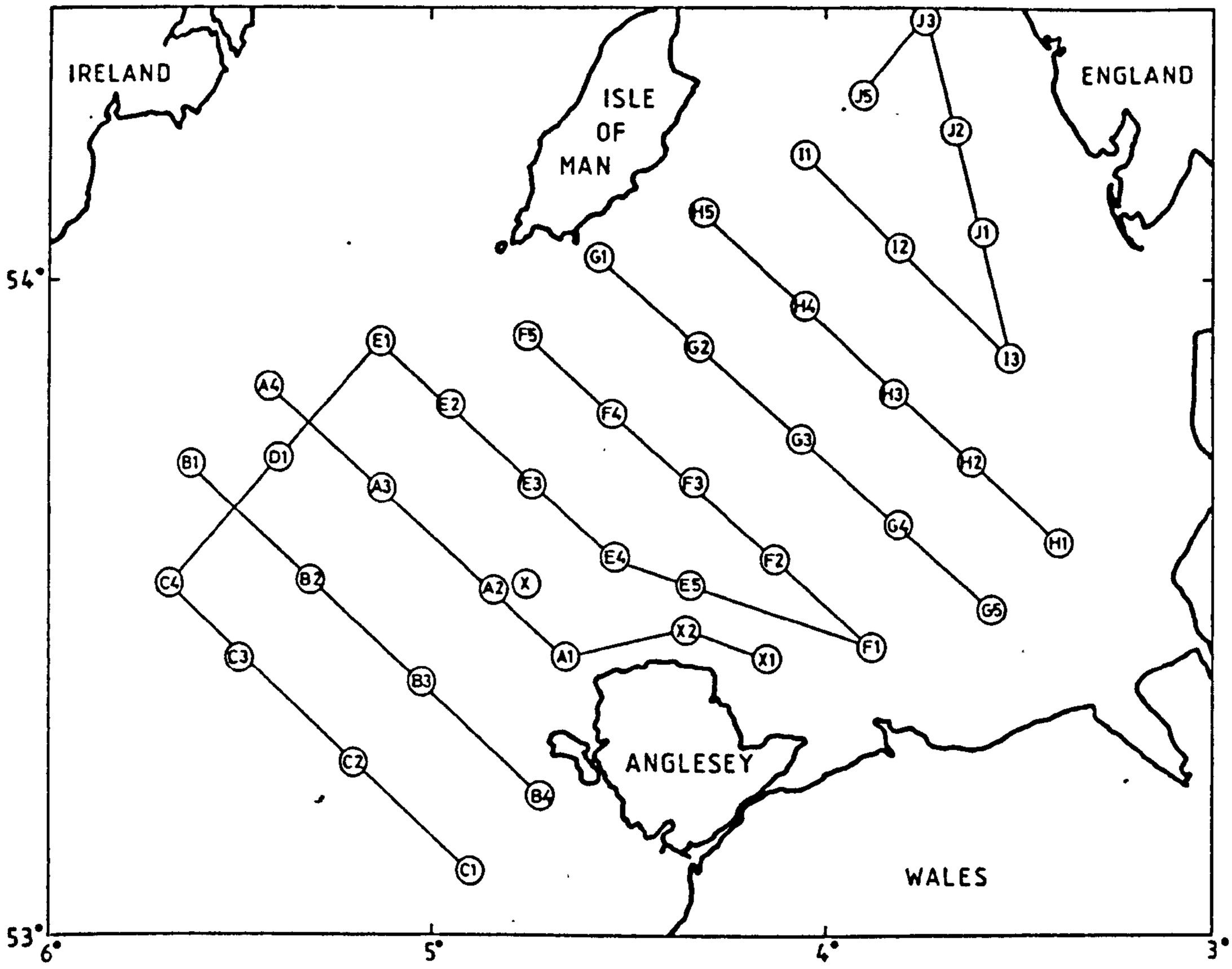

Figure 4.5. Grid of stations for vertical profiles of CTD measurements, in 1987. Station X is the location of the mooring, in 75 m water depth.

TABLE 6 MOORING POSITIONS IN 1987

Depl.	Water depth (m)	Duration Time (GMT)	Date	Lat.	Long.	Depth(m) RCM	Depth(m) TRANS
1	82.0	1130	6.4.87	53° 33.3'	4° 46.6'	26.0	27.0
		to				75.0	76.0
		1620	12.5.87				
2	77.0	1730	28.5.87	53° 32.71'	4° 47.85'	17.0	18.0
		to				75.0	76.0
		2230	29.6.87				
3	77.0	1900	29.6.87	53° 32.91'	4° 47.3'	21.0	22.0
		to				75.0	76.0
		1130	4.8.87				
4	77.0	1100	3.8.87	53° 32.72'	4° 48.48'	20.0	19.0
		to				75.0	76.0
		0630	8.9.87				
5	77.0	0600	8.9.87	53° 32.69'	4° 48.86'	22.0	21.0
		to				75.0	76.0
		1630	12.10.87				

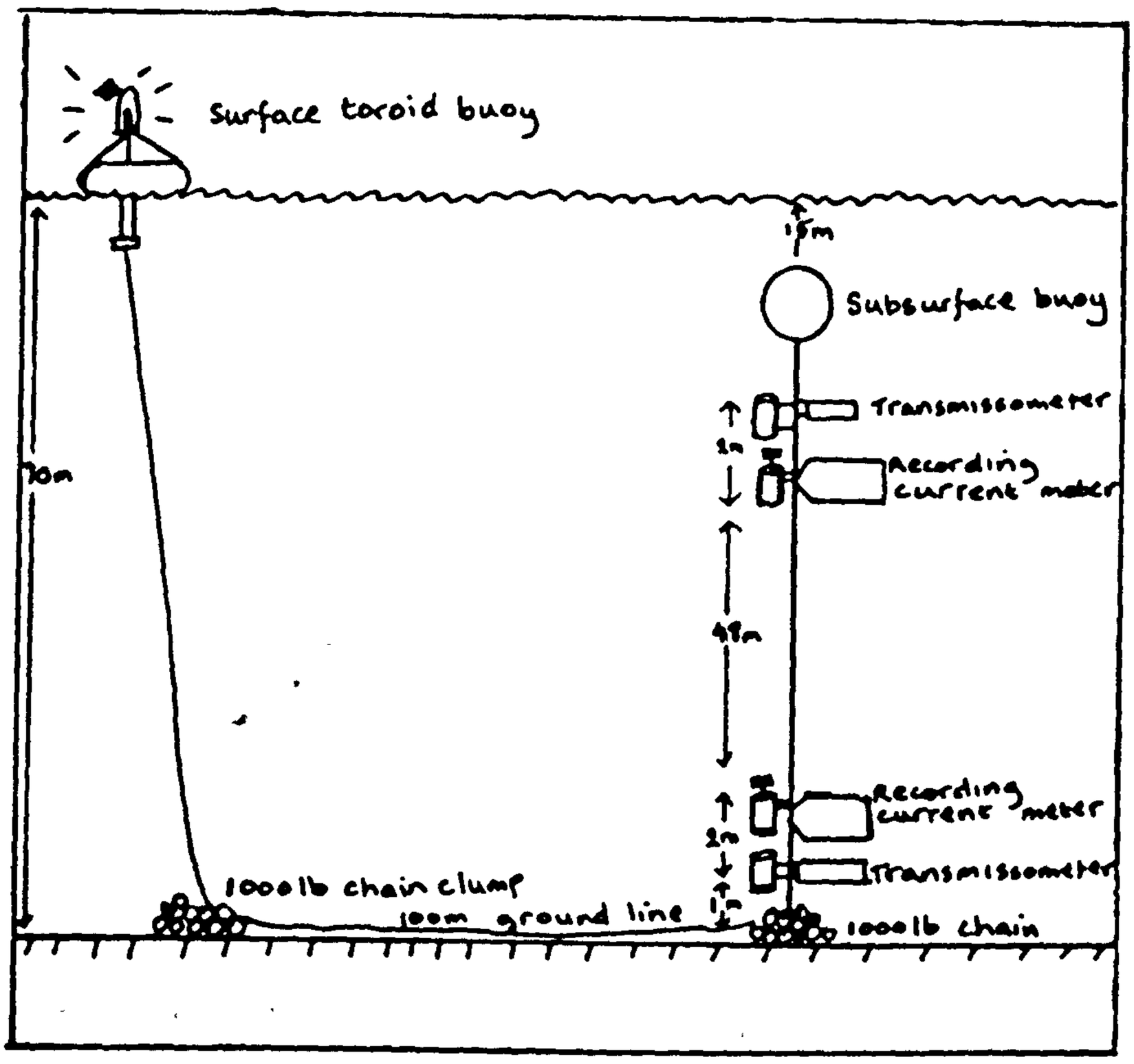

Figure 4.6. The design of the mooring. Instruments were deployed in pairs, a transmissometer and a current meter, as shown in the diagram.

4.4.2. The transmissometer.

The design of the transmissometer is described in 4.2.1. In order to determine the effect of ambient daylight entering the instrument, and the drift in the dark response, a facility was incorporated to switch the light beam off for part of the series of measurements. An Aanderaa thermistor logger was used to log the output from the transmissometer. A nine volt battery was used as the power supply. A regulated -6V DC was passed to a programmable current source, taking 2 mA to drive the LED. In series with the LED there was a switch circuit. This was driven from a timer circuit which was activated when the the LED was switched on. The Aanderaa loggers make a series of 12 measurements. These are refered to as channels 1 to 12 in the text. During the first six measurements, the LED was switched on, and during the last six the LED was switched off.

The photodiode was connected across a -6V supply. The DC offset voltage was used to set the dark current so that when the LED was switched off the voltage signal was 2.25V, referenced to the -6V rail.

The logger employs a bridge balancing system to record the signal from the transmissometer.The voltage required to balance the bridge is recorded into binary by means of an encoder, and then recorded onto magnetic tape. A built-in quartz clock triggered the measuring cycle at regular intervals.

Before deployment, the instruments were set up as described in 4.2.2., and switched on. Several sets of readings were taken using a direct readout unit. Beam attenuation was calculated as follows:

Channels 2 - 6 = Transmittance in air $= [[\Sigma Ix]/5] = I_L$

Channels 7 - 12 = Dark value (0%) $= [[\Sigma Iz]/6] = I_D$

were x = channels 2 to 5, and z = channels 7 to 12.

100% Transmittance in air, I_o

$= (I_L - I_D)$

and beam attenuation, where I = reading in water

$$c = 1/r \cdot \ln [[(((\Sigma Ix)/5) - (((\Sigma Iz)/6))] / I_o]$$

Intercalibration of transmissometers.

In order to ensure that there was no loss of signal from the transmissometer during deployment from fouling of the optical windows by algae, a series of measurements were made at the end of each deployment before and after the windows were cleaned. There was no loss of signal from fouling.

There was not always a complete record of beam transmittance for each deployment. This was due either to battery failure in the logger or to the entanglement of the tape. However all but one of the time series presented in this thesis were complete records. Different instruments were used for the deployments. In order to achieve a coherent time series, the moored transmissometer measurements were normalised to the transmissometer on the CTD. This was done by attaching the moored instruments to the CTD frame at the beginning and at the end of each deployment and aqcuiring a set of simultaneous measurements from both instruments. A correction factor for each deployment was calculated, so that all measurements were normalised to the CTD transmissometer. The standard deviation of the correction factor was $0.2m^{-1}$.

Data processing

The data on the magnetic tapes were read onto the Vax mainframe computer, using an Aanderaa tape reader. Beam attenuation was calculated as shown above. The data were then plotted as a time series for each depth.

4.4.3. Aanderaa recording current meters.

The RCM's , model no. 4, had sensors to measure current speed and direction, depth and temperature and conductivity. The last two parameters were not processed. The instruments were set to record at the same time as the transmissometers, at 30 minute intervals.

Six values were recorded onto tape, the first was a reference number used to identify tapes. Pressure was measured by a potentiometer driven by a bourdon tube. As the instrument aligned itself with the current ,the direction was measured by the orientation of the instrument by means of a magnetic compass in the recording unit. Current speed was sensed by a rotor at the top of the recording unit. Each revolution of the rotor was transferred magnetically to the inside of the recording unit and a counter counted the number of revolutions in a sampling interval. Table 7 shows the specifications of the sensors and the instrument. The near sea-bed sensors were the Savonius, or paddle rotor. Those at 20m were the "straight-face" rotor type.

Calibration and data processing.

Speed.

It was assumed that the manufacturers constants were correct.

$$\text{Speed} = a + (b * N)$$

where N = no. of revolutions in a sampling period.

$$a = 1.5 / 100 \text{ ms}^{-1} \text{ (Manufacturers specifications)}$$

$$b = 42 * \left[\frac{\text{revolutions per count}}{\text{no. of seconds in sampling interval}} \right] / 100 \ (\text{ms}^{-1})$$

TABLE 7 SPECIFICATIONS FOR AANDERAA R.C.M. SENSORS

Parameter	Range	Accuracy	Resolution
Pressure	0 - 100 p.s.i	1% of range	0.1% of range
Current direction	0^{o} - 360^{o}	7.5 for speed 2.5 - 5 cm/s or 100-200cm/s. 5 for speed 5 - 100 cm/s	0.35
Current speed	2.5 - 250 cm/s	1 cm/s, or 2% of speed	

Direction.

Calibrations were supplied for each compass, with the instrument , from NERC RVS at Barry. An assessment was made of the linearity of the relationship between compass direction and the output values from the compass sensors. These are tabulated in table 8.The regression gave r^2 values of 99% and so the regression coefficients were used as the constants a and b where

$$\text{Direction} = a + (b * N)$$

where a = regression constant, b = slope, N = encoded reading from RCM.

Pressure.

In order to ensure that the wire to which the instruments were attached had remained vertical in the water during each deployment, the pressure data was processed. Calibration was supplied by RVS for each instrument, and a regression was calculated, as for the direction calibration.The calibration constants were used to calculate pressure where

$$\text{Pressure} = a + (b * N)$$

TABLE 8 PRESSURE AND DIRECTION CALIBRATIONS FOR RECORDING CURRENT METERS

Depl.	Depth (m)	Meter no.	Direction const	Direction slope	Pressure const	Pressure slope
1	21	6753	2.71	0.348	-4.54	0.0740
3	22					
5	26					
1	75	3311	4.65	0.346	-4.88	0.0760
3	75					
5	75					
2	17	5229	3.14	0.349	-3.43	0.0736
4	20					
2	75	5912	-0.07	0.355	-5.51	0.0774
4	75					

Current meter data was processed as described, to produce files listing pressure ,speed, direction, east velocity and north velocity.

East velocity = Speed * sin (Direction * 2π / 360)

North " = " " cos (" " ")

4.5. Laboratory measurements.

4.5.1. Introduction.

The purpose of this section is to quantify the relationship between beam attenuation and the concentration of SPM, and, if possible, to calculate a predictive algorithm for SPM concentration using measurements of c. Since c (at 660 nm) is proportional to the absorbance and scatterance of particles in the light beam, it is important to establish how much the absorbing and scattering properties of the particles influence the relationship between c and SPM concentration. The important light absorbing and scattering properties of particles are particle size, refractive index and pigment composition, discussed in Chapter 3.

Water samples were taken by means of the rosette multi-sampler at 5m below the sea-surface and from 5 to 10 metres above the sea-bed, during vertical deployments of

the CTD and beam transmissometer. This provided parallel measurements of beam attenuation and SPM concentration, since the rosette multisampler was immediately above the CTD and transmissometer. The concentration of SPM was calculated as the weight of the dried solid material per unit volume of sea-water. The analysis of the relationship between c and SPM concentration follows in section 4.5.2.

An assessment of the variation in the refractive indices of the SPM was achieved by examining the proportion of organic and inorganic SPM. It was considered important to quantify the absorbance of the light beam by chlorophyll as there is a spectral absorbance peak at 670 nm and the wavelength of the transmissometer light source was 660 nm (± 11nm). Since light scattering is dependant on particle size, for particles under 3 μm, it was necessary to examine the particle size distribution. Additional information about the size and nature of the particles was acquired by microscopic analysis.

The measurement of SPM concentration by gravimetric means and of chlorophyll concentration by fluorometry are discussed in section 4.5.2. The results are discussed in section 4.5.3. Section 4.5.4. gives an account of the methods for particle size distribution

analysis, scanning electron microscope techniques and analysis and includes a discussion of the results. An assessment of the use of the transmissometer to measure SPM concentrations follows in section 4.5.5.

4.5.2. Measurement of SPM and Chloropyll concentrations

4.5.2.1.Total SPM (TS), inorganic SPM (IS), and organic SPM (OS).

Total SPM concentration (TS) were measured by the method described in Strickland and Parsons (1972). Whatman GF/C glass filter papers were used, which have a retention capacity for particles greater than 1.2 μm. During each cruise a number of replicate samples were taken from the same cast in order to quantify the precision of the measurement used. Replicates were also taken using GF/F filter papers, with a retention capacity of).7 μm, in order to assess the percentage loss of particles in the range of 0.7 to 1.2 μm.

The filter papers were numbered with a ball-point pen and then washed with distilled water to remove loose fibres. They were dried in an oven at 90.0^{o} C and stored in a desiccator. They were then weighed on a Mettier balance, which was accurate to 10^{-6} g. The weighing chamber was supplied with fresh desiccant regularly to minimise the absorbance of moisture by the filter papers, after their removal from the desiccator.

At sea a known volume of water was filtered through a numbered filter paper. The volume was typically 2 to 4 litres, but depended on the concentration of SPM in the water. The filter paper was washed with 20ml of distilled water to remove salts, wrapped loosely in aluminium foil, labelled and freeze-dried. In order to quantify the handling error, every 10th filter paper was processed in the same way but sea- water was not filtered through it.

At the laboratory, the filter papers were unfrozen, dried for 12 hours at 90.0° C, and cooled in a dessicator. They were weighed on the same balance as was used in the preparation of the filter papers. This gave the value of the total SPM concentration per volume of sea- water filtered (TS). The filter papers were then placed in a muffle furnace set at 550° C for 12 hours to oxidise the organic fraction. This was expected to remove the carbon compounds, but may leave some skeletal material. The filter papers were cooled in the dessicator and weighed on the same balance as before. This gave the weight of inorganic SPM concentration per volume of sea-water filtered.

Blanks were processed in the same way. After the drying process, the mean blank value for each cruise was

calculated, giving the handling correction, X. After the ashing process, the mean blank value was calculated, to give the ashing correction, Y.

The concentration of total SPM per unit volume of sea-water is given by

$$TS = \frac{W_2 - W_i - X}{V}$$

$$X = (W_{2b} - W_{ib})$$

where W_i = filter paper weight; W_2 = weight after drying; X = handling correction; V = volume of water filtered; b = blank.

The concentration of the inorganic SPM per unit volume of sea-water is given by

$$IS = \frac{W_3 - W_i * Y}{V}$$

$$Y = \frac{W_{3b}}{W_{2b}}$$

where W_3 = weight after ashing; Y = ashing correction.

Table 9 gives the values for X and Y for the cruises in 1986 and 1987, for both GF/C and GF/F filter papers.

TABLE 9 a) HANDLING (X) AND ASHING (Y) CORRECTIONS FOR GF/C FILTER PAPERS.

Cruise	Date	X (mg)	s.d.	Y	s.d	N
48	30.6-4.7.86	1.0225	1.0007	0.989	0.280	13
50	4-6.8.86	1.0225	1.0007	0.989	0.280	13
51	22-25.9.86	1.0225	1.0007	0.989	0.280	13
52	18-22.11.86	1.023	1.0007	0.989	0.280	13
53	30.3-4.4.87	2.015	0.898	0.983	0.680	11
55	11-15.5.87	2.015	0.898	0.983	0.680	11
56	29.6-3.7.87	0.395	0.600	0.986	0.266	11
57	3-7.8.87	0.944	0.586	0.986	0.008	16
59	12-16.10.87	2.722	1.327	0.974	0.667	14

b) HANDLING (X) AND ASHING (Y) CORRECTION FOR GF/F FILTER PAPERS.

56	29.6-3.7.87	2.923	1.101	0.973	0.112	11
57	3-7.8.87	2.415	0.687	0.979	0.005	16
59	12-16.10.87	1.8	1.77	0.980	0.561	4

N = number of samples.

The results from the comparison of replicate GF/C filtered water from the same casts gave the following values:

Standard deviation TS = 1.828 mgl^{-1}

" " IS = 1.315 "

" " OS = 1.286 "

The comparison between the retention of solids on the GF/C and the GF/F filter papers showed that the GF/F filters retained an average of 35.1% more SPM than the GF/C filters (s.d.=28.2%).

This suggests that the use of GF/C filter papers may cause the underestimation of SPM by at least a third, but the fluctuation in the relationship between GF/C and GF/F filter papers does not indicate that this can be corrected confidently by the use of CF/F filter papers. In addition , the filtering of sea-water through GF/F filter papers is extremely slow, and clogging of the filters frequently occurs. The use of GF/F filter papers is not recommended. Careful consideration was applied to the best choice of filter paper to use for the gravimetric analysis. Nuclepore or millipore filters were favoured because they were considered to be more reliable in terms of pore size and weight. Their weight was small compared to that of the SPM filtered in the samples and so the signal to noise ratio was small.

However their use was rejected due to the expense of the filters and in the difficulty of ashing the samples to determine the inorganic fraction of the SPM.

4.5.2.2. Chlorophyll

Chlorophyll-a was measured by the fluorometric method described by Strickland and Parsons (1972) and Tett (1987). A known volume of sea-water (typically 100-200ml) was filtered through a Whatman GF/C 4.7cm filter paper. The filter paper was wrapped loosely in foil and immediatly freeze-dried. At the laboratory the filter paper was placed, still frozen, in a centrifuge tube and 10ml of buffered 90% analar acetone was added to extract the pigment into solution. The samples were stored at 10 °C for a minimum of 10 and a maximum of 72 hours. They were then centrifuged, shaken by hand, and centrifuged again in order to separate the particles from the solution. The extract was poured into a cuvette and the fluorescance was measured on a Turner Model 10 fluorometer. The fluorometer illuminates the extracted chlorophyll with blue light which excites it and causes it to fluoresce. The intensity of the fluorescance is proportional to the concentration of chlorophyll in the sample.

The instrument was calibrated before each batch of samples were processed. This was achieved by measuring the optical density of a chlorophyll standard on a spectrophotometer, an SP 500 , at the peak absorbance wavelength. This enabled the concentration of the chlorophyll standard to be calculated. The fluorescence of the same standard, and a series of dilutions, were then determined in order to calculate concentrations of chlorophyll-a per ml per unit fluorometric units.

Chlorophyll-a decays to form phaeopigments, which also fluoresce in response to blue light. In order to quantify the chlorophyll-a concentration, it is necessary to convert all the chlorophyll-a into phaeopigments, by adding dilute hydrochloric acid, and then to measure the fluorescence. The difference between this and the original measurement gives the concentration of chlorophyll-a. The ratio between the two measurements gives an indication of the health of the phytoplankton.

Cuvettes were rinsed four times with 2ml of 90% acetone, to remove traces of previous samples. Blanks were processed every 10th sample in order to quantify any contamination from previous samples.

4.5.3. Comparison of measurements of beam attenuation and total,inorganic and organic SPM, and chlorophyll concentrations.

The coefficient of determination (r^2) of total, inorganic and organic SPM and chlorophyll concentrations and beam attenuation, are shown in Table 10. There is considerable variation in these values, shown for each cruise , covering a period from March to October in 1987. It is evident that the relationship between c and total SPM does not remain constant. This may be because the particle size distribution varies.

Figure 4.7. shows two examples of the relationship between SPM concentrations and c. Figure 4.7.a. shows total SPM concentrations and values of c from April 1987, and Figure 4.7.b. shows inorganic SPM concentrations and values of c from May, 1987. Inorganic SPM is presented from the cruise in May be_cause the proportion of organic material in the SPM was 28% at that time, causing a greater degree of variation in the relationship between SPM and c than during April. In order to assess the accuracy of the measurement of beam attenuation to measure SPM a regression of c on SPM was calculated. The regression line is shown for the two examples in Figure 4.7. This is discussed more fully on page 118.

The highest values of r^2were in April, early July and

TABLE 10 COEFFICIENT OF DETERMINATION (R^2) OF C WITH TOTAL (TS),INORGANIC (IS), ORGANIC (OS) AND CHLOROPYLL (CHL) CONCENTRATIONS.

CRUISE (Date)	C,TS	C,IS	C,OS	C,CHL	TS,OS
53 (30.3.-4.4.87)	0.440	0.462	0.131	0.202	0.992
55 (11-15.5.87)	0.110	0.108	0.068	0.041	0.961
56 29.6.-3.7.87)	0.193	0.160	0.125	0.086	0.716
57 (3-7.8.87)	0.392	0.618	0.000	0.024	0.803
58 (7-11.9.87)	0.129	0.259	0.225	0.071	0.093
59 (12-16.10.87)	0.353	0.311	0.000	0.013	0.906
ALL DATA	0.364	0.443	0.035	0.000	0.946

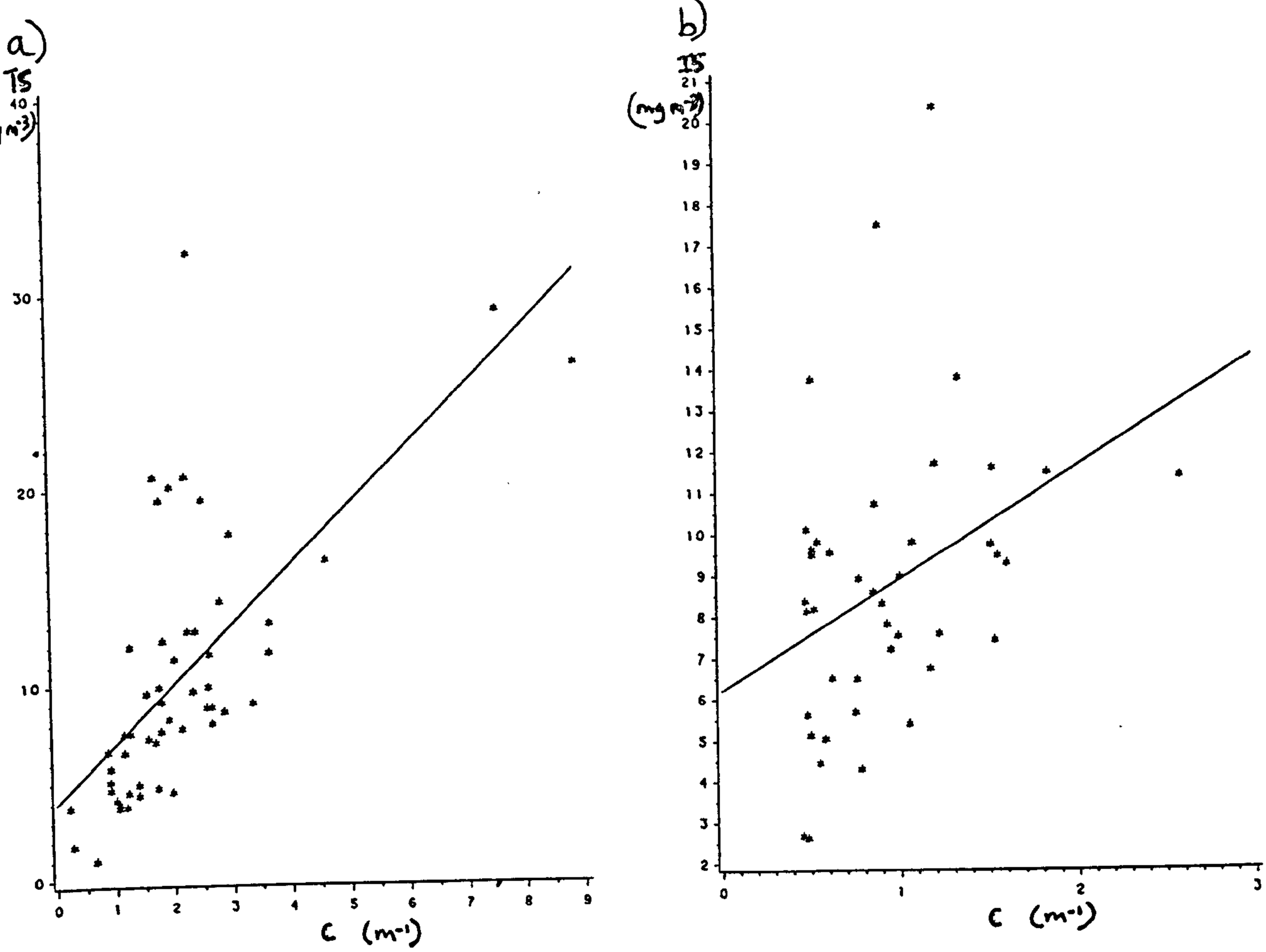

Figure 4.7.
Calibration diagrams for SPM and c.
The diagrams show examples of the relationship between SPM and c during 2 periods in 1987.

a) 30/3/87-4/4/87
Total SPM (mg m^{-3}) is plotted against c (m^{-1}). Water bottle samples were taken at 5m below the sea-surface and at 5m above the sea-bed.

b) 11/5/87-15/5/87
Inorganic SPM (mg m^{-3}) is plotted against c (m^{-1}). Sampling procedure as in (a). Inorganic SPM is presented here as at this time of year the organic component of the SPM was 34%, causing a greater degree of variation in the relationship between SPM and c than at times when the proportion of organic SPM was small. Therefore the ashed samples (inorganic SPM) show a closer relationship to c.

The regression line is included in the figures and the details of the fit of the regression are tabulated in Table 13.a. The graph has been plotted this way, with the Y and X axes as SPM and c respectively (after Joseph, 1955) as the aim of the exercise is to predict the concentration of SPM from c. In other words the concentration of SPM is the dependent variable and c is the independent variable and we want to use the measurements of c to predict the concentration of SPM .

The plots presented here show examples of good and poor relationships between SPM and c. In a) the regression model fits the scattered data reasonably well, but in b) the data is so scattered that the value of the model to predict SPM is limited. Indeed Table 13a shows a standard deviation of 3.3 mg m^{-3}.

TABLE 11 TOTAL, INORGANIC ORGANIC SPM AND CHLOROPHYLL CONCENTRATIONS AND BEAM ATTENUATION AVERAGED FOR EACH CRUISE

CRUISE	c, s.d. (m^{-1})	TS, s.d (mg/l)	IS, s.d. (mg/l)	OS, s.d (mg/l)	CHL, s.d (µg/l)
53	2.13, 1.51	10.37, 6.78	9.63, 5.98	0.83, 1.06	0.75, 0.60
55	0.93, 0.46	12.10, 4.41	8.74, 3.49	3.35, 1.18	5.83, 6.84
56	0.76, 0.52	3.59, 2.43	2.45, 1.76	1.19, 1.76	1.87, 2.60
57	0.56, 0.55	1.51, 1.42	1.12, 1.13	0.39, 0.64	0.68, 0.58
58	0.82, 0.72	6.40, 6.10	6.04, 5.53	0.72, 1.52	0.79, 0.45
59	0.82, 0.28	2.37, 1.34	3.00, 1.26	-0.07, 0.36	0.51, 0.46

October. However in July the mean value of SPM for each cruise was very low (shown in Table 11), and close to the error limits of the measurement method. The handling corrections for the measurement of SPM are discussed in section 2. High values for r^2 in April and October can be attributed to the comparatively low proportion of organic material in the SPM in the spring and autumn (shown in figure 4.8.). It is suggested that values of organic SPM over 20% may contribute to the attenuation of the light beam of the transmissometer. The seasonal chlorophyll maximum was during May, which would indicate a high proportion of organic SPM (Table 11). This may contribute to the attenuation of the light beam.

In order to determine the additive effects to attenuation of the several parameters measured, a multiple regression analysis was calculated with c as the dependant variable and total, inorganic and organic SPM and chlorphyll concentrations as the independant variables. The results, in Table 12, indicate that total and inorganic SPM were the most important determinants of c and that the additive effects of OS and chlorophyll concentration did not improve the ratio of the expected to the unexpected sum of suares (F value).

The data for each cruise were divided according to their

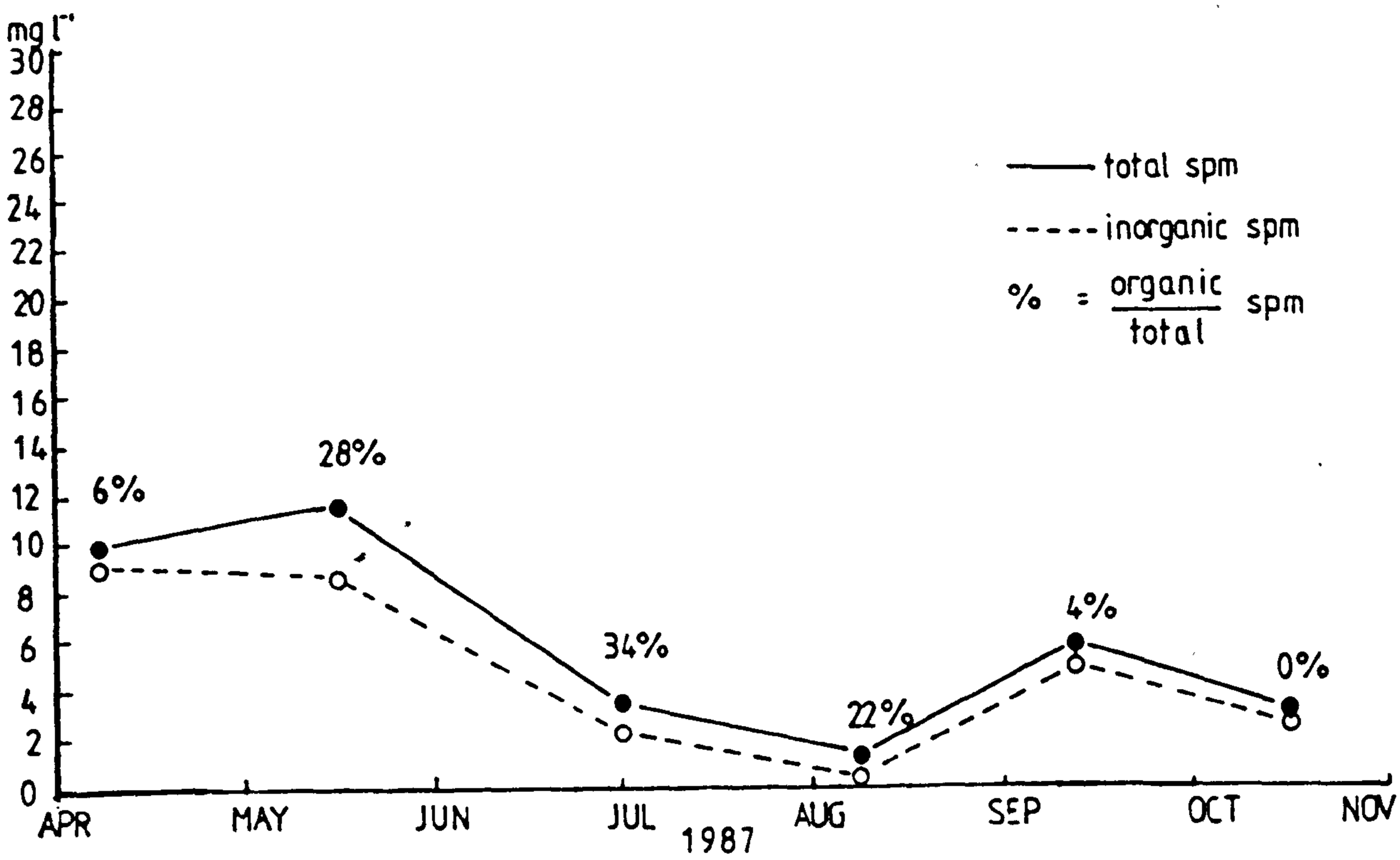

Figure 4.8. Time series (from 1987) of values of total, inorganic concentrations (mgl^{-1}), averaged for each cruise. The percentage of organic material in the total SPM is given for each cruise.

TABLE 12 REGRESSION OF C BY TS,IS: MULTIPLE REGRESSION OF C BY TS,IS AND CHL.

N = number of samples; R^2 = the coefficient of determination, F = the variance distribution; P = the probability of the relationship between the parameters ocurring by chance.

CRUISE	C:PRED	N	R^2	F	P
53	TS	52	0.440	41.9	0.000
"	IS	"	0.462	45.63	0.001*
"	TS,IS,CHL	"	0.483	17.2	0.000
"	TS,CHL	"	0.469	23.98	0.000
"	IS,CHL	"	0.487	25.70	0.000
55	TS	41	0.110	6.06	0.018
"	IS	"	0.108	5.95	0.019
"	TS,IS,CHL	"	0.094	2.42	0.081
"	TS,CHL	"	0.106	3.43	0.043
"	IS,CHL	"	0.114	3.65	0.035
56	TS	86	0.193	21.31	0.000*
"	IS	"	0.160	17.34	0.000
"	TS,IS,CHL	"	0.239	9.99	0.000
"	TS,CHL	"	0.217	12.91	0.000
"	IS,CHL	"	0.248	15.15	0.000

TABLE 12 (CONTINUED)

57	TS	97	0.392	63.52	0.000
"	IS	"	0.618	157.88	0.000*
"	TS,IS,CHL	"	0.641	58.74	0.000
"	TS,CHL	"	0.386	31.55	0.000
"	IS,CHL	"	0.614	78.18	0.000
58	TS	13	0.129	2.93	0.113
"	IS	"	0.259	5.55	0.036*
"	TS,IS,CHL	"	0.397	3.85	0.045
"	TS,CHL	"	0.080	1.56	0.252
"	IS,CHL	"	0.199	2.62	0.117
59	TS	19	0.353	11.38	0.003*
"	IS	"	0.311	9.58	0.006
"	TS,IS,CHL	"	0.288	3.56	0.038
"	TS,CHL	"	0.329	5.65	0.013
"	IS,CHL	"	0.280	4.69	0.024
ALL	TS	308	0.364	176.69	0.000
DATA	IS	"	0.443	245.38	0.000*
"	TS,IS,CHL	"	0.477	94.38	0.000
"	TS,CHL	"	0.383	96.26	0.000
"	IS,CHL	"	0.448	125.49	0.000

location in order to assess the response of the transmissometer to regional differences in SPM. This improved the fit of the regression in three instances in the WIS, and on one occasion off the north coast of Anglesey.

The best regression calculations for each cruise are marked in table 12, and these have low values of p. The probability of the relationships ocurring by chance are in all cases less than 0.2%.

The calibration of the transmissometer for the measurement of SPM concentration is shown in Table 13a, for each cruise. This was calculated for both total and inorganic SPM concentrations. A better fit (r^2) was generally found for inorganic SPM. The results show that over the season there was considerable variation in the standard deviation of the regression, with high values in September, April and low values in May.

The average of the slopes of the regressions of TS with c were 2.835 . (s.d.= 0.817). For IS the average was 2.583 (s.d.= 1.05). This compares well to values of the slope of attenuation vs. mass concentration found by other workers, shown in Table 13b. The equivalent inverse value for this study is 0.353 .

Table 14 shows examples of the predicted total and inorganic SPM concentrations, calculated using the coefficients in Table 13 , and values of c. Mean

TABLE 13.a. CALIBRATION OF TRANSMISSOMETER

TS = A + B * c and

IS = A + B * c

where TS = total SPM and IS = inorganic SPM concentration (mgl^{-1}); A = the intercept; B = the slope; r^2 = the coefficient of determination.

CRUISE	TS/IS	A	B	r^2	s.d (SPM,mg/l)
53	TS	3.94	3.01	0.440	5.076
	IS	3.84	2.72	0.462	4.384
55	TS	8.88	3.46	0.110	4.163
	IS	6.21	2.71	0.108	3.300
56	TS	1.96	2.09	0.193	2.183
	IS	1.40	1.39	0.160	1.615
57	TS	0.583	1.64	0.392	1.109
	IS	0.198	1.63	0.618	1.476
58	TS	3.300	3.78	0.129	5.690
	IS	2.480	4.34	0.225	4.756
59	TS	-0.099	3.03	0.353	1.080
	IS	0.801	2.69	0.311	1.048
ALL	TS	2.08	3.56	0.364	4.523
DATA	IS	1.22	3.36	0.443	3.625

TABLE 13.b. COMPARATIVE FIELD CALIBRATION OF BEAM TRANSMISSOMETERS, ATTENUATION VS. MASS CONCENTRATION.

(For references in this table see Baker and Lavelle,1984).

REFERENCE	LOCATION	REGRESSION SLOPE
Otto (1986)	Wadden Sea Netherlands	0.088
Jones and Wills (1956)	Thames estuary U.K.	0.12
Joseph (1955)	North Sea	0.16
E.T.Baker (unpublished)	Duwamish estuary Washington,USA	0.22
Jones and Wills (1956)	Plymouth Sound U.K.	0.22
McCarthy et al. (1974)	Anclote estuary Florida.	0.30
Baker (1983)	Alaskan coast.	0.30
Calloway et al. (1976)	New York Bight.	0.32
Heathershaw and Simpson (1974)	Irish Sea.	0.33
Drake et al. (1972)	Southern California shelf.	0.37
Gordon and Smith (1972)	Biscayne Bay, Florida.	0.38
Nyquist (1979)	Orust-Tjorn fjord, Sweden.	0.48
Baker et al.(1983), Baker (1984)	Puget Sound, Washington.	0.46-0.62
Peterson(1977)	Oregon Shelf	0.50-0.62
E.T.Baker (unpublished)	Washington continental slope	0.50
McCave (1983)	Novia Scotia continental rise.	0.83
This study	Irish Sea	0.353

TABLE 14 PREDICTION OF C FROM REGRESSION COEFFICIENTS (TABLE 13a)

TS = a + b * c
IS = a + b * c

a = the intercept; b = the slope (Table 13a); s.d. is the standard deviation also from Table 13a ; c is the average beam attenuation coefficient for each cruise, from Table 11.

CRUISE	TS/IS	a	b	c (m^{-1})	TS/IS (pred)	s.d (mg/l)	s.d./TS (IS)
53	TS	3.94	3.01	2.13	10.35	5.1	0.49
	IS	3.84	2.72	2.13	9.63	4.4	0.46
55	TS	8.88	3.46	0.93	12.09	4.0	0.33
	IS	6.21	2.71	0.93	8.73	3.30	0.38
56	TS	1.96	2.09	0.76	3.55	2.18	0.61
	IS	1.40	1.39	0.76	2.46	1.62	0.66
57	TS	0.58	1.64	0.56	1.50	1.11	0.74
	IS	0.20	1.63	0.56	1.11	1.48	1.33
58	TS	3.30	3.78	0.82	6.40	5.70	0.89
	IS	2.48	4.34	0.82	6.04	1.05	0.35
59	TS	-0.099	3.03	0.82	2.38	1.08	1.08
	IS	0.80	2.69	0.82	3.006	1.05	0.35
ALL DATA	TS	2.08	3.56	1.003	6.45	4.52	0.70
	IS	1.22	3.36	1.003	4.59	3.63	0.79

averages of c for each cruise were used (Table 11).The ratios of the standard deviation of the regression to these predicted values of SPM concentration are shown in the last column in Table 14. This ratio was smaller in April, May and October, indicating that the transmissometer was a better measure of SPM at these times.

This can be explained by the fact that the proportion of organic material was high in July and August, thus increasing the attenuation of the light beam, either by absorption or by a change in the refractive index of the SPM. No explanation for the better fit of the regression in May can be offered.

The regression for the entire data set shows a higher standard deviation than those for single cruises, which suggest that the attenuating properties of the SPM vary significantly with time.

4.5.4. The size distribution and nature of the SPM.

4.5.4.1. Particle size distribution.

The particle size distribution analysis was carried out using the Coulter Counter for samples taken during two cruises during 30 June to 4th July, and during 12-17th October 1987. Water samples were taken at sea by

means of the rosette multisampler, at 5 metres below the surface and from 5 to 10 metres above the sea-bed. 500ml of sea-water was stored in particle-free glass jars and 50ml of 20% buffered formaldehyde was added to preserve the sample. This gave a 2% formaldehyde concentration. The formaldehyde had been previously filtered through Whatman GF/F (0.7 μm) glass fibre filter papers using particle free glassware. The particle size distribution was measured within a week of the cruise, and the jars were shaken daily to prevent flocculation.

The particle size analysis was carried out on a different Coulter Counter for each batch of samples. In June a Model 2A was used, while in October measurements were made with a Model ZM.

Calibration of the Model 2A.

Measurements of particle size distribution were made on the Coulter Counter with 70μm and 200μm apertures . This gave a range of measurement 1.5 to 80 μm (2% of the minimum and 40% of the maximum aperture sizes). The instrument was calibrated using latex beads of a known volume and resistivity, suspended in sea-water which had been filtered (retention capacity > 0.45 μm.) The resistivity of the particles in the samples was then converted into a size distribution, and the data presented as a percentage volume for each size interval.

Calibration of the Model ZM.

The samples taken in October 1987, using a Model ZM Coulter Counter, were measured using a 50 μm and a 100 μm aperture, giving a range of measurement from 1 to 40 μm. The instrument was calibrated as described for the Model 2A. However counts below the equivalent size range of 6 μm were extremely high in the calibration of the 100 μm aperture. A similar effect was noted for counts below the equivalent of 4 μm diameter for the 50 μm aperture. Therefore the range of measurement for samples taken in October was limited from 4 to 40 μm.

An intercalibration of the two instruments was carried out using the same aperture (100 μm). A known volume of a water sample was passed through each Coulter Counter. Total particle concentrations were 0.673 mg l^{-1} and 2.392 mg l^{-1} for the Models 2A and the ZM respectively.

Results.

The results from the Coulter Counter measurements can be summarised by presenting the particle size distribution from two regions where there was a marked difference in tidal stirring, during June and October, 1987.

The first region was near the coast of Anglesey (Figure 4.5.) where the water was well mixed throughout the year. The surface and near bottom particle size

distributions are presented in Figure 4.9. (Station X2,figure 4.9.a; station A2,figure 4.9.b.) This shows that in June the largest percentage of the volume was for particles of less than 4μm. However in October, although the greatest volume was in the small size fraction, there were larger particles (>20μm) in the sample. There was no significant difference in size distribution between the surface and bottom water samples.

The second region was in deeper water (100m) in the WIS. (Stations A4,figure 4.9.c; station B1,figure 4.9.d). This shows that in June, during stratification , there was a much higher percentage of small particles in the near-bottom water than in the surface water. In October, however, when the water was mixed, there was little difference in the size distribution of the particles in the surface and near bottom waters. As in June, the largest percentage of the volume was in the size fraction smaller than 4μm, and in October there were some particles in the size fraction greater than 20μ m. However, since the Model ZM Coulter Counter, used for the measurements made in October, did not give reliable measurements for the particles less than 4 μ m, any comparison between the samples taken in June and in October must be viewed as partly due to the change in instrumentation.

Figure 4.9. Volume (%) of SPM of discrete size intervals from

a) Station X2, (29/6/87-3/7/87) in mixed water,depth 70m.

b) Station A2 (12-16/10/87) in mixed water,depth 70m.

c) Station A4 (29/6/87-3/7/87) in stratified water,depth 100m.

d) Station B1 (12/10/87-16/10/87) in mixed water, 80m).

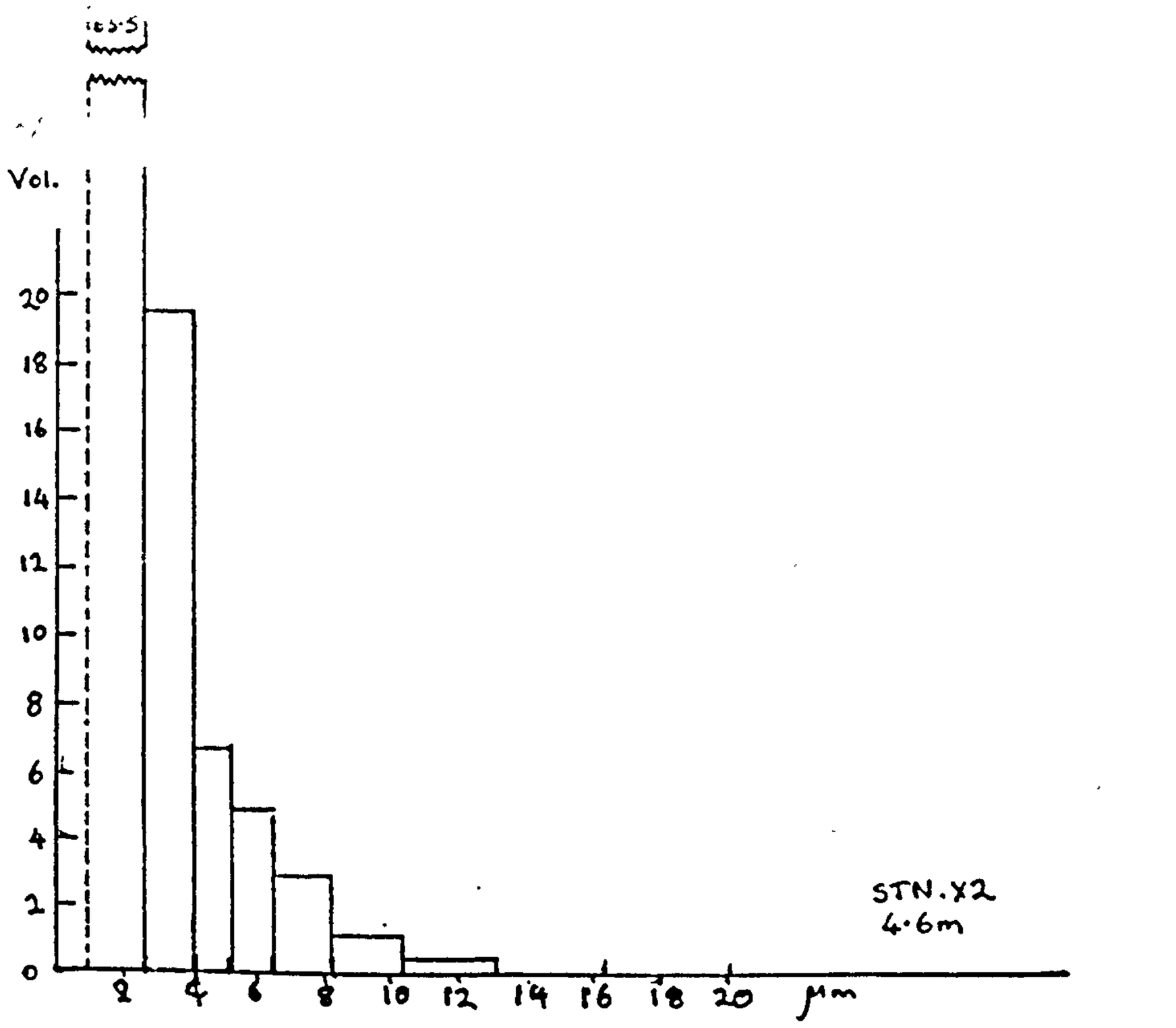
65·5
Vol.
20
18
16
14
12
10
8
6
4
2
0
2
4
6
8
10
12
14
16
18
20
μm
STN.X2
4·6m

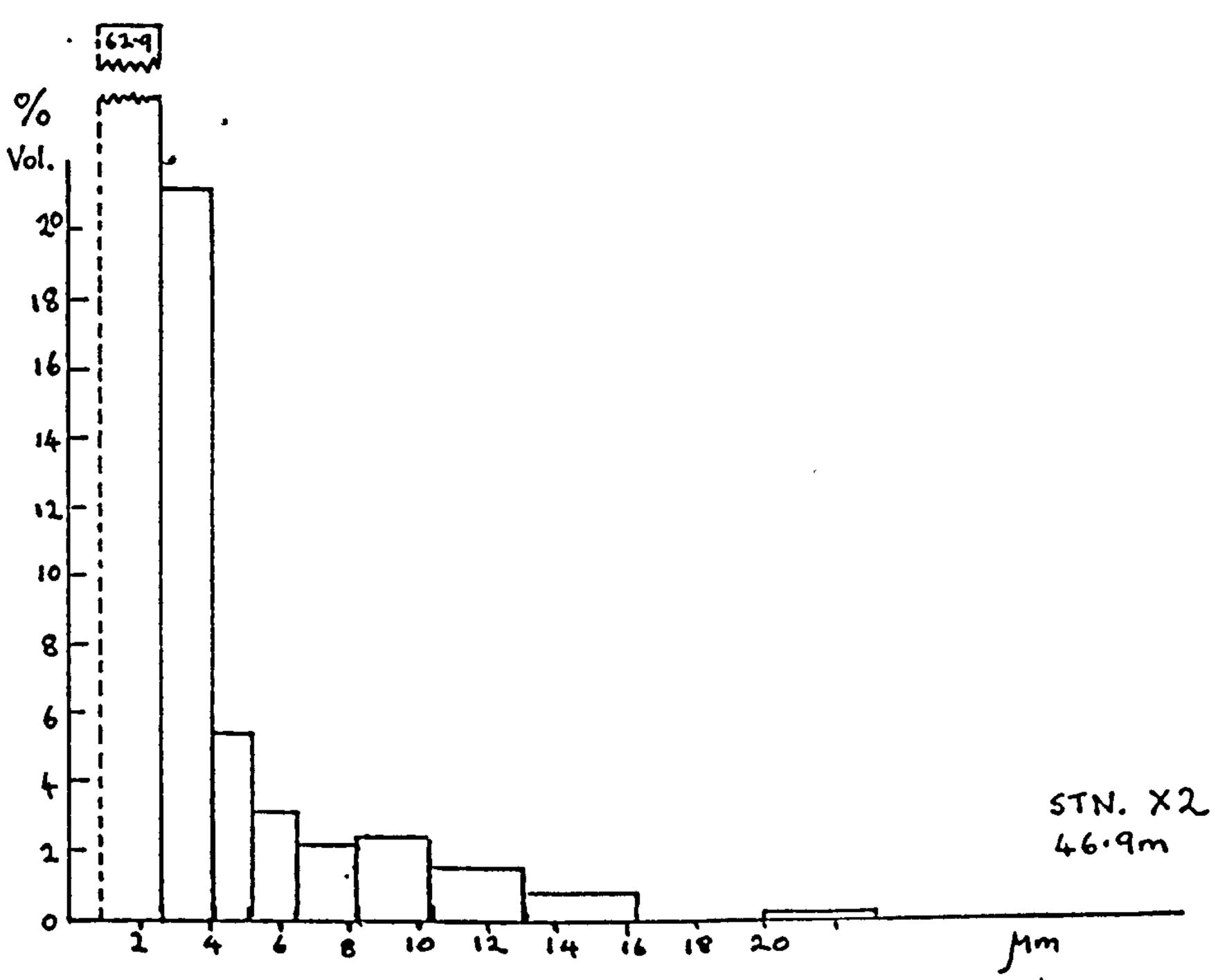
62·9
%
Vol.
20
18
16
14
12
10
8
6
4
2
0
2
4
6
8
10
12
14
16
18
20
μm
STN. X2
46·9m

(b)

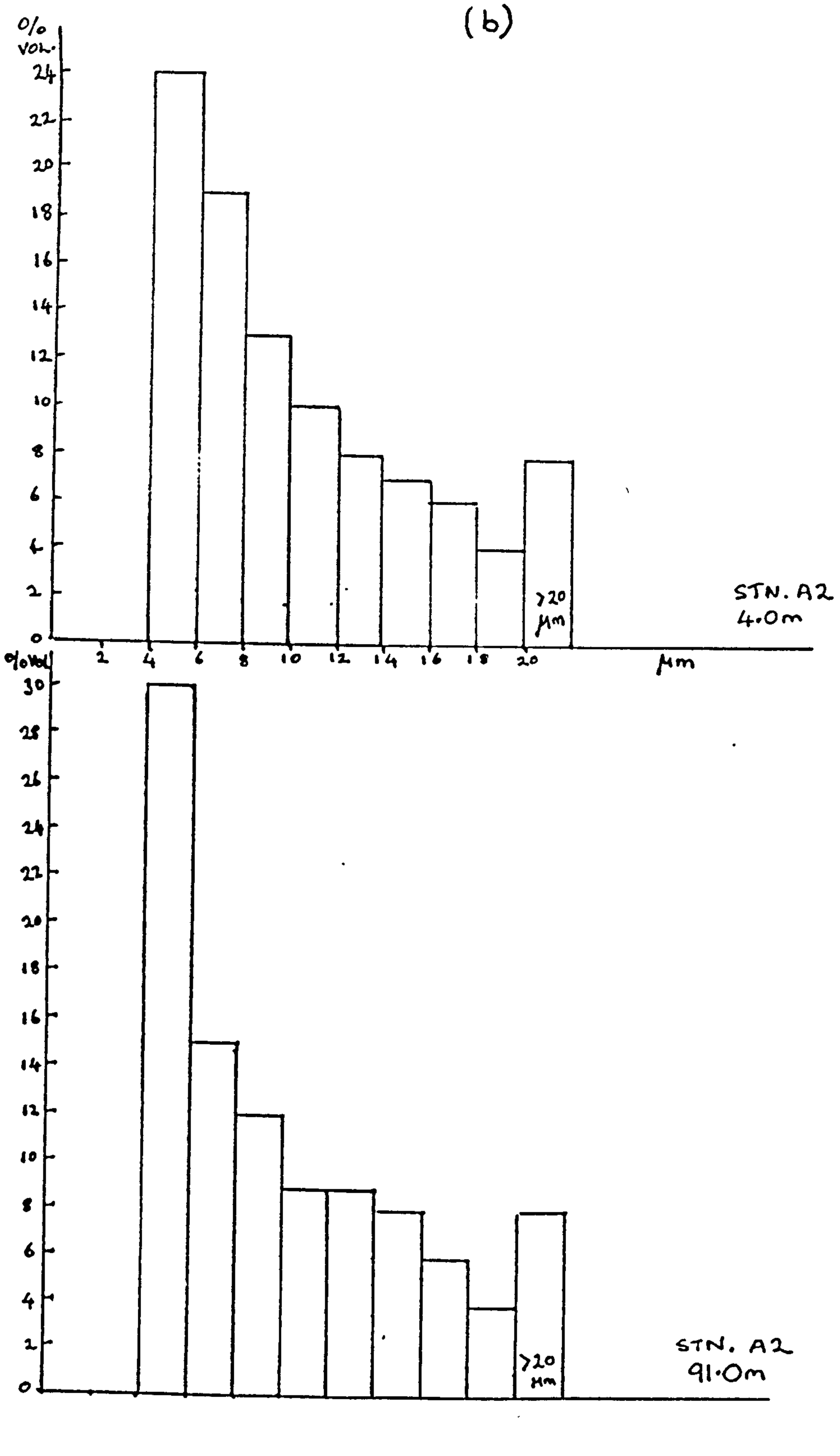
0/0 VOL.
24
22
20
18
16
14
12
10
8
6
4
2
0
2
4
6
8
10
12
14
16
18
20
>20 µm
µm
STN. A2
4.0m
0/0 Vol
30
28
26
24
22
20
18
16
14
12
10
8
6
4
2
0
>20 Hm
STN. A2
91.0m

(c)

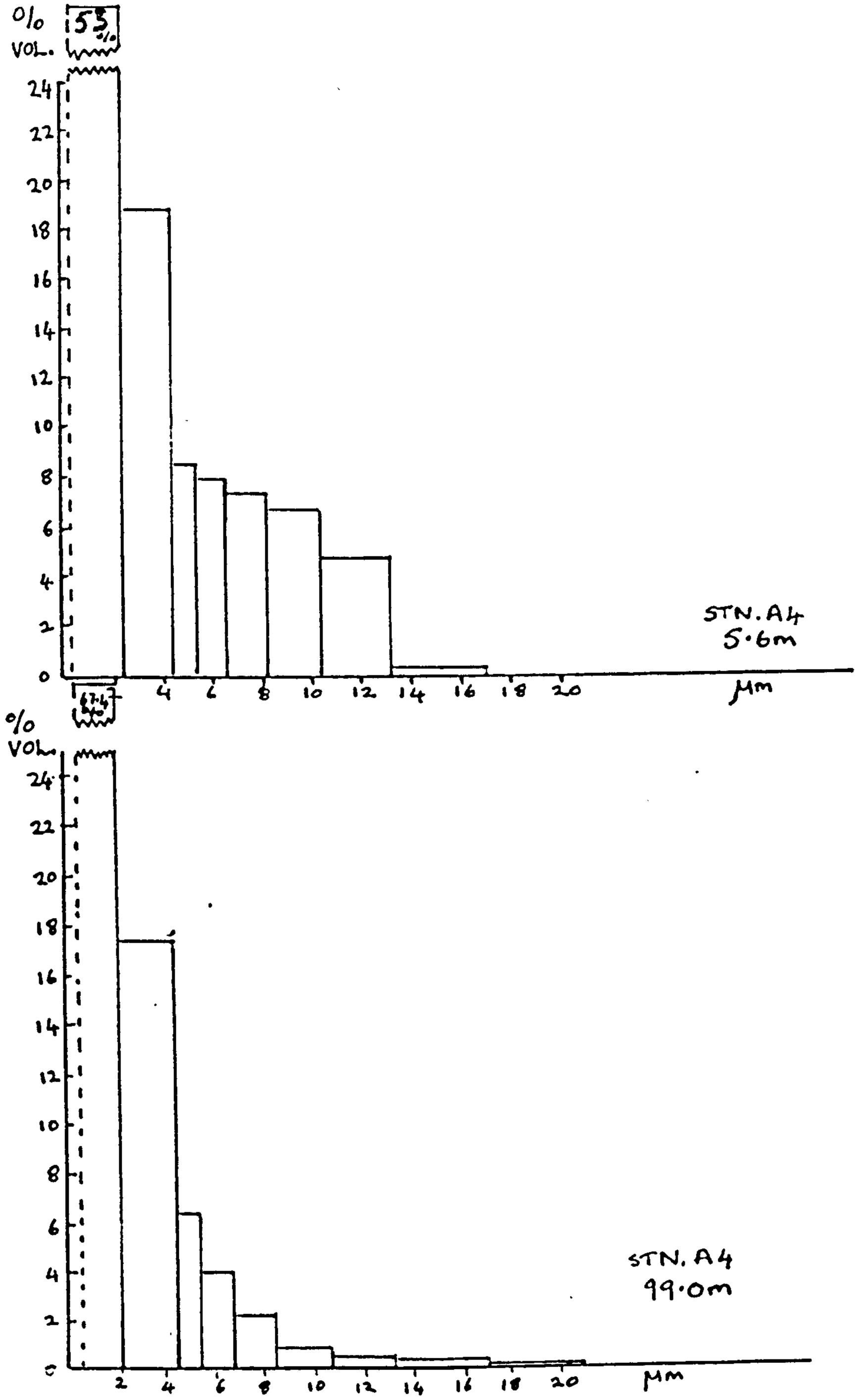
0/0
VOL.
53%
24
22
20
18
16
14
12
10
8
6
4
2
0
4
6
8
10
12
14
16
18
20
μm
STN. A4
5·6m
0/0
VOL.
24
22
20
18
16
14
12
10
8
6
4
2
0
2
4
6
8
10
12
14
16
18
20
MM
STN. A4
99·0m

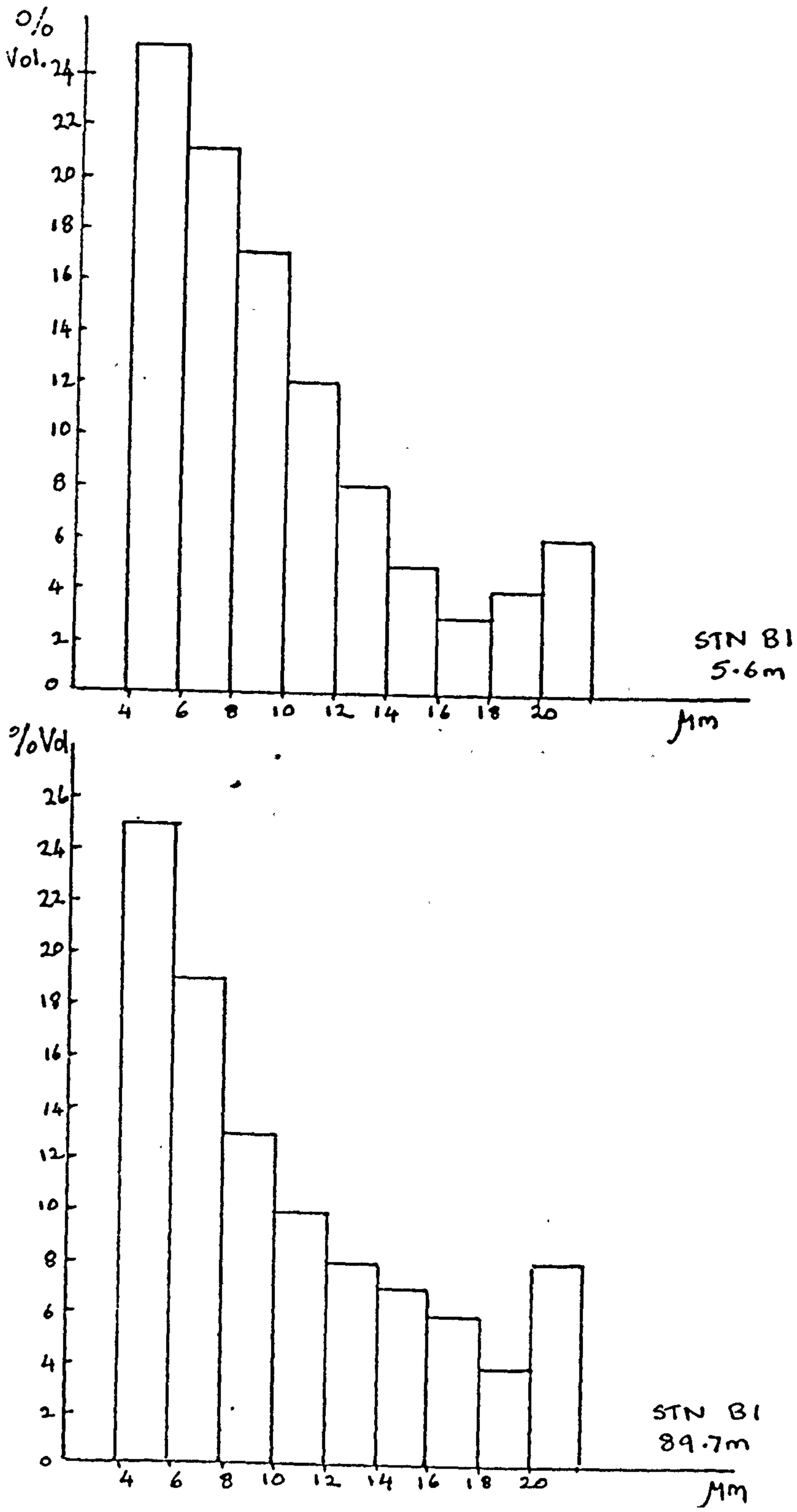
0/0
Vol.
24
22
20
18
16
14
12
10
8
6
4
2
0
4
6
8
10
12
14
16
18
20
μm
STN B1
5·6m
%Vd
26
24
22
20
18
16
14
12
10
8
6
4
2
0
4
6
8
10
12
14
16
18
20
μm
STN B1
89·7m

Summary

The results suggest that in mixed water, there is little difference between the particle size distribution in the surface and near-bottom waters. Other studies in the Irish Sea (Boudjelas,1988) show that within 1km there is no significant difference in the size distribution of particles. This study suggests that there are marked differences in particle size distribution over several months. It also shows that in stratified water there is a considerable difference in the particle size distribution between surface and near-bottom waters.

4.5.4.2. The Scanning Electron Microscope Analysis.

The composition of the SPM was studied by photographing sections of filter papers which were scanned with a Hitachi Scanning electron microscope, model S520.

The procedure for collecting and preserving the samples was the same as that described for the particle size analysis. A certain amount of water was filtered through a 0.2 μm nuclepore filter paper. The amount filtered depended on the concentration of SPM determined by gravimetric analysis. It was important that only an even coating, with a single layer of particles, should be distributed on the filter paper.

After filtration, the filter paper was washed with distilled water to remove salts, and then dried in sterilized Petri dishes at room temperature. A central square was cut from each filter and it was mounted on aluminium stubs. The specimens were coated with a very thin layer of gold in a Polaron E500 Sputter Coater. Photographs of the SPM on the filter papers were taken.

Because the particles were not evenly distributed on the filters, it was not possible to make a quantitative analysis of the different particle types present. It was, however, possible to identify a number of main groups, and main particle size groups.

The samples were taken from mixed water at a station offshore of the Menai Straits (station F1 in figure 4.5.) on 15th October 1987. A series of photographs, in figure 4.10.a and b show that the SPM was composed mainly of aggregates, from 20 to 30 μm in size. These were often in the form of faecal pellets. The aggregates were generally composed of plate-like fragments, probably clay minerals. These were typically from 2 -3 μm in size, In addition, many organic fragments were observed, some of which were identified as parts of coccolithophores and diatoms. Some examples of these are shown in figures 4.10.c. These fragments, of organic origin, were of the order of 40

Figure 4.10.

Scanning electron microscope photographs of SPM from station F1 ,on 15/10/87 .

Figures a) and b) show that the particles were frequently aggregates of in the size range of 20 to 30 μm, but that these were composed of particles less than 4 μm in size. Fragments of organic debris can be observed.

Figure c) shows intact phytoplankton cells.

a)

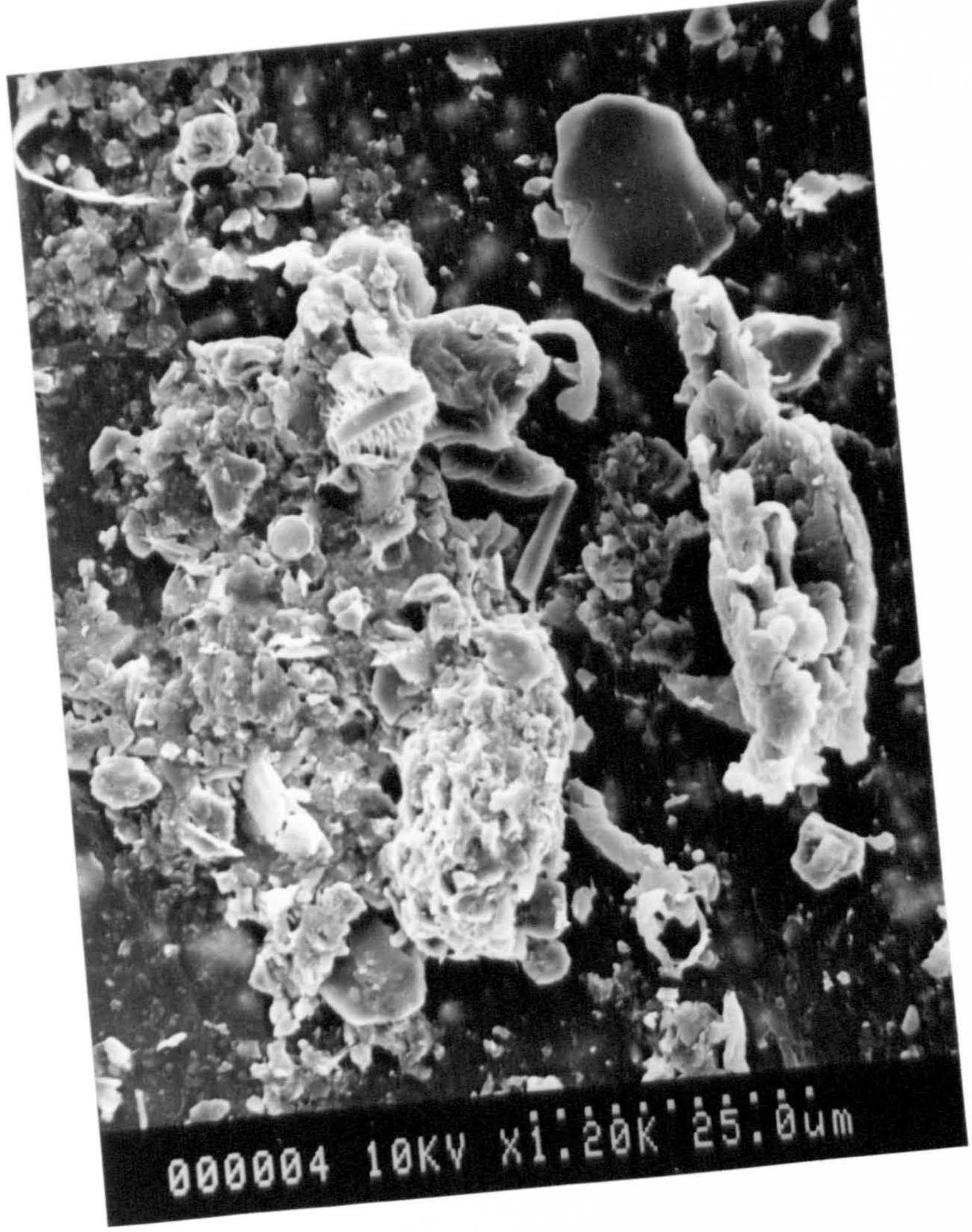

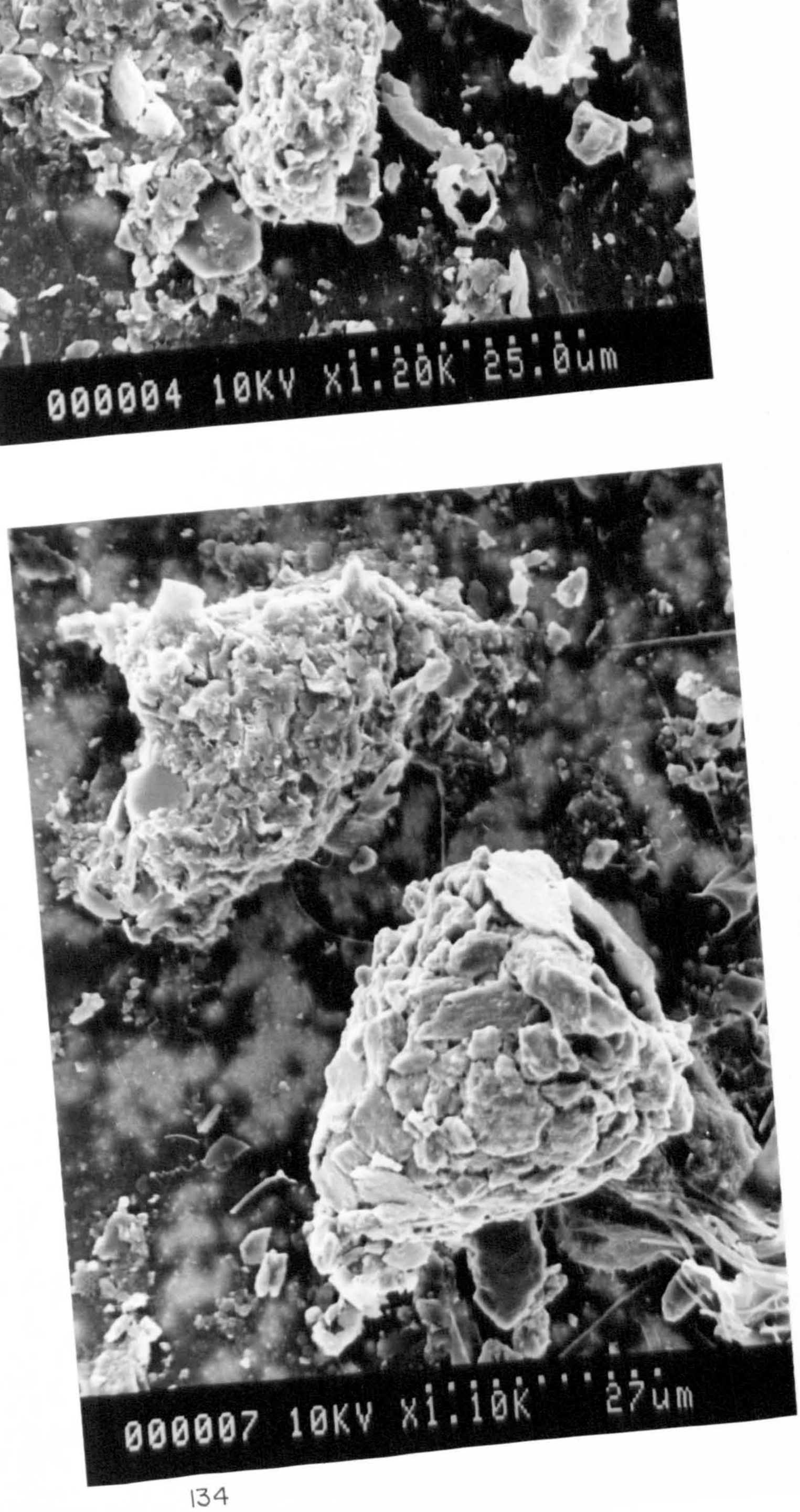

b)

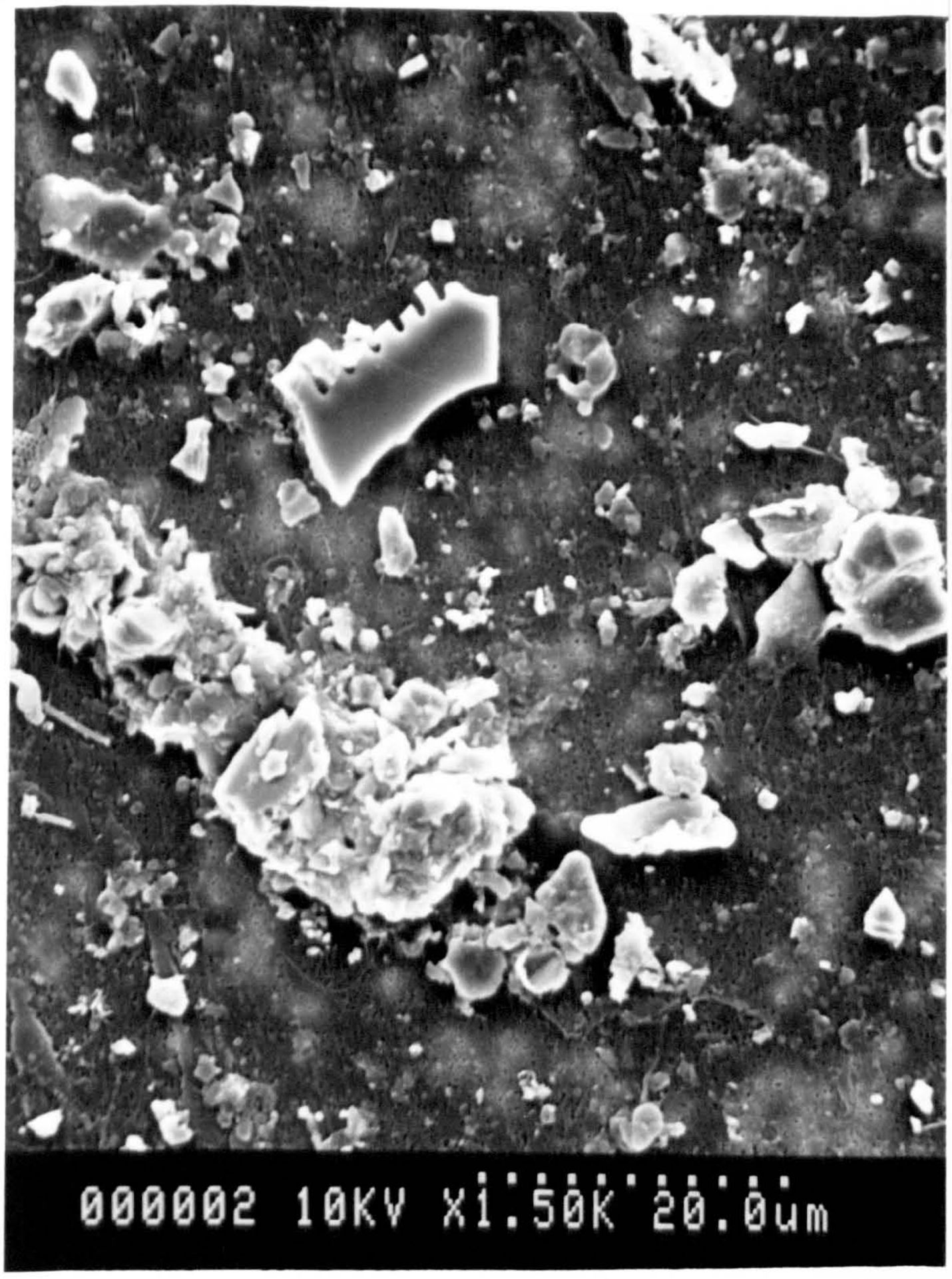

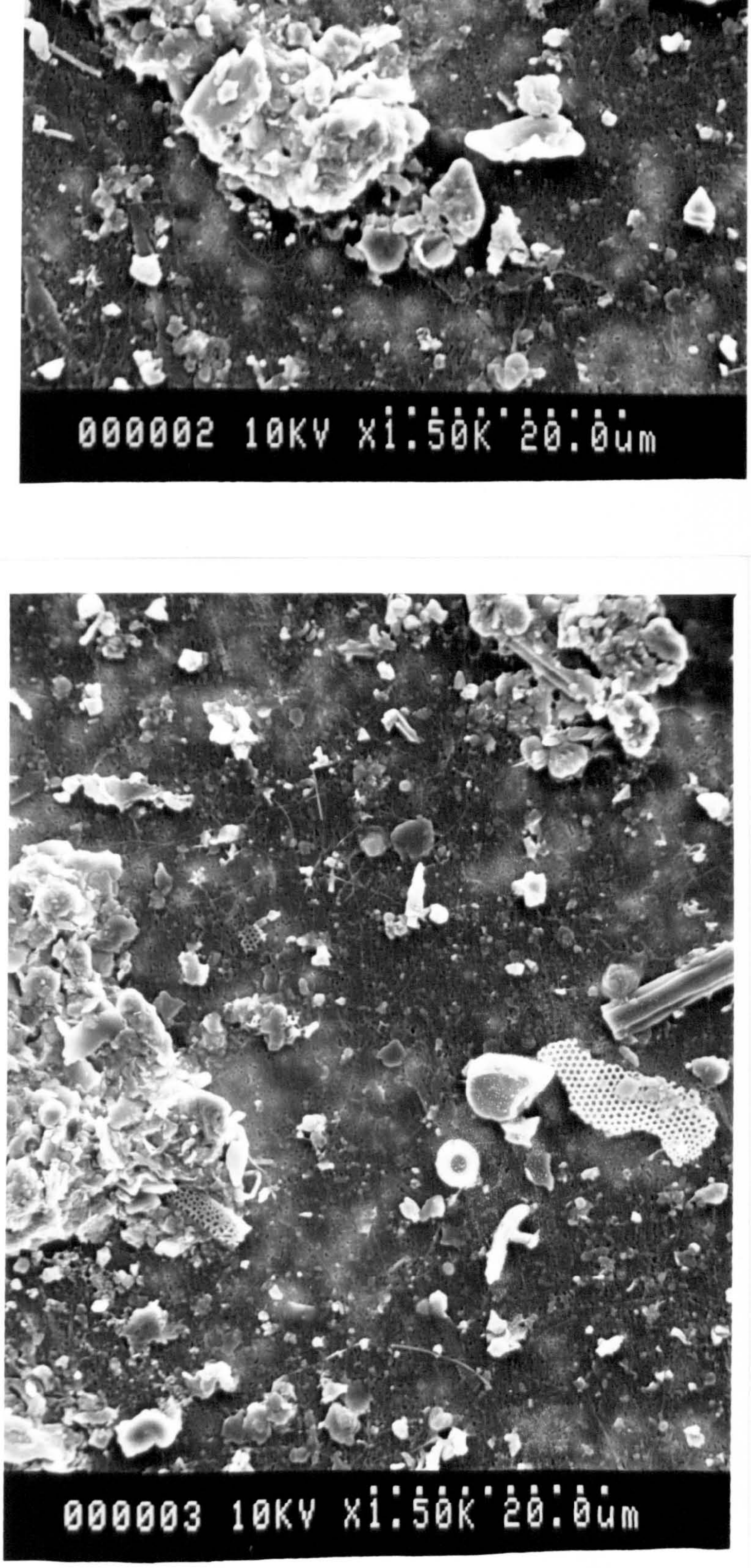

c)

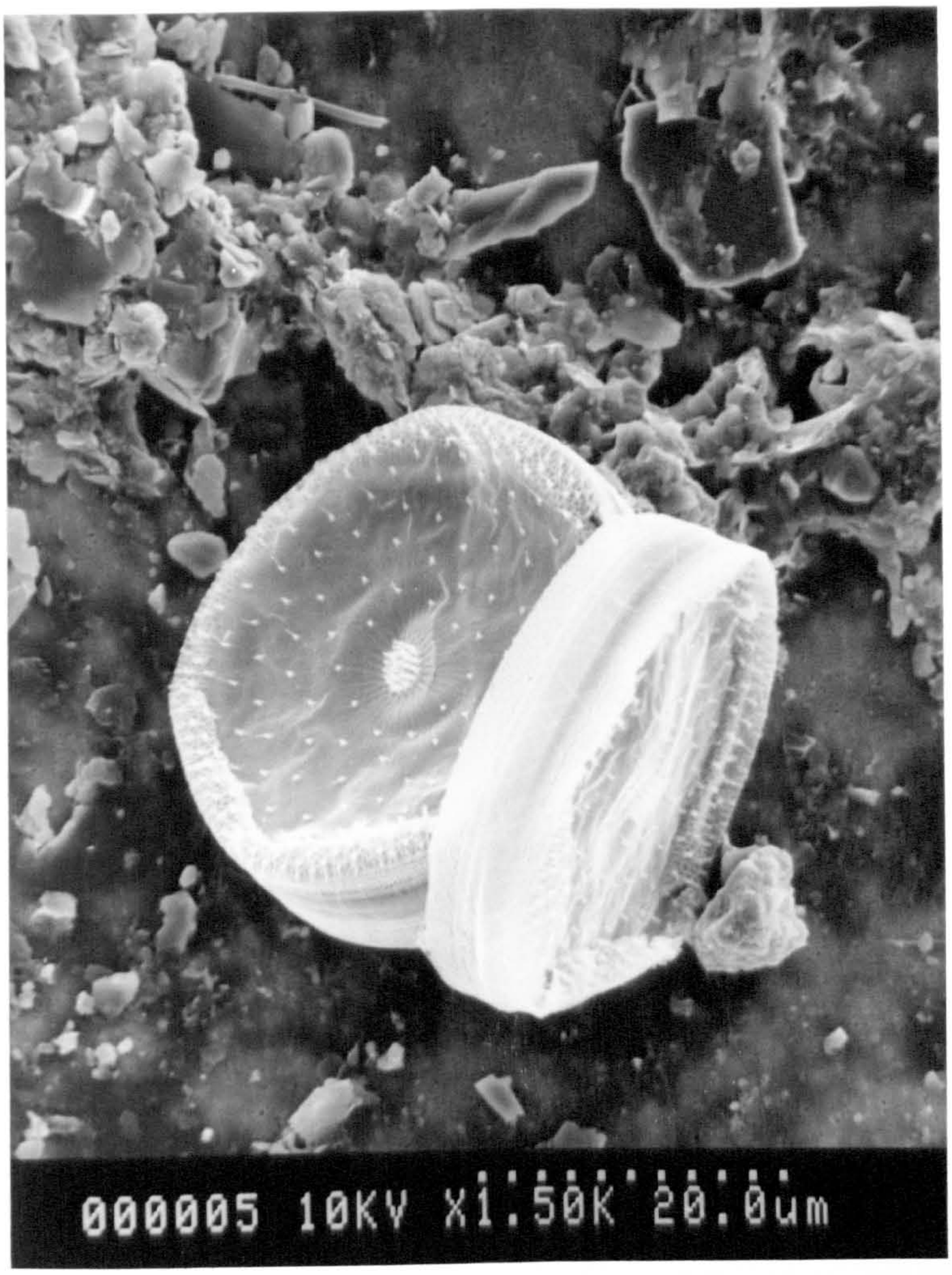

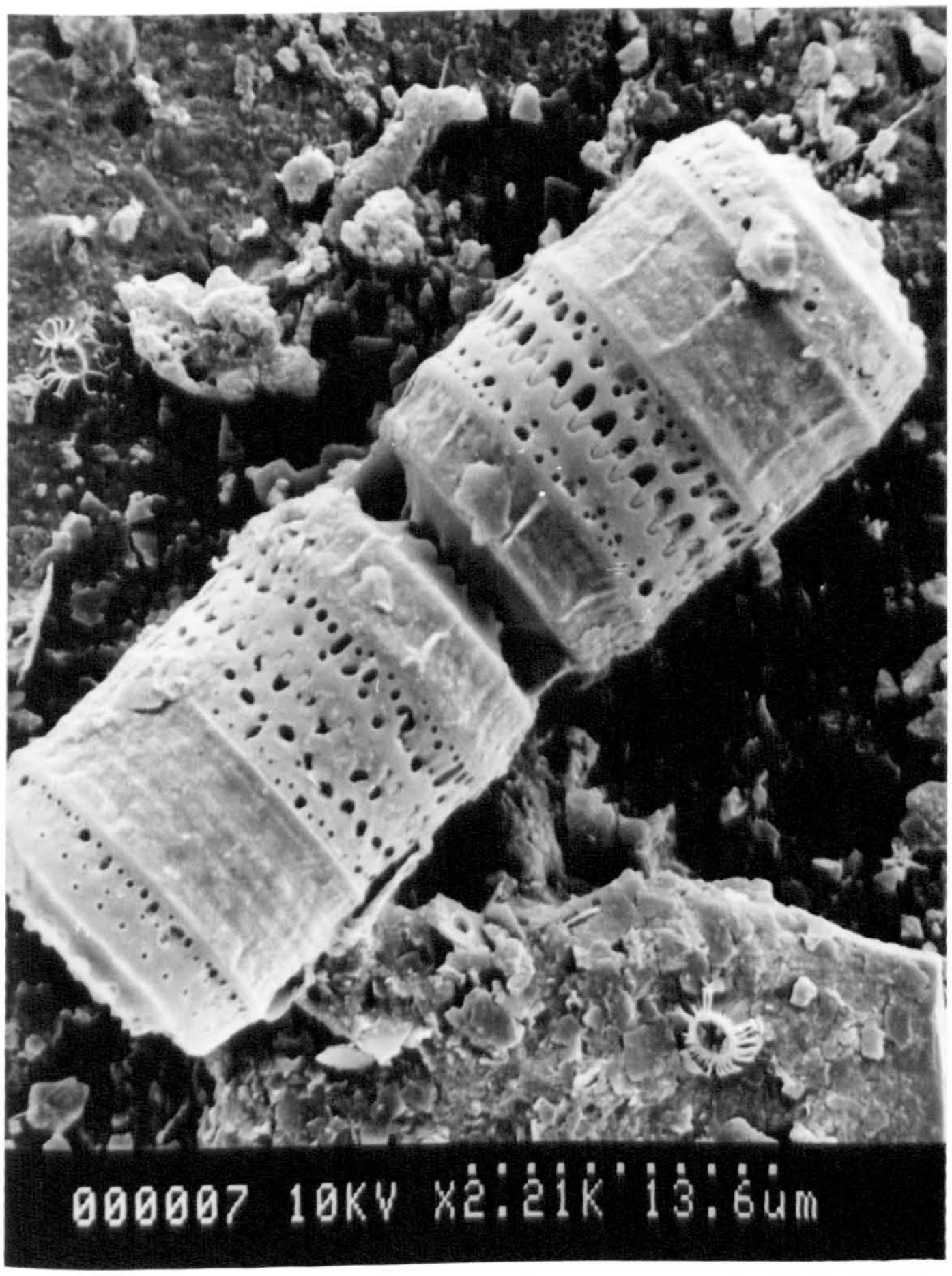

μm in size, and were sometimes larger. There were also complete phytoplankton cells, shown in Figure 4.9.c.

Summary

These observations of the sizes of particles are not inconsistent with the measurements of size distributions discussed in 4.5.4., in which the greatest volume of particles were in the size fraction less than 4μm, with some larger particles present. The action of the Coulter Counter mechanisms causes disaggregation. Therefore the large aggregates observed in the SEM photographs would have been broken up.

4.6. Conclusions.

These observations show that a relationship exists between c and SPM, but it is only a general guide, and is no substitute for gravimetric measurements. However, the use of c widely extends the survey capability. SPM concentrations can only be determined by beam transmittance with a rather large degree of uncertainty of the order of 50%.

Reasons for the variation in beam attenuation are evidently partly due to the changing proportion of organic material in the SPM and the seasonal change in chlorophyll concentrations since the variance in the relationship between c and SPM is greatest in the late

spring and early summer. It is suggested that this is due to the different light absorbing and scattering properties of the phytoplankton and detritus in the water at this time of year. It is also probable that a variation in the particle size distribution would cause a change in the relationship between c and SPM. The evidence from the SEM analysis reveals that particle shapes are extremely variable and so would be expected to influence the measurement of c if these variations were spatially and seasonally inconsistant.

These observations indicate that although the measurement of beam attenuation over a wide area may be limited when interpreting the data in terms of the concentration of SPM, it may be more useful for measurements at a fixed point, where the characteristics of the particles are consistent. In addition, at the present time there is no better way to make a large number of measurements of the concentration of SPM.

CHAPTER 5

RESULTS OF THE SURVEY

5.1. Introduction

The experimental work was carried out over a two year period, from the R.V.S. Prince Madog, a purpose built research ship ,owned by U.C.N.W. In 1986 four sites were selected for a detailed survey of variations in beam attenuation and physical parameters. These sites had contrasting tidal flows and water depths. The positions of the stations are shown in figure 5.1.a, and the details are in Table 15. The sites were surveyed at approximately monthly intervals, from March to November when continuous vertical profile measurements of temperature, conductivity, depth and beam attenuation were recorded using the CTD. The measurements were made at 30 minute intervals, for a duration of 13 hours at each station, in order to assess the response in the attenuation record to any tidal resuspension. Measurements of current speed and direction at 5m below the surface were made with an NBA profiling current meter.

The programme of fieldwork in 1987 consisted of a survey of a grid of stations, shown in figure 5.1.b., where continuous vertical profile CTD and beam attenuation

a)

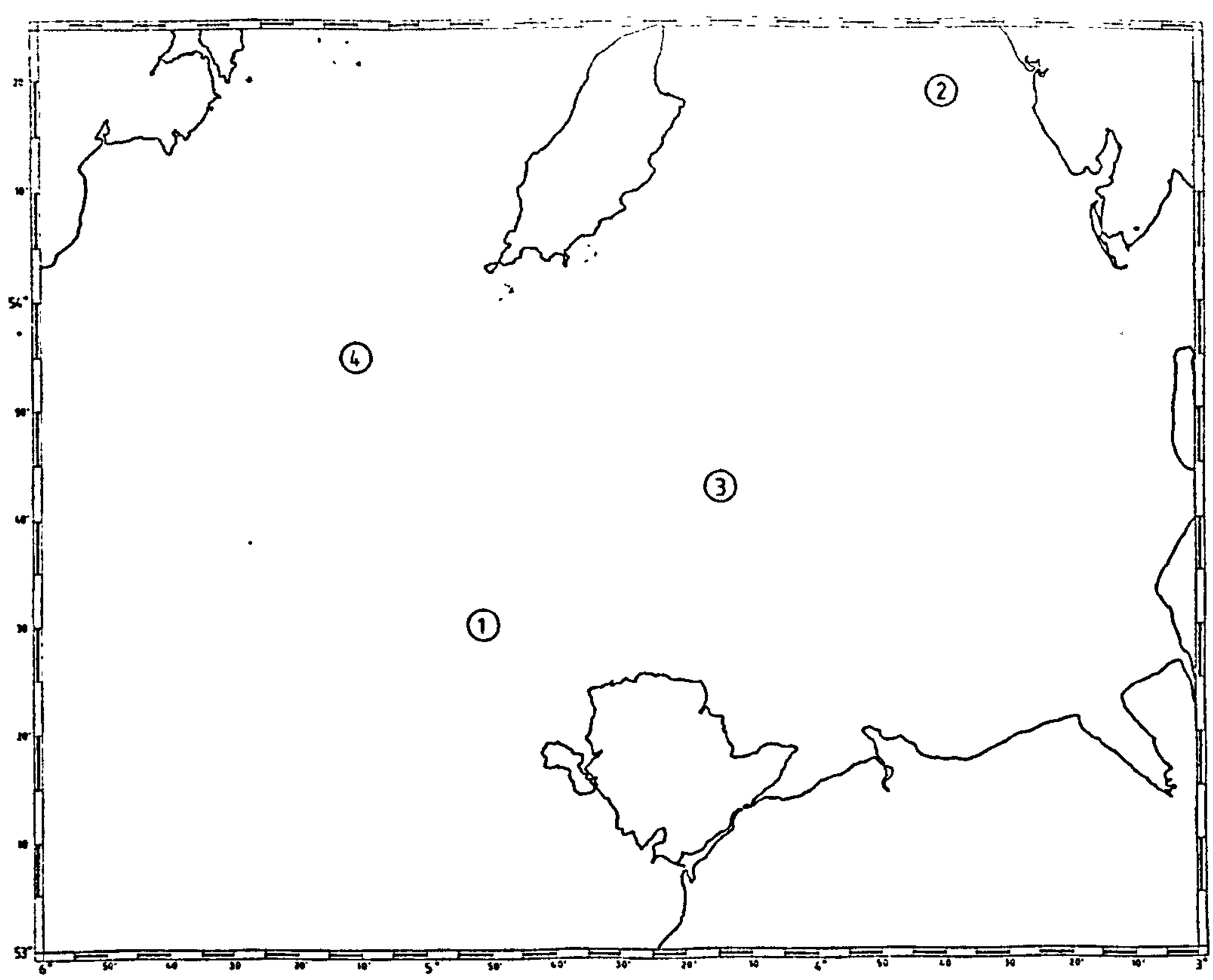

a

b)

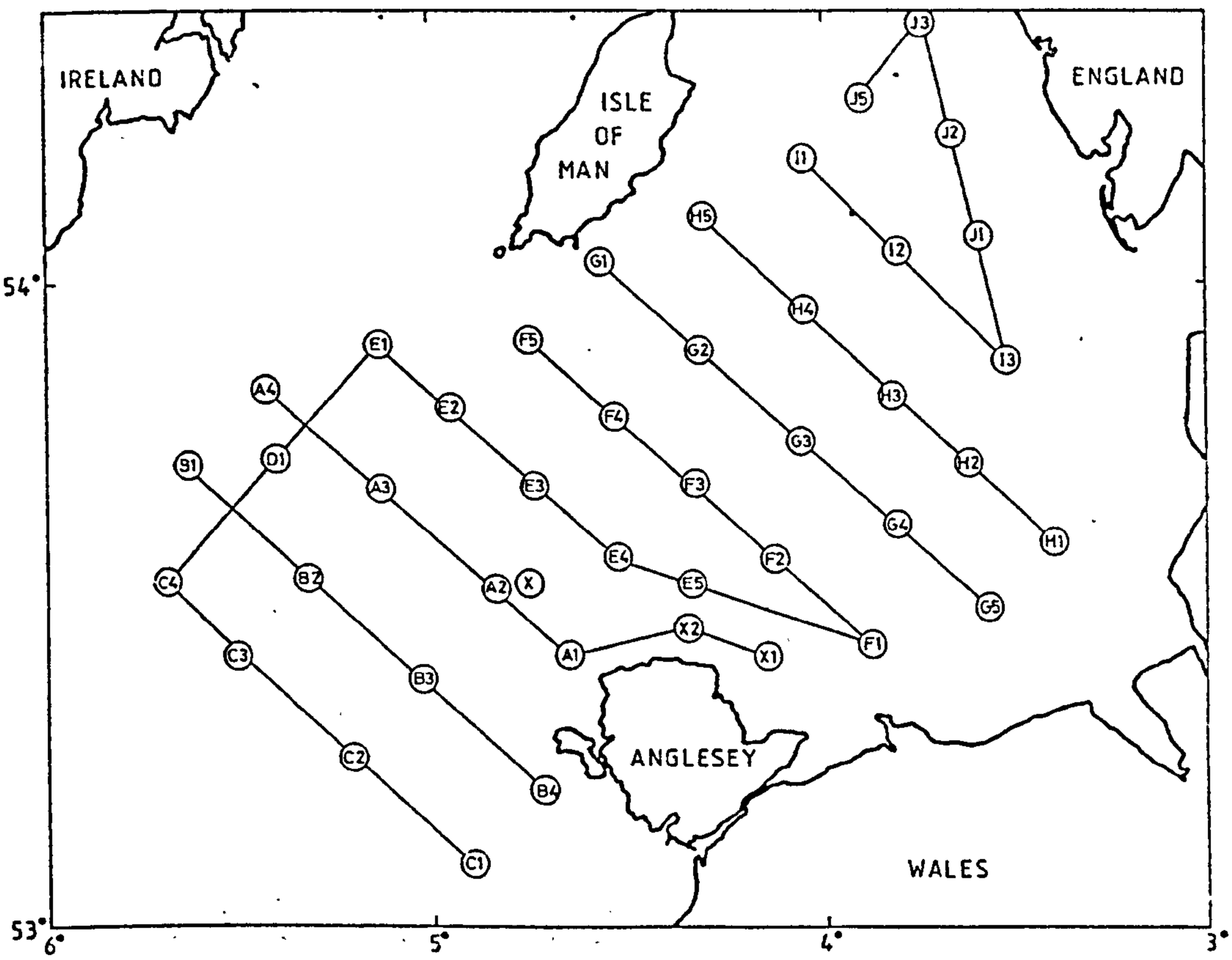

Figure 5.1. a)Positions of stations for CTD and beam attenuation measurements in 1986.

b)Grid of stations for CTD and beam transission measurements in 1987.

TABLE 15 STATION SUMMARIES - 1986

cruise	date	stations	duration (hrs)	parameters
45	17/3/86- 21/3/86	1,3	13	d,t,tr
47	7/5/86- 9/5/86	2	13	d,t,tr
48	30/6/86- 4/7/86	1,2,3 4	13 3	C,T,D,c
50	4/8/86- 6/8/86	2	13	C,T,D,c
51	22/9/86- 25/9/86	1,2,3 4	13 6	C,T,D,c C,T,D
52	19/11/86- 22/11/86	1,2,	single station	C,T,D,c

d,t,= depth and temperature

tr= transmittance , using a prototype of the CTD/transmissometer system described in chapter 3.

C,T,D,c = conductivity, temperature,depth,beam attenuation using the instrumentation described in chapter 3.

casts were recorded. Surveys were made at monthly intervals at times close to neap tides. Details of the surveys are in Table 16.

In addition a mooring was deployed on 6th April 1987 (station X in figure 5.1.b),serviced during the cruises, and finally recovered on 12th October 1987, giving 6.5 months of time series data. The mooring is described in detail in Chapter 4, and the results are described in Chapter 6.

Details of the bathymetry, tidal regime and sediment composition are given in Chapter 2.

5.2. The CTD survey : Spatial distributions of beam attenuation in the northern Irish Sea.

The results from the surveys in 1986 and 1987 indicated that the distribution of beam attenuation was highly differentiated in the northern Irish Sea. This is illustrated in figures 5.2.a. and b. which show the distribution of beam attenuation, c, at 5m below the surface, and at 5m above the sea-bed, in early April 1987.

High values of c were observed near the surface in the region north of Anglesey, with low values to the north-west and the north-east of the region. The corresponding

TABLE 16 STATION SUMMARIES - 1987

cruise	date	transects of stns. completed(fig 5.2)
ISIS 53	30/3/87- 4/4/87	A,B,E,F,G,H
ISIS 55	11/5/87- 15/5/87	A,B,E,F,G
ISIS 56	29/6/87- 3/7/87	A,B,C,E,F,G,H
ISIS 57	3/8/87- 7/8/87	A,B,C,E,F,G,H,I,J
ISIS 58	7/9/87- 11/9/87	A,B,C,E,
ISIS 59	12/10/87- 16/10/87	A,B,C,E

Figure 5.2. Survey during 30/3/87-4/4/87.
a) Beam attenuation (m^{-1}) at 5m below the surface .
b) Beam attenuation (m^{-1}) 5 m above the sea-bed.
c) Sigma-t at 5m below the surface.
d) Sigma-t at 5m above the sea-bed.

a)

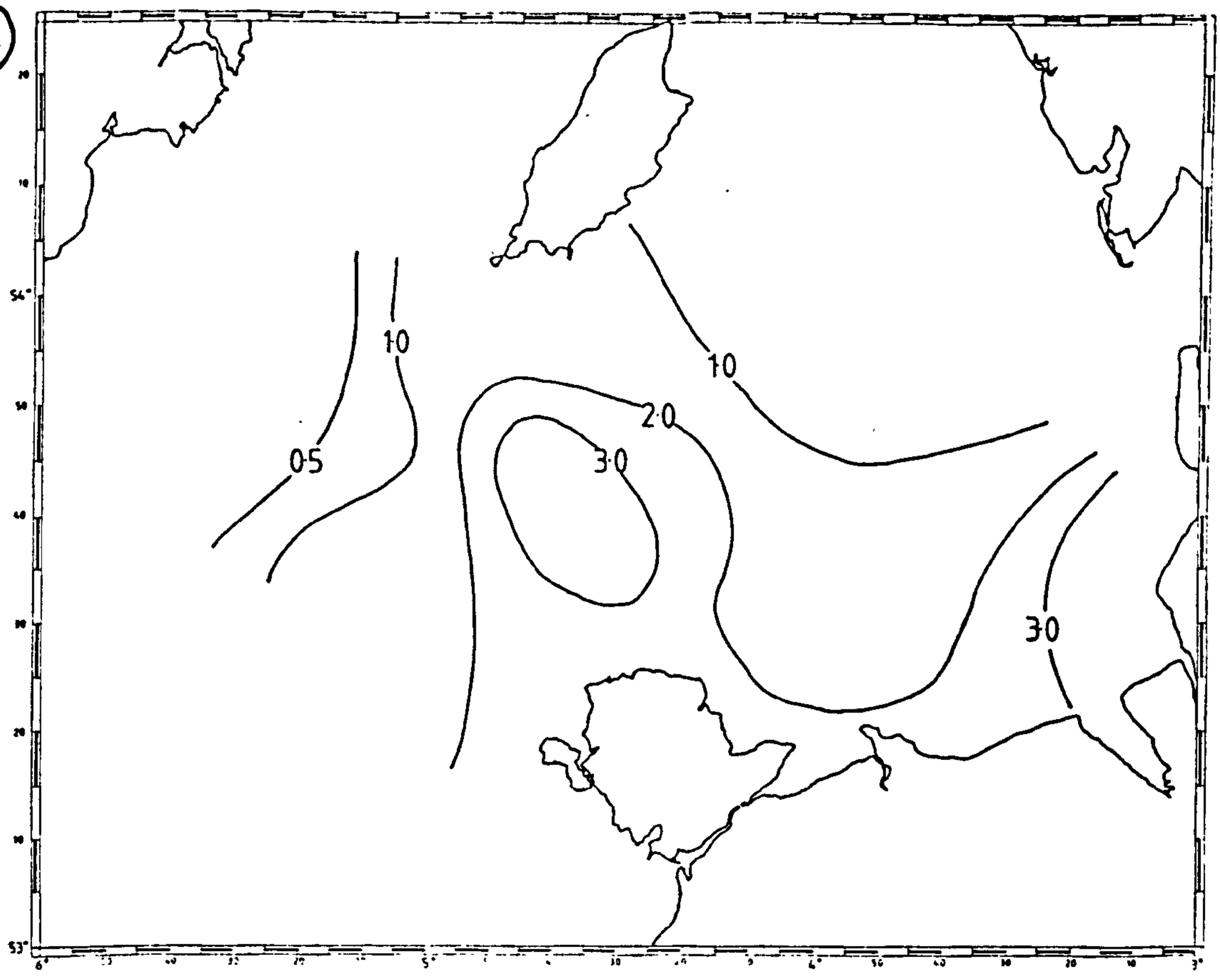

b)

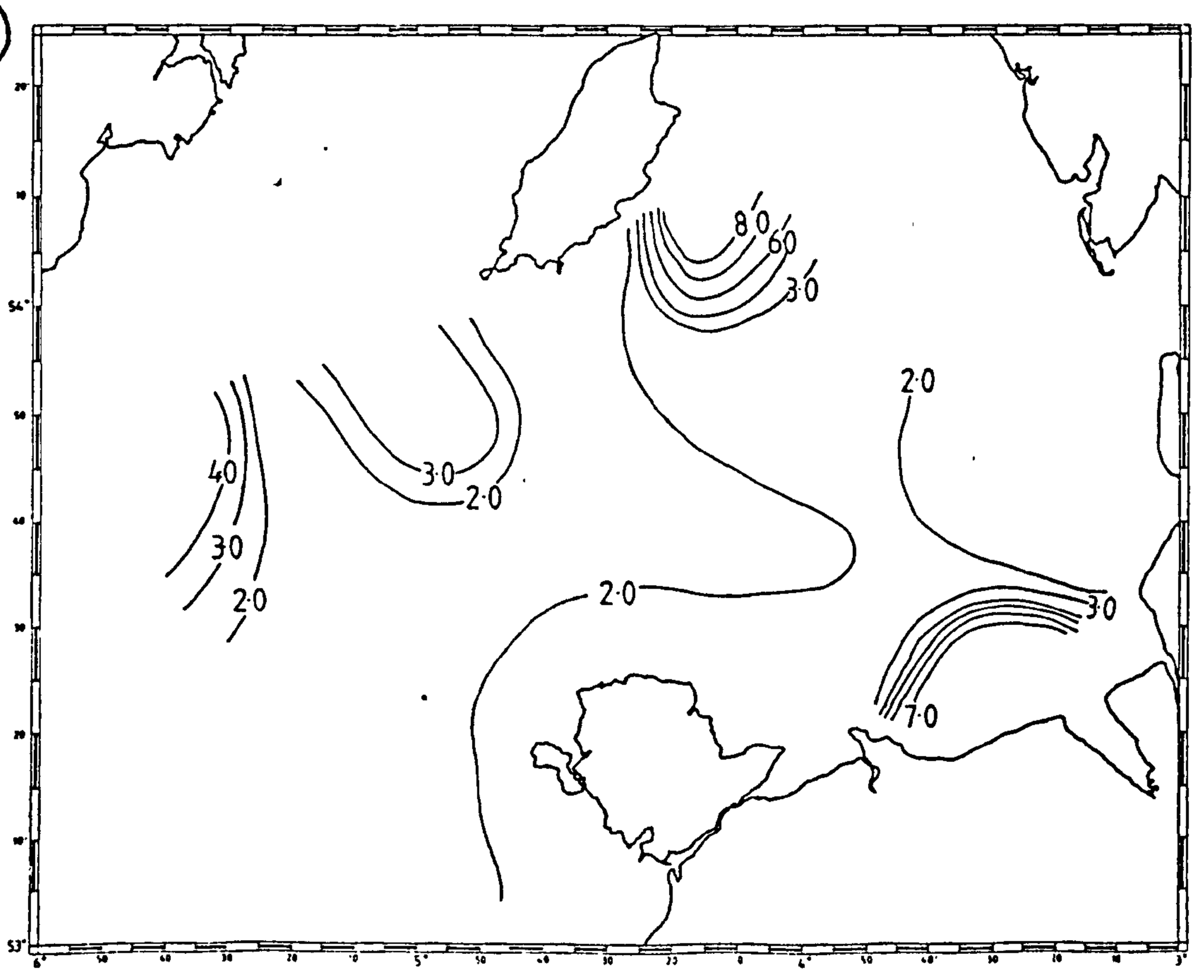

c)

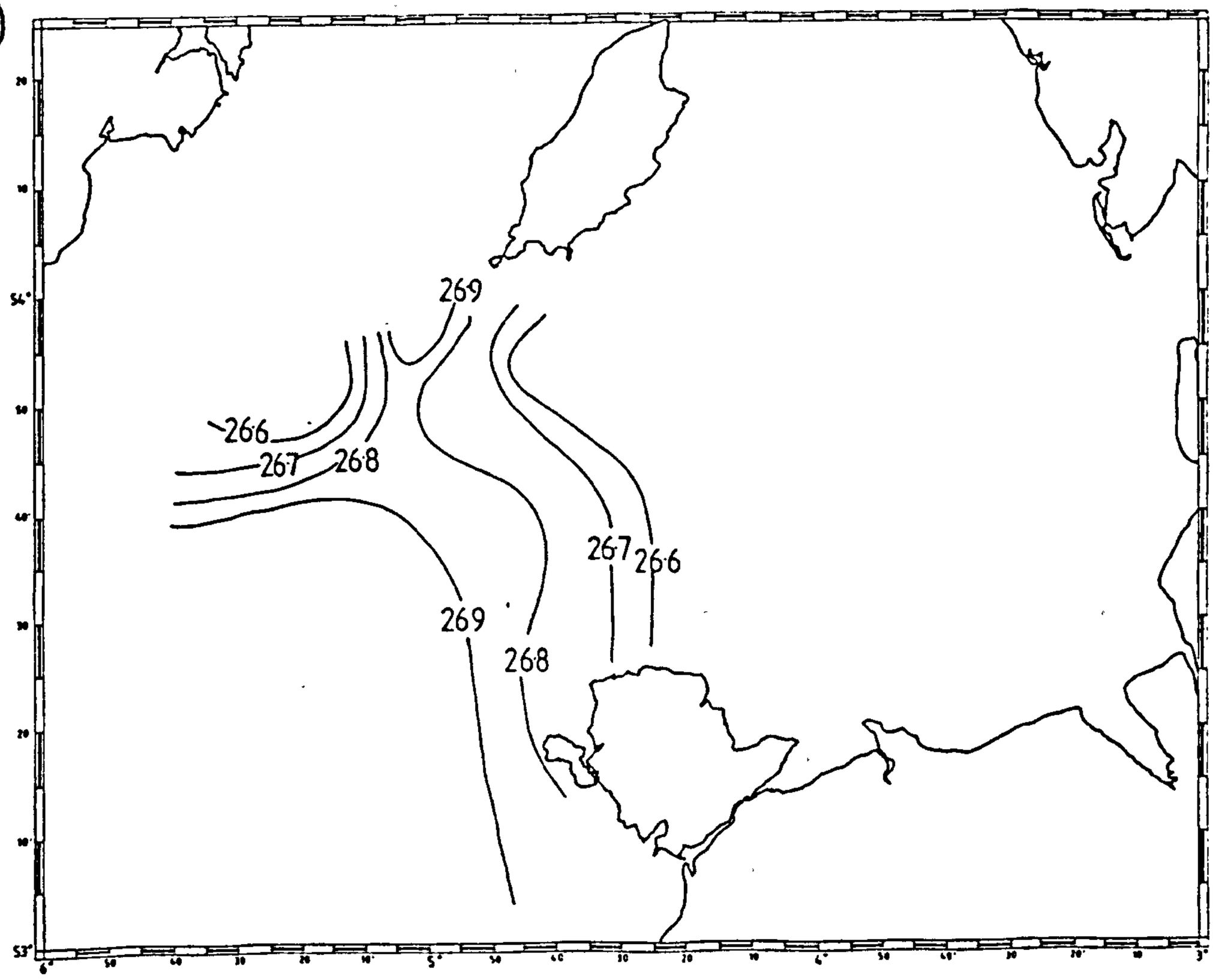

d)

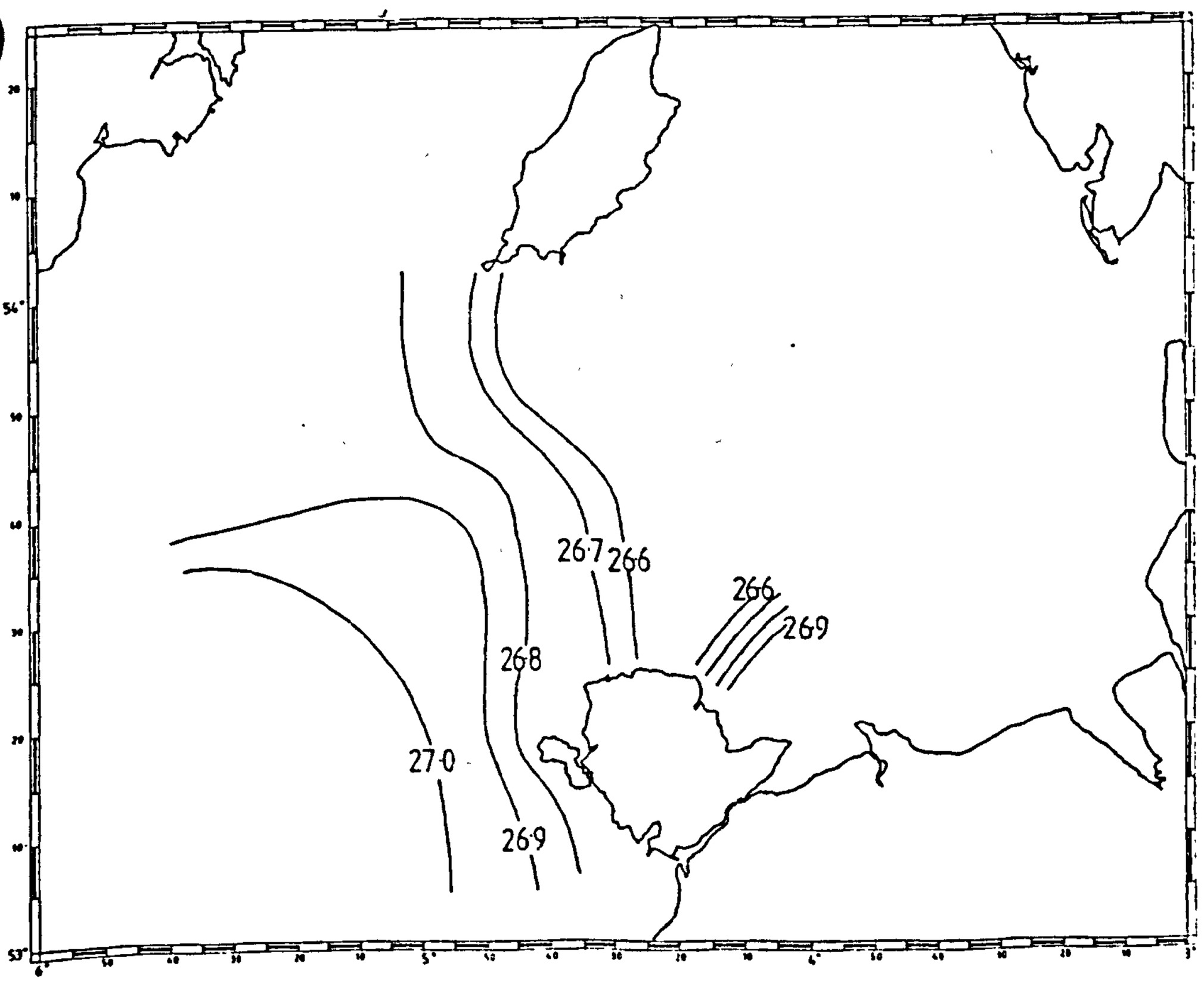

values of total SPM concentrations near the surface were in the range of 2 to 12 mgl^{-1}, and are shown in figure 5.3.

The surface distribution of c ,in March 1987, was similar to the characteristic pattern of sea-surface radiance in the CZCS imagery (Channels 1,2 and 3) from that time of year, an example of which is shown in figure 2.2., from 4/4/80. There is typically an isolated maximum in reflectance in the region centred on 53°40'N, 4° 40'W, and low values to the north-west and to the north-east of the region.

A sharp horizontal gradient south-west of the Isle of Man was oberved in the distribution of c at 5 m below the sea-surface, (Figure 5.2.). This a feature frequently observed in the CZCS images at this time of year (Figure 2.2.). A horizontal density gradient observed at the same location is in the region of the tidal mixing front of the western Irish Sea . The measurements of the distribution of sigma-t values in figure 5.2. do not extend east of 4°W due to a change in instrumentation during the cruise.

Near sea-bed values of c were observed to be high close to the coast of Anglesey (2 m^{-1}) , but were higher still in the western Irish Sea (WIS) ,Liverpool Bay and south-east of the Isle of Man (up to 7.0m^{-1}).

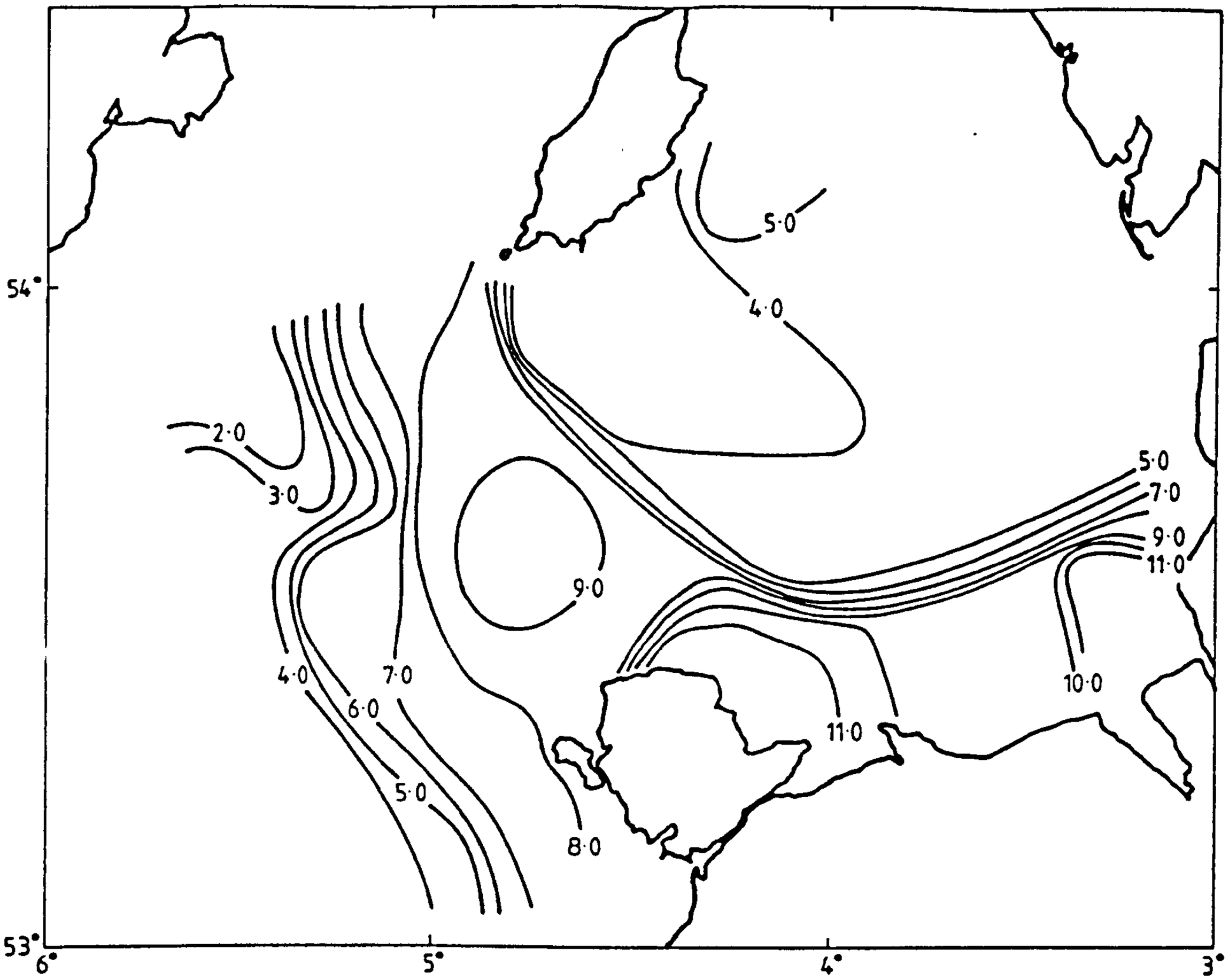

Figure 5.3. Distribution of SPM concentrations (mgl^{-1}) at 5 m below the surface during 30/3/87-4/4/87.

The spatial variation in c in early April is further illustrated by a section of vertical profiles of measurements of c from a transect of stations from A1 to A4, (shown in Figure 5.4.) . The location of the stations is shown in figure 5.1.b. A section of the vertical profile of sigma-t values is included in figure 5.4. Values of c and sigma-t were vertically uniform near the Anglesey coast (station A1). In the WIS (Station A4) there was a marked difference in c from the surface to the sea-bed, which was associated with a difference in sigma-t.

5.3. The CTD survey : Seasonal development of beam attenuation.

5.3.1. Horizontal distribution of beam attenuation in 1987.

There was a marked seasonal change in the values of c in 1987. This is illustrated by the series of distribution maps of c at 5m below the surface and at 5m above the sea-bed from the survey in 1987, shown in figures 5.2,5.5 to 5.9. in which the values of sigma-t are also presented. In order to obtain a coherent time series, the monthly surveys were always carried out at times close to neap tides. The tidal range in the survey area was up to 15km at spring tides, and up to 8km at neaps. Since the resolution of the survey grid was in the order of 10km, variations in the state of the tide at neaps did not significantly cause bias in the data.

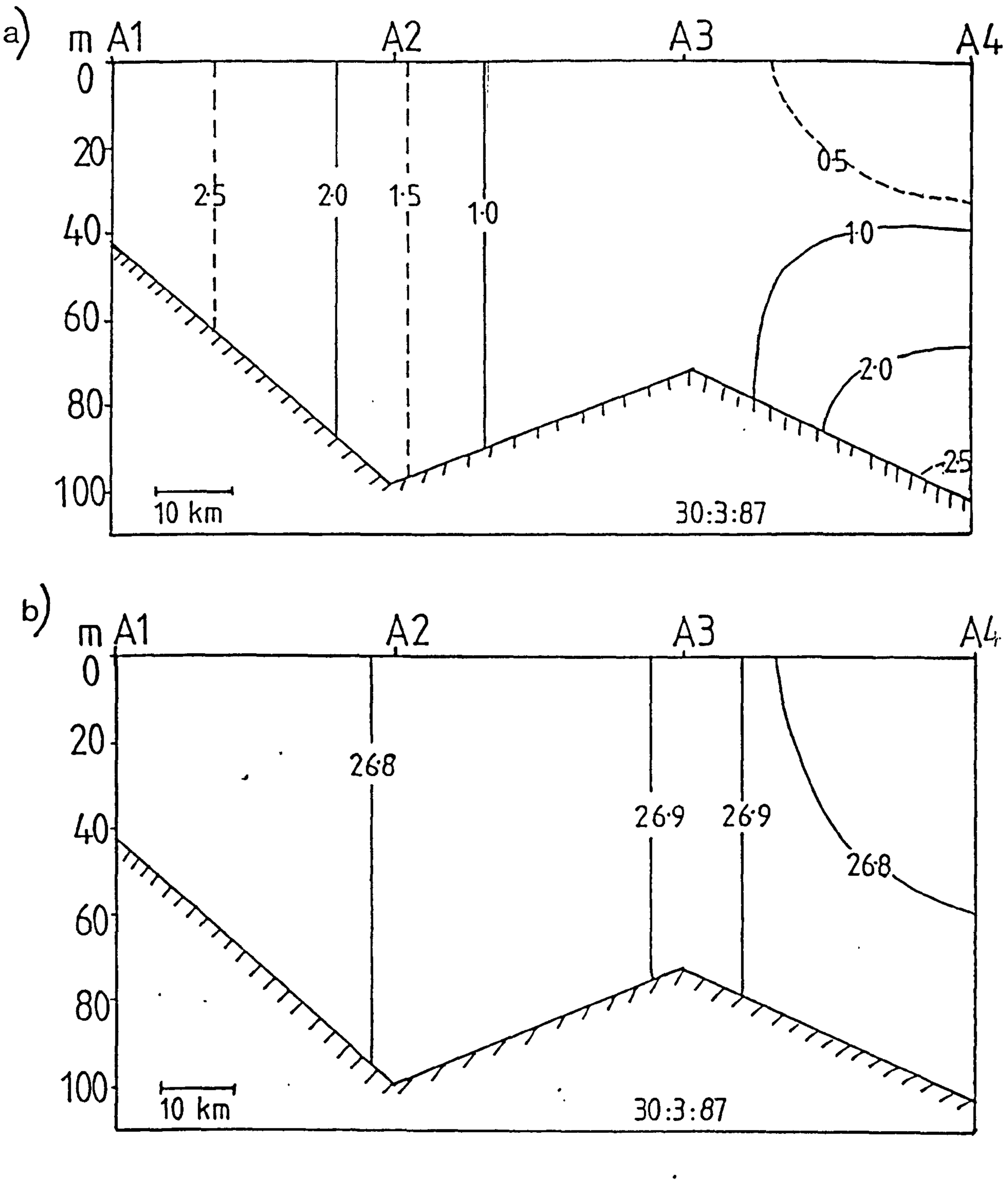

Figure 5.4. Section of vertical profiles of measurements of a) beam attenuation, b) sigma-t along transect A (figure 5.1.b)

The spatial distribution of c in early April 1987 has been described in section 5.2. Clearer water was associated with water of lower density near the surface in the western Irish Sea (WIS). There was a weak density front in the WIS.

During May (figure 5.5.) there were generally lower values of c in the whole region than in early April.In addition to the WIS front, a second density front had formed running from north Anglesey towards the Lancashire coast. While there were low values of c in the less dense surface water in the WIS, there were high values of c in the less dense water to the south of the front east of Anglesey.

There were lower values of c in the central part of the survey area in late June (figure 5.6), but values of c in the deep water in the WIS and to the north-east of the region were higher than during May. The horizontal density difference across the survey area was 1.5 sigma-t units.

In early August (figure 5.7.) the distribution of c was relatively unchanged from the previous cruise, but the gradient in sigma-t had increased to 2.0, due to the increase in temperature of the shallow water in the east.

Surface values of c in early September (figure 5.8) were higher than during August near the Anglesey coast, and in the deep water in the WIS. There was an area of relatively less dense water north-east of Anglesey.

Figure 5.5. Survey during 11/5/87-15/5/87.
a) Beam attenuation (m^{-1}) at 5m below the surface.
b) Beam attenuation (m^{-1}) at 5 m above the sea-
c) Sigma-t at 5m above the surface.
d) Sigma-t at 5m above the sea-bed.

a)

b)

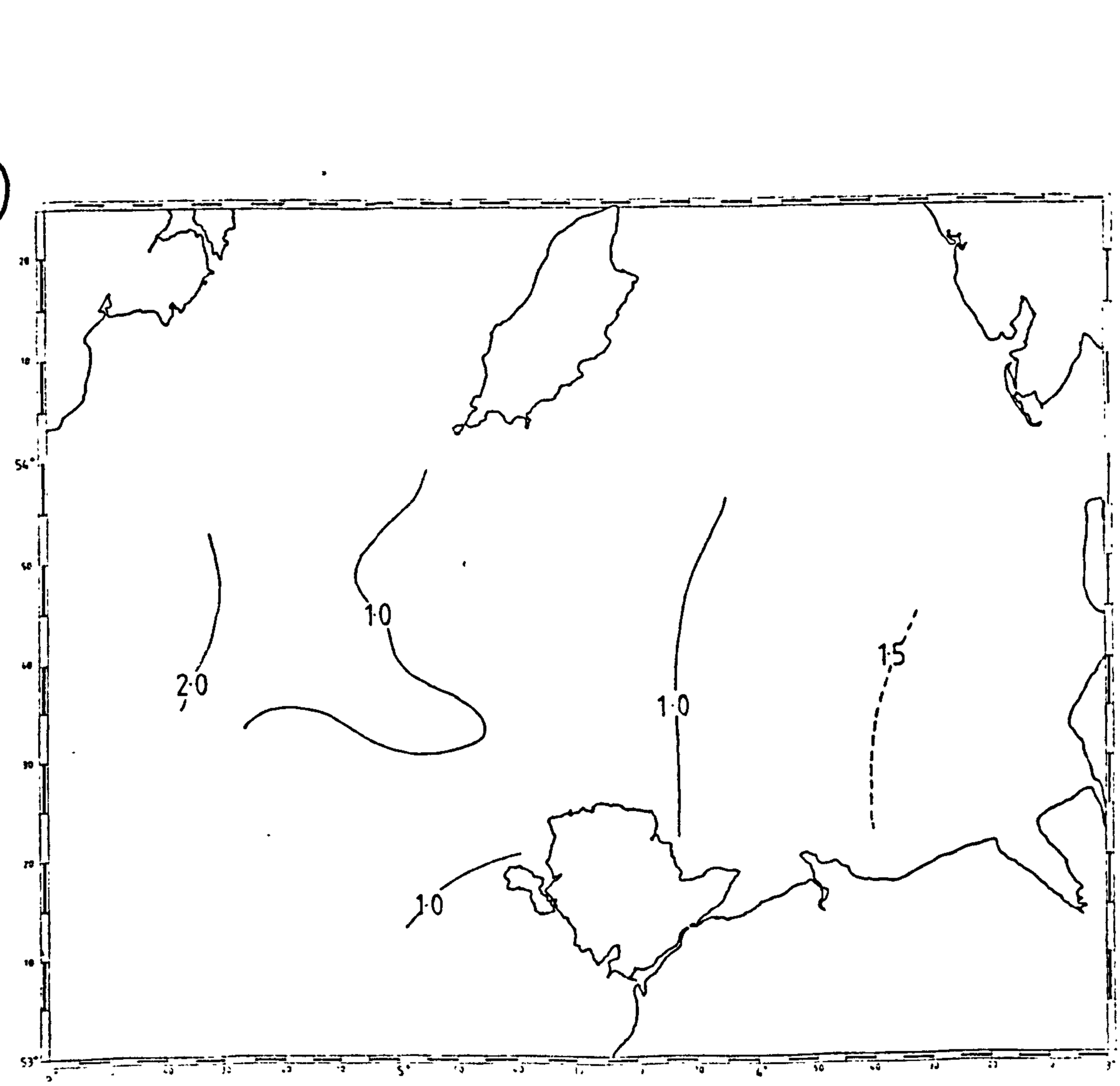

c)

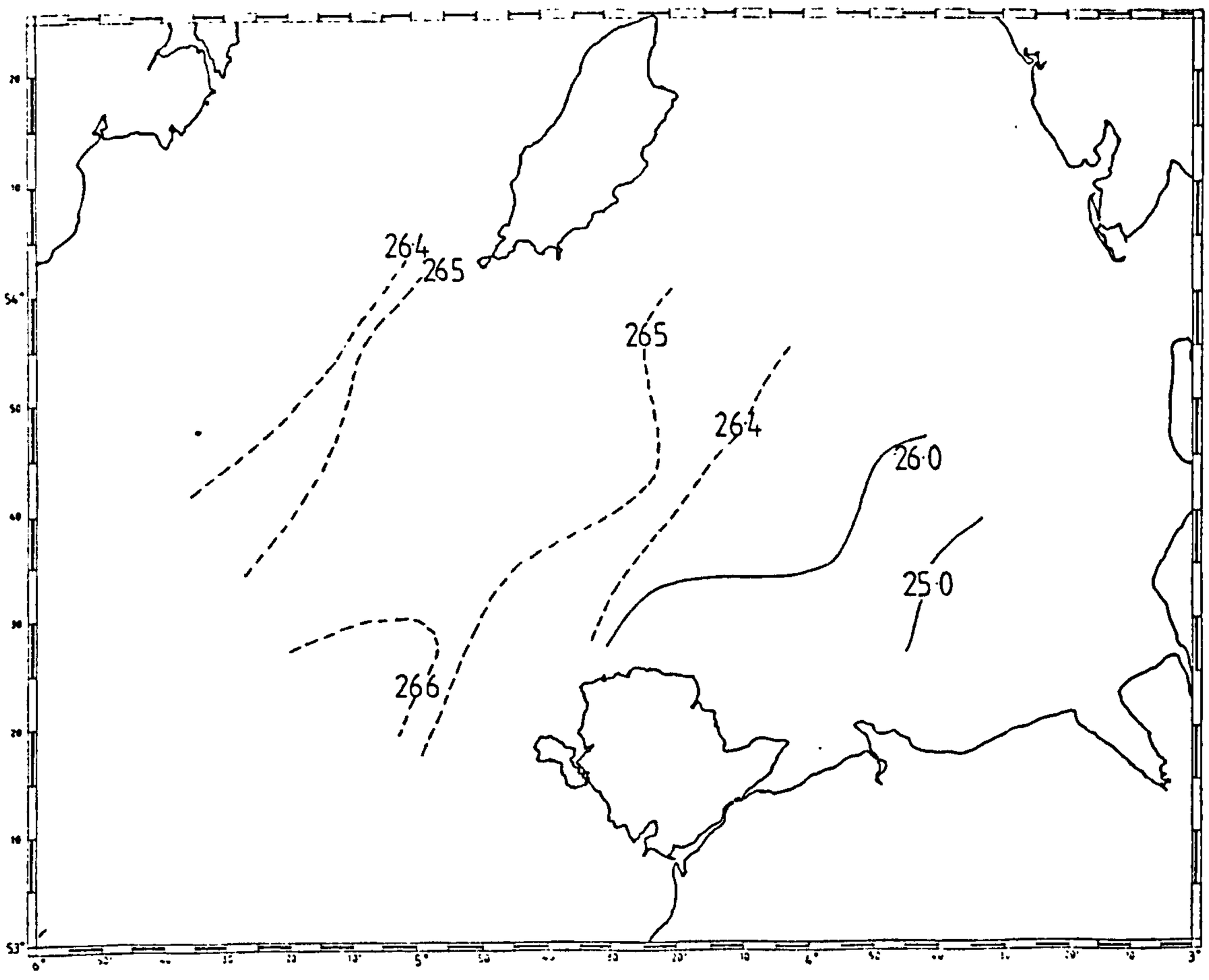

d)

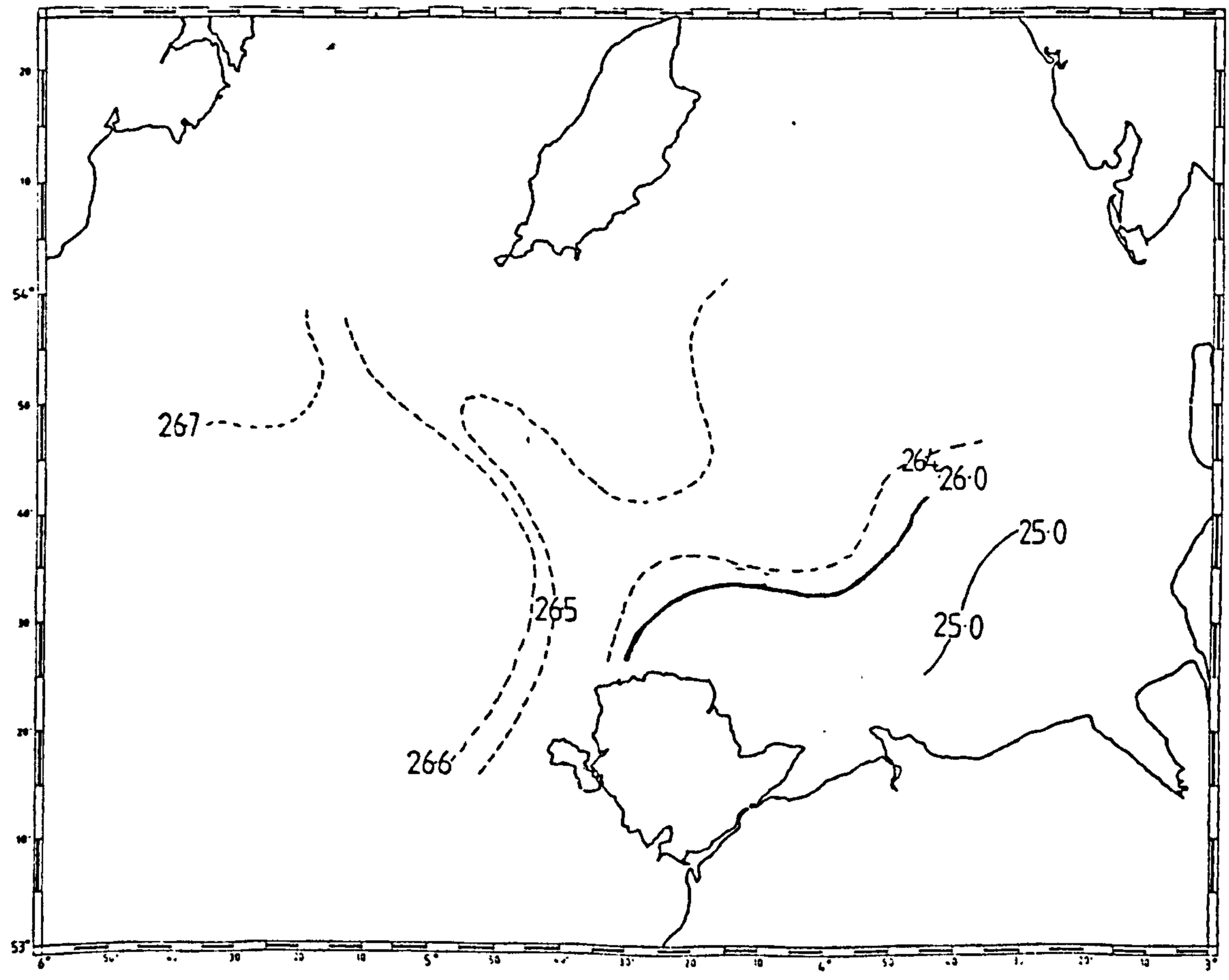

Figure 5.6. Survey during 29/6/87-3/7/87.
a) Beam attenuation (m^{-1}) at 5m below the surface.
b) Beam attenuation (m^{-1}) at 5m above the sea-bed.
c) Sigma-t at 5m below the surface.
d) Sigma-t at 5m above the sea-bed.

a)

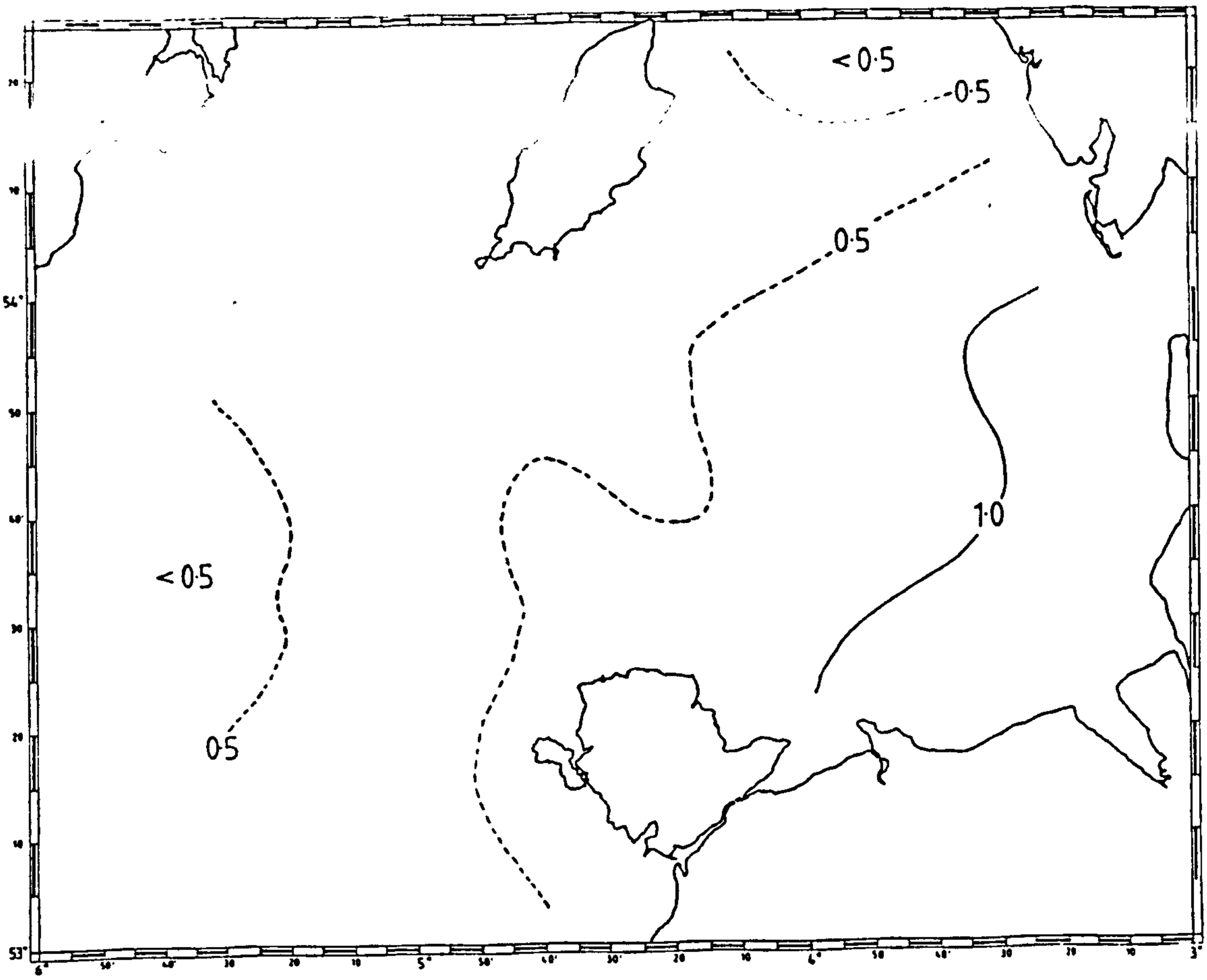

b)

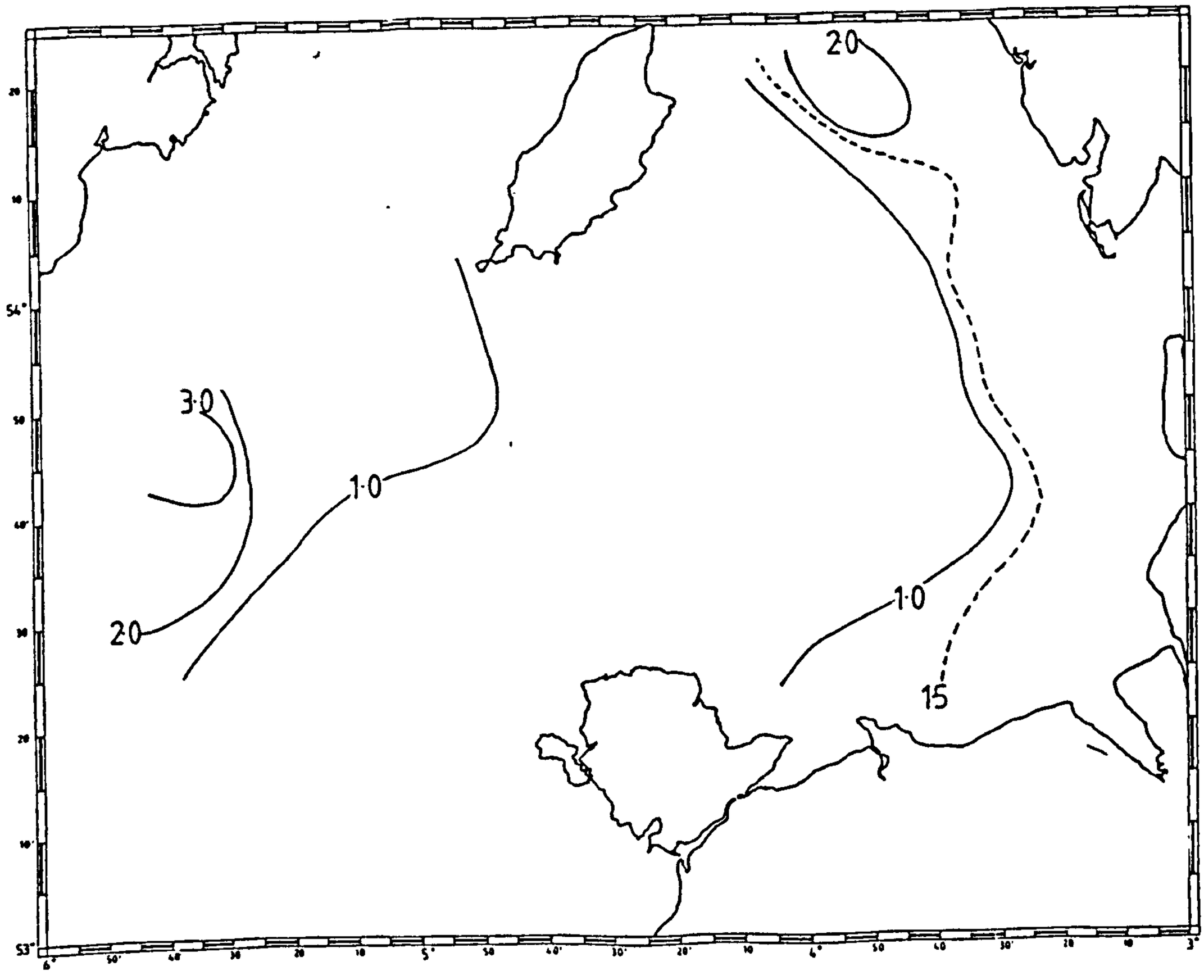

c)

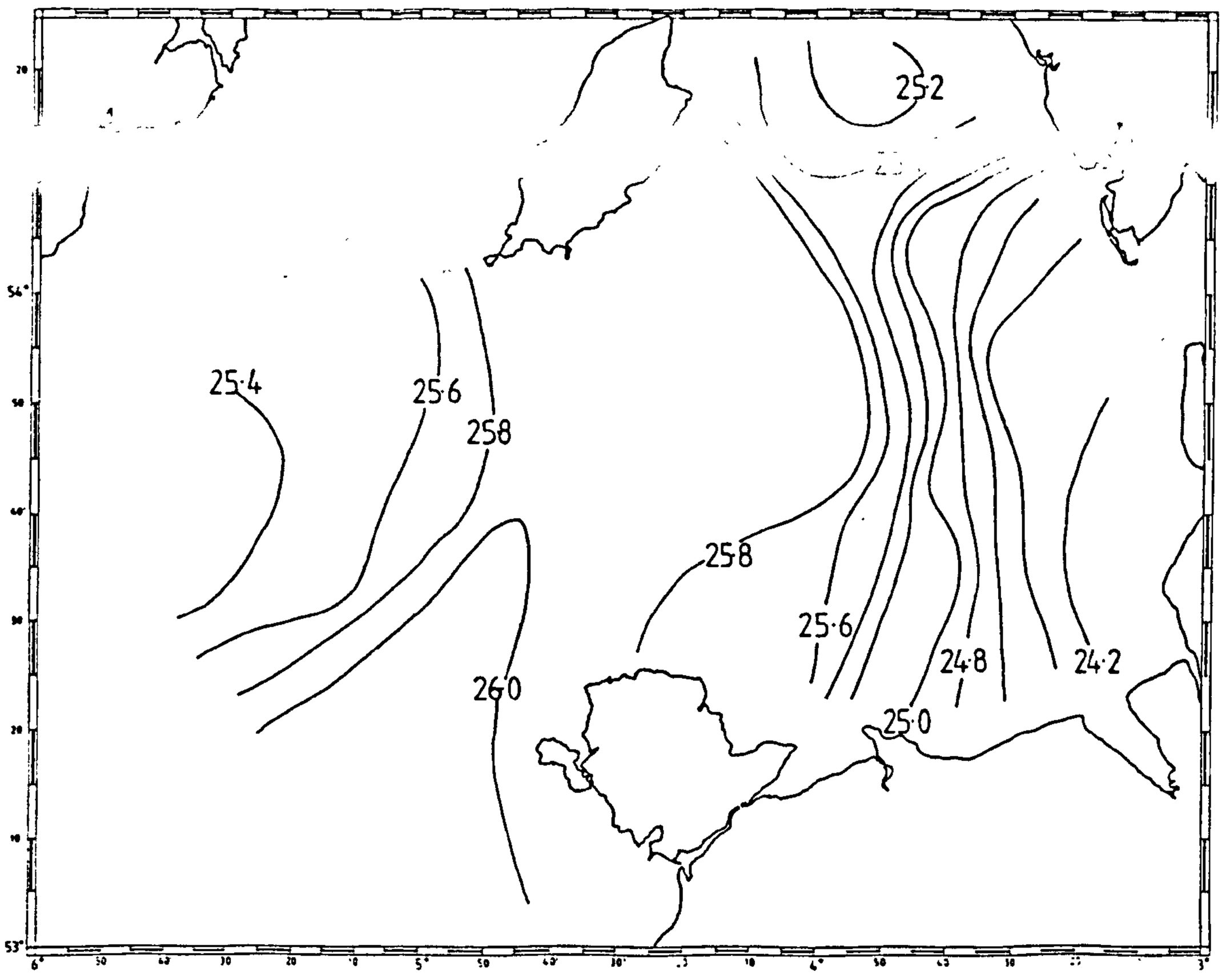
25·2
25·4
25·6
25·8
26·0
25·8
25·6
24·8
24·2
25·0

d)

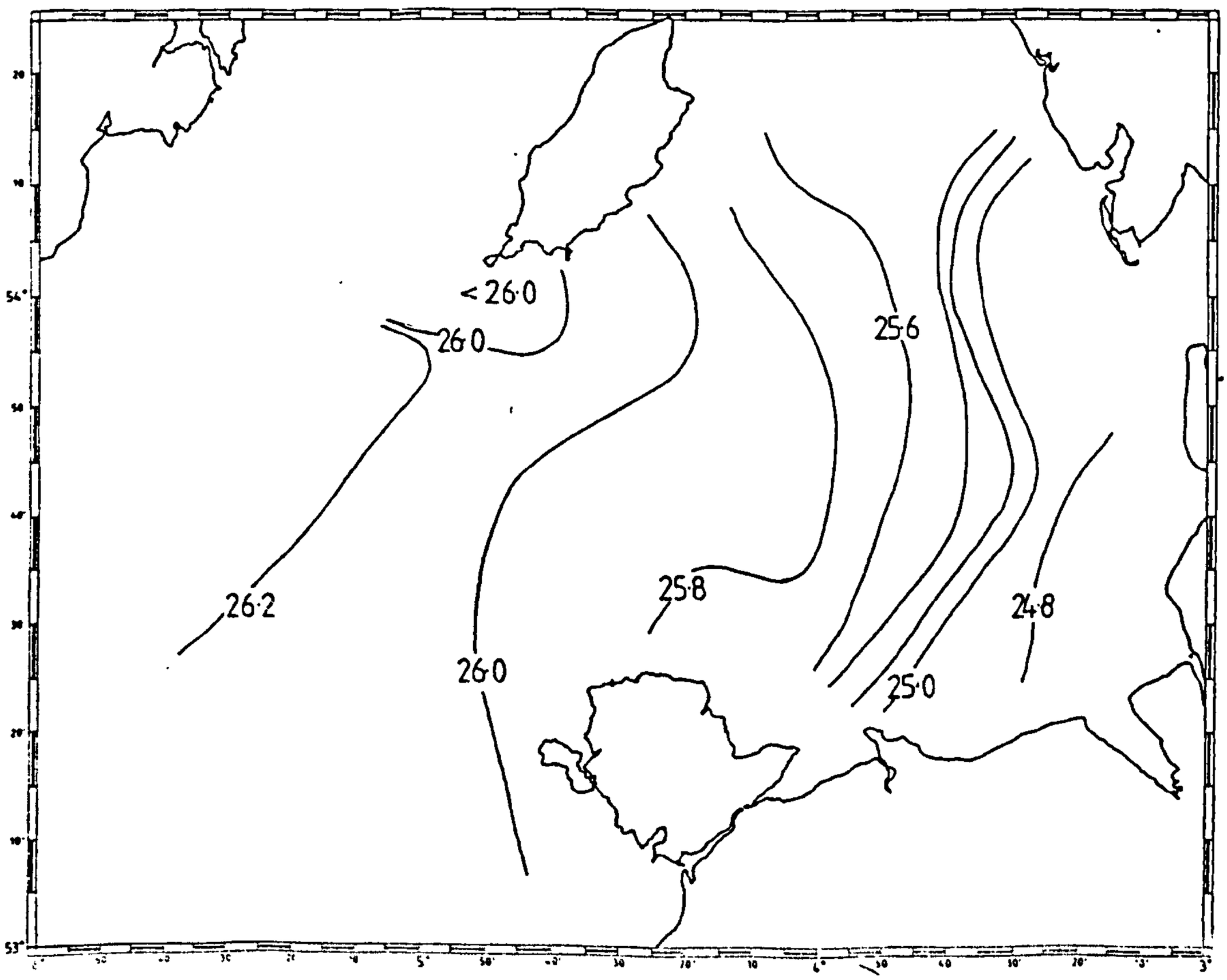
< 26·0
26·0
25·6
26·2
25·8
24·8
26·0
25·0

Figure 5.7. Survey during 3/8/87-7/8/87.
a) Beam attenuation (m^{-1}) at 5m below the surface.
b) Beam attenuation (m^{-1}) at 5m above the sea-bed.
c) Sigma-t at 5m below the surface.
d) Sigma-t at 5m above the sea-bed.

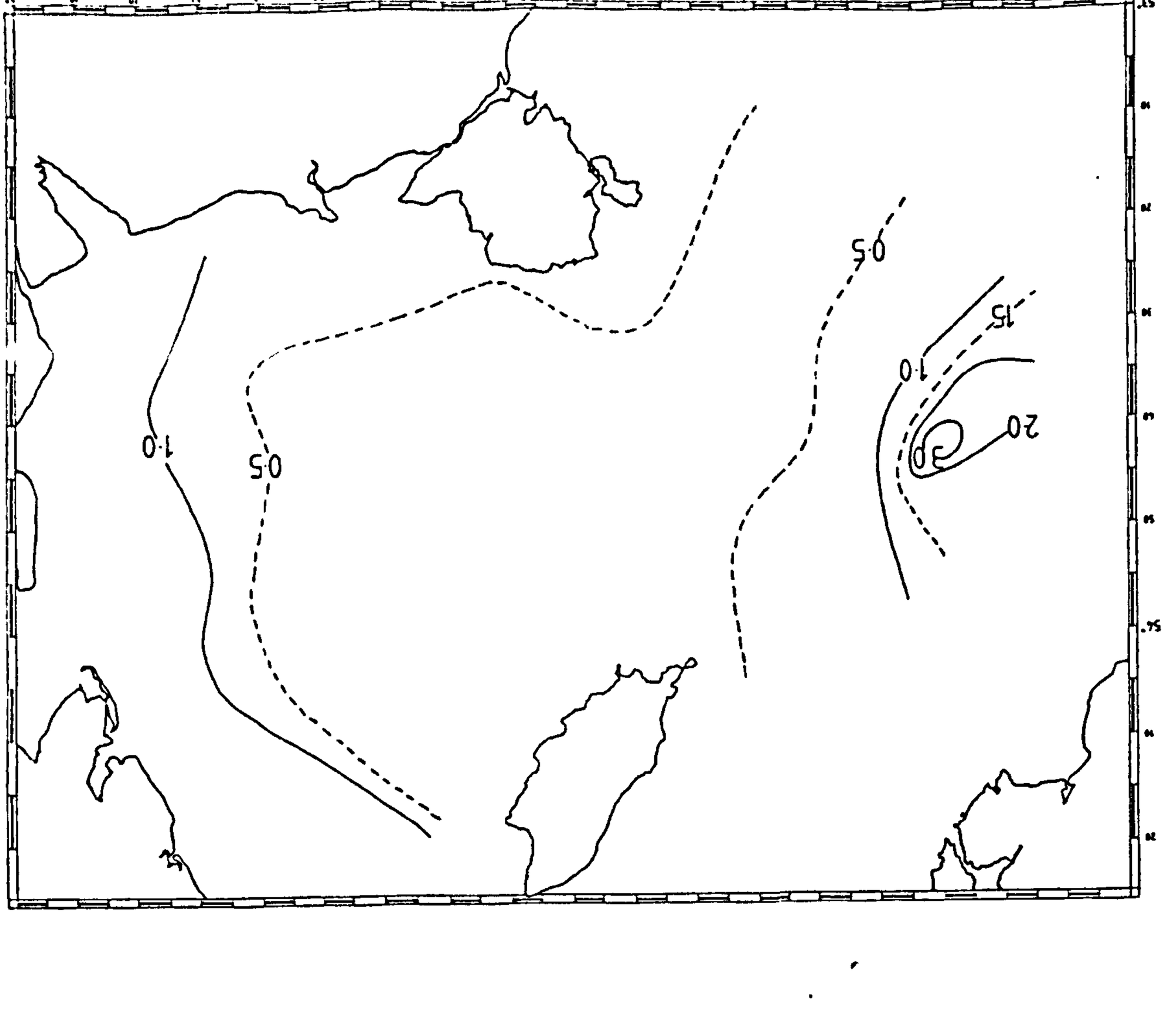
1·0
0·5
0·5
1·0
15
20
30
0·5
(a)

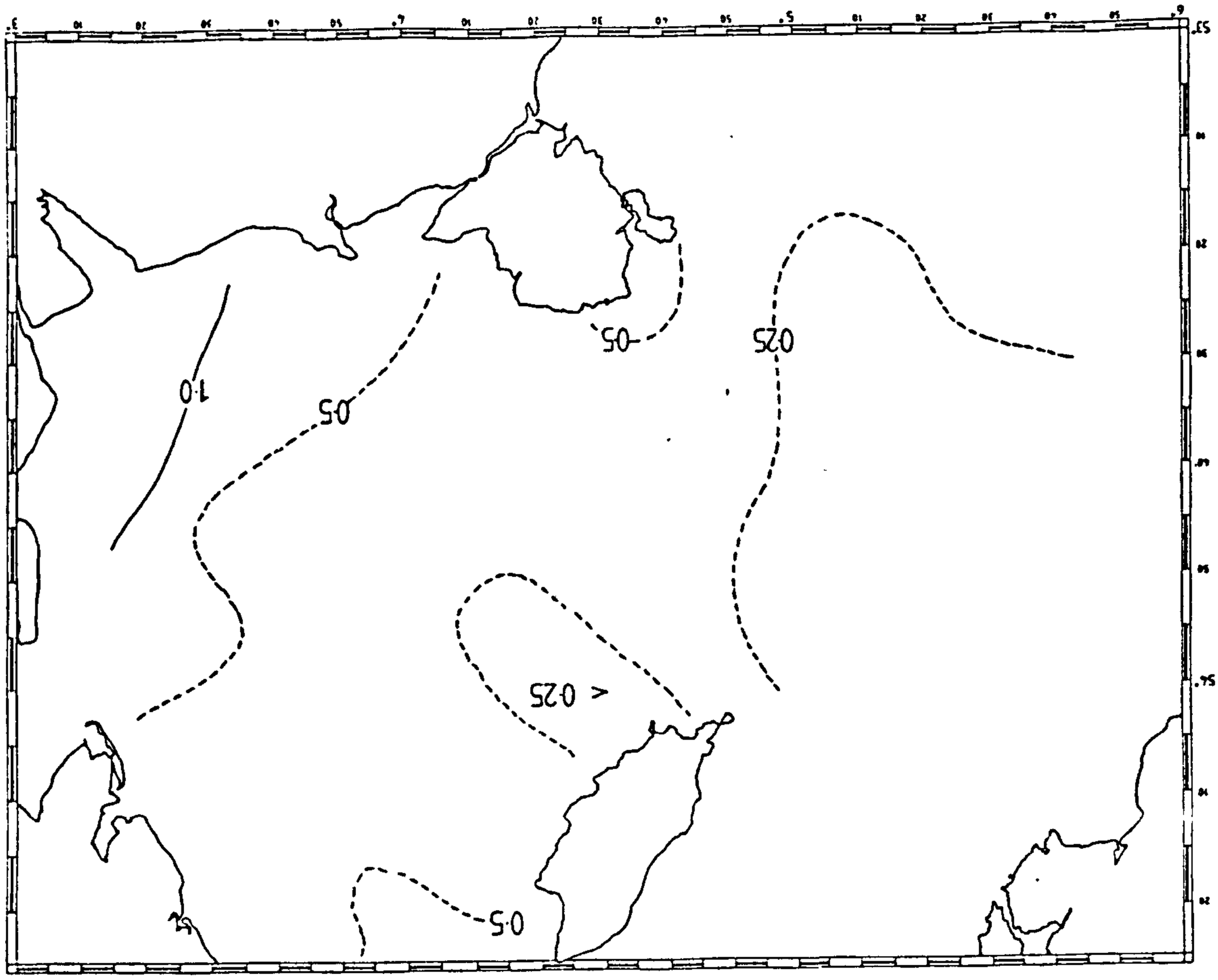
1·0
0·5
0·5
0·25
< 0·25
0·5
(b)

c)

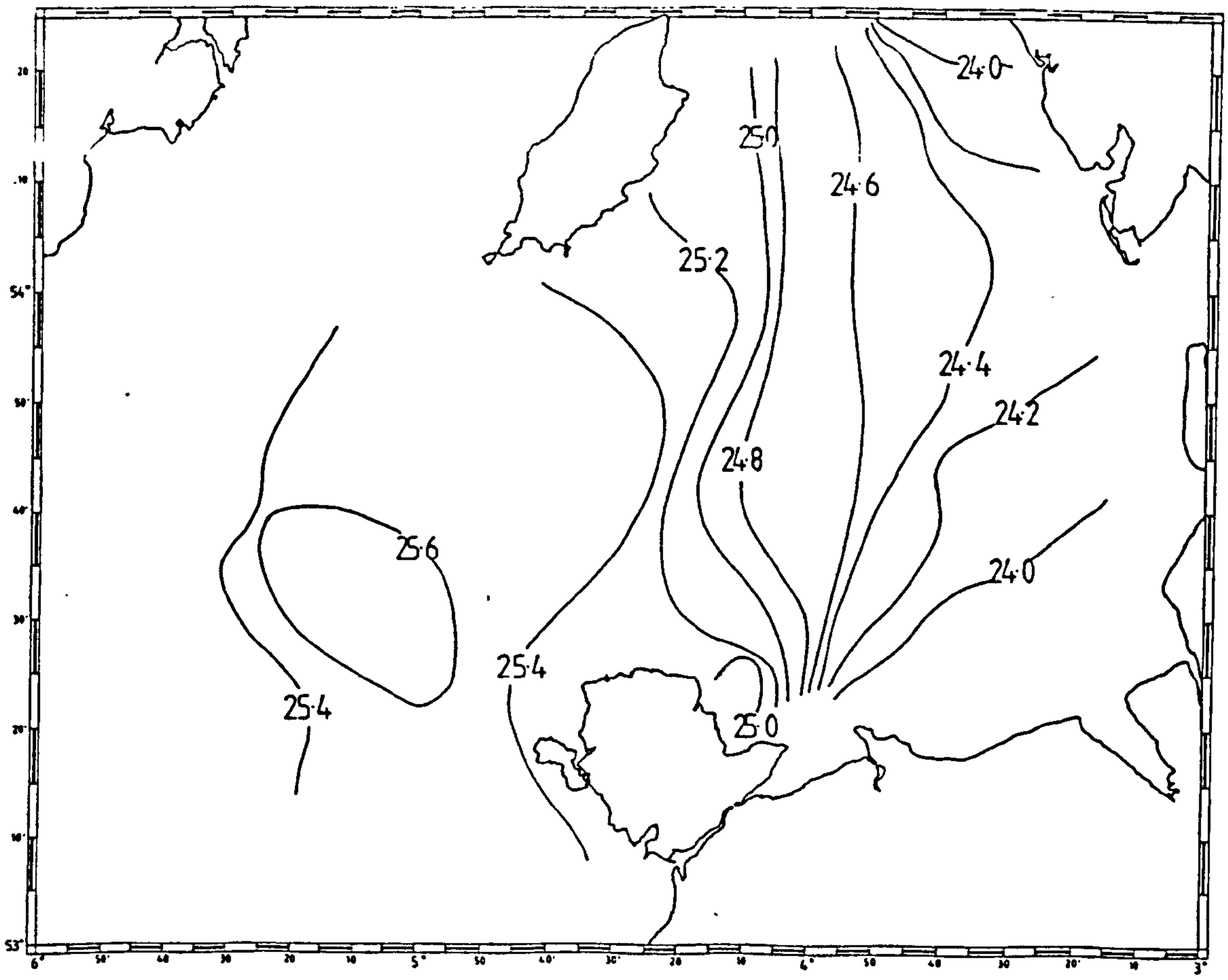
25·0
24·6
24·0
25·2
24·4
24·2
24·8
25·6
24·0
25·4
25·4
25·0

d)

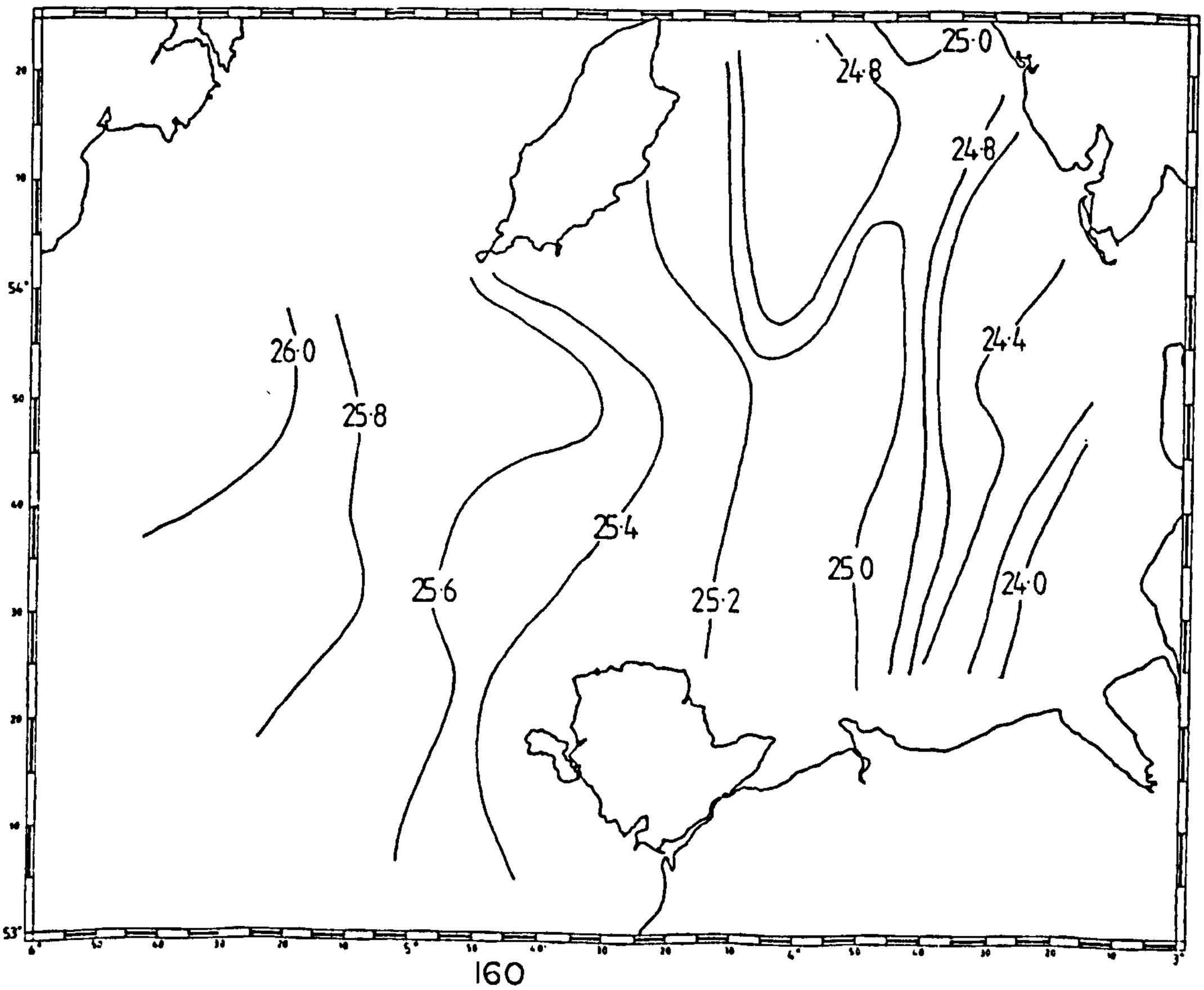
25·0
24·8
24·8
26·0
24·4
25·8
25·4
25·6
25·2
25·0
24·0

Figure 5.8. Survey from 7/9/87-11/9/87.
a) Beam attenuation (m^{-1}) at 5m below the surface.
b) Beam attenuation (m^{-1}) at 5m above the sea-bed.
c) Sigma-t at 5m below the surface.
d) Sigma-t at 5m above the sea-bed.

a)

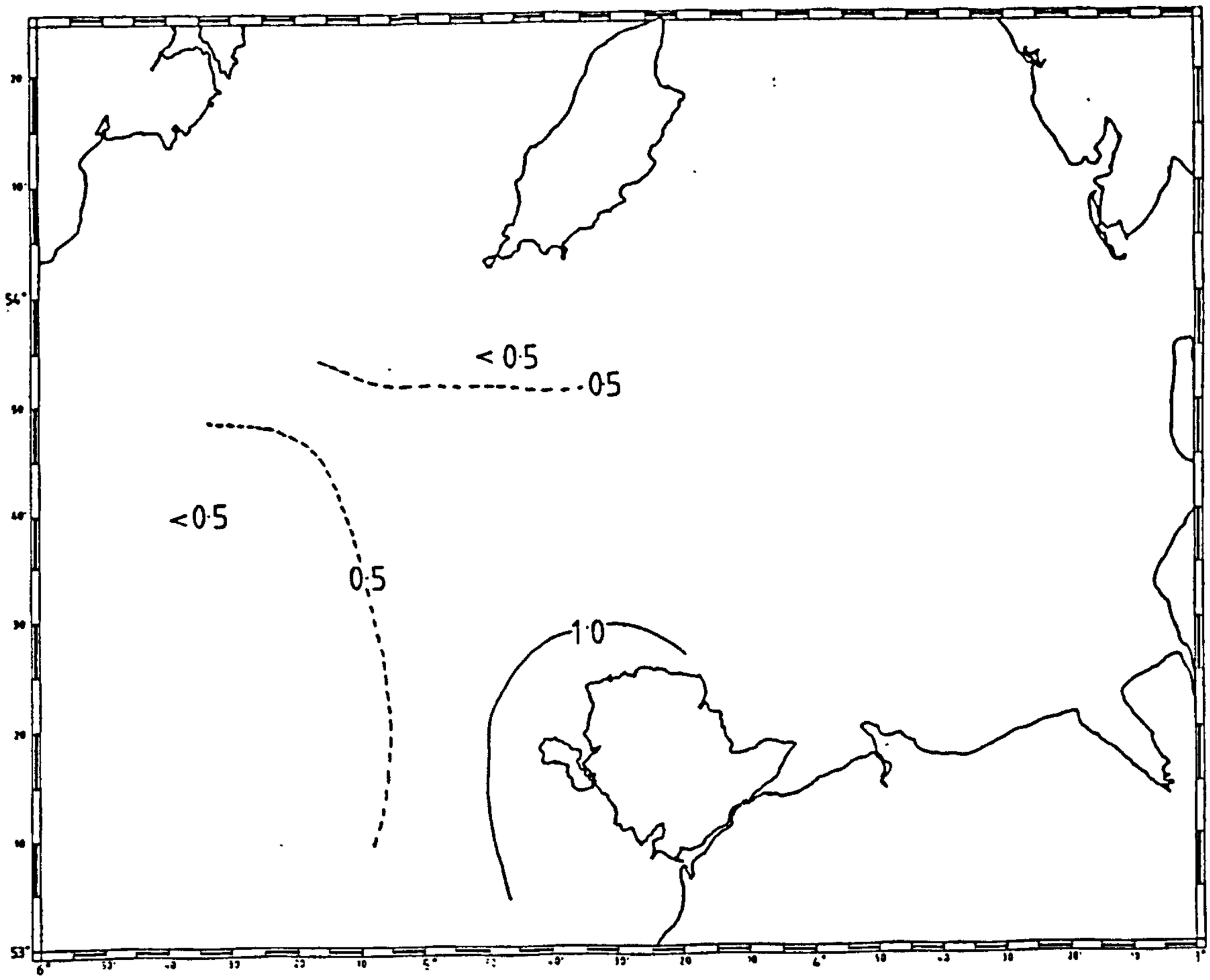

b)

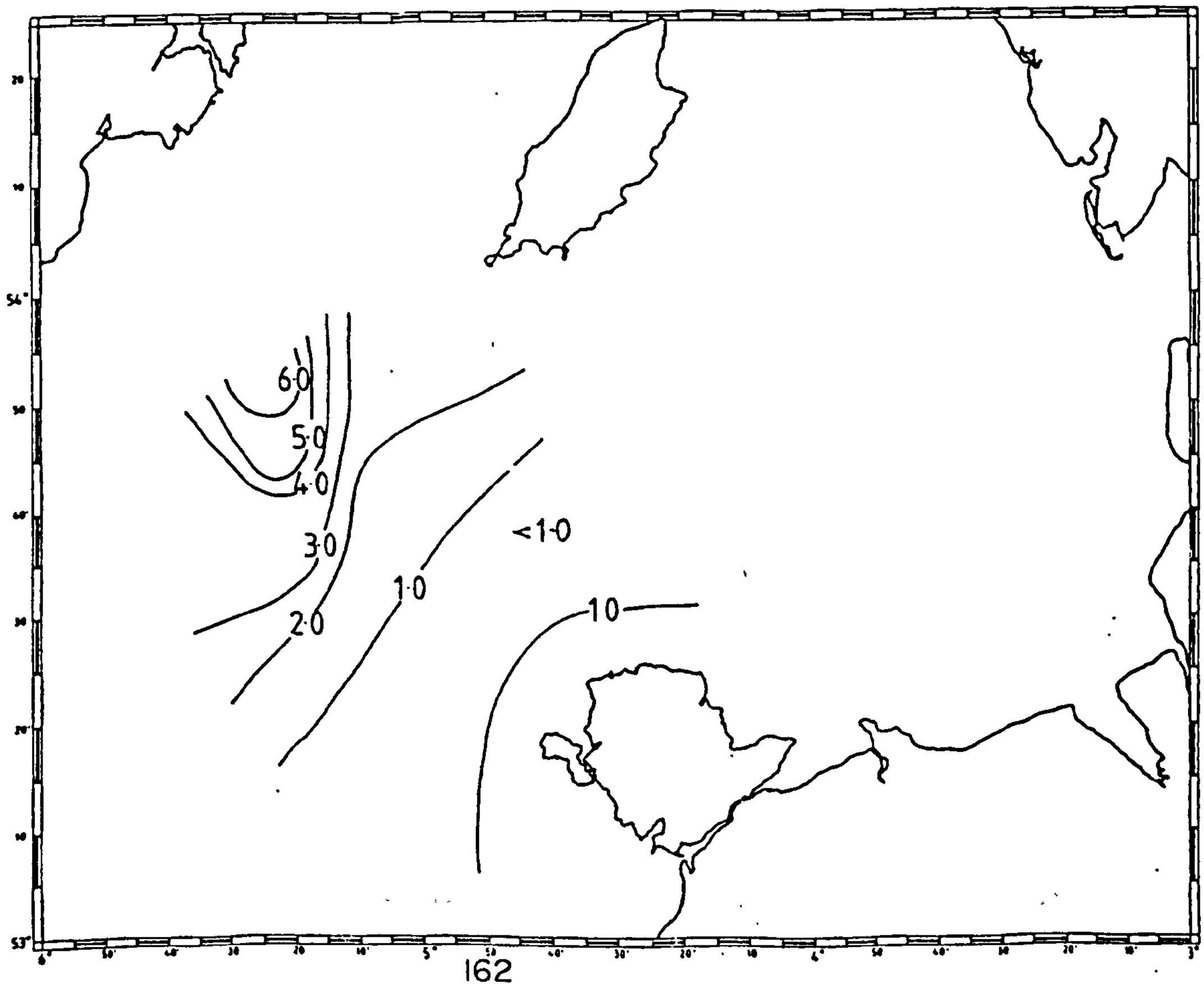

c)

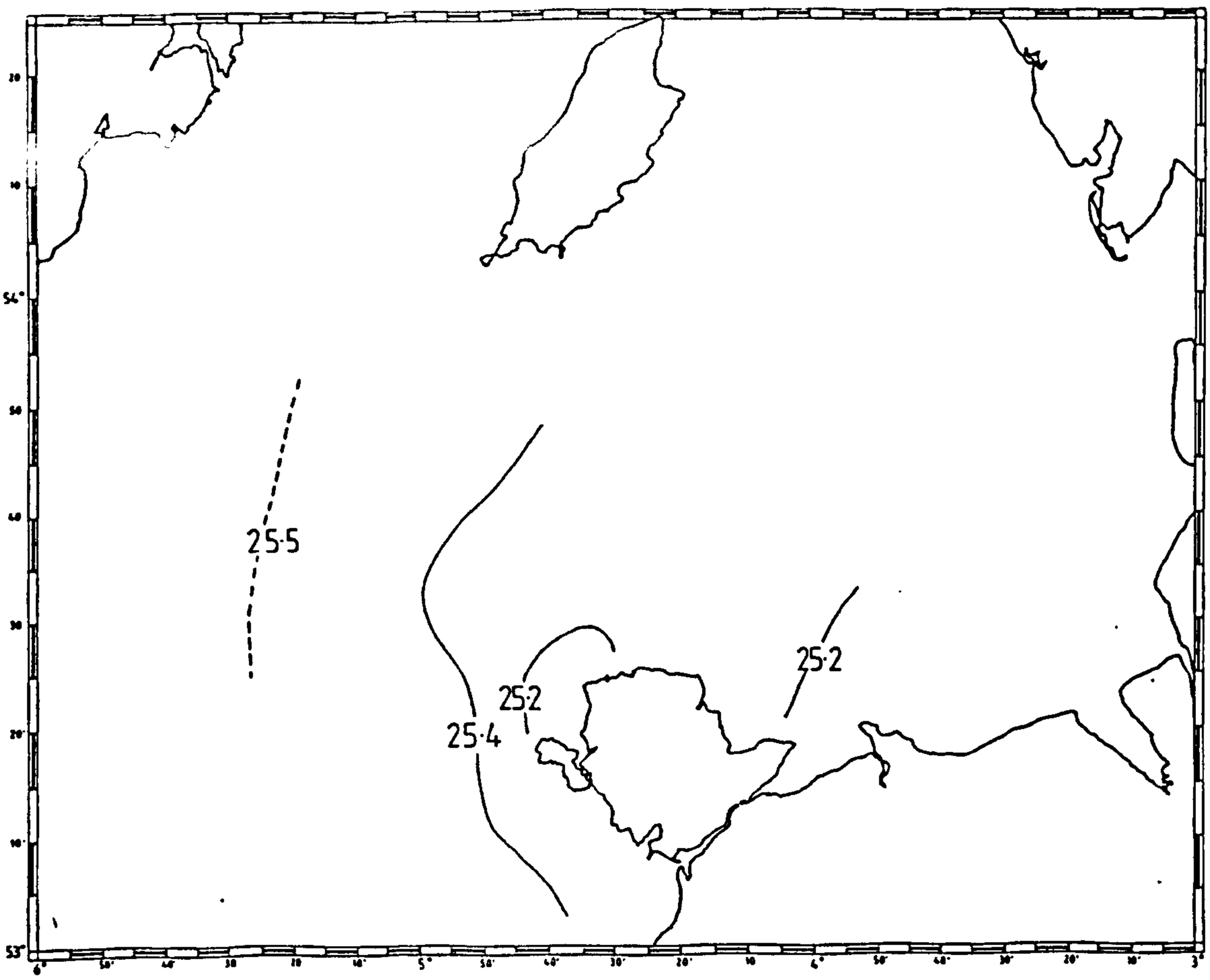

d)

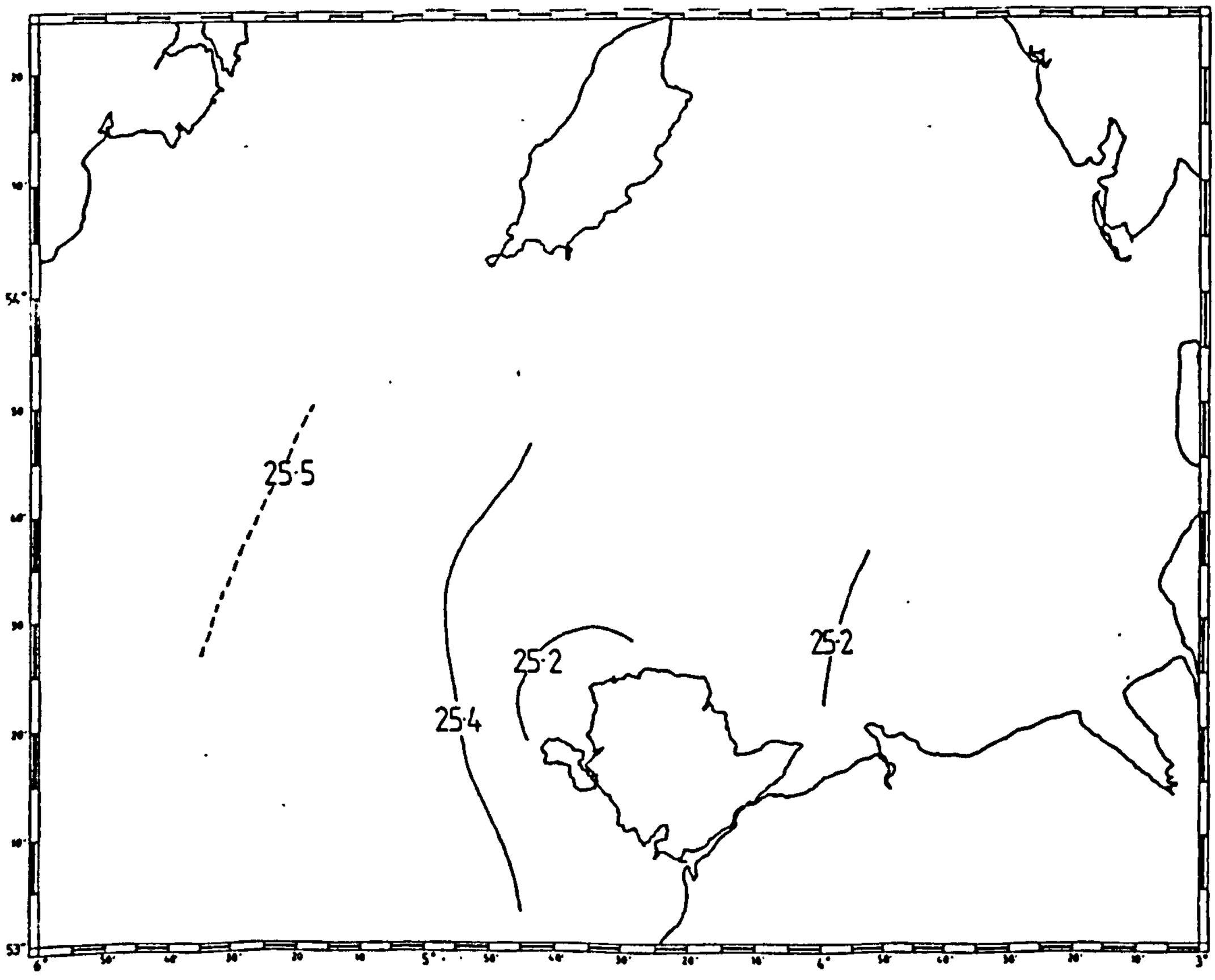

Figure 5.9. Survey from 12/10/87-16/10/87.
a) Beam attenuation (m^{-1}) at 5m below the surface.
b) Beam attenuation (m^{-1}) at 5m above the sea-bed.
c) Sigma-t at 5m below the surface.
d) Sigma-t at 5m above the sea-bed.

a)

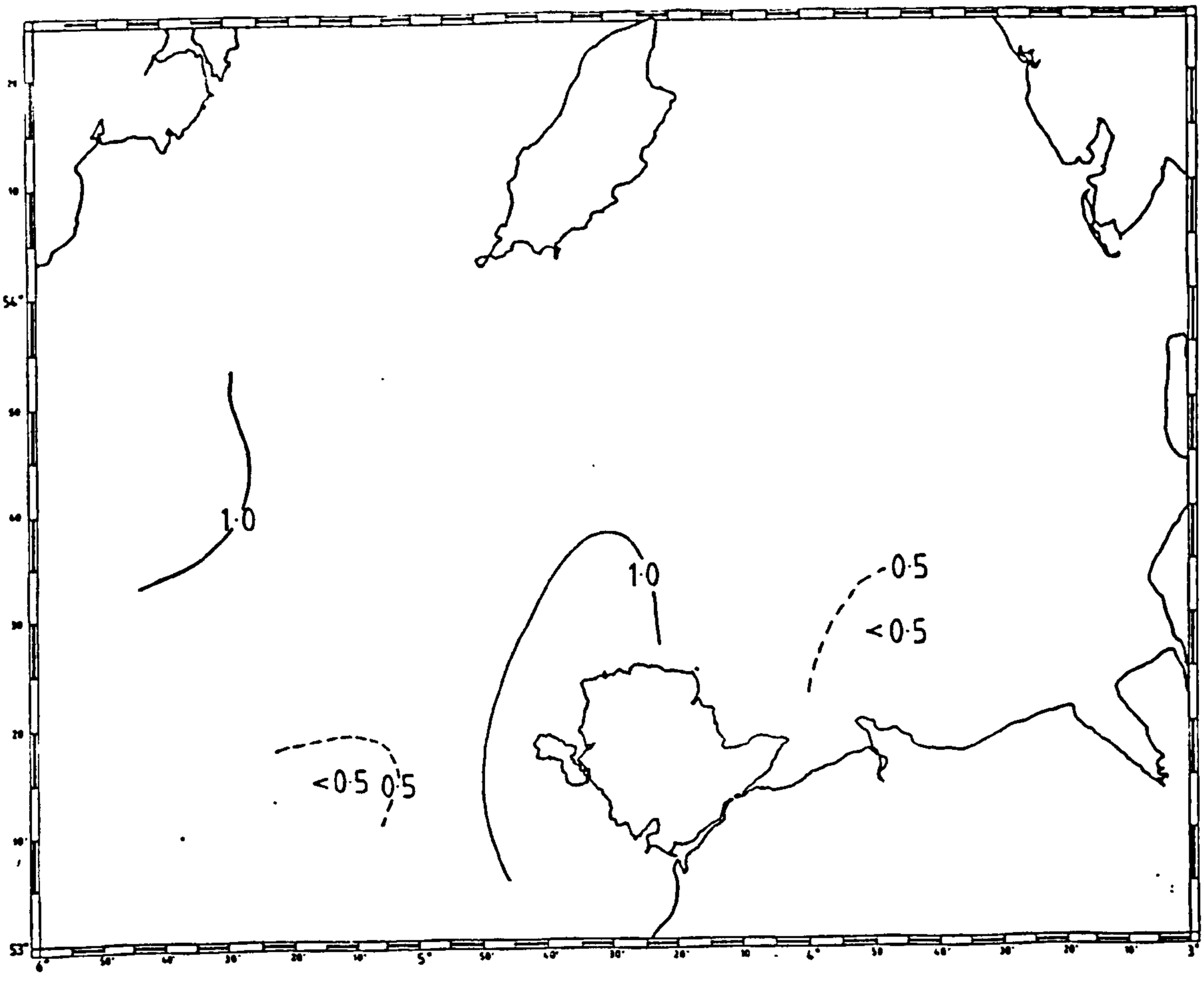

b)

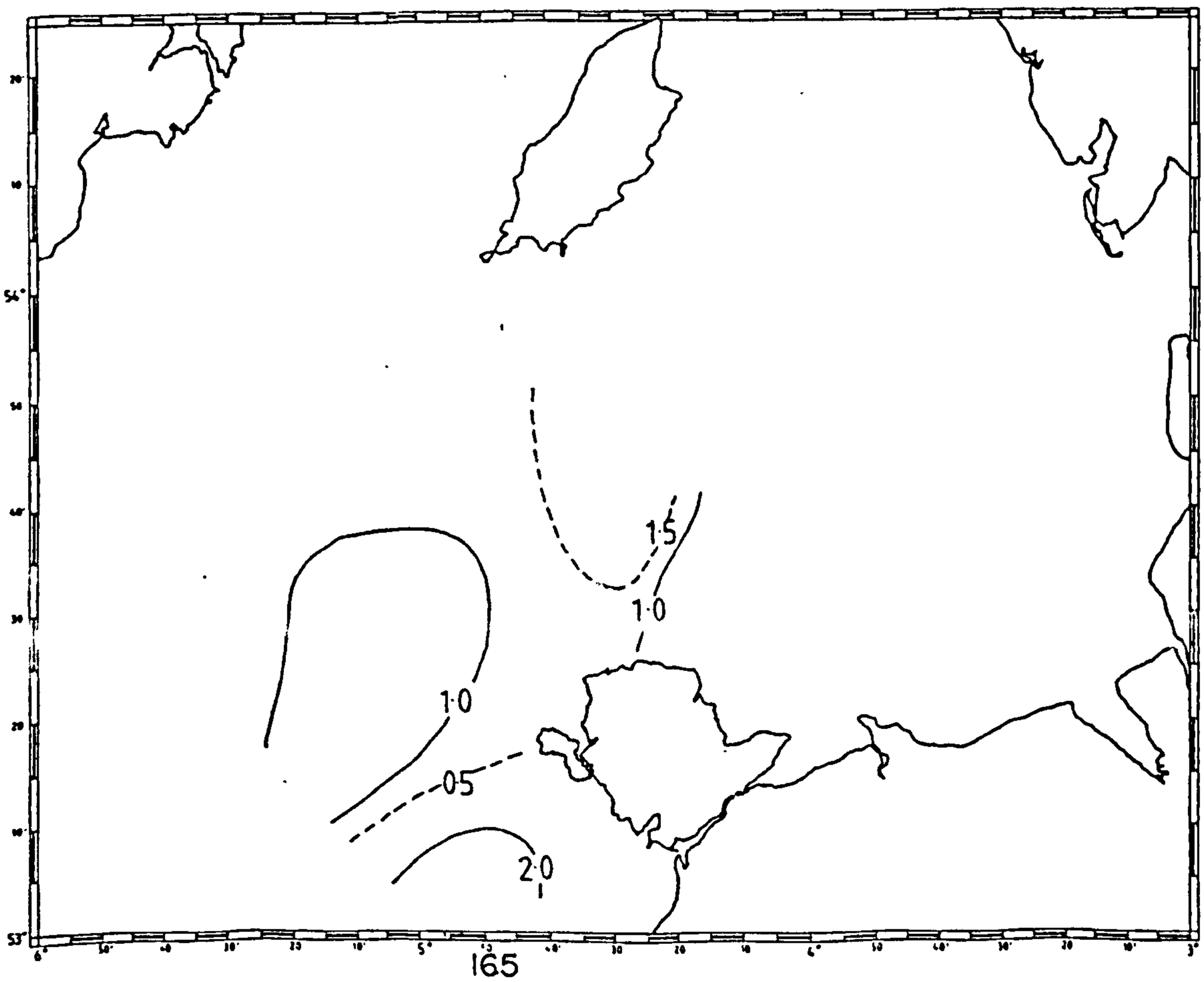

c)

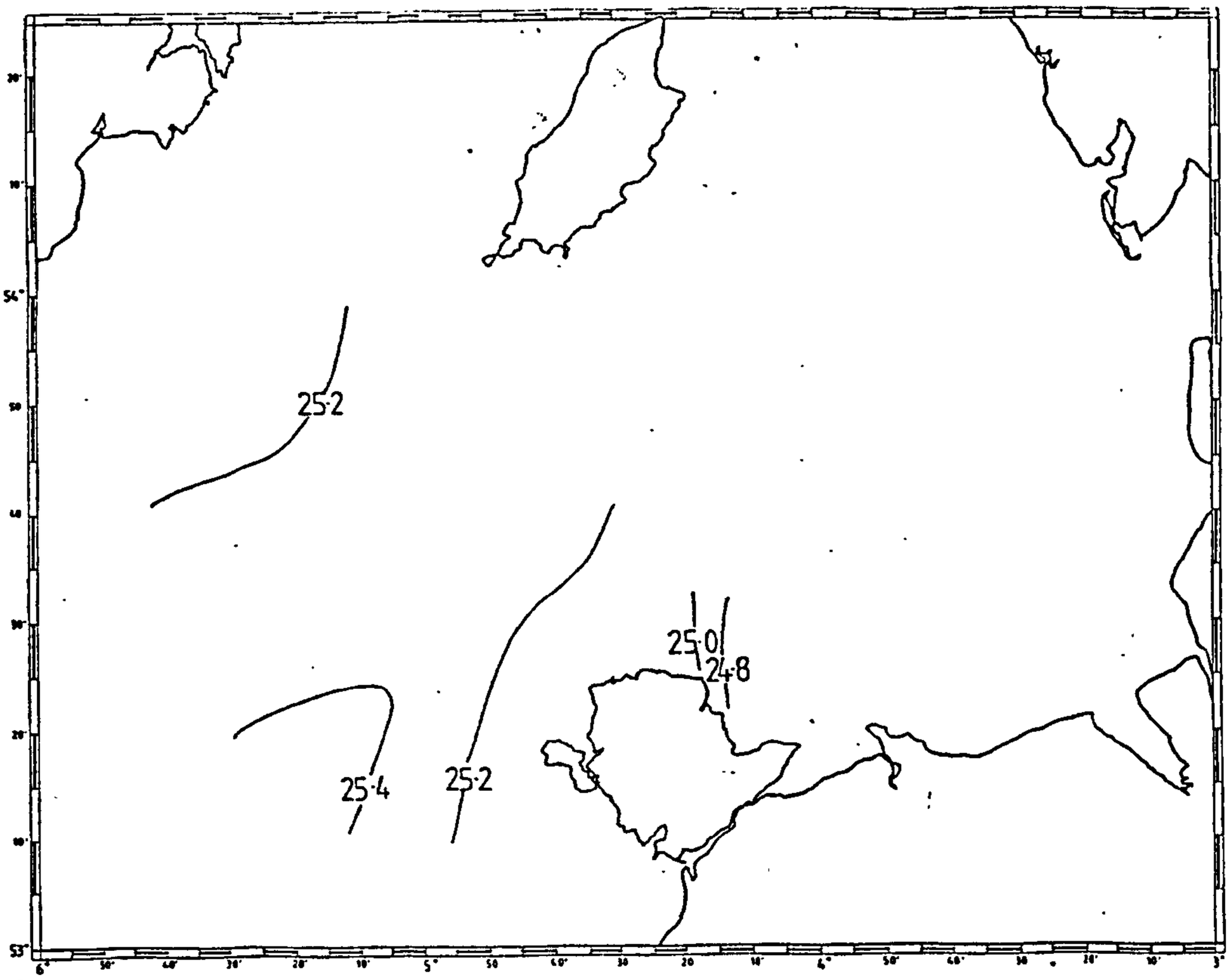

d)

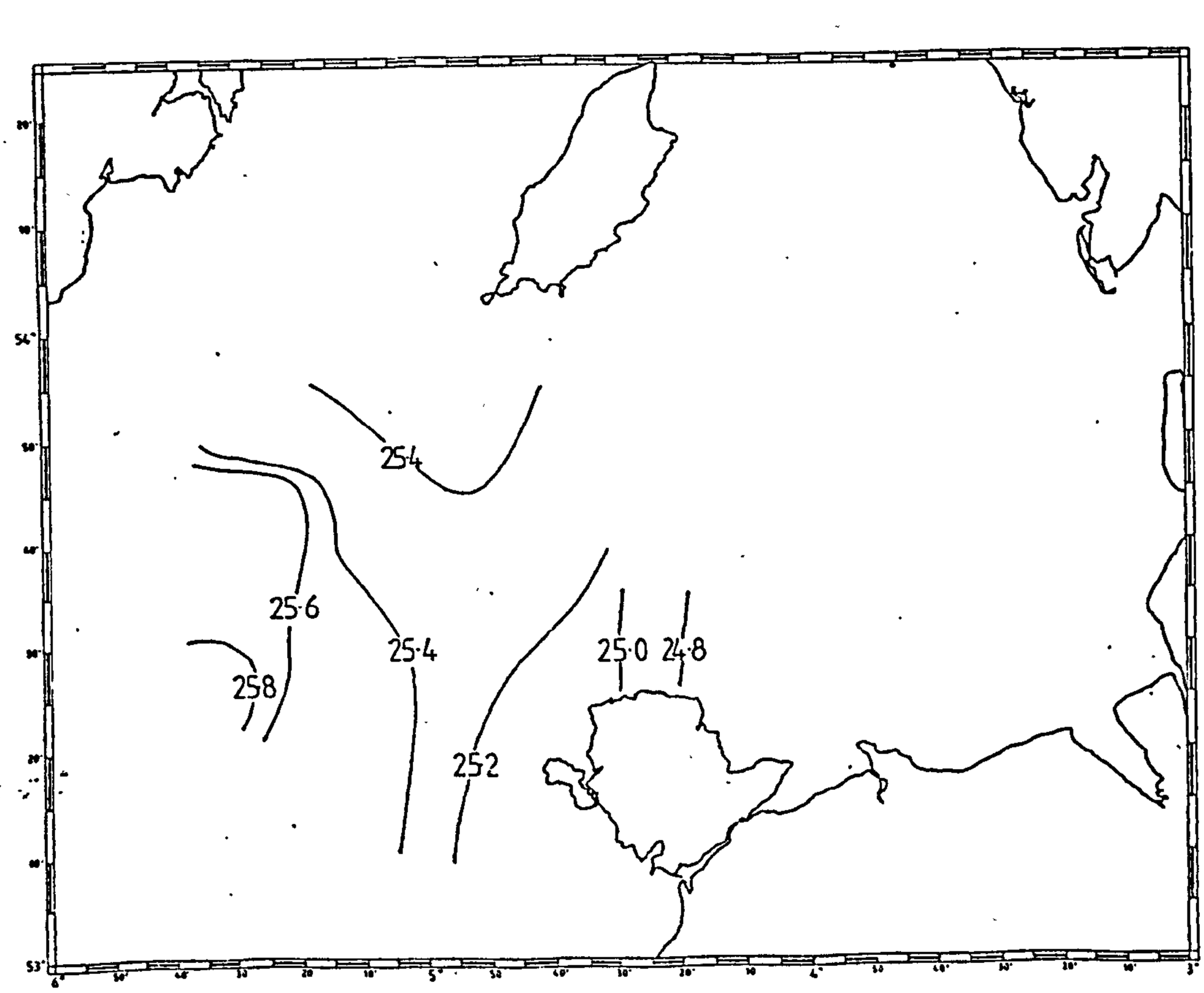

In mid-October (figure 5.9) values of c were higher generally and more spatially uniform throughout the water column than during the previous cruise.Values of sigma-t were also more uniform than for the previous surveys in 1987.

5.3.2. Vertical distribution of beam attenuation in 1987. The seasonal variation in the vertical distribution of c in 1987 is illustrated by a time series of vertical profiles of measurements in three sections of transects A,B and C . The location of the transects is shown in figure 5.1.b.. The sections are presented in figures 5.10 to 5.12, and they include sections of the vertical distribution of sigma-t.

The vertical distribution of c in section B in early April was similar to that in section A, described in section 5.2. Values of c were vertically unifom in the mixed water near the Anglesey coast (stations A1,B4) but a vertical gradient in c was observed in deep, weakly stirred water (stations A4, B1). The difference in sigma-t from the surface to the sea-bed in the WIS was less than 0.2 σ_t units.

The time series of sections A,B and C show that the values of c in the mixed water north of Anglesey were high in April and May and decreased in June, July and August. Values of c increased in September and October.

This pattern is confirmed by an annual composite time

Figures 5.10, 5.11. and 5.12.

Time series(1987) of sections of vertical profiles of measurements a) of beam Attenuation, b) of sigma-t. Positions of transects are shown in Figure 5.1.b.
The date for each transect is shown in the section.

Fig.10 - Section A.
Fig.11 - Section B.
Fig.12 - Section C.

Figure 10.

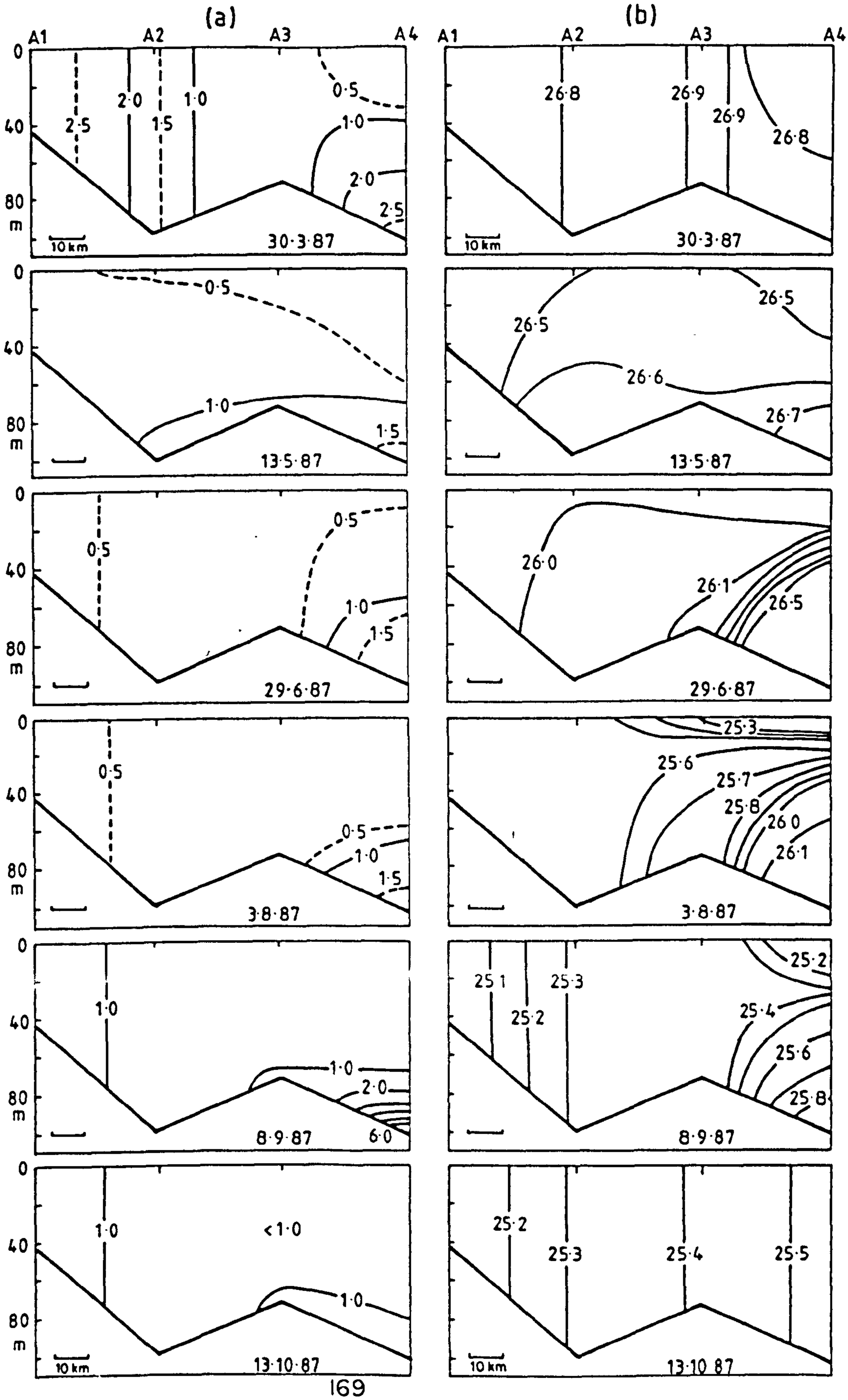
(a)
(b)
A1
A2
A3
A4
0
40
80
m
10 km
30·3·87
2·5
2·0
1·5
1·0
0·5
26·8
26·9
13·5·87
29·6·87
3·8·87
8·9·87
6·0
25·3
25·6
25·7
25·8
26·0
26·1
25·2
25·4
<1·0

Figure 11.

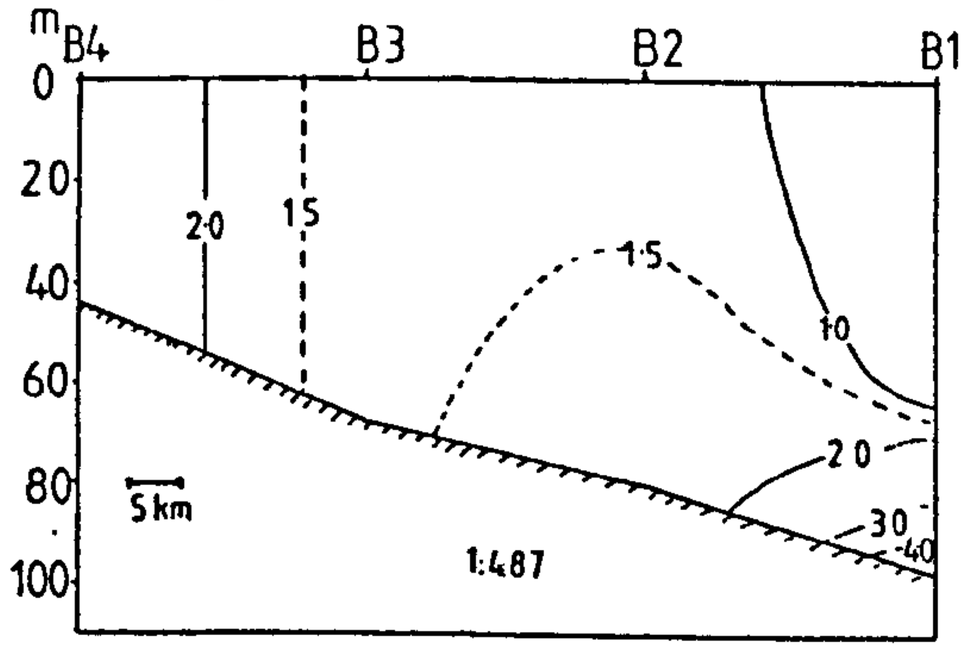
m
B4
B3
B2
B1
0
20
40
60
80
100
2·0
1·5
1·0
2·0
3·0
40
5 km
1:4:87

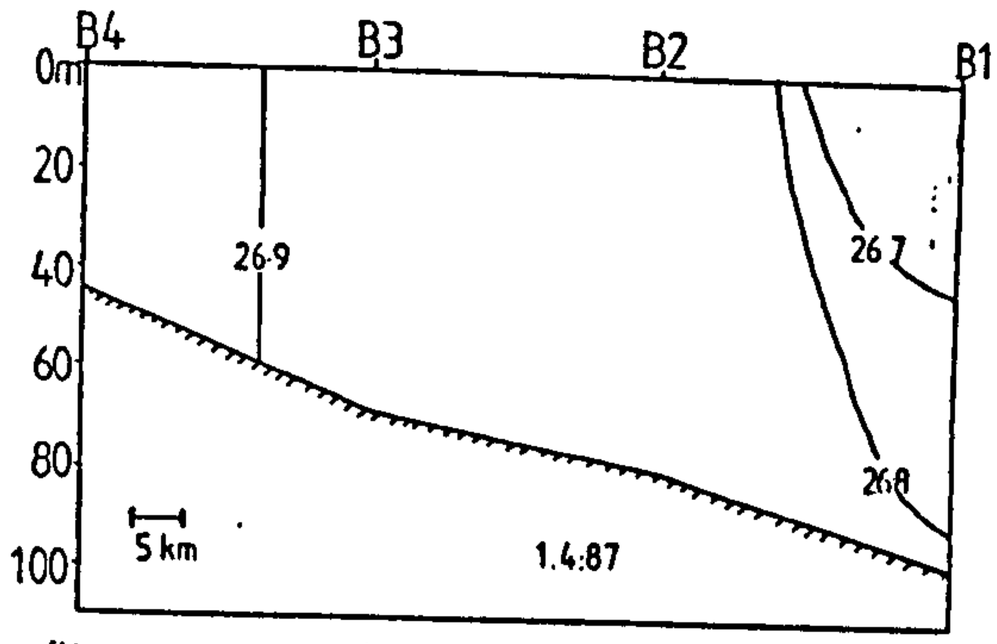
B4
B3
B2
B1
0m
20
40
60
80
100
26·9
26·7
26·8
5 km
1.4:87

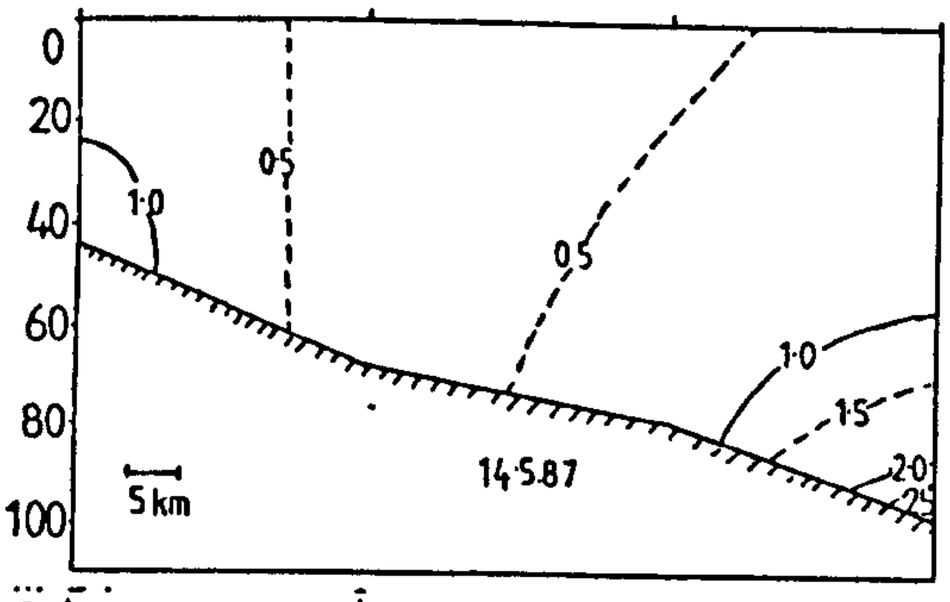
0
20
40
60
80
100
1·0
0·5
0·5
1·0
1·5
2·0
2·5
5 km
14·5·87

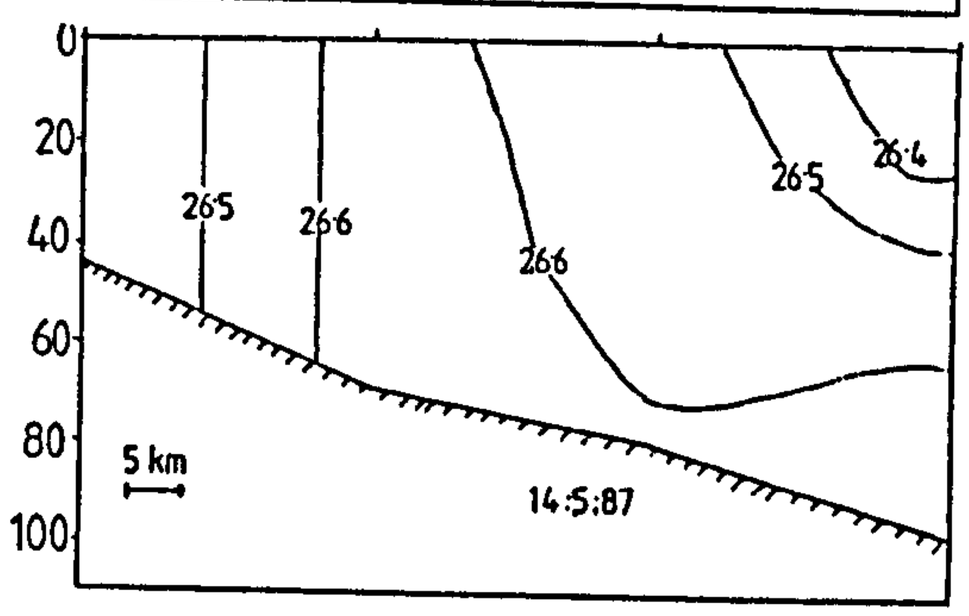
0
20
40
60
80
100
26·5
26·6
26·6
26·5
26·4
5 km
14:5:87

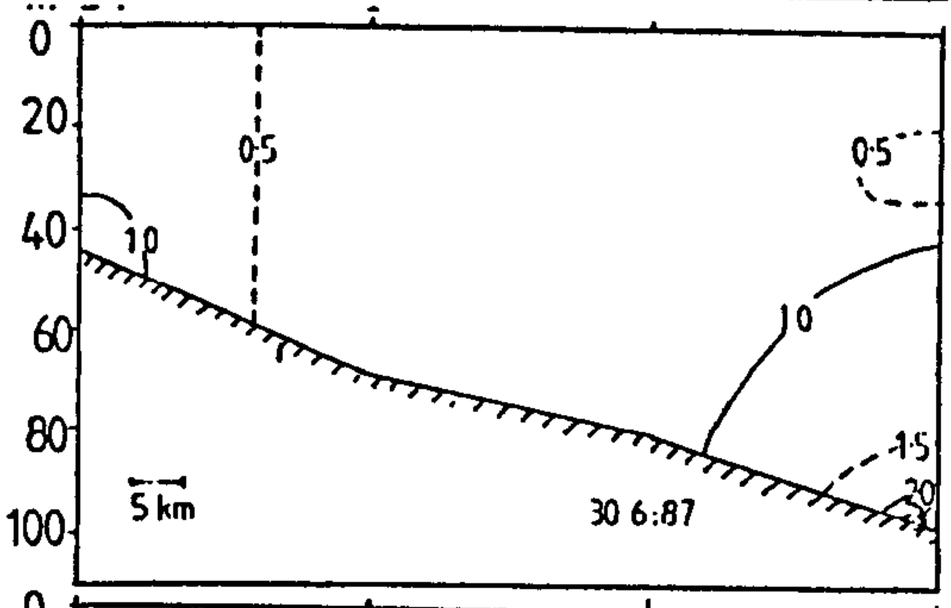
0
20
40
60
80
100
1·0
0·5
0·5
1·0
1·5
2·0
5 km
30 6:87

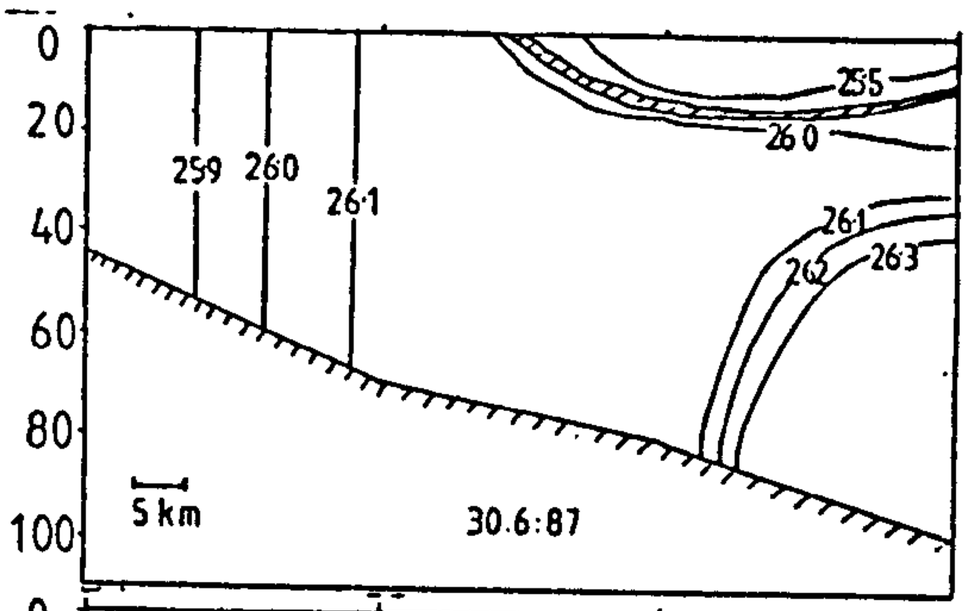
0
20
40
60
80
100
25·9
26·0
26·1
26·1
26·2
26·3
5 km
30.6:87

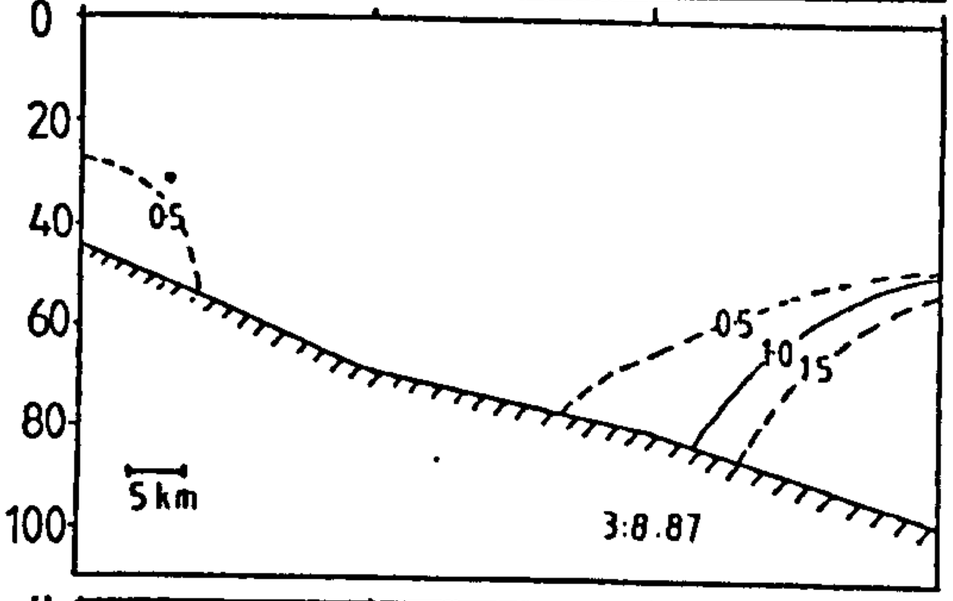
0
20
40
60
80
100
0·5
0·5
1·0
1·5
5 km
3:8.87

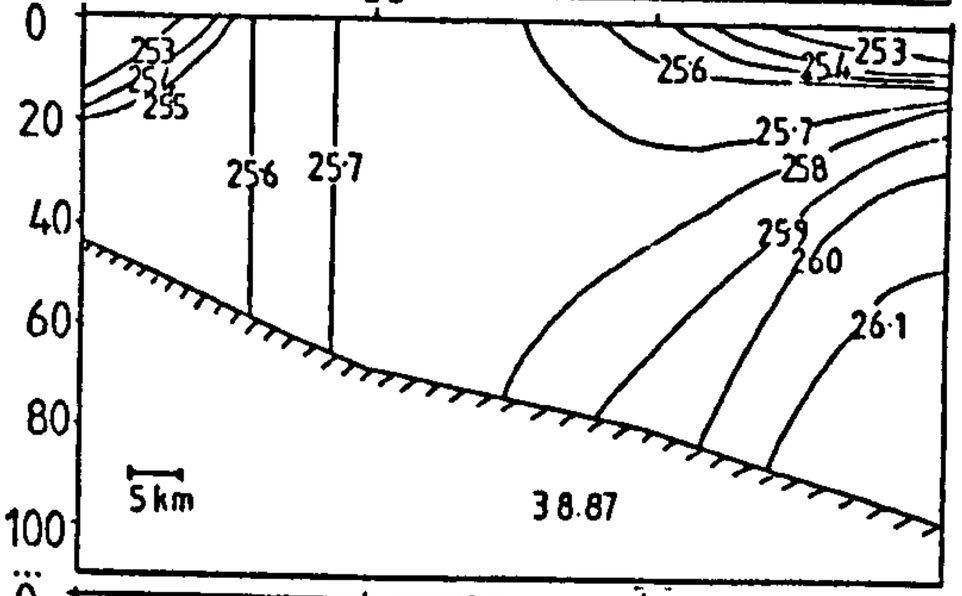
0
20
40
60
80
100
25·3
25·4
25·5
25·6
25·4
25·3
25·7
25·6
25·7
25·8
25·9
26·0
26·1
5 km
3 8.87

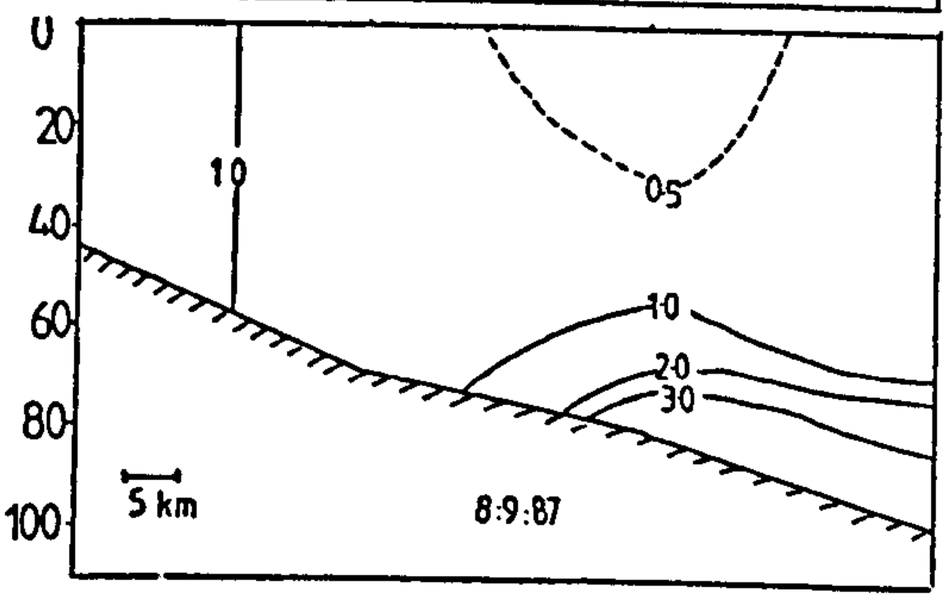
U
20
40
60
80
100
1·0
0·5
1·0
2·0
3·0
5 km
8:9:87

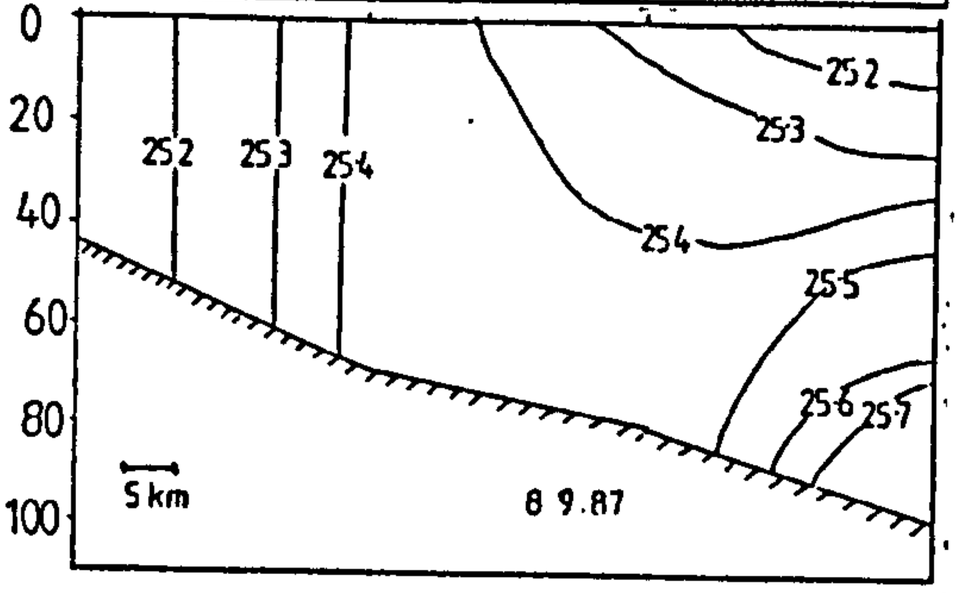
Ö
20
40
60
80
100
25·2
25·3
25·4
25·2
25·3
25·4
25·5
25·6
25·7
5 km
8 9.87

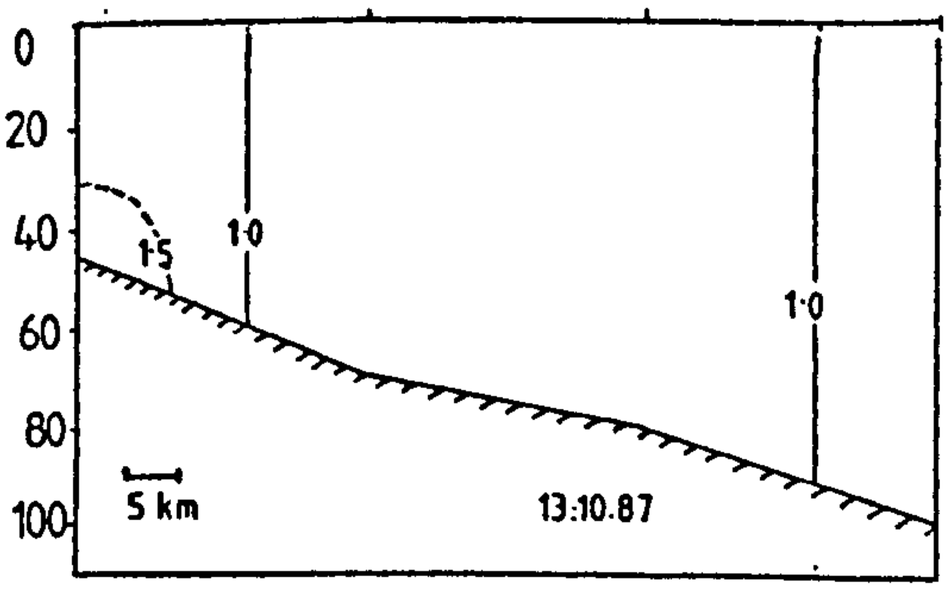
0
20
40
60
80
100
1·5
1·0
1·0
5 km
13:10.87

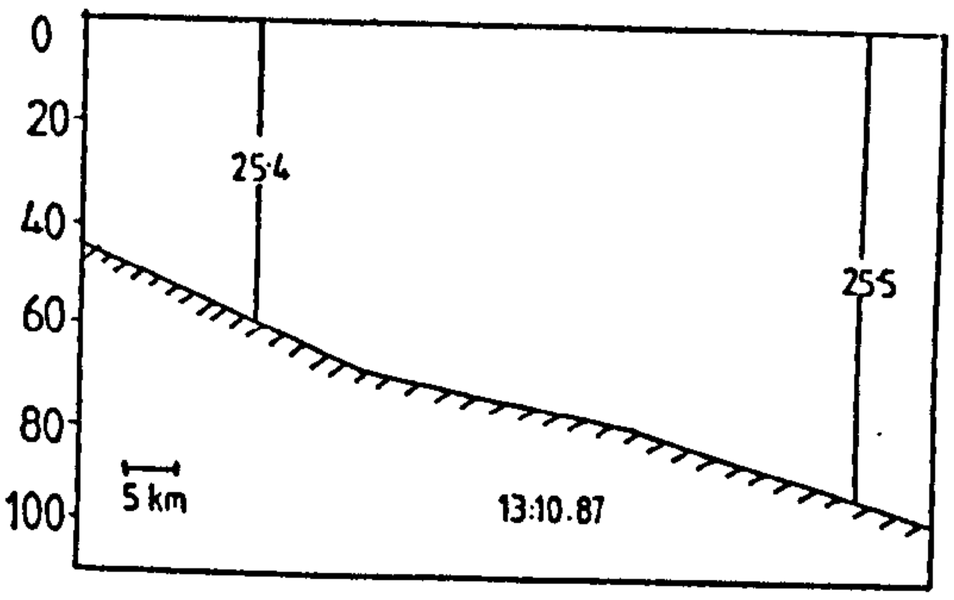
0
20
40
60
80
100
25·4
25·5
5 km
13:10.87

Figure 12.

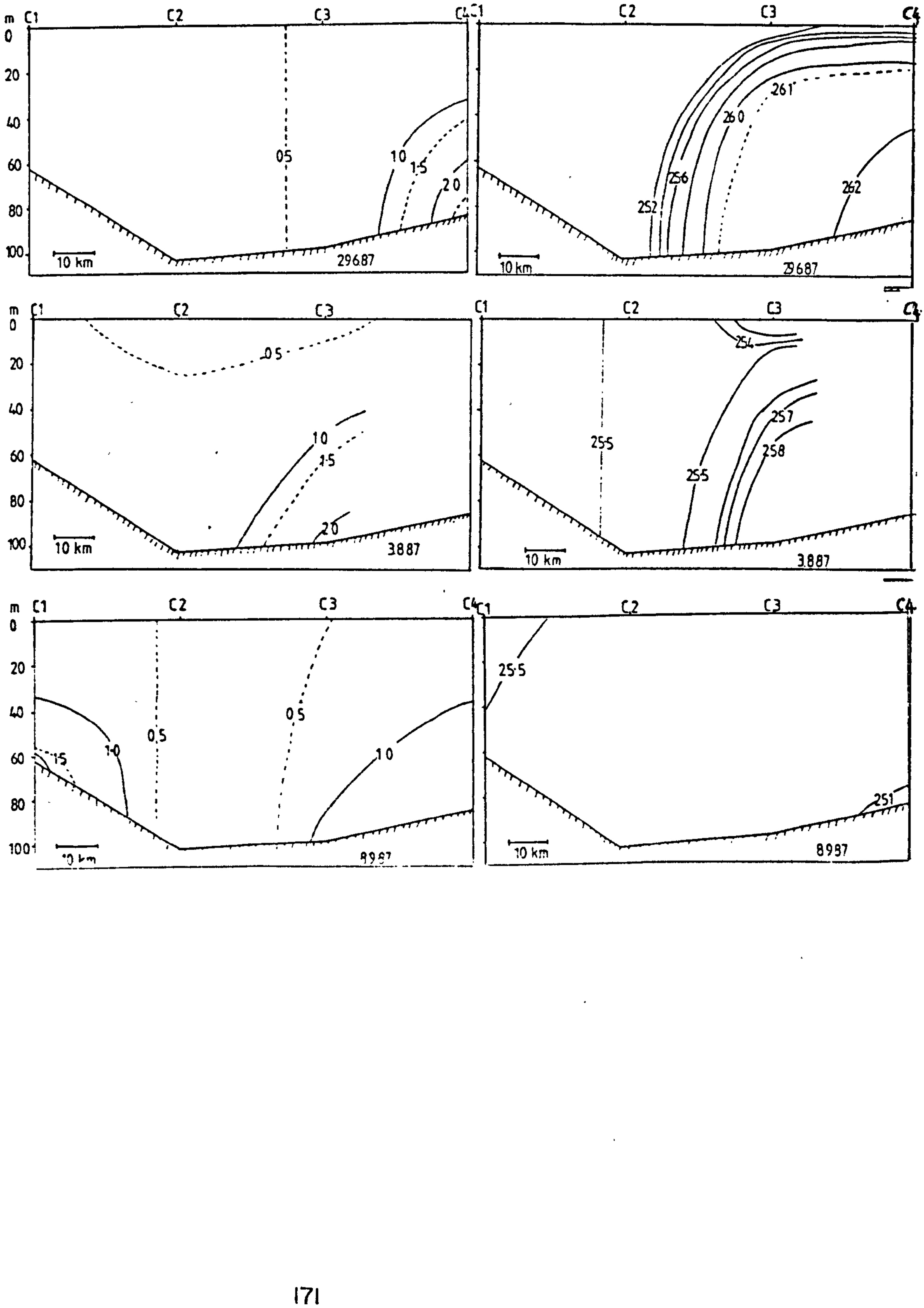
m
C1
C2
C3
C4
0
20
40
60
80
100
05
10
1·5
2·0
10 km
29687
261
260
256
252
262
254
257
255
258
3887
25·5
99·87
8987
251

series of SPM concentrations (mgl^{-1}), shown in figure 5.13. The measurements were taken from weighed near surface and near sea-bed samples from station A2 in 1986 and 1987. Some data from a survey in 1981 is included (Mitchelson, 1984). These measurements were averaged from a number of mixed water stations south of the WIS front. The value for each station was an average of samples taken from the surface to 20m. The time series shows high values of SPM concentrations in April, with lower values in June, July and August. Concentrations of SPM increased again in September and October.

The inorganic, and organic SPM and the chlorophyll concentrations are included in Figure 5.14. This shows that when values of chlorophyll were high ,in May, the organic SPM concentration was high. Values of beam attenuation are also included in the time series.

The vertical profiles of c in figures 5.10. to 5.12. indicate that as the summer developed, water with high values of c became confined to an area nearer the coast of Anglesey. At the same time the vertical density gradient in the WIS increased, and the stratified water extended toward the south-east. High values of c were associated with the deep layer of dense water.

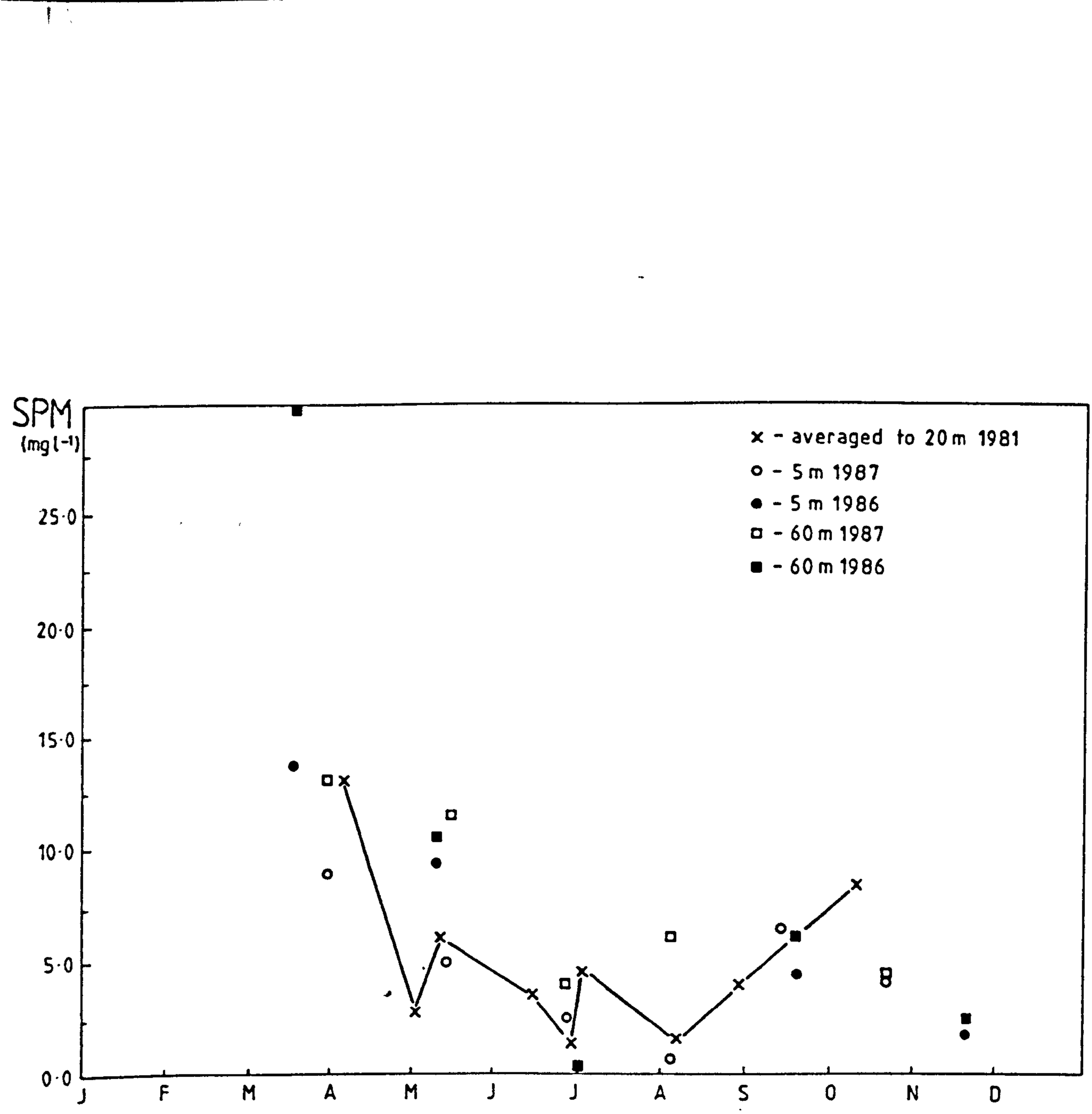

Figure 5.13. Composite annual time series of SPM concentrations (mgl^{-1}) in the region of mixed water north of Anglesey. X = data averaged from the surface to 20m below from a number of stations in the region of mixed water south of the WIS front (Mitchelson,1984). Other values were taken from single samples at 5 m below the surface and 5m above the sea-bed from station A1, in 1986 and 1987.

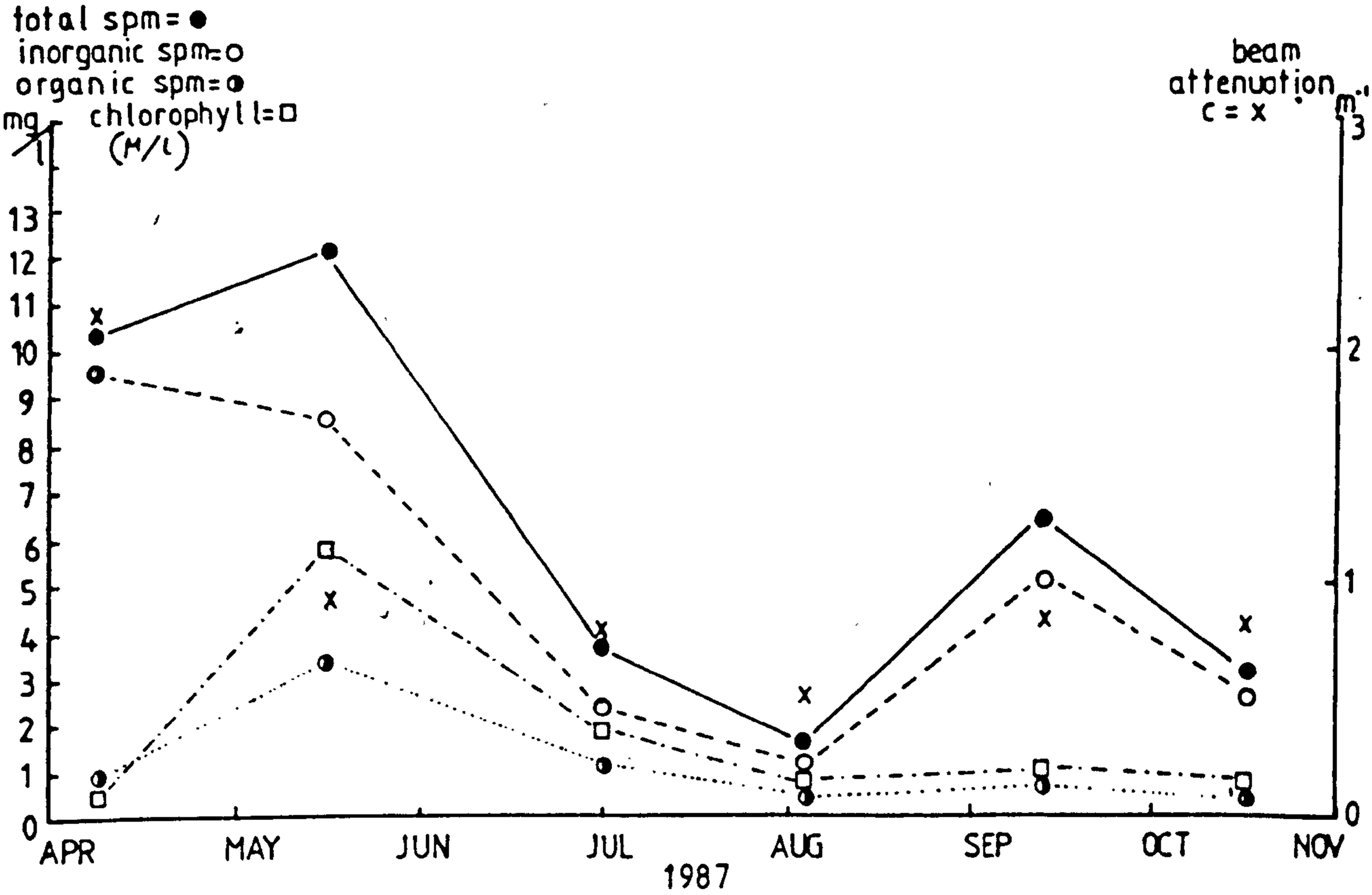

Figure 5.14. Time series (from 1987) of values of total, inorganic and organic SPM concentrations (mgl^{-1}), chlorophyll a concentrations ($\mu g\ l^{-1}$), and beam attenuation (m^{-1}), averaged for each cruise.

It was not possible to construct a seasonal time series of stations in the eastern part of the survey area as bad weather sometimes prevented completion of the surveys during the cruise. However highly attenuating water in this area was observed to be associated with a lower , dense layer when stratification developed. This is illustrated by a section of vertical profiles of measurements of c and sigma-t in early August from Liverpool Bay to the WIS,(figure 5.15) Highly attenuating water is associated with isolated basins of deeper, dense water in the stratified regions in the extreme east and west of the section.

5.4. Relation of beam attenuation to tidal stirring.

The spatial distribution of c was extremely varied in 1987, particularly during the first cruise in early April and in May. The distribution pattern of near-surface c is similar to that of the tidal stirring parameter h/u^3 (Simpson and Hunter, 1974), shown in figure 2.1. This similarity strongly suggests that the availability of turbulent kinetic energy from the tidal flow exerts the main control on the level of particulate suspensions. Figure 2.1. shows that vertical mixing is predicted for values of h/u^3 less than 2.7. These regions were associated with high surface values of c in early April 1987.

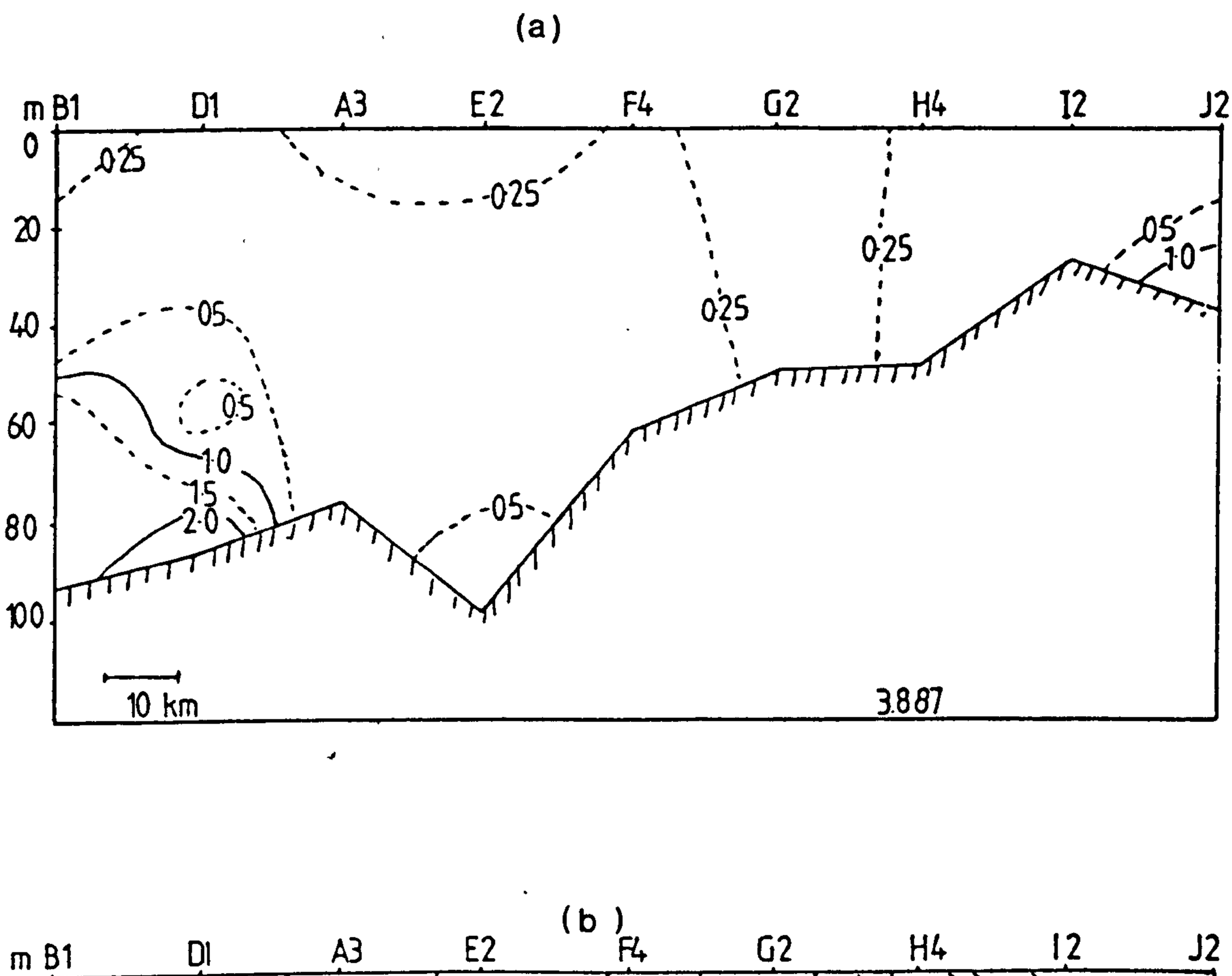

Figure 5.15. Section of vertical profiles of measurements of beam attenuation (a) and sigma-t (b) along a transect from Liverpool Bay (J2) to the western Irish Sea (B1).

In order to examine this link with tidal mixing further, a regression was performed of the near surface values of c and the amplitude of the M2 tidal current (Robinson,1979).The results for cruises in 1987 are summarised in Table 17. An example of the data from the cruise in April is plotted in Figure 5.16. These results showed that there was a relationship between surface values of c and the M2 tidal flow in 5 cases out of 6. The link was most evident in April and May, decreasing to a minimum in July and increasing in September. In October, when convective cooling may have dominated the breakdown of stratification, there was apparantly no relationship between the parameters.

A more explicit quantitative indication of the availability of TKE from the tidal flow is the parameter u^3/h which was calculated for each station. A regression analysis was performed of surface values of c on u^3/h. The results, summarised in Table 18, shows that surface values of c were closely related to u^3/h from April to September. Again there was no relationship between the parameters in October. Figure 5.17. shows an example of the regression from the cruise in April/ May, and Figure 5.18. shows a similar plot for all the data from the cruises in 1987. When the constant and the slope of the

TABLE 17 COEFFICICIENTS OF DETERMINATION (R^2) for C AT 5m AND THE M2 TIDAL CURRENT SPEED.

CRUISE	MONTH	R^2	d.f
53	APRIL	0.313*	21
55	JUNE	0.277	20
56	JULY	0.043	42
57	AUGUST	0.121	44
58	SEPT.	0.298	17
59	OCT.	0.000	22

R^2 = coefficient of determination. d.f. = degrees of freedom.

* Regression is plotted in Fig. 5.16.

TABLE 18 COEFFICIENTS OF DETERMINATION (R^2) FOR C AT 5m AND U^3/H.

CRUISE	MONTH	R^2	d.f.	constant	slope	p
53	APRIL	0.754	11	0.703	97.6	0.000
55	JUNE	0.658	20	0.486	29.2	0.000
56	JULY	0.320	42	0.437	23.6	0.000
57	AUGUST	0.393	44	0.277	15.5	0.000
58	SEPT.	0.664	17	0.426	34.9	0.000
59	OCT.	0.000	22	0.768	0.12	0.989
ALL DATA 1987		0.225	161	0.452	29.8	0.000

p = probability of the relationship between the parameters ocurring by chance.

* Regression is plotted in 5.17.

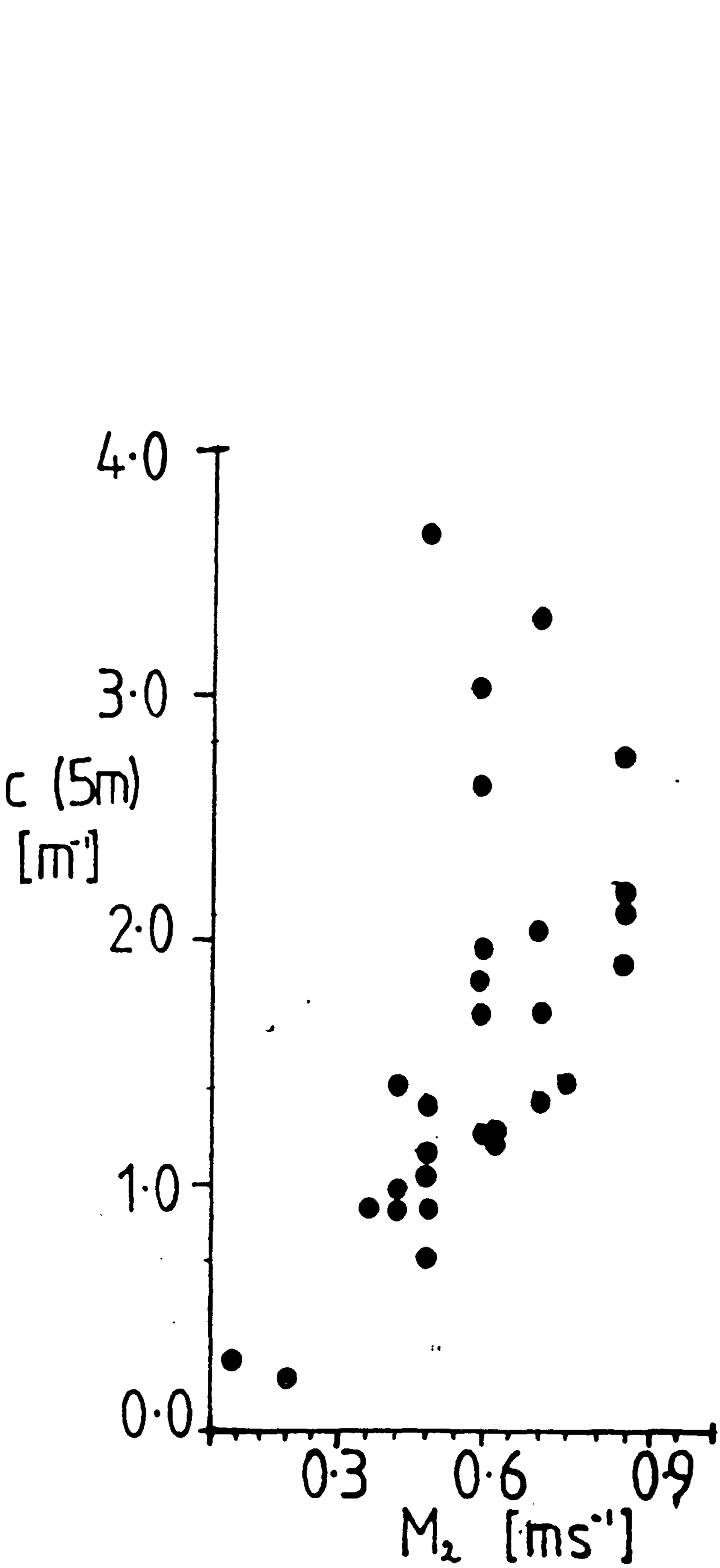

Figure 5.16. Beam attenuation during 30/3/87-4/4/87 at 5m below the surface plotted against M_2 tidal current from a model by Robinson(1979).

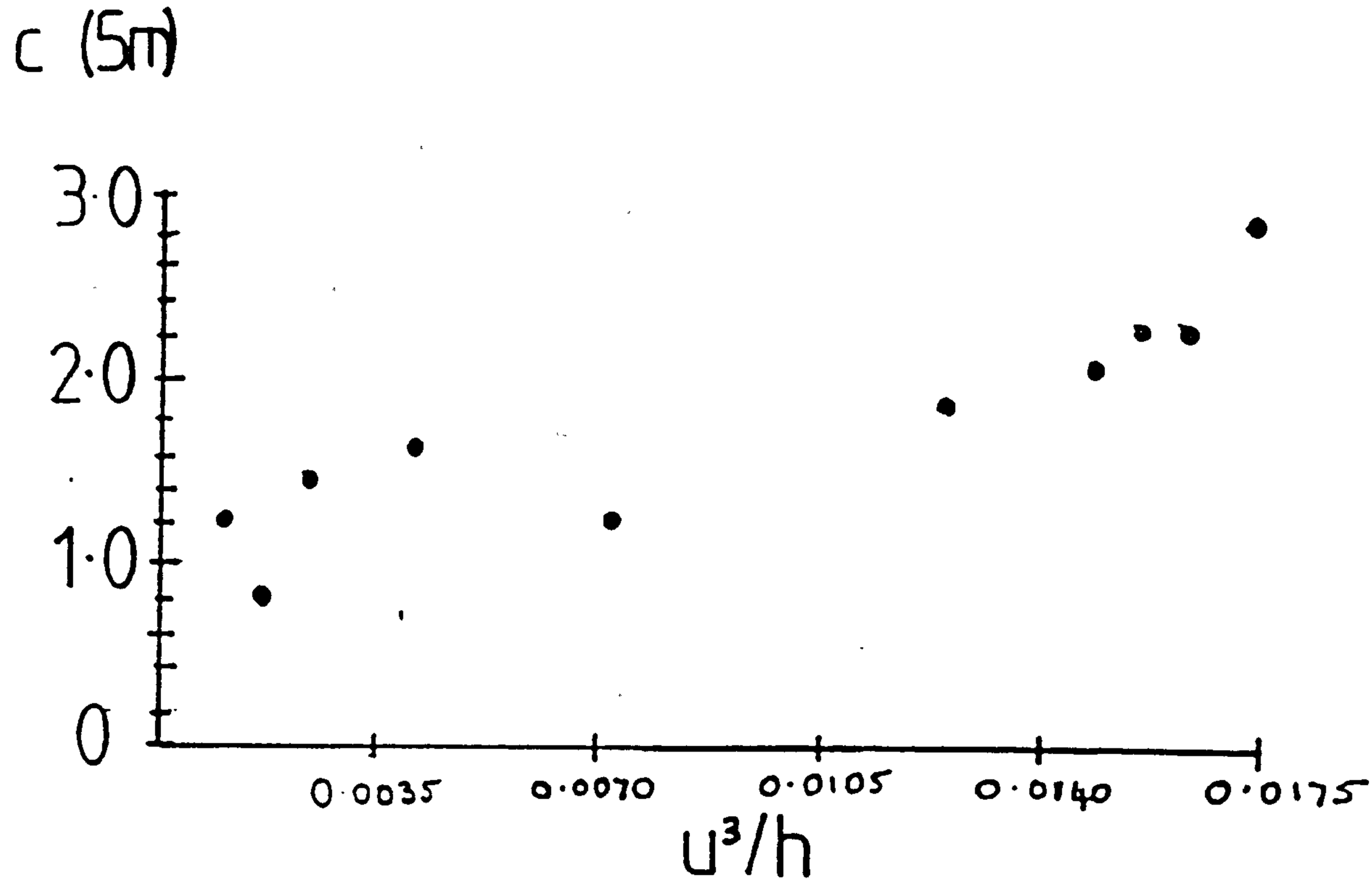

Figure 5.17. Beam attenuation (c) at 5m plotted against u^3/h from the cruise during 30/3/87-4/4/87.

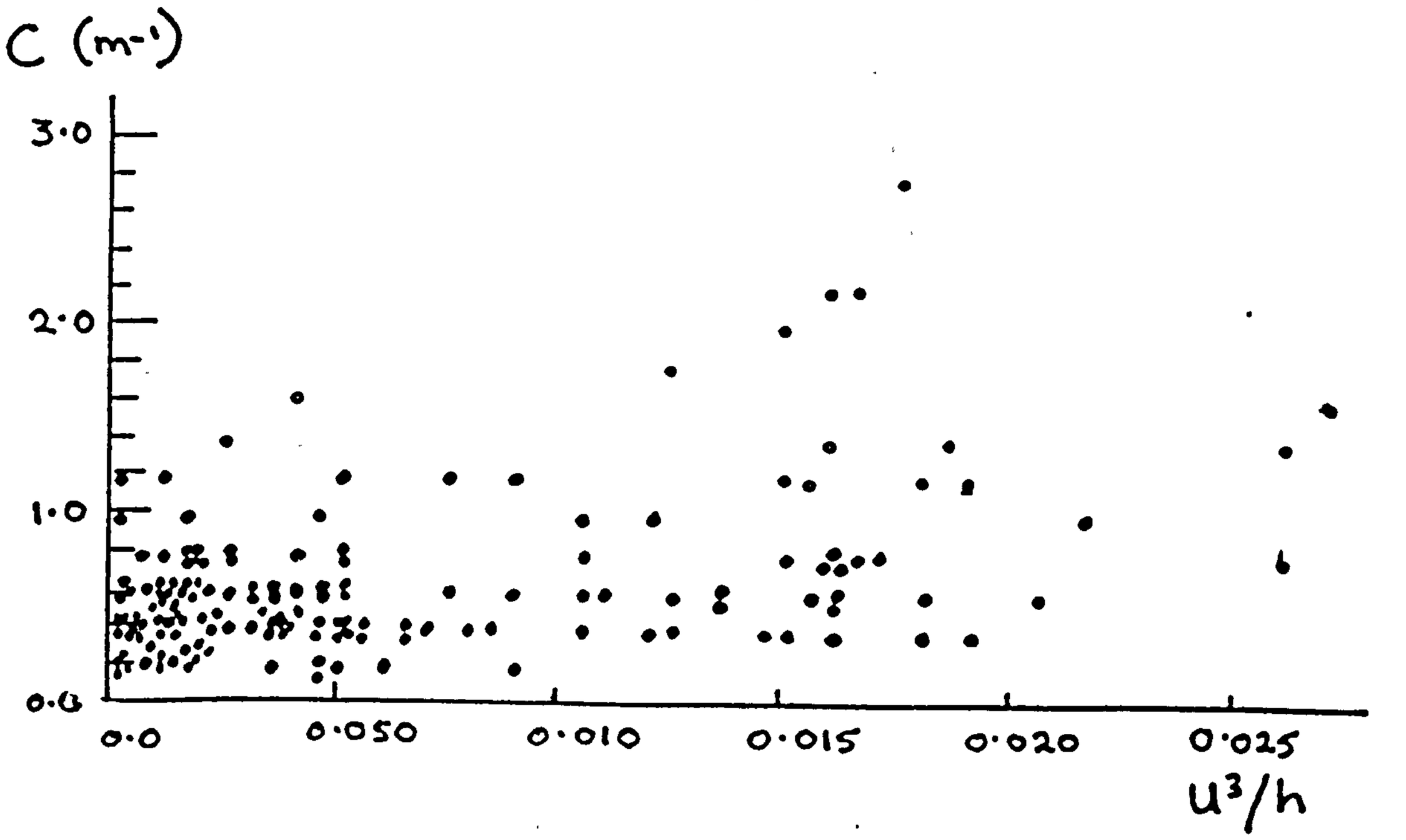

Figure 5.18. Beam attenuation (c) at 5m below the surface plotted against u^3/h from all the data collected in 1987.

regressions are examined (Table 18) it is noted that the relationship between the parameters over the season is not constant. High values of the constant and slope are observed in April and September, with low values in August. This indicates that seasonal processes are involved in SPM concentrations. It was noted earlier in this chapter that stratification was most intense during August.

An abrupt change in surface beam attenuation at the boundary between weakly and strongly mixed waters, may occur because there are layers of varying concentrations of SPM in weakly mixed water, with low surface values and high values nearer the sea-bed. In well mixed waters the vertical distribution of SPM is uniform.

An indicator of the TKE available to oppose the sinking velocity of the SPM is the potential energy anomaly, ϕ, described in Chapter 2. This takes into account the seasonal increase in buoyancy due to the heat input to surface waters. Values of ϕ were calculated from the data for each station in 1987 and regressions of c on showed consistently high values of the coefficient of determination, r^2 (Table 19). An example, from the cruise in August, is plotted in Figure 5.19.

TABLE 19 COEFFICIENTS OF DETERMINATION (R^2) FOR ΔC AND ϕ

CRUISE	MONTH	R^2	d.f
53	APR/MAY	0.354	11
55	JUNE	0.352	20
56	JULY	0.406	42
57	AUGUST	0.705*	44
58	SEPT.	0.543	17
59	OCT.	0.496	22

* Regression is plotted in Figure 5.19.

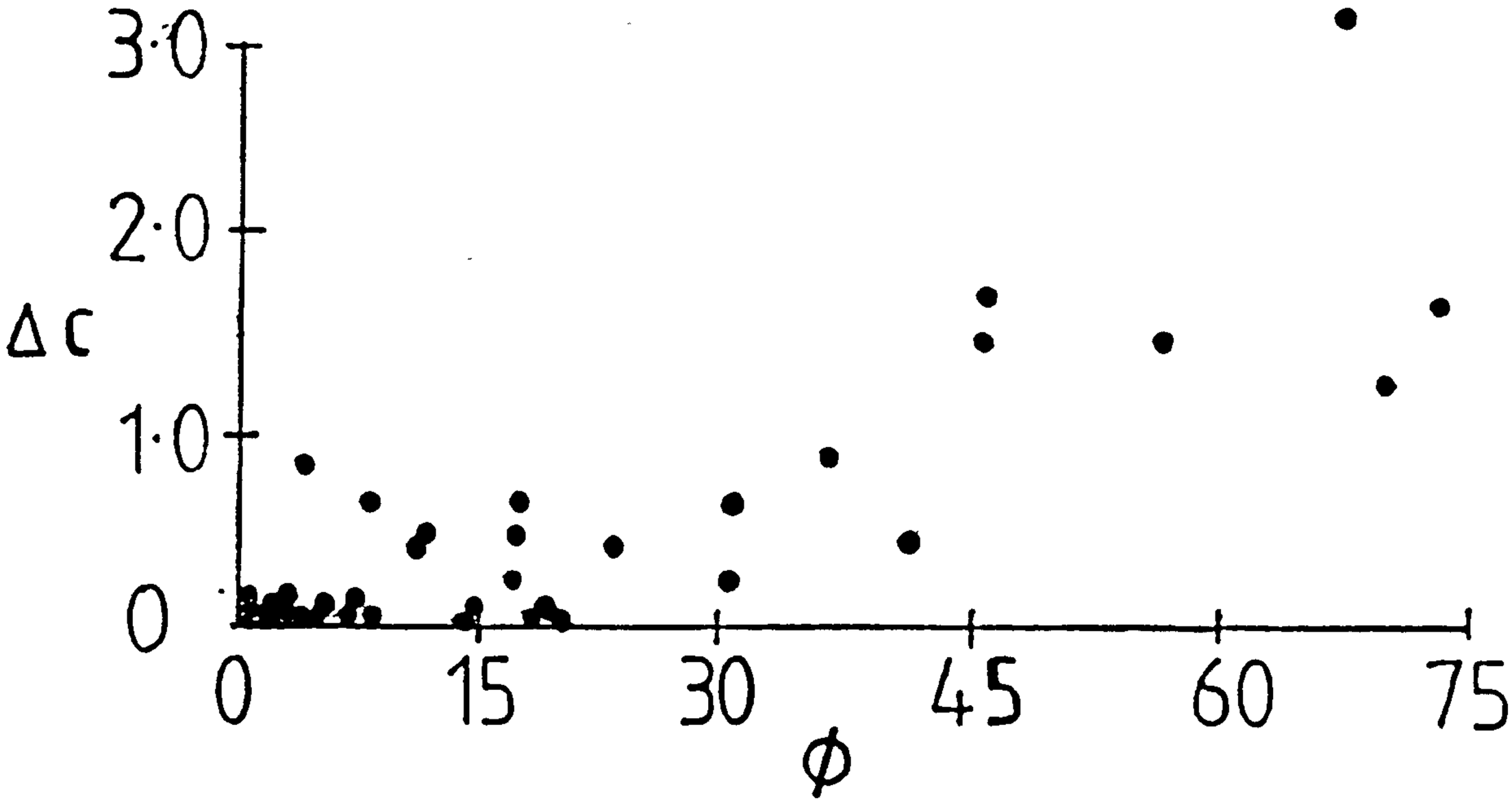

Figure 5.19. The difference between surface and near-bottom values of beam attenuation (m^{-1}) during 30/3/87-4/4/87 plotted against the potential energy anomaly (ϕ).

5.5. Discussion

These observations show that there is a direct relationship between c and the level of TKE available to mix the water .This hypothesis is supported by the low p values ,in Table 18, which are 0 except during the cruise in October. A value of p is the probability of the relationship between the variables occurring by chance.

However seasonal processes are also involved since it is evident from the data in Table 18 that there is a reduction in both the constant and the slope of the regressions of c on u^3/h during the summer. This may be determined by the level of stratification which exists during the summer seasonal heating, as the relationship between c and ϕ remains relatively constant from April to September (Table 19). Therefore tidal stirring also exerts a secondary effect through stratification on c.

An increase in the intensity of stratification, caused by solar heating of the surface waters, may inhibit the upward movement of SPM through the thermocline. Any SPM falling downward will become trapped in the lower dense layer during the summer months. The development and extension of stratification into previously mixed water enlarges the area where there are high concentrations of SPM in the deep layer.

An increase in the cohesion of sediment on the sea-bed may be caused by more vigorous benthic activity and the subsequent production of mucal films. It may also be caused by reduced erosion of sediment from turbulence generated by surface wave action and storm surge currents during the summer.

The seasonal variation in the surface distribution of c shows a marked similarity to the sequence of sea-surface radiance images from the CZCS (figure 2.2.). Highly reflecting water, corresponding to high values of c, became confined to the Anglesey coast in May and June, as the darker, clearer water , with low values of c, extended from the WIS to the south. It is, however, important to remember that the images and distributions were not from the same year, although they are representative of consistent seasonal pattern.

CHAPTER 6

Beam attenuation time-series observations and determinant processes.

6. 1. Time series observations.

A mooring with self-recording transmissometers and current meters was deployed at a site north of Anglesey (at X, in figure 5.1.b.) from 6/4/87-12/10/87. The site was chosen as it was strongly tidally mixed for the whole year. It was within 2 to 3 hours journey from Menai Bridge which allowed regular servicing at approximately monthly intervals (Table 6). This was done at times close to neap tides since there are strong tidal currents in the region at springs and it was considered to be preferable to service the mooring during times of weaker tides. The water depth was 75m and the sea-bed was composed of rock and gravel, with small patches of mud in sheltered hollows (I.Rees, personal communication).

Measurements of beam transmittance, current speed and direction were recorded every 30 minutes by instruments 20m below the sea-surface and 1m above the sea-bed . However only 50% of the beam transmittance records provided high quality data, although all the current meter data were acceptable. There were complete

records from 4 out of 5 of the instruments deployed at 20m. Only one of the deployments near the sea-bed provided a good record. This may have been because the instruments were only one meter from the anchor chain clump, which may have caused the instruments to become entangled in the chain. Beam attenuation was calculated from the beam transmittance measurements by the method described in Chapter 4. The current meter data was converted into values of current speed and direction by applying calibration factors,and eastward and northward velocity was calculated. Hourly wind speed measurements, in knots, were obtained from the meteorological station at RAF Valley, in Anglesey.

The time series from instruments deployed at 20m below the surface are shown in Figures 6.1 to 6.4. The deployments were from four to five weeks in duration (Table 6) in April, June, July and September 1987. The figures show time series of measurements of beam attenuation, current speed, easterly and northerly velocity at 20m and wind speed.

In the first record (Fig.6.1) and in the last (Fig.6.4.) the values of beam attenuation exhibited strong tidal signals. High values of c were associated with maxima in speed, with the highest maxima of c at spring tides. The records from June (Fig.6.2) and July

Figure 6.1. to 6.4.
Time series of measurements at 20m below the surface of
a) beam attenuation (m^{-1}).
b) current speed (ms^{-1}),
c) eastward velocity (ms^{-1}).
d) westward velocity (ms^{-1}).
e) windspeed (knots)

6.1. 6/4/87-12/5/87,at 20m.
6.2. 28/5/87-29/6/87, at 20m.
6.3. 29/6/87-4/8/87,at 20m.
6.4. 7/9/87-12/10/87,at 20m.

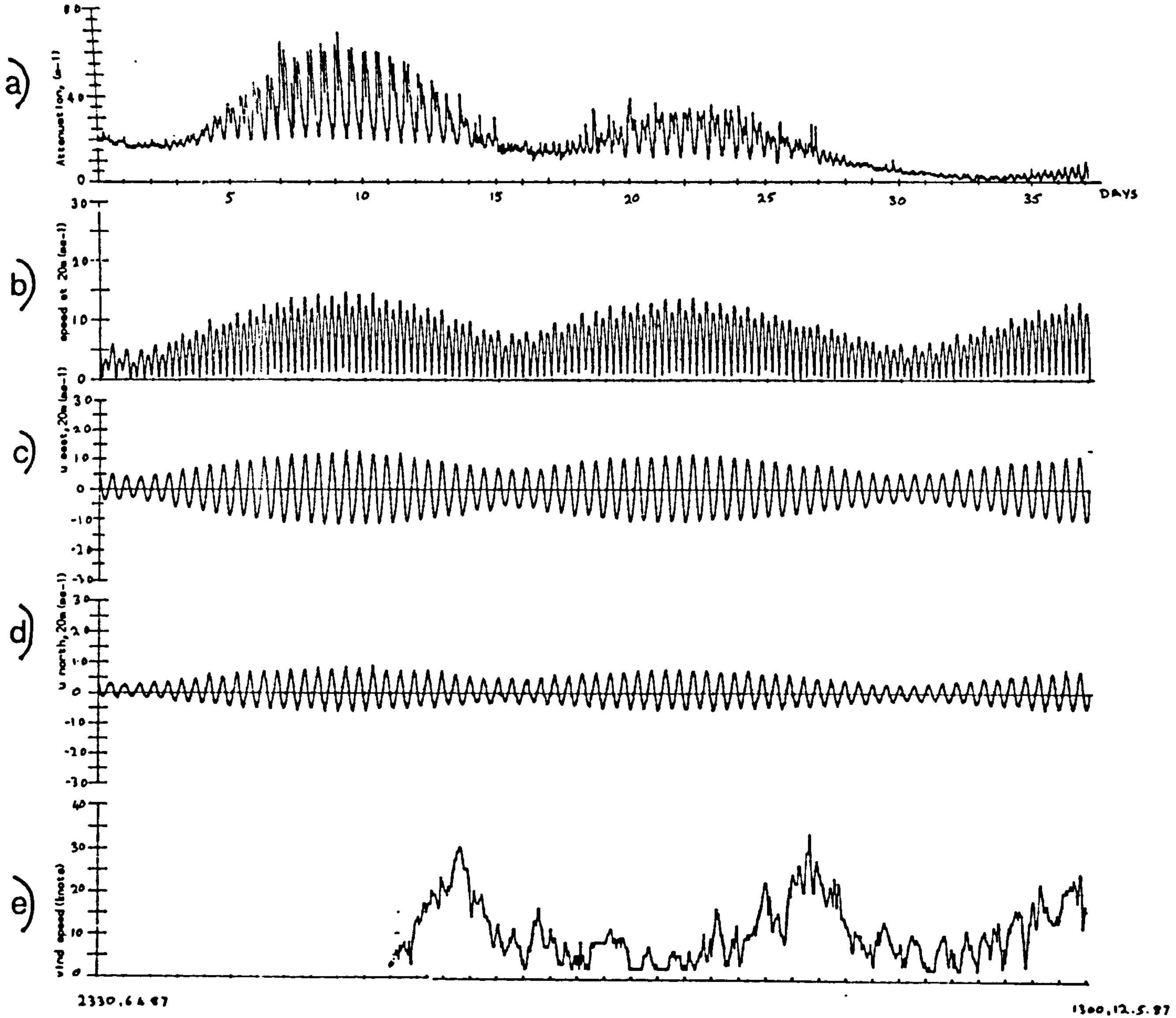
a)
Attenuation, (s-1)
0
4.0
8.0
5
10
15
20
25
30
35
DAYS
b)
speed at 20m (ms-1)
30
20
10
0
c)
u east, 20m (ms-1)
30
20
10
0
-10
-20
-30
d)
v north, 20m (ms-1)
30
20
10
0
-10
-20
-30
e)
wind speed (knots)
40
30
20
10
0
2330, 6 & 7
1300, 12.5.97

Figure 6.1

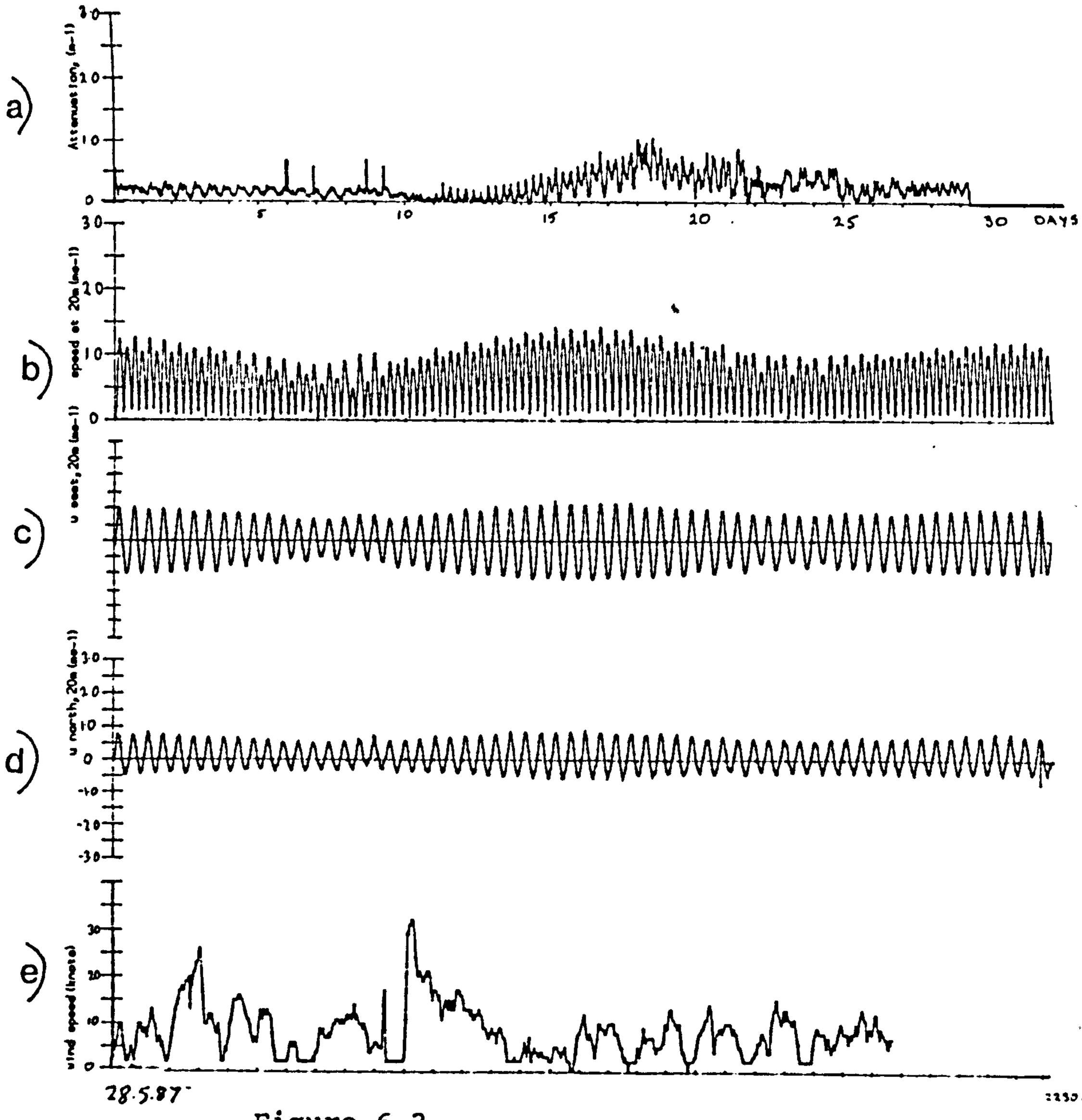
a)
Attenuation (dB)
30
20
10
0
5
10
15
20
25
30 DAYS
b)
speed at 20m (ms-1)
30
20
10
0
c)
u east, 20m (ms-1)
d)
u north, 20m (ms-1)
30
20
10
0
-10
-20
-30
e)
wind speed (knots)
30
20
10
0
28.5.87
2250.29 6.87

Figure 6.2

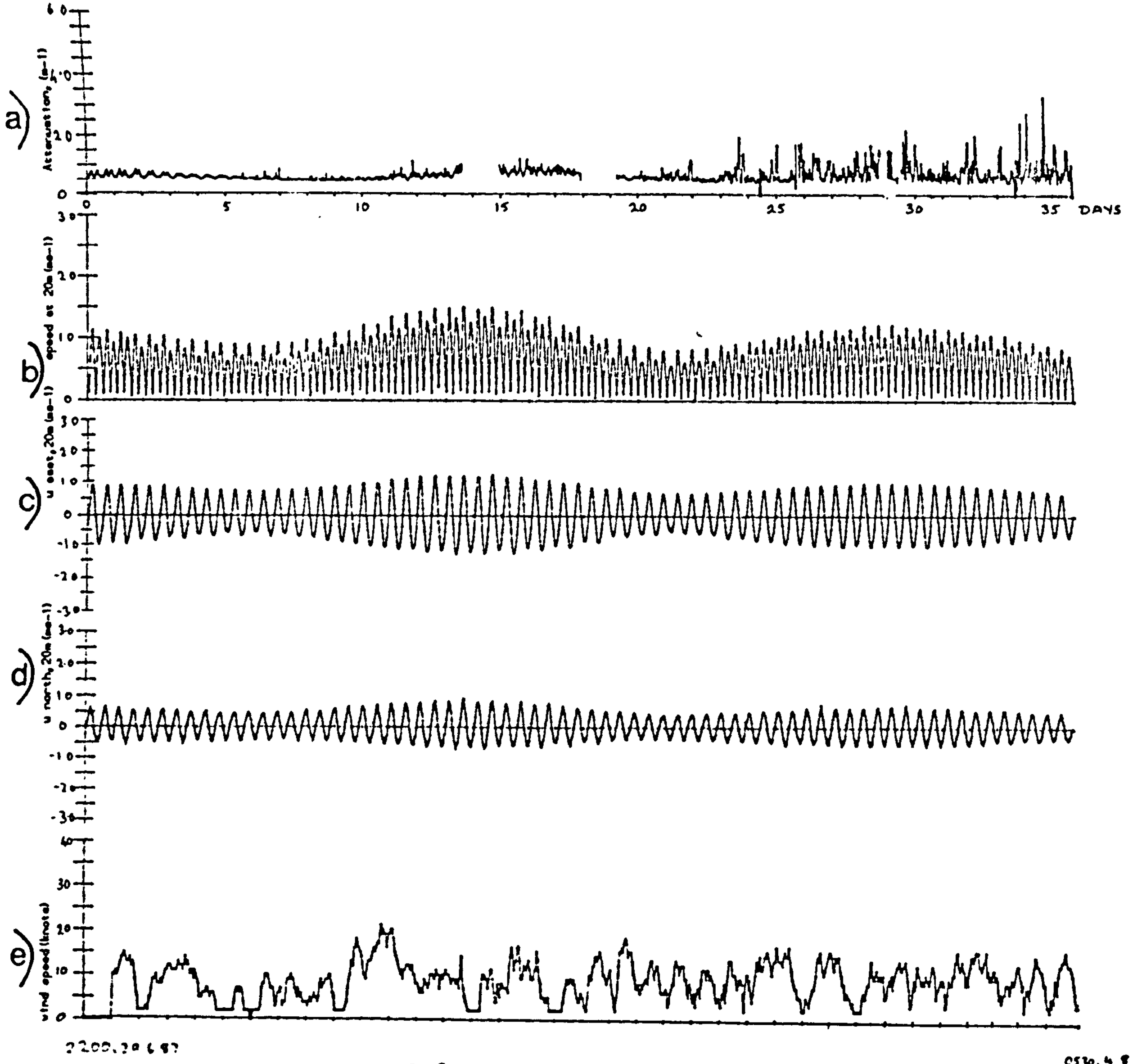
a)
Attenuation, (m-1)
0
5
10
15
20
25
30
35
DAYS
b)
speed at 20m (ms-1)
c)
u east, 20m (ms-1)
d)
u north, 20m (ms-1)
e)
wind speed (knots)

Figure 6.3

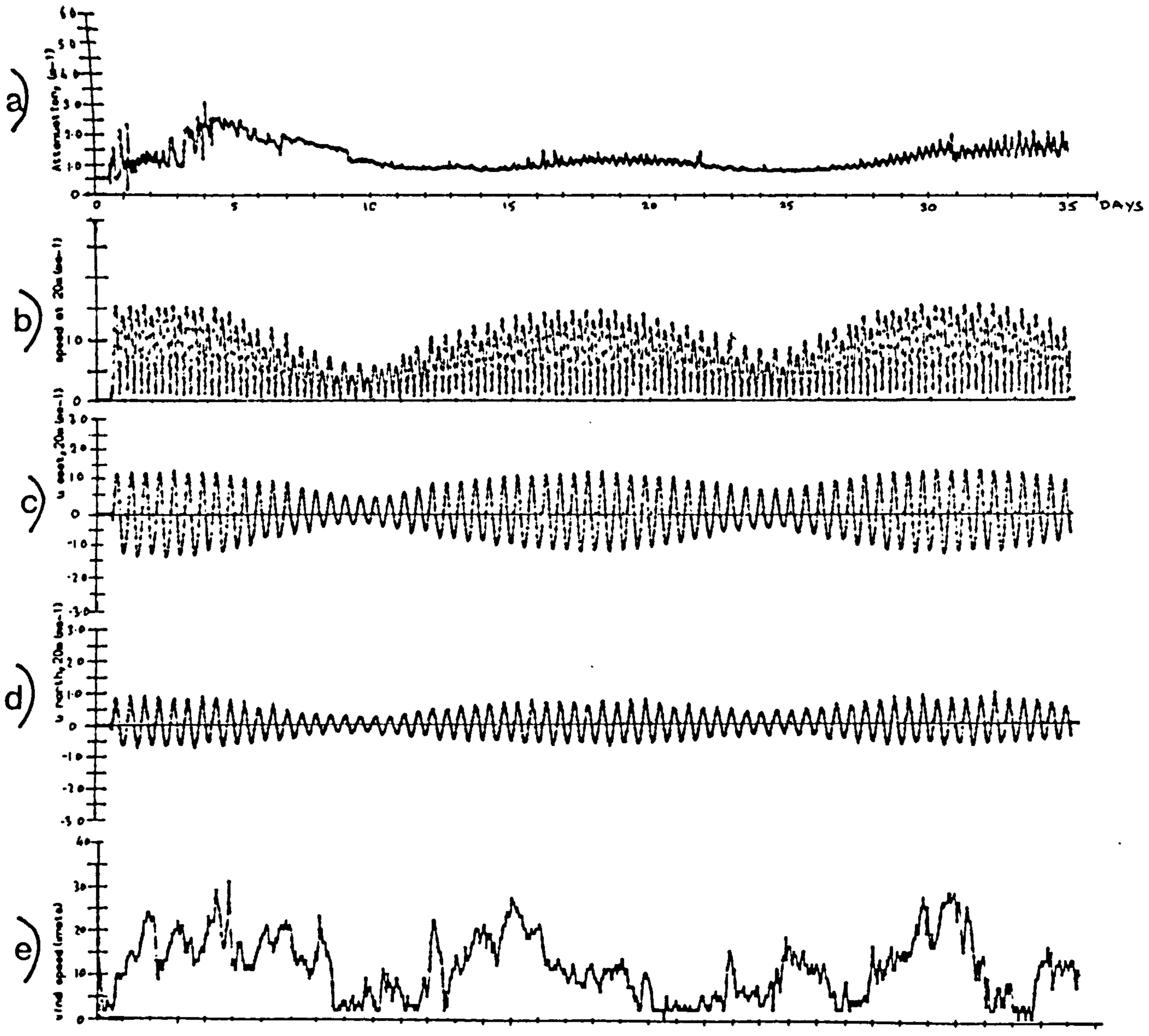

Figure 6.4.

(Fig.6.3) do not show this feature so strongly. In addition, the mean values of c reach higher values during the first and the last deployments, whereas values of c remain low in June (6.2) and (6.3) at the same sites. During the deployment in April (Fig.6.1) maximum values of c were 6.3 m^{-1} at times of spring tides. Because surveys were always made during neap tides these high values were only observed in the record from the mooring and not during the surveys.

The beam attenuation records in figures 6.1, 6.2 and 6.3 show a return to a baseline value approximatly every 12 hours. This suggests that there was tidal advection of turbid water into the region of the mooring. This occurs to some extent in the record from the deployment in October (Fig.6.4.). In addition, the baseline values were higher during the spring and autumn (6.1, and 6.4) than in the summer (6.2. and 6.3). This is consistent with the seasonal trend observed in the mixed water region near the mooring described in Chapter 5. This observation is supported by a time series from all the instruments deployed at 20m which is presented in Figure 6.5.

There was, surprisingly, no increase in beam attenuation 20m during times of strong winds (Figures 6.1 to 6.4). This shows that turbulence induced by wave action did not cause local resuspension of sediment from the sea-bed. Therefore there was no further investigation of the

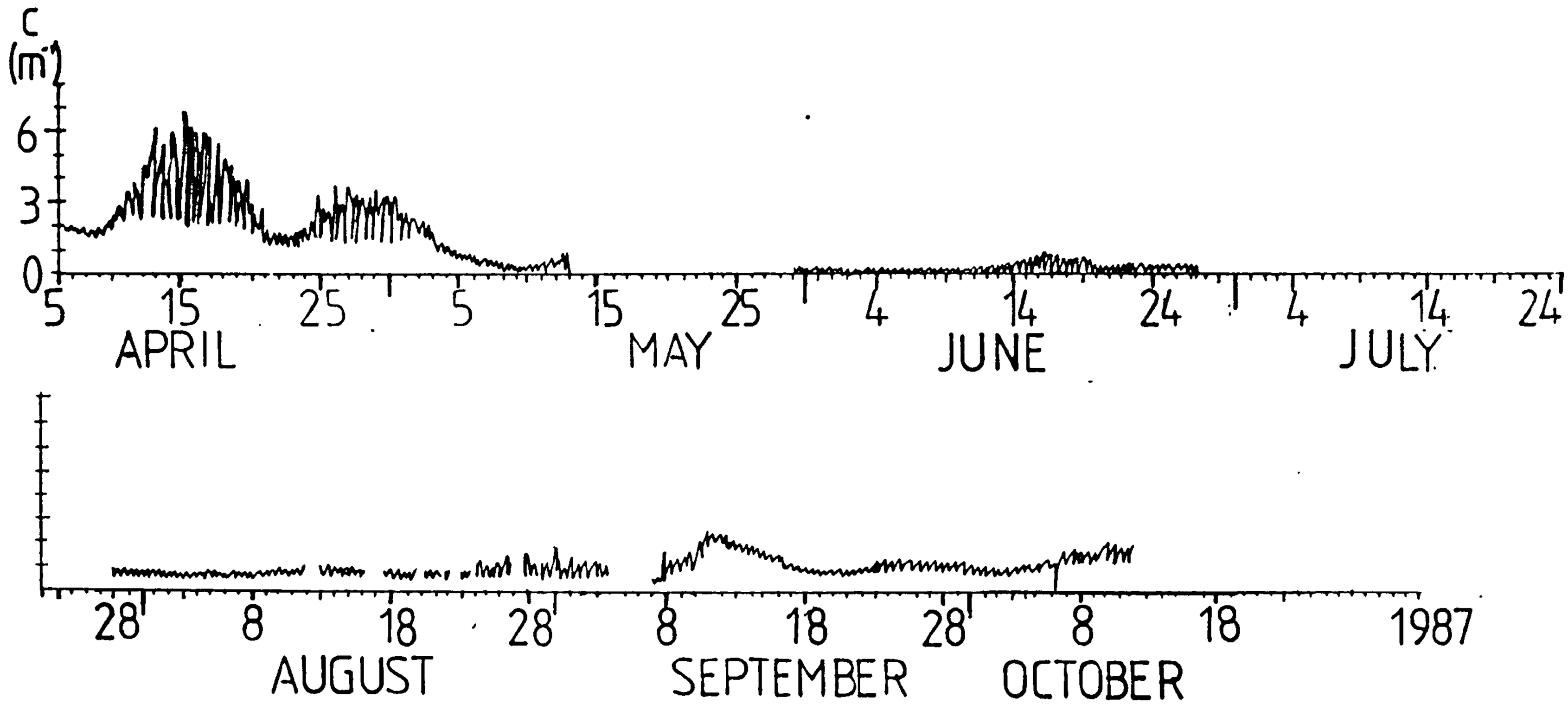

Figure 6.5. Time series of beam attenuation (m^{-1}) at 20m below the surface from the deployments in 1987.

effect of waves on resuspension of sediment.
In order to examine the relationship between the beam attenuation coefficient and the tidal forcing , a section of the time series data was selected from the seasonal record and expanded. The time series in figure 6.6. shows a five day section of beam attenuation, current speed and easterly velocity from the April/May record (figure 6.1) close to the first spring tide. In addition to an M_2 signal, there was a double maxima at the M_4 frequency. The M_4 signal was at approximately the time of the maximum current speed, though it was consistently slightly offset , with a maximum just after the peak in westerly current (a) and one just before the peak in easterly current (b).

The principal minima in beam attenuation (c,e in figure 6.6.) are coincident with the high water slack whereas the maxima are coincident with the low water slack (d). This strongly suggested that there was a horizontal gradient of SPM which oscillated in the tidal flow.

The same features were observed in a second expanded section of the April/May record at times of a spring tide, shown in figure 6.7. However when sections of data at neap tides are examined, in figures 6.8. and 6.9., the beam attenuation record is observed to be more uniform, as expected in a diminished tidal flow.

The tidal ellipse at the mooring site was almost

Figures 6.6.to 6.9.
Expanded time series of measurements of beam attenuation , current speed and eastward velocity ,at 20m.

Fig.6.7. from 14/4/87-18/4/87, spring tides.
Fig.6.8.from 26/4/87-30/4/87, spring tides
Fig.6.9. from 18/4/87-22/4/87,neap tides.
Fig.6.10. from 4/5/87-8/5/87, neap tides.

Figure 6.6.

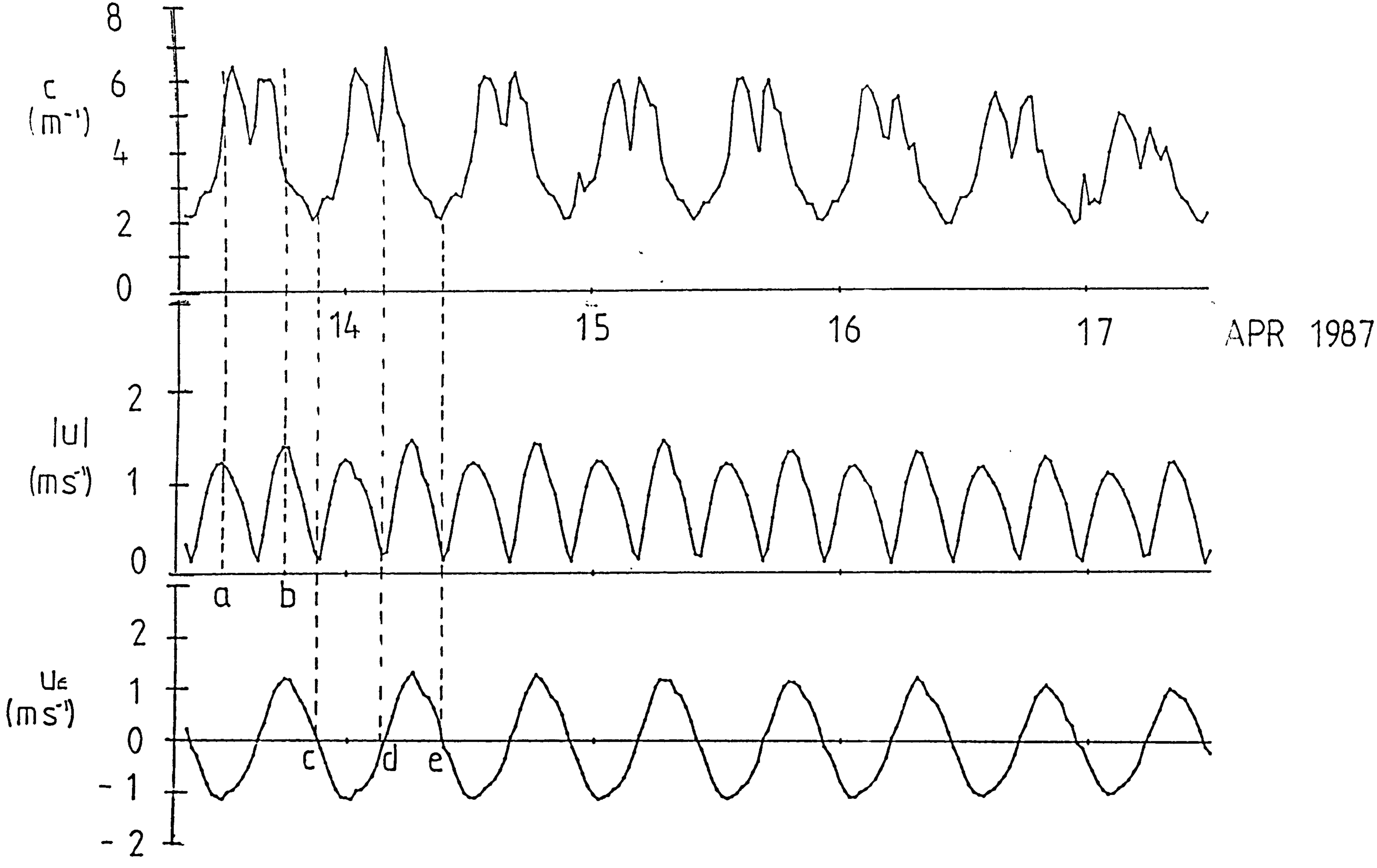

Figure 6.7.

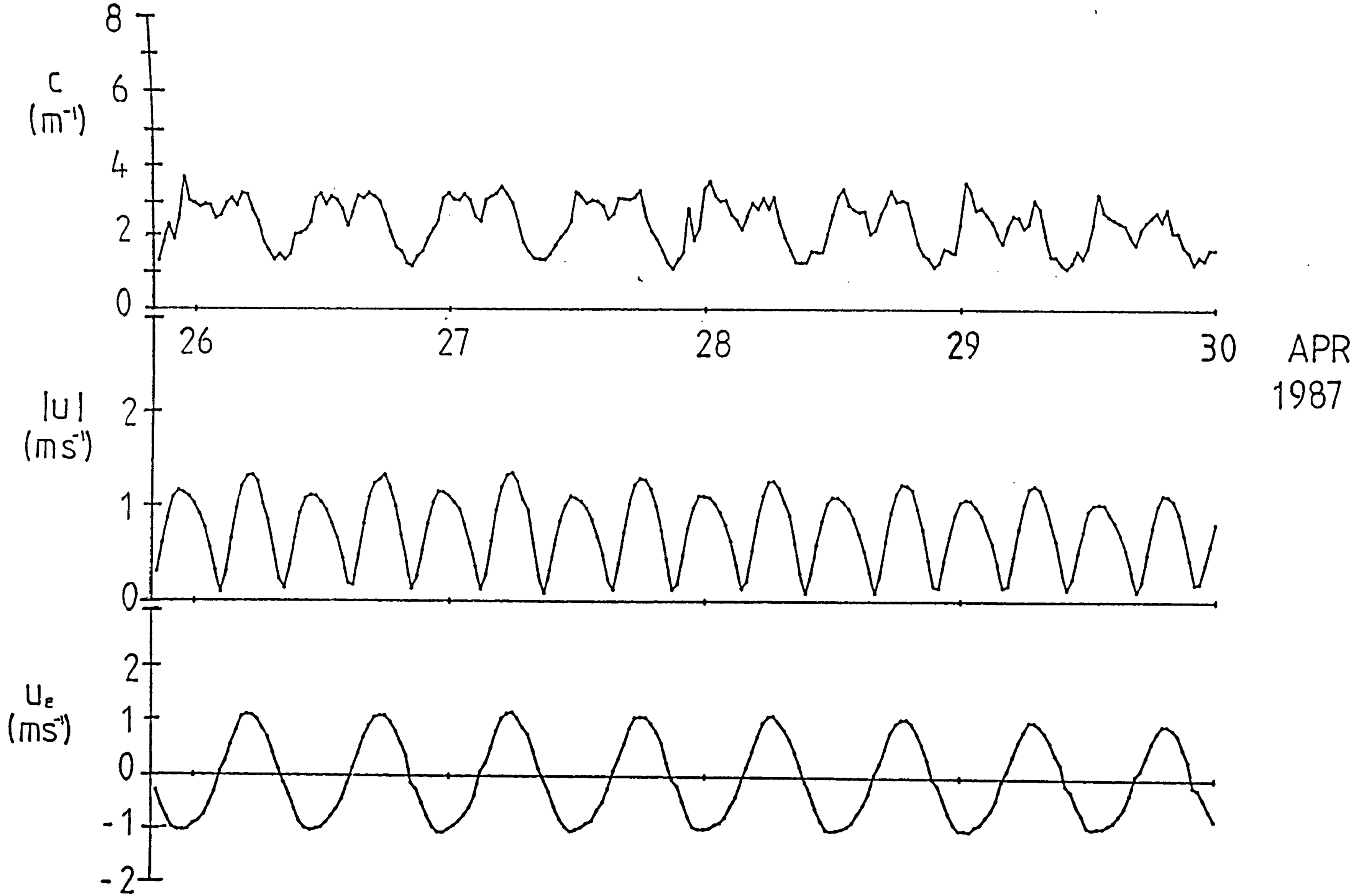

Figure 6.8.

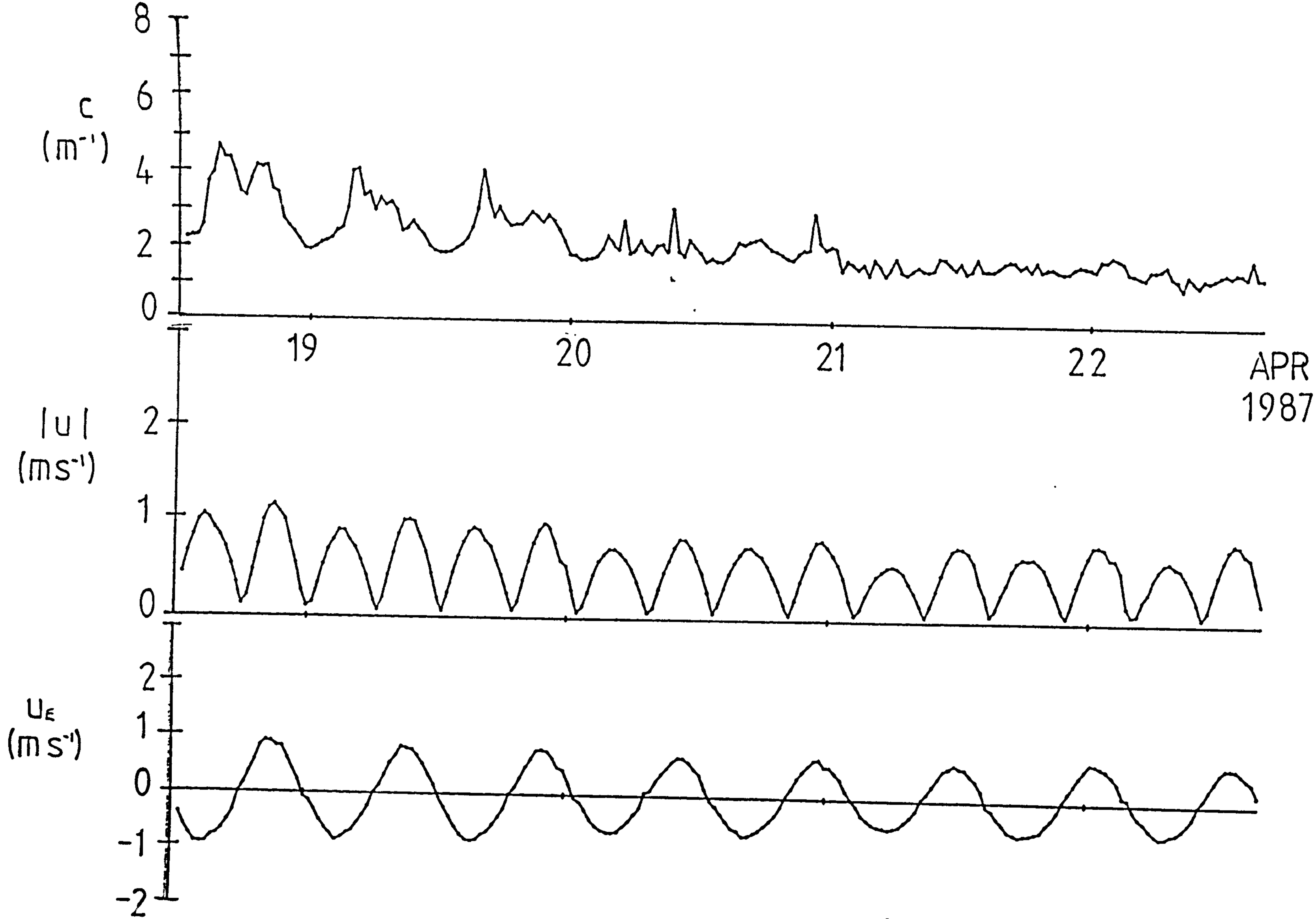

Figure 6.9.

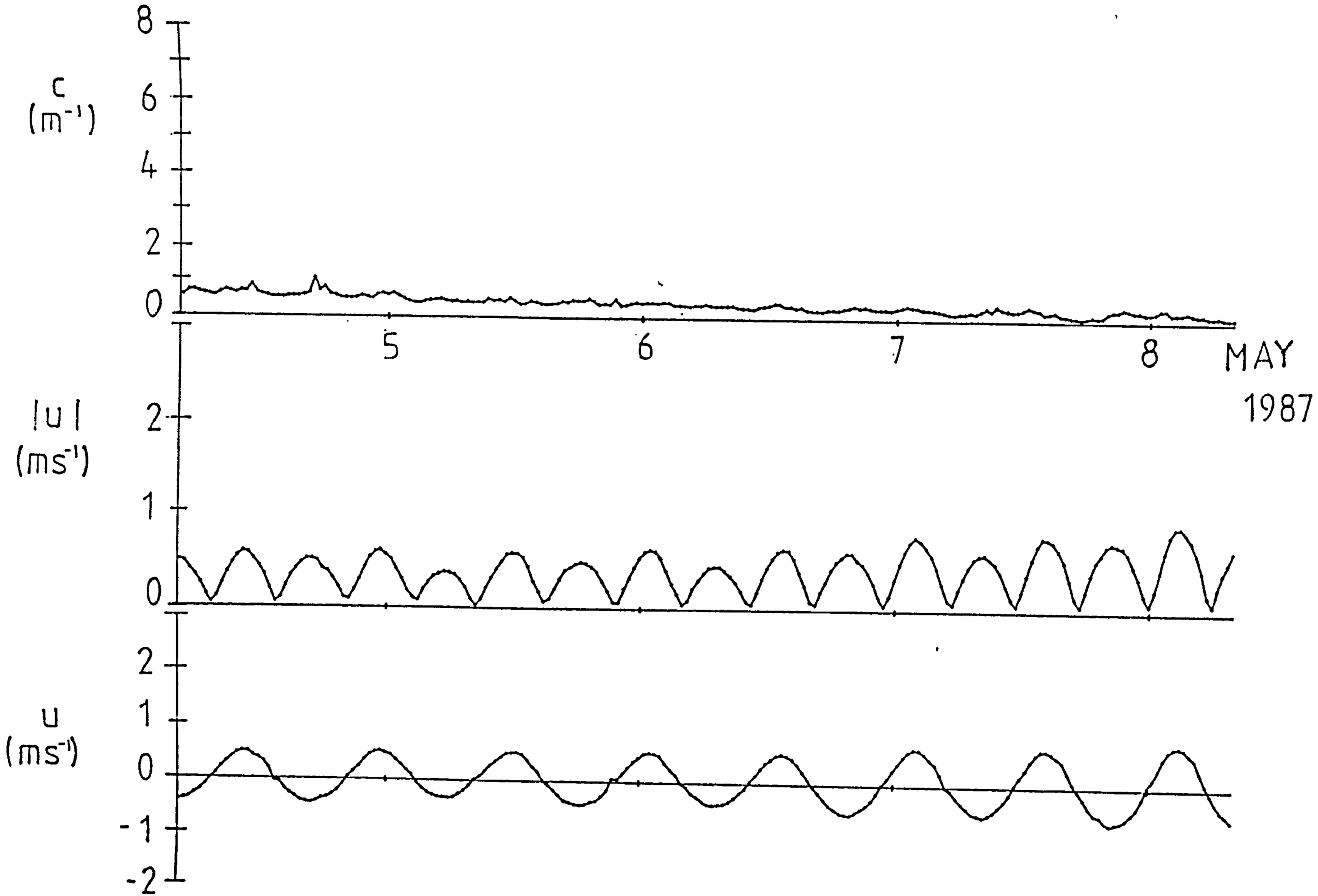

rectlinear. This is illustrated by a plot of eastward and northward velocity values taken from a four day period at times of spring tides in the April/May record (figure 6.10).The eastward velocities were greater than the those in the northerly direction, and there was a northerly residual of 0.1ms^{-1}.

Confirmation of the trends in the time series observations in 1987 were found, in part, in the vertical profiles of CTD and beam attenuation measurements made from the ship in 1986 over 13 hour periods. Figure 6.11 shows a time series of vertical profile measurements of temperature and beam attenuation and surface current speed in the region of the mooring, (53° 30.38'N,4° 50.36'W) on 30/6/86. Warm, less dense, turbid water was observed at LW slack tide (0030) when there is the maximum south-westerly displacement of the water column. Cool, dense, clear water was observed at HW slack, during the maximum north-easterly displacement. This is consistent with the idea of a horizontal gradient in SPM producing time dependant variations at a point in an oscillating tidal flow. There was no evidence of resuspension in the time series. This may have been due to weak tidal velocities.

A second time series of vertical profiles of temperature, beam attenuation and surface current speed from the region (53°41.53'N,4°21.71'W) on 22/9/86 showed

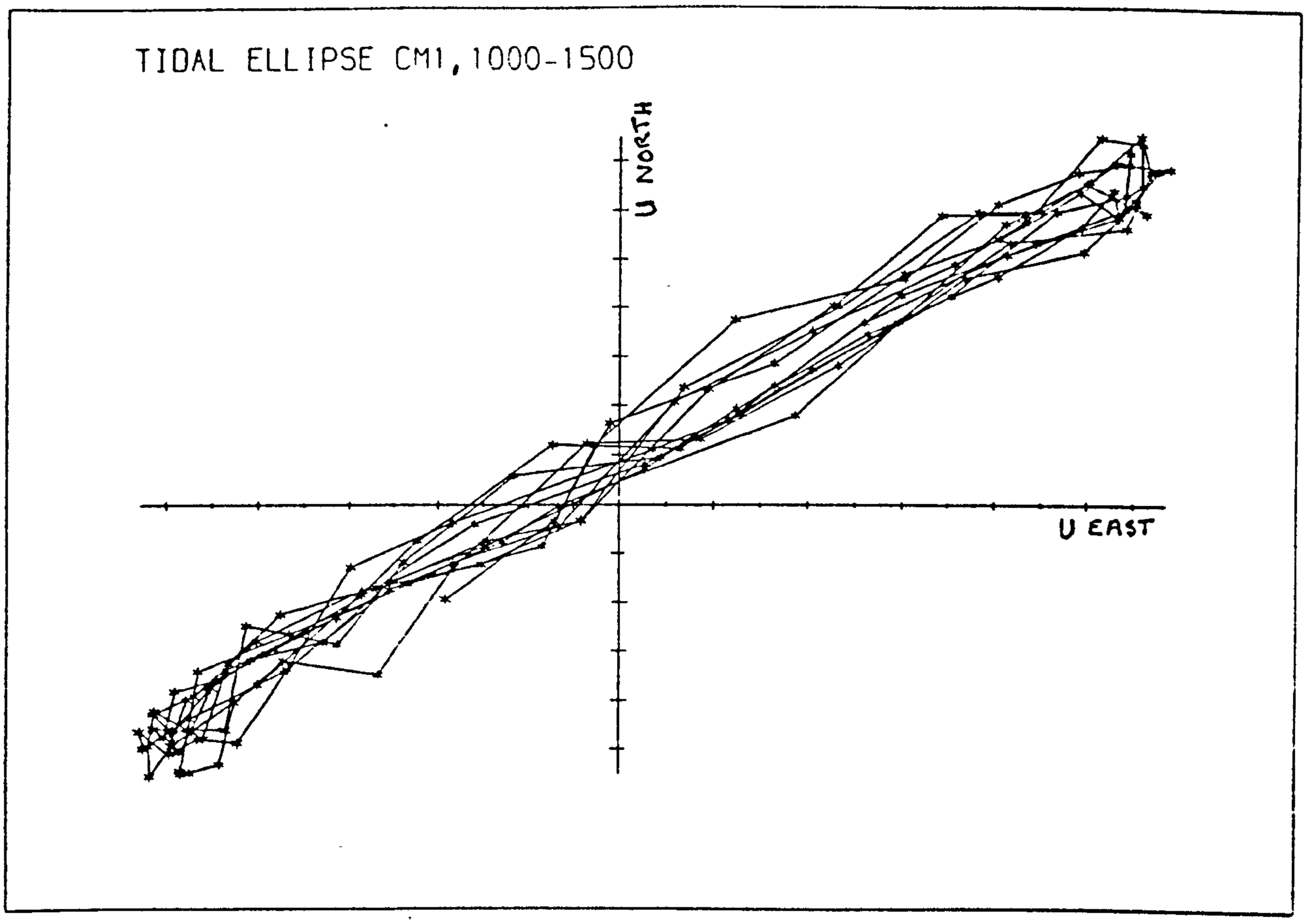

Figure 6.10. Tidal ellipse taken from part of velocity time series at a depth of 20m , from 26/4/87-6/5/87. Intervals on axes = 1 cms^{-1}.

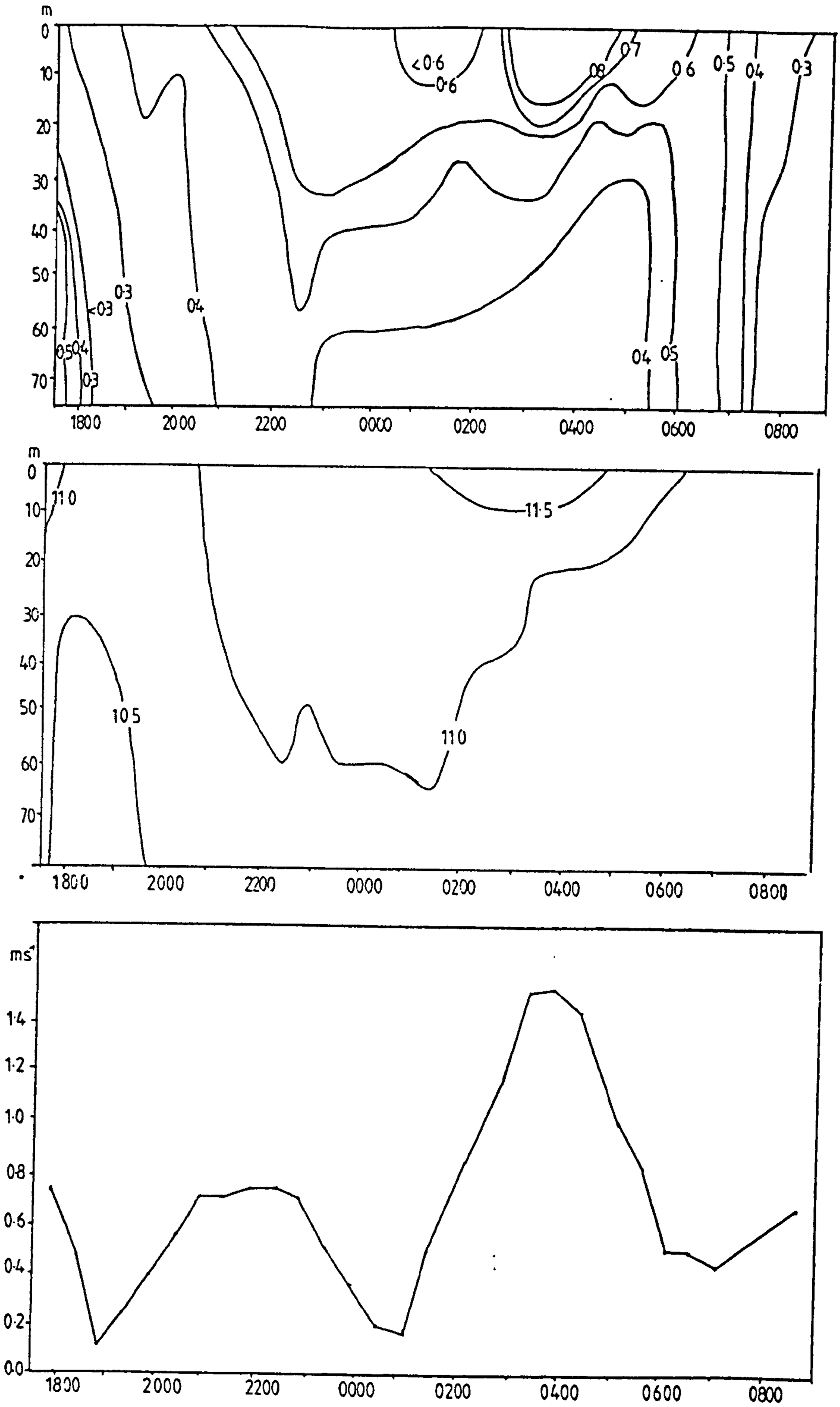

Figure 6.11. 13 hour time series of vertical profiles of measurements of a)beam attenuation,b) temperature,c) subsurface measurements of current speed near to station A2 ,at 53° 30.38'N,4° 50.36'W on 30/6/86.

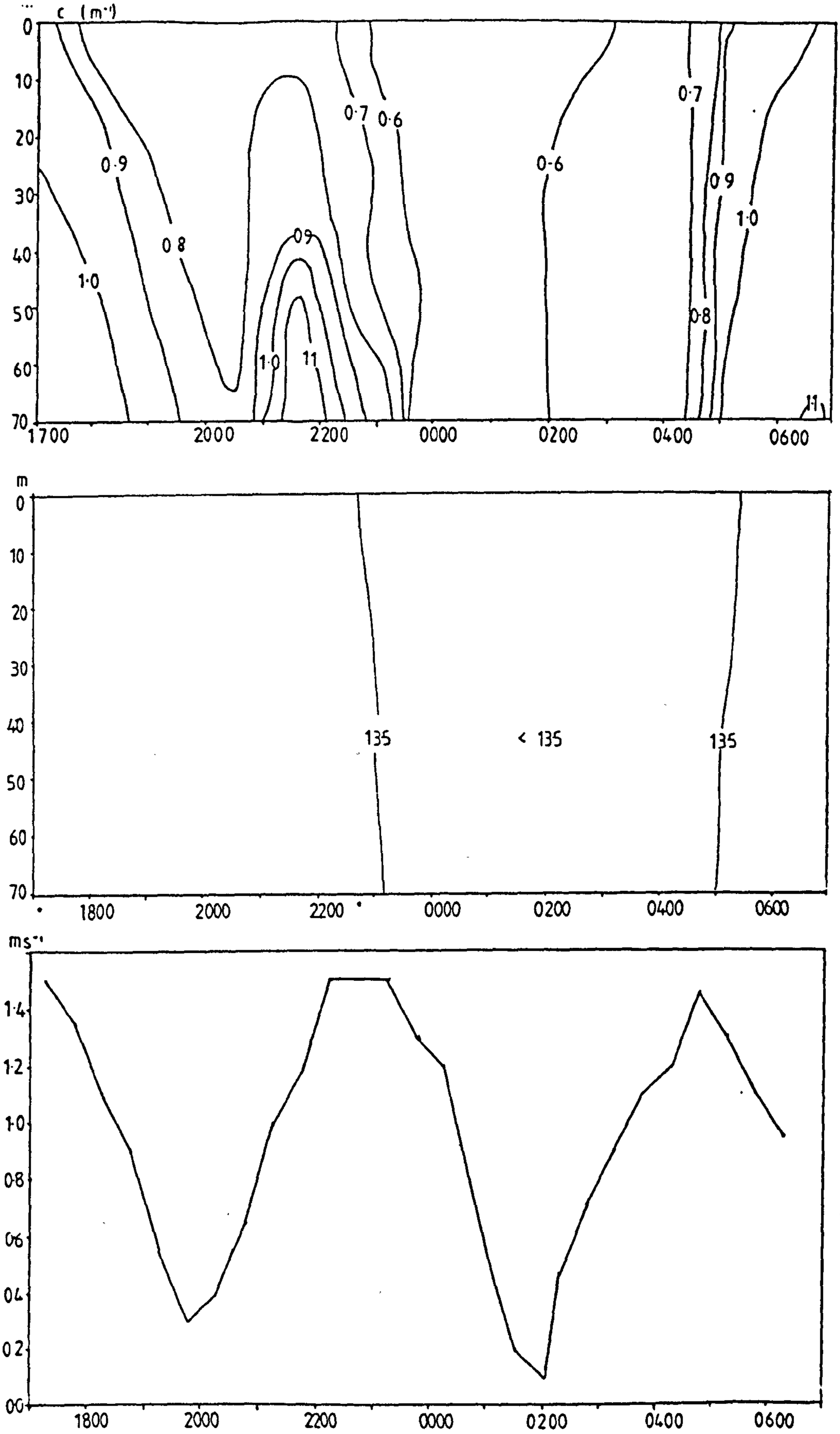

Figure 6.12. 13 hour time series of vertical profiles of measurements of a) beam attenuation, b)temperature, c) subsurface current speed near to station F3 ,at 53° 41.53'N,4° 21.71'W, on 22/9/86.

a similar trend (figure 6.12.). The horizontal temperature gradient was small but again clear water was observed at high water, slack tide, attributed to the flow from the south-west. More turbid water was observed at low water, slack tide, advected from the north-east.

Furthermore, there is some evidence of local resuspension of SPM during the maximum flood tide flow,between 2100 and 2200.

To establish the consistency of the processes observed at the location north of Anglesey, a time series from a second location was examined. The vertical profiles of measurements of temperature and beam attenuation and surface current speed were made off the coast of Cumbria at station J3 (in figure 5.1.b.) at 54° 19.67'N,3° 41.01'W. The sea-bed is composed of mud at this location and tidal currents are typically less than 0.4 ms^{-1}. Figure 6.13. shows a 12 hour time series from 2/7/86. The water was thermally stratified, with higher values of c below the thermocline. The vertical gradient in c was disturbed just after the maximum current at 2230, suggesting that there was resuspension near the sea-bed.

A second time series from the Cumbrian location, station J3 (at 54° 19.19'W,3° 42.2'W) on 23/9/86 is shown in

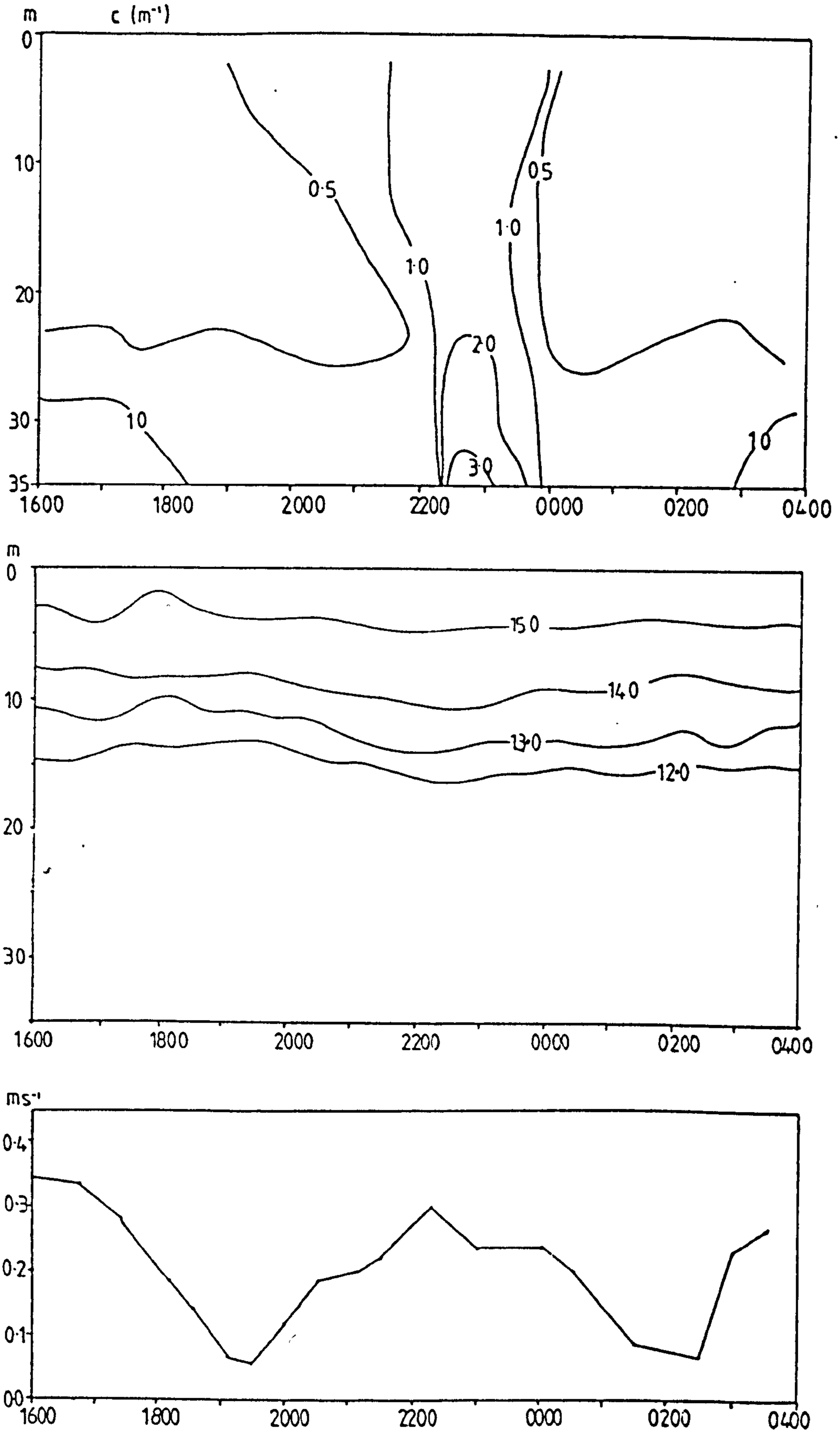

Figure 6.13. 13 hour time series of vertical profiles of measurements of a)beam attenuation, b) temperature, c) subsurface current speed at station J2 , at 54° 20.0'N, 3° 41.0'W on 2/7/86.

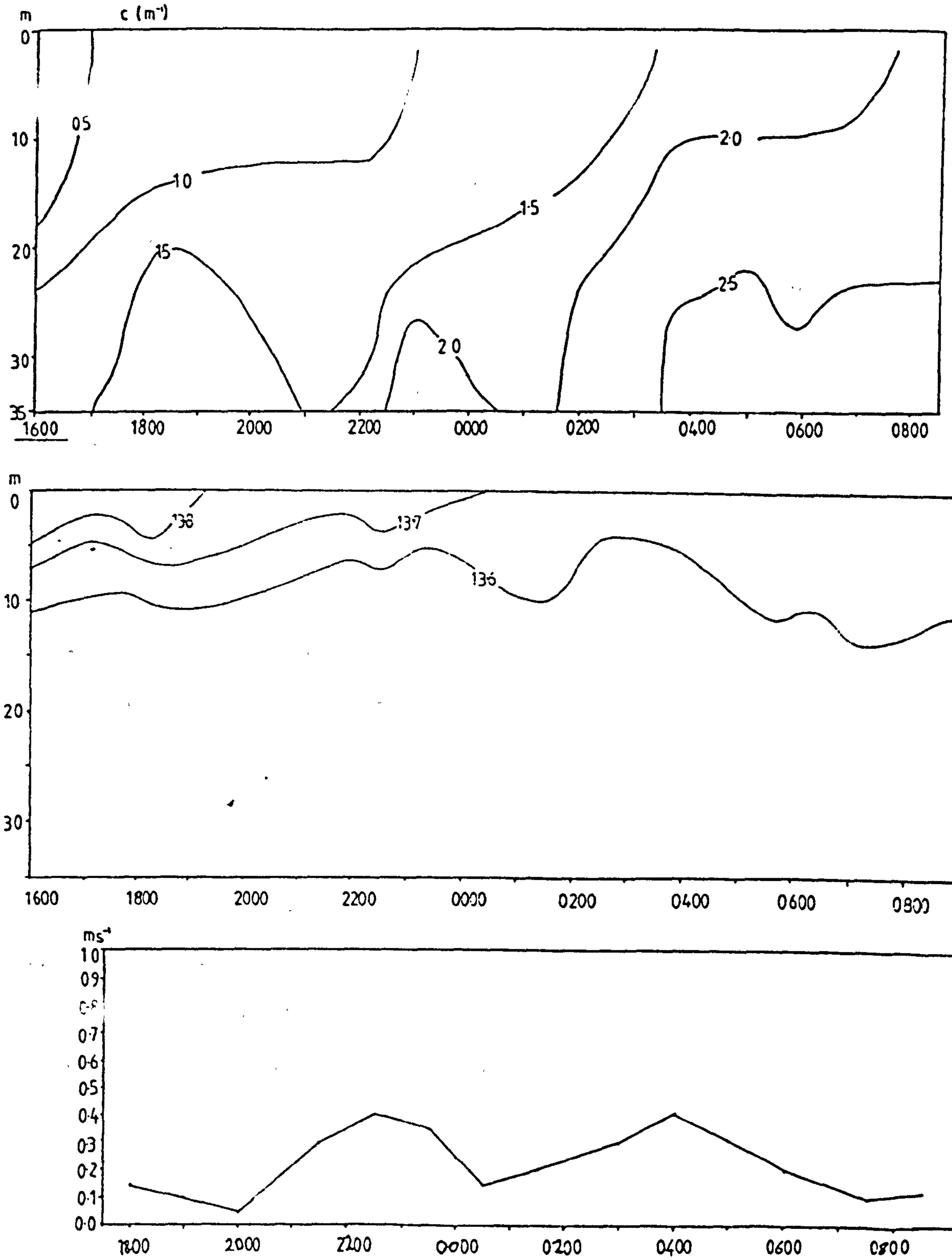

Figure 6.14. 16 hour time series of vertical profiles of measurements of a) beam attenuation, b) temperature, c) subsurface current speed at station J2 , at 54° 20.0'N, 3° 42.0'W on 23/9/86.

figure 6.14. Thermal stratification had almost broken down, and the vertical profile of c was more uniform than in July. Values of c were generally higher than in July. There were high values of c associated with velocity maxima, suggesting resuspension of sediment by the tidal flow. High values of c observed at slack water may be caused by horizontal advection of SPM.

Conclusions.

A strong seasonal cycle, consistent with the observations in Chapter 5, was observed in the beam attenuation record from the moored transmissometers. The records were tidally dominated during the spring and autumn, but in June,July and August showed rather little tidal response. It is somewhat surprising that that there was no apparent influence of waves on the level of SPM in the water. It may be that the effect of waves on resuspension is confined to shallower areas and so is not observed in the record from the mooring which was in a water depth of 70m. The seasonal response can be observed in the record for the whole season and was so marked during the spring that it clearly observed in the record from the deployment in April.

Closer examination of the record from April 1987 suggested that local resuspension of sediment from the sea-bed and tidal oscillation of a horizontal gradient of SPM concentrations appeared to be responsible for variations in the time series measurements of c.

These observations were supported by data from the surveys in 1986, in which vertical profiles of measurements were recorded over 13 hour periods using instruments lowered from the ship.

The extent of the relationship between tidal flow and beam attenuation is examined further in section 6.2.

6.2. A conceptual model of variations in beam attenuation.

Beam attenuation, recorded at a fixed position in the sea, varies with resuspension of sediment from the sea-bed and with advection of water masses with different concentrations of suspended material. A schematic diagram of these processes is shown in figure 6.15.

The conceptual model (figure 6.15) describes a region where there is a linear horizontal gradient of the beam attenuation coefficient, with increasing values to the east, and a rectilinear tidal current orientated in the east to west direction. Every 12.42 hours, the M_2 tidal period, there are maximum and minimum values of c at the mooring, at slack water. The graph in Figure 6.15(a) shows the change in beam attenuation with time. If $dc/dx = 0$, there will be no change in c. But if $dc/dx > 0$, values of c will be lowest when the water is displaced furthest to the east, and highest, when it is displaced furthest to the west.

In Figure 6.15.(b) the mooring is in the same

a)

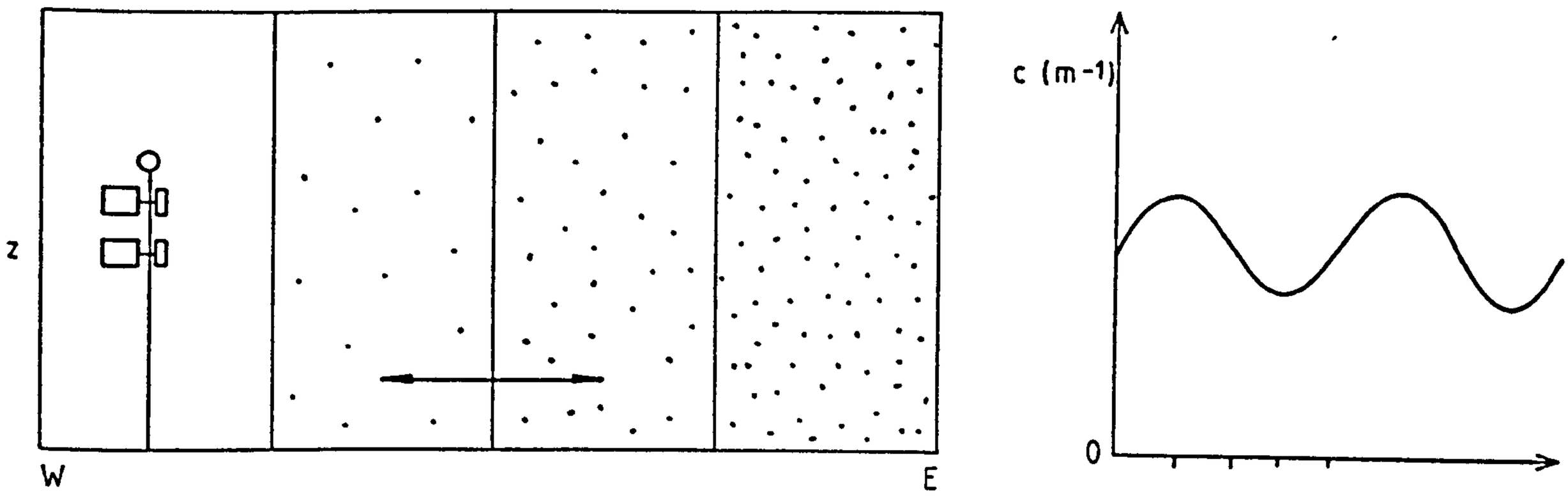

b)

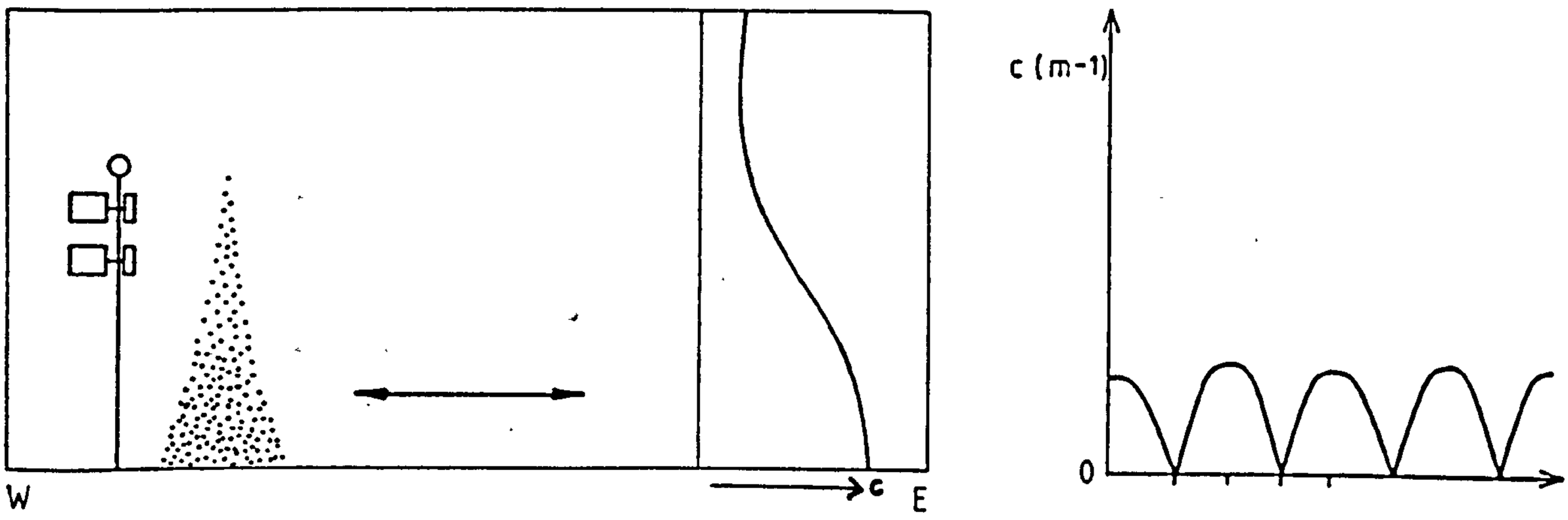

c)

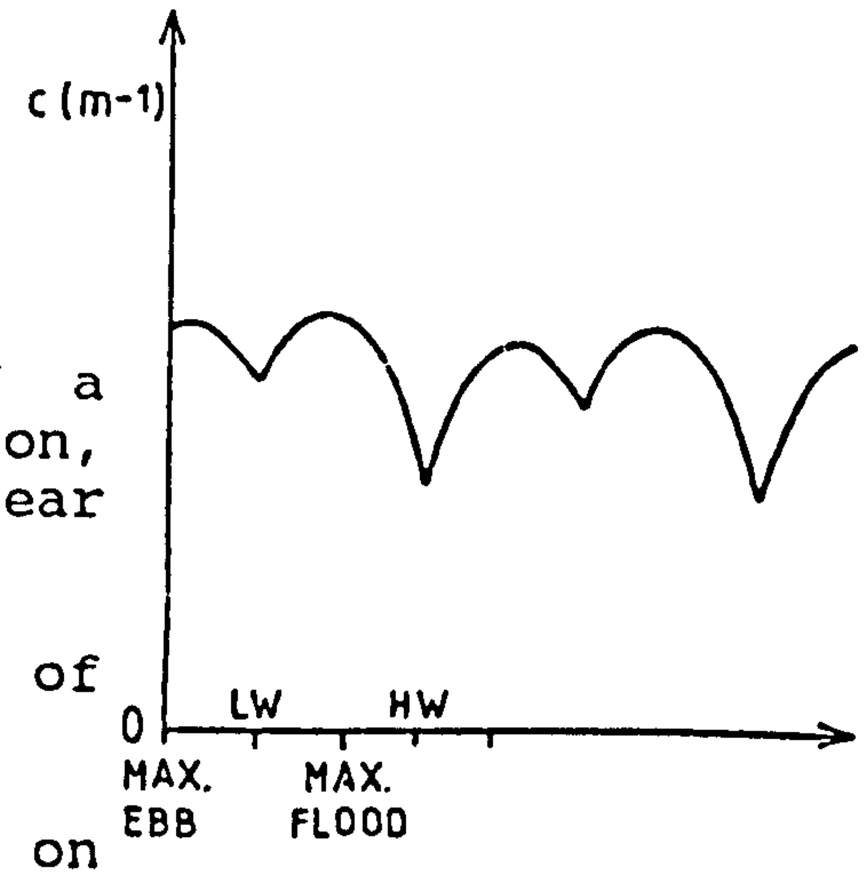

Figure 6.15.

a) The effect of the oscillation of a horizontal gradient in beam attenuation, increasing to the east, in a rectilinear tidal flow, on values of c.

b) The effect of tidal resuspension of sediment on values of beam attenuation.

c) The combined effect of (a) and (b) on beam attenuation,c.

oscillating tidal current but the sediment is resuspended from the sea-bed in response to the shear-stress, and is deposited when the current relaxes. Every 6.21 hours there are maximum values of c at the same time as maximum current speeds.

When the two curves ,in a) and b), are summed (c) the two peaks in c at M_4 frequencies are offset from the maxima in current speed, as they are in the expanded records of c in figures 6.6. and 6.7 .Furthermore there is an M_2 signal in (c) when u = 0, equivalent to low and high water slack tide. This is also observed in the data.

The conceptual model qualitatively fits the data as shown in figure 6.16 , where sections of measurements of beam attenuation (a),current speed (b) and tidal displacement to the east (c) are shown for a period of 4 days near spring tides.

This may be represented in the form

$$\hat{c} = \alpha x + \beta |u|^n + \gamma$$

$\hat{c}$ = predicted attenuation (m^{-1}); x is the tidal displacement (in km) of a horizontal gradient of c (α); $|u|$ = the modulus of velocity, assumed to be horizontally uniform(ms^{-1}); β = the sediment pick-up rate. α, β, γ, n are coefficients to be determined.

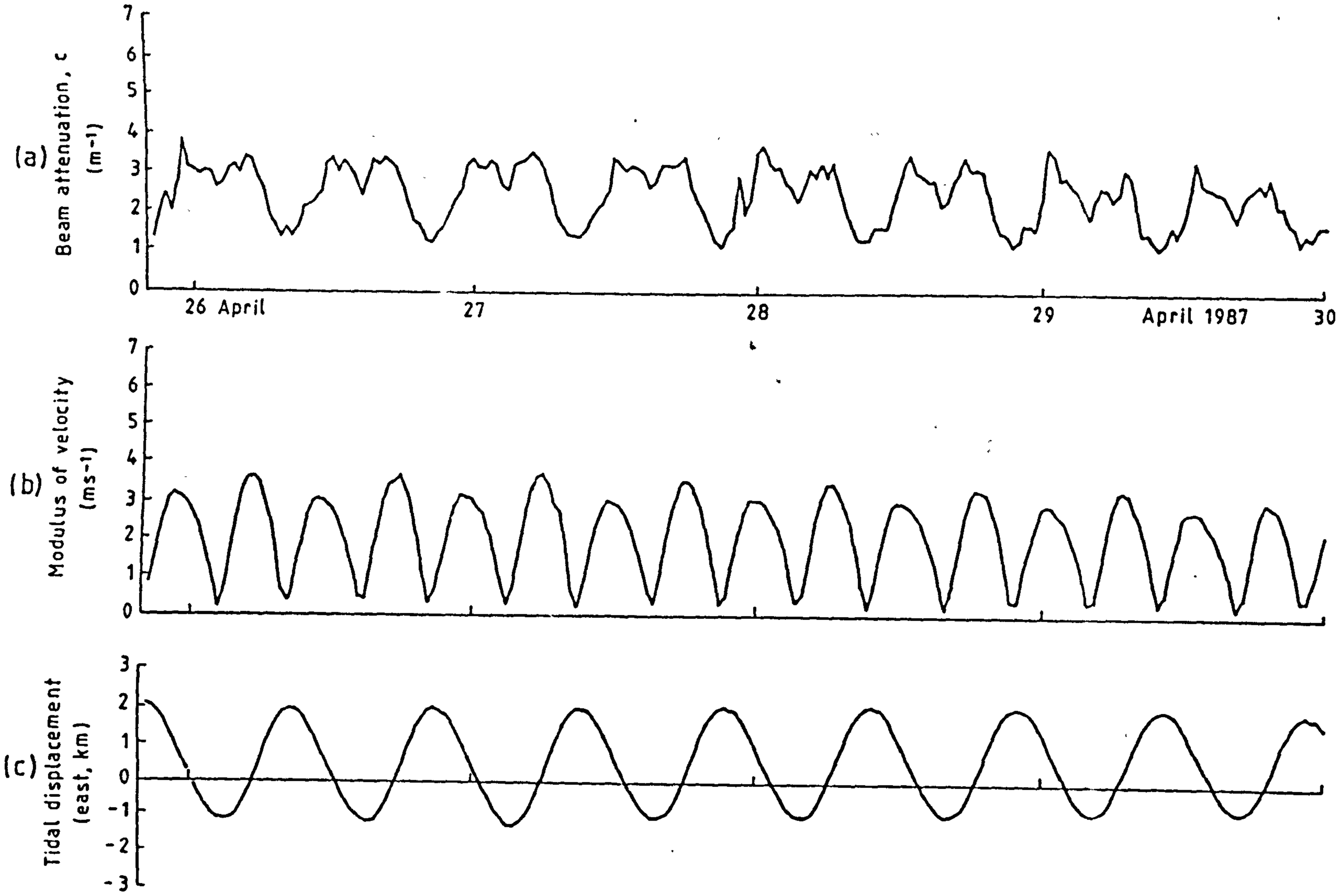

Figure 6.16. Expanded time series from 26/4/87-30/4/87 from 20m of
a) beam attenuation (m^{-1}).
b) current speed (ms^{-1}).
c) eastward tidal displacement (km).

Values of $|u|$ were taken from current speed measurements. x was calculated from velocity measurements where

$$x = \int u.dt$$

The residual current was filtered from the values of x so that only the tidal displacement was calculated.

In order to quantify the coefficients α, β, γ a regression was calculated using the time series measurements of c and current speed and direction from the deployment in April/May 1987. $|u|$ was simply the current speed; x was calculated by integrating easterly velocity with time. Since the tide was rectilinear (Figure 6.10) , the displacement, x, was always in the same plane. The regression was repeated with values of n from 0.25, 0.5, 0.75, 1.0 and 2.0.

Table 20 shows that when n was set at 0.5 the model provided the best fit to the variance in the data, giving an r^2 value of 35.4%. The relationship between the model and the data is significant at the 0.1% level. Since there was little difference in the regression for different values of n , the value was set at 1 for all the following calculations.

The constants α, β, γ, n were then used to calculate c, with

TABLE 20 REGRESSION ANALYSIS FOR THE TIME SERIES OF C (APRIL,1987) AND THE MODEL (SEE TEXT).

$\hat{c} = \alpha x + \beta|u|^n + \gamma$

Data from deployment during 6/4/87-12/5/87

n	γ	α	β	F	r^2 (%)	s.d. (m^{-1})
0.25	-0.0601	-0.0815	2.59	520.6	34.2	1.42
0.5	0.281	-0.0849	2.46	549.76	35.4	1.13*
0.75	0.585	-0.0857	2.28	525.46	34.4	1.14
1.0	0.800	-0.0857	2.05	497.55	33.2	1.15
2.0	1.23	-0.0825	1.56	414.48	29.3	1.18

the time series of $|u|$ and x from the April/ May deployment. The simulated beam attenuation for the time series is shown in figure 6.17 where a) is the attenuation data, b) is the predicted attenuation and c) is the difference between the two. The least difference between the data and the predicted c is in the central part of the record, but somewhat larger at the extremities.

As the CTD spatial survey indicated a change in the spatial gradient of c over the time of the deployment, the value of α was expected to be variable over the duration of each deployment. Figure 6.18 shows the variation in the spatial variation of c during 30/3/87-4/4/87 and during 12/5/87-15/5/87. This shows that the horizontal gradient in beam attenuation decreased from April to May. Furthermore since a better relationship was found between c and u at spring tides (figures 6.1,), it was expected that the model should provide a better fit to the variation in the data for short time series.

The data was therefore divided into sections of 4 days and the regression was calculated for these sections.

The best estimates of c from the model are shown in table 21. The model explained 70% of the variation in c

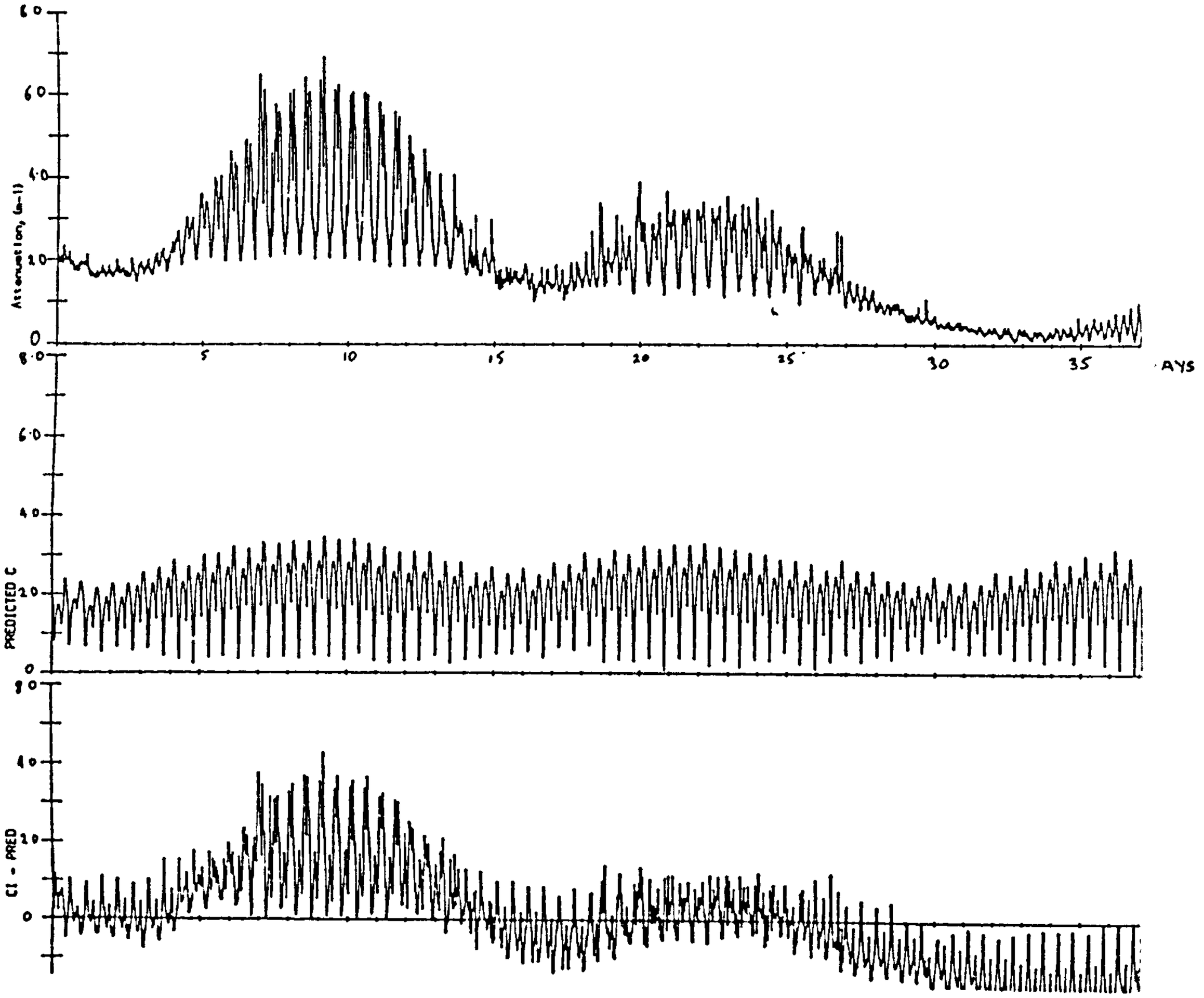

Figure 6.17 Time series of from 6/4/87-12/5/87 at 20m of
a) beam attenuation (m^{-1}), c.
b) beam attenuation (m^{-1}) predicted from the model, $\hat{c}$.
c) $c - \hat{c}$.

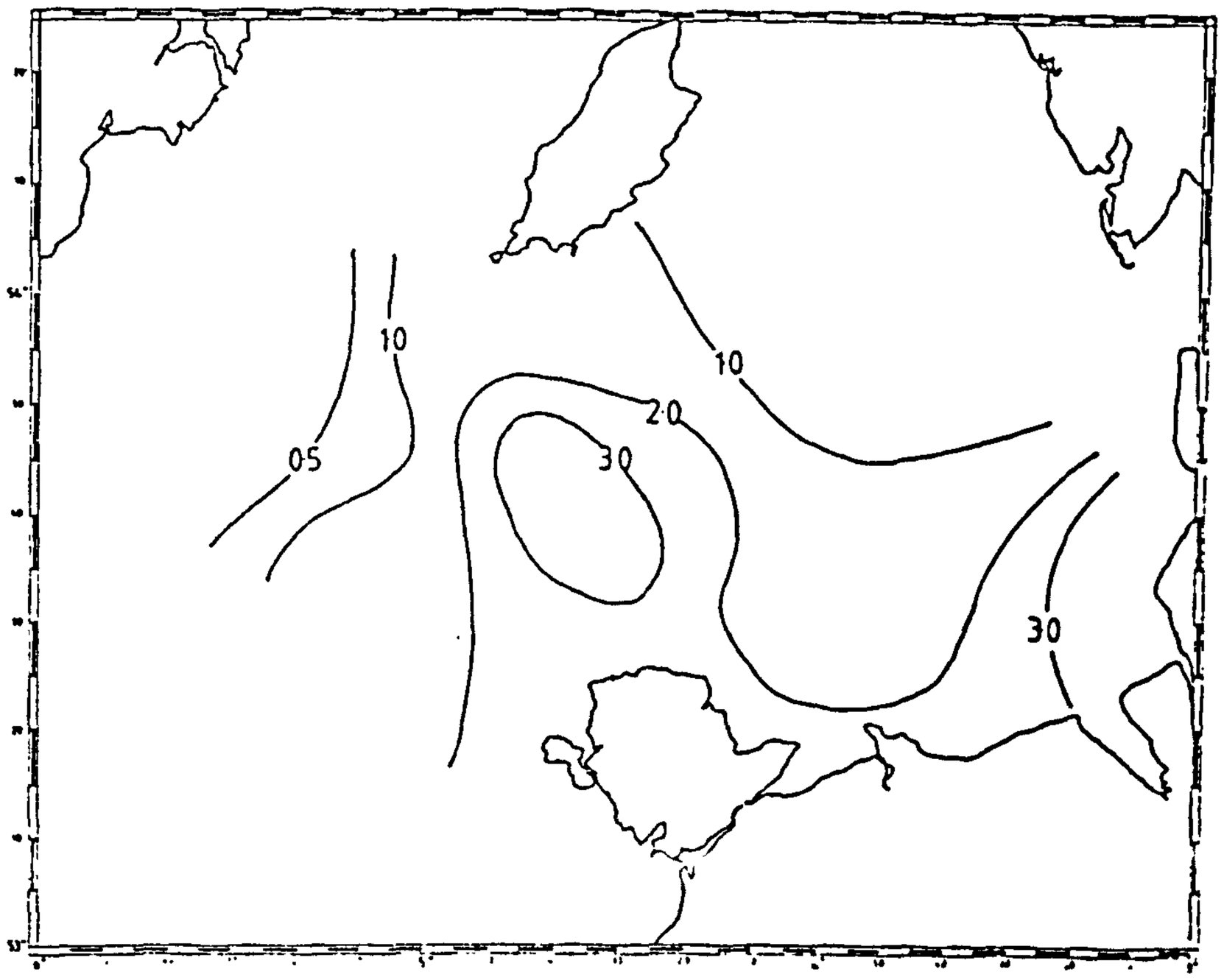

Figure 6.18. Spatial distribution of beam attenuation at 5m below the surface
a) from 30/3/87 to 4/4/87,
b) from 11/5/87-15/5/87.

TABLE 21 VALUES OF α AND β WHEN n = 1, FOR TIME SERIES OF 4 DAYS, FROM THE PERIOD DURING 6/4/87 to 12/5/87.

DAYS AFTER START	CONST	α	β	R^2	LUNAR PHASE
0-4	1.66	-0.0127	0.569	0.300	
4-8	2.87	-0.149	1.13	0.532	
8-12	4.00	-0.214	0.403	0.718	S
12-16	1.58	-0.051	1.15	0.213	
16-20	1.33	-0.020	0.949	0.333	
20-24	1.94	-0.089	0.926	0.738	S
24-28	0.842	-0.013	0.997	0.293	
28-32	0.402	-0.0235	-0.001	0.167	
32-36	0.0537	-0.002	0.417	0.663	S

at times of spring tides. At neap tides, the corresponding values were ~ 30%. This is illustrated by figures 6.19 and 6.20. which are time series of the sections of data, of predicted attenuation, and of the difference between the data and the model for two sections near spring tides.

A comparison was made between the estimates of α and $\Delta c/\Delta x$ the predicted and the measured horizontal attenuation coefficient gradient.The measured values were taken from the survey cruises at the beginning and at the end of the deployment. Table 22 shows that α was smaller than the measured parameter $\Delta c/\Delta x$ by a factor of 4 to 5. It also shows that the values of both α and $\Delta c/\Delta x$ decreased in 6 weeks by a factor of 2, due to the seasonal reduction in SPM.

Conclusions.

The model predicting beam attenuation from values of current speed and tidal displacement explains 35% of the variation in the beam attenuation record in a 5 week period from April to May 1987.

When the data was divided into shorter sections, the model predicted 70% of the variation in the data at times of spring tides, but only 30% at times of neap

Figures 6.19 and 6.20.
Expanded time series of a) beam attenuation, at 20m, b) predicted beam attenuation, $\hat{c}$, using coefficients from the model for this section of the time series, c) $c-\hat{c}$:

Fig.6.19. From 14/4/87-18/4/87

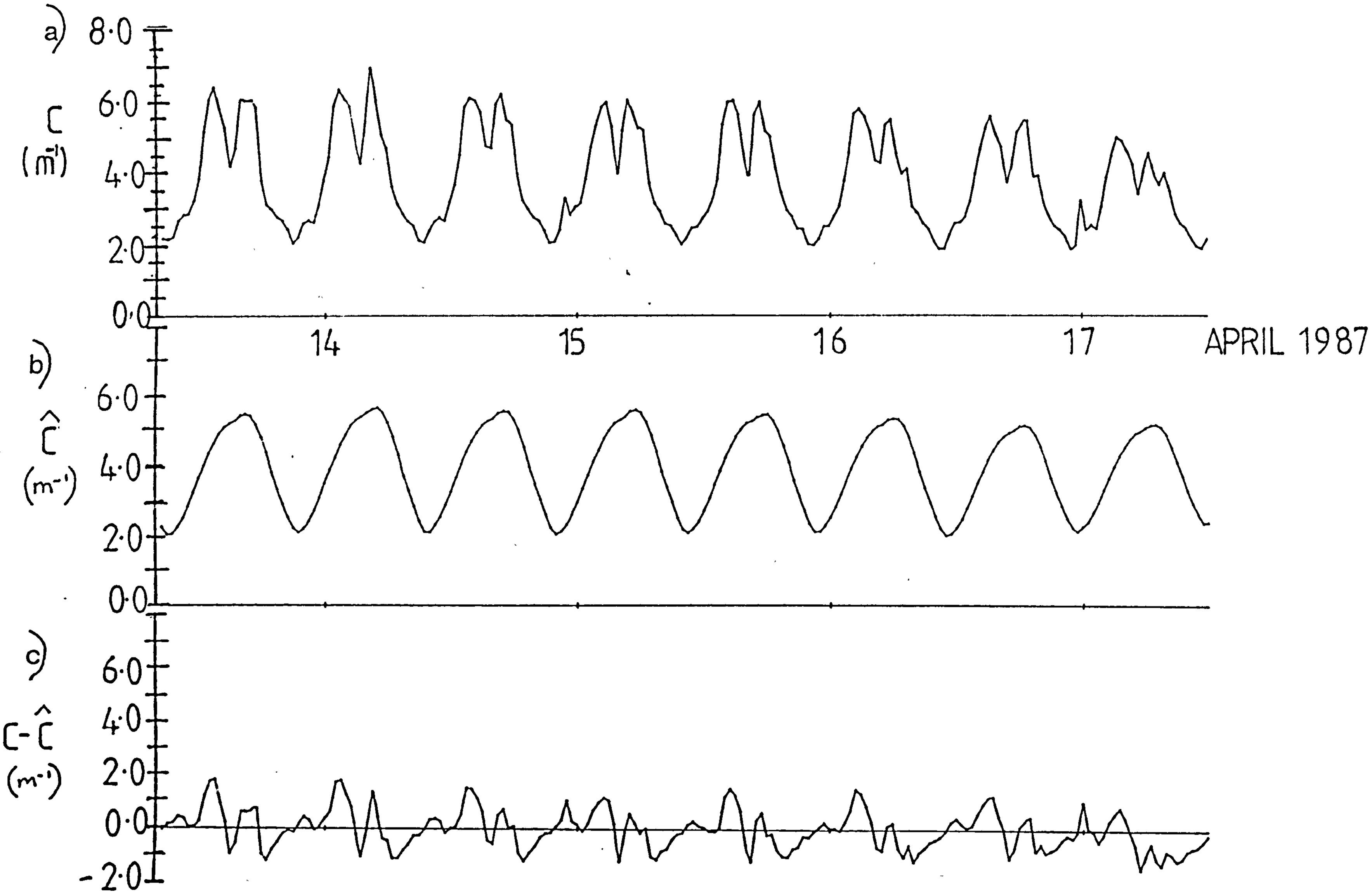

Fig.6.20. From 26/4/87-30/4/87.

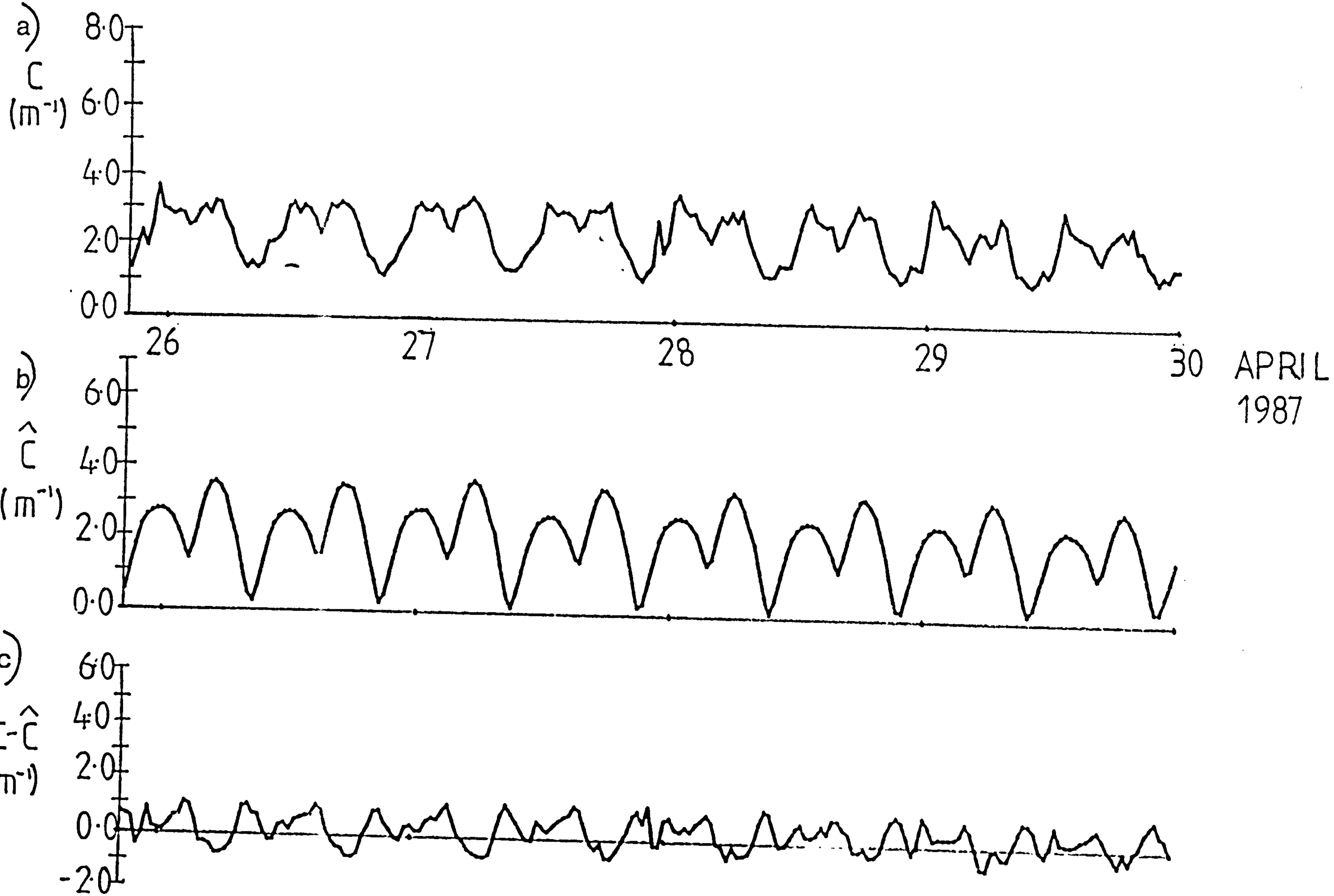

TABLE 22 VALUES OF THE OBSERVED AND PREDICTED HORIZONTAL GRADIENT OF C.

date	gradient direction	observed $\Delta c/\Delta x (m^{-1}km^{-1})$	model	$\alpha /(\Delta c/\Delta x)$ (%)
30/3/87	E-W	0.05	0.0136	27.0
12/5/87	E-W	0.03	0.0060	20.0

tides. Close observation of the results of the regression analysis show that from the beginning to the end of the deployment, the constant becomes smaller. This corresponds to the seasonal reduction in the background values of beam attenuation. The values of the horizontal gradient in c also become smaller throughout the deployment. However , there is a consistent pattern of the movement of clear water from the west coming into the region of the mooring. The values for the pick-up function , β , remain close to 1, with several exceptions where there were smaller values for β .

These observations indicate that the dominant processes, which cause variations in beam attenuation , originate from the tidal flow in the region of the mooring. The fit of the data to the model is reduced over a time period of more than four days.

CHAPTER 7 DISCUSSION

Recognition of the important biological and chemical role of SPM in the shelf seas has highlighted the scarcity of observational data, and the technical difficulties of making widespread measurements of SPM concentrations. The design and the construction of the beam transmissometer in this study was undertaken to acquire a time series of observations and surveys of the spatial distribution of the concentration of SPM.

These developments enabled a spatial survey to be made , with a wide area of coverage over a two year period in the northern Irish Sea. A time series was obtained for a six month period, from the moored transmissometers. Both of these achievements would not have been possible with solely traditional methods of measuring SPM, such as gravimetric determination of SPM concentrations.

However, the information from the transmissometer measurements was quantitatively limited, due to the comparison of beam attenuation with gravimetrically determined SPM concentrations. This is not altogether surprising as other workers have spent considerable effort calibrating their measurements of beam attenuation to give units of SPM concentration (Bishop,1986; Baker and Lavelle,1984).

However, although the observations are quantitatively limited, the use of transmissometers to measure SPM is the only realistic approach to the problem at the present time, if the objective is to aquire data over a wide area and for a substantial period of time.

The observations from the distributions of beam attenuation in the spatial survey showed a strong similarity to the patterns of upwelling radiance from the imagery from satellite-mounted sensors (CZCS). For the first time these patterns showed a resemblance with those of tidal stirring. A quantitative relationship has been shown between beam attenuation and the level of TKE. There is evidence of an additional effect by stratification on the distribution of beam attenuation. This was suggested in earlier work by Heathershaw and Simpson (1974). This is shown clearly in the data from October 1981 in which the surface values of c show no relationship with the level of TKE, but show a significant relationship to the stirring parameter ϕ. Convective cooling during this time may have masked the effect of tidal stirring.

For the first time a time series of beam attenuation has been obtained for a period of six months, giving valuable insight into the seasonal and shorter frequency variations and processes controlling SPM in the shelf

seas. Although there are time series of the variations in SPM concentrations in straits (Buchan et al.,1964) and in estuaries (e.g. Assinder et al,1985), the observations offshore in the shelf seas are limited. A notable example is the work by Joseph (1955) who made a time series of transmissometer measurements over several tidal cycles.

This study reveals a strong seasonal signal in beam attenuation, particularly in strongly mixed water, and in the concentration of SPM, with higher values in the spring and autumn than in the summer months. In the spring and autumn there was a strong tidal response, but this was not apparent in the observations in the summer. The tidal response in the beam attenuation record is observed to be a combination of advection and re-suspension, and as the model in Chapter 6 shows, contributes as much as 70% of the variation in the values of beam attenuation at times of spring tides.

A particularly interesting observation was that there is no apparent response in beam attenuation to the surface wind, although other workers (e.g. Pejrup ,1986) found wind to have a significant effect on the level of SPM concentration in a shallow estuary. It may be that surface winds cause more stirring of the sediment near the coasts .

A synthesis of the dominant processes forcing changes in SPM concentrations is presented in Figure 7.1. The seasonal cycle of variations in SPM concentrations is driven by biological and physical processes, which overshadow the relatively constant seasonal tidal processes. Although there is no direct evidence in this study of binding of the sediment during the summer, it may account for the reduction in tidal re-suspension of material from the sea-bed and in the coastal margins. It may be an important control in the decrease in the horizontal gradient in beam attenuation observed during the summer. The sediments on the sea-bed may, therefore, not be available for re-suspension as in the winter, spring and autumn.

In addition, stratification has been shown to exert a secondary control on beam attenuation. This may occur by forming a barrier to the upward movement of SPM out of the deep stratified water. Areas such as the WIS and off the Cumbrian coast become stratified during the summer and may be a source of the fine sediments which remain in suspension for long periods. Stratification may effectively isolate these regions of high concentrations of SPM from the main body of water, although material from the surface layers can still sink downwards through the pycnocline. Stratified water may act as a trap for suspended particulates during the summer (Figure 7.1.)

The processes whch control the seasonal variations in

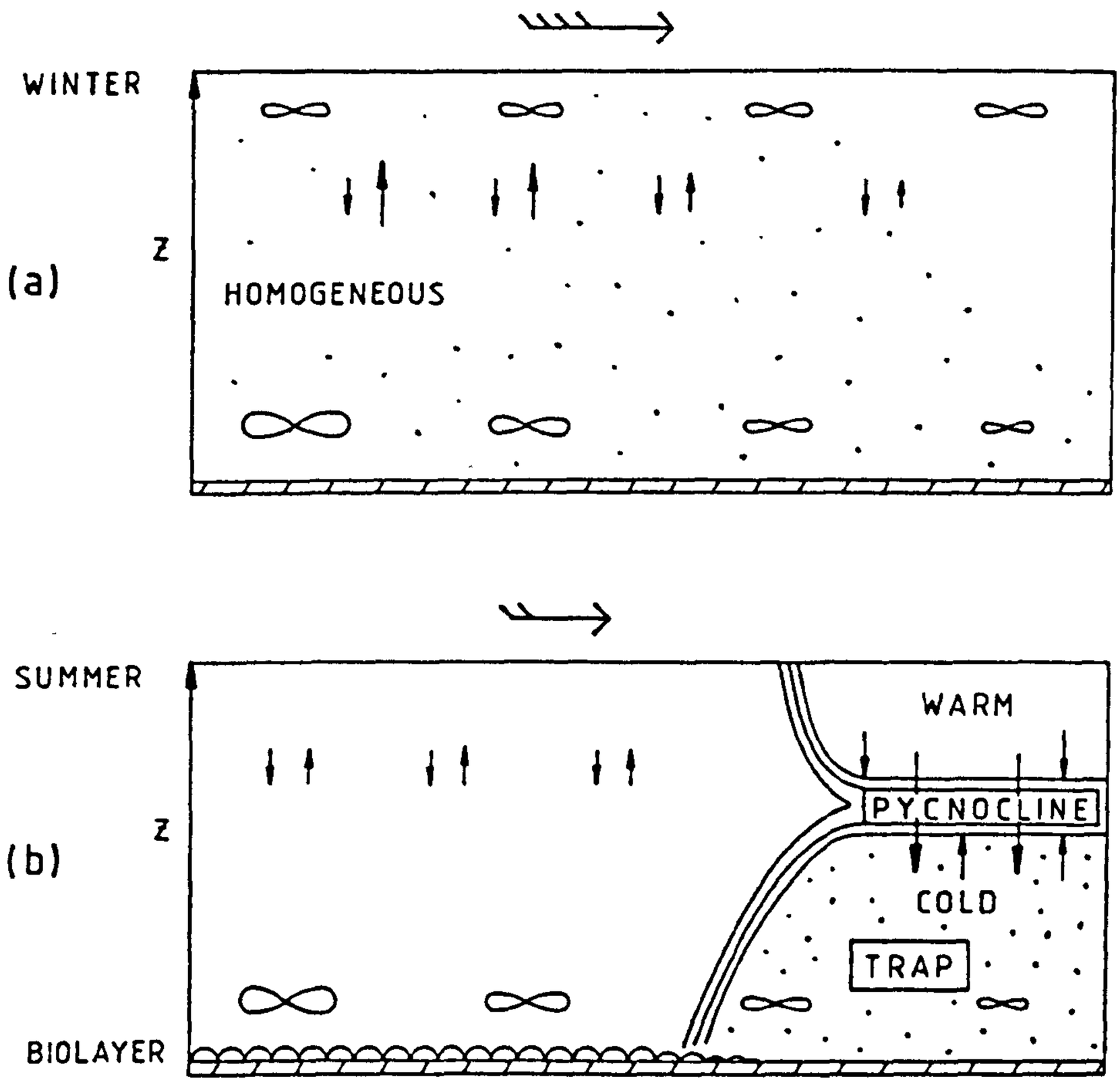

Figure 7.1. A schematic diagram of the processes controlling SPM concentrations in the shelf seas in
(a) winter.
(b) summer.
∞ = turbulent mixing; ↝ = wind above the sea surface; ↑↓ upward and downward movement of SPM.

SPM concentrations in the shelf seas are a combination of wind stirring, the binding of the sediment and stratification. Further work should include more extensive observations to be made near the coasts to determine the contribution of surface winds, of seasonal changes in the sediment to SPM concentrations and of temporal variations of SPM concentrations in stratified waters.

During the preparation of this thesis further work by C.Jago and S.Jones (University College of North Wales) has revealed that tidal advection and resuspension are dominant processes controlling SPM concentrations in their study of the North Sea. The model developed in this thesis has been applied with some success to time series data from transmissometers attached to their moorings.

It is evident that the use of transmissometers to measure SPM concentrations is limited because of the large uncertainty in the calibration. It would be useful to develop better algorithms for quantifying SPM concentrations from measurements of beam attenuation. This should include the improvement of water filtering techniques and more extensive size distribution analyses to determine the optical significance of a wide range in the particle size distribution. There should be further investigation into the variability of beam attenuation measurements with different proportions of organic material in the SPM.

REFERENCES

Agnew, M. M. 1983. A study of the use of sea colour for determining phytoplankton pigments and seston concentrations in coastal waters. M.Sc. thesis, University of Wales.

Allen, G. P., Sauzady, G., Castaing, P.,Jouanneau, J. M. 1977. Transport and deposition of sediments in the Gironde estuary. In, Estuarine Processes,2. Ed. Wiley.M., Academic Press, New York, 63-81.

Amos, C. L., Topliss, B. J. 1985. Discrimination of suspended particulate matter in the Bay of Fundy using Nimbus 7, CZCS. Can. J. Rem. Sens., 11, 85-92.

Assinder, D. J. 1982. The geochemistry of artificial radionuclides in the Irish Sea. Ph.D. thesis, University of Lancaster.

Assinder, D. J., Kelly, M. and Aston, S. R., 1985. Tidal variations in dissolved and particulate phase radionuclide activities in the Esk estuary, England, and their distribution coefficients and particulate activity fractions. J. Env. Radioactivity. 2,1-22.

Bader, H. 1970. The hyperbolic distribution of particle sizes. J. Geophys. Res. 75, 2822-2830.

Bagnold, R. A. 1956. Flow of cohesionless grains in fluids. Phil. Trans. R. Soc. London. A249, 235-297.

Baker, E. T., Lavelle, J. W. 1984. The effect of particle size distribution and chlorophyll on beam attenuation spectra. Appl. Optics. 21,3913.

Bartz, R., Zaneveld, J. R. V., Pak, H. 1978. A transmissometer for profiling and moored observations in water. Ocean Optics. 60,102-108.

Belderson, R. H. 1964. Holocene sedimentation in the western half of the Irish Sea. Mar. Geol. 2,147-163

Bishop, J. K. 1986. The correction and suspended particulate calibration of Sea Tech transmissometer data. Deep Sea Res. 33,121-134.

Boudjelas, S. 1988. Characteristics of fine suspended sediment in the Irish Sea. M.Sc.thesis, University of Wales.

Buchan, S., Floodgate, G. D., Crisp, D. J. 1967. Studies of the seasonal variation of the suspended matter in the Menai Straits. Limn. Oceanogr. 12,419-431

Bukata, R. P., Jerome, T. H., Bruton, S. C., Jain, S. C., Zwich, H. H., 1981. Optical water quality model of Lake Ontario: Determination of the optical cross sections of organic and inorganic particulates in Lake Ontario. Appl.Opt.20, 1696-1703.

Burt, W. V. 1953. Interpretation of Spectrophotometer readings in Chesapeake Bay waters. J. Mar. Res. 14, 33-46.

Burt, W. V. 1956. A light scattering diagram. J. Mar. Res. 15, 76-80.

Campbell, D. E., Spinrad, R. V., 1987. The relationship between light attenuation and particle characteristics in a turbid estuary. Est. Shelf. Mar. Sci. 25, 53-63.

Chester, R. 1982. The concentration, mineralogy and chemistry of total suspended matter in sea-water. In Pollutant Transfer and Transport in the Sea, 2, Ed. Kullenberg, G., CRC Press, Boca Raton, Florida.

Clarke, D. K., Baker, E. T., Strong. A. E., 1980. Upwelled spectral radiance distribution in relation to particulate matter in sea water. Bound. Layer. Met. 18, 287-298.

Czitrom, S. P. R. 1982. Density stratification and an associated front in Liverpool Bay. Ph.D. thesis, University of Wales.

Dobson, M. R., Evans, W. E., James, K. H. 1970. The sediments on the floor of the southern Irish Sea. Mar. Geol. 11,27-69.

Duursma, E. K, Eisma, D. 1973. Theoretical, experimental and field studies concerning reactions of radioisotopes with sediments and suspended particles of the sea : Applications to field studies. Neth. J. Sea. Res. 6, 265.

Duursma, E. K., Smies, M. 1982. Sediments and transfer at and in the bottom interfacial layer. In Pollutant Transfer and Transport in the Sea, II, Ed. Kullenberg,G.

Dyer, K. R. 1986. Coastal and estuarine processes. J.Wiley and Sons. pp. 342.

Eakins, J. D., Lally, A. E., Burton, P. J., Kilworth, D.R.,Pratley, F.A. (1982)Studies of environmental radioactivity in Cumbria. Part.5. The magnitude and mechanism of enrichment of sea-spray with actinides in west Cumbria, UK. United Kingdom Atomic Energy Authority Report No.AERE-R10127.

Frostick, L. E, McCave, I. N. 1979. Seasonal shifts of sediment within an estuary mediated by algal growth. Est. Coast. Mar. Sci. 9, 569-576.

Hamilton, E. I. 1981. Alpha-particle radioactivity of hot particles from the Esk esturay. Nature 290,690-693.

Haven, Morales-Alamo. 1968. Occurrence and transport of faecal pellets in suspension in a tidal estuary. Sed. Geol. 2, 141-151.

Heatherington, J. 1976. The behaviour of plutonium nuclides in the Irish Sea. In Environmental Toxicity of Aquatic Radionuclides:Models and Mechanisms, Ann Arbor Series, Michigan. eds. Miller.M.W., Stannard, J. H. 81-106.

Heathershaw, D. C., Simpson, J. H. 1974. The fine structure of light attenuation and its relation to temperature in the Irish Sea. Est. Coast. Mar. Sci. 2,91-103.

Holland, A. F., Zingmark, R. B., Dean, J. H. 1974. Quantitative evidence concerning stabilisation of sediments by marine benthic diatoms. Mar. Biol. 27, 191-196.

Jago, C. F. 1981. Sediment response to waves and currents on the N.Yorkshire shelf of the North sea. Spec. Publ. Int. Ass. Sediment, 5, 283-301.

Jerlov, N. G. 1968. Optical Oceanography, Elsevier.

Joint, I. R., Pomroy, A. J. 1981. Primary Production in a turbid estuary. Est. Coast. Shelf. Sci. 12, 303-316.

Jonasz, M. 1987. Non-sphericity of suspended marine particles and its influence on light scattering. Limn. Oceanogr. 32,1059-1063.

Jones, D., Wills, F. 1956. Attenuation of light in the sea and estuarine waters in relation to the concentration of suspended and solid matter. J. Mar. Biol. Ass. U.K. 35,431-444.

Jones, R. F. 1960. The accumulation of nitrosyl ruthenium by fine particles and marine organisms. Limn. Oceanogr. 5, 312.

Joseph, J. 1955. Extinction measurements to indicate distribution and transport of watermasses. Proc. UNESCO. Symp. Phys. Oceanogr., Tokyo. 59-75.

Kershaw, P., Young, A. 1988. Scavenging of 234Th in the eastern Irish sea. J. Env. Radioactivity. 6,61-23.

Kershaw, P., Pentraeth, R. J., Gurbett, P. A., Woodhead, D. S., Durance, J. A., Camplin, W. C. (in press) Modelling the behaviour of long-lived radionuclides in the Irish sea:comparison of model predictions with field observations. Methods for Assessing the reliability of Environmental Transfer Models Predictions. Elsevier Applied Science Publishers.

Kirby, R., Parker, W. R. 1983. Distribution and behaviour of fine sediment in the Severn estuary and inner Bristol Channel. Canadian. J. Fish. Aquat. Sci., 40,81-95.

Kirby, R. 1987. Sediment exchanges accross the coastal margins of N.W. Europe. J. Geol. Soc. London. 144,121-126.

Kirk, J. T. O. 1980. Spectral absorption properties of natural waters: contributions of the soluble and particulate fraction to light absorption in some inland waters of S.E.Australia. Aust. J. Mar. Freshwater Research. 31, 287-296.

Kirk, J. T. O. 1983. Light and photosynthesis in aquatic ecosystems. Cambridge Univ.Press.

Kitchen, J. C., Zaneveld, J. R., Pak, H. 1982. The effect of particle size distribution and chlorophyll content on beam attenuation spectra. Appl.Optics. 21, 3913.

Kranck, K. 1974. The role of flocculation in the transport of pollutants in the marine environment. Presented at the International Conference on the Transport of Persistent Chemicals in Aquatic Ecosystems, Ottowa, Canada. May,1974.

Lee, A. J., Foulkard, A. R. 1969. Factors affecting turbidity in the southern North sea. J.Conseil International pour Exploration de la Mer, 32, 291.

Lewis, A. G., Svyvetski, J. P. H. 1983. The interaction of plankton and suspended sediments in fjords. Sed. Geol. 36,81-92.

Mare,M.F. (1942) A study of a marine benthic community with special reference to the micro-organisms. J.Mar.Biol.Ass. 25,517-554.

McCave, I. N. 1979. Suspended sediment. In Estuarine Hydrography and Sedimentation. Ed. Dyer, K. 144-184.

Mehta, A. J, Parthianedes, E. 1975. An investigation of the depositional properties of flocculated fine sediments. J. Hydraul. Res. 4,361-381.

Meir-Reil, L. A. 1980. Bacterial activity in sandy sediments. in Biological features of the Baltic. Proceedings, Keiler Meeresforschingen,

Mie, G. 1908. Beitrage zur optik truber median, spexiell kolloidalen metallsunger. Ann. Physik, 25,377.

Ministry of Agriculture Fisheries and Foods, 1987, Aquatic Environment Monitoring report, Ed. R.R.Dickson, Irish Sea status report of the Marine Pollution Monitoring Management Group., M.A.F.F.

Mitchelson, E. G. 1984. Phytoplankton and suspended sediment distribution in relation to physical structure and water-leaving colour signals. Ph.D.thesis, University of Wales.

Moody, J. A., Butman, B., Bothner, M. H. 1986. Near bottom suspended matter concentration on the Continental Shelf during storms: estimates based on in-situ observations of light transmission and particle size dependent transmissometer calibration. Cont. Shelf. Res. 7,609-628.

Morel, A. Y., Prieur, L. 1977. Analysis of variations in ocean colour. Limn. Oceanogr., 22,709-722.

Newton, A. 1986. Nitrogen nutrition and succession in phytoplankton. M.Sc.thesis. University of Wales.

Nichols, M. H. 1985. Effects of fine sediment resuspension in estuaries. In Cohesive Sediments, Springer-Verlag.

Nowell, A. R. M., Jumars, P. A., Eckman, J. E. 1981. Effects of biological activity on the entrainment of marine sediments. Mar. Geol. 42,133-153.

Officer, C. B. 1980. Physical dynamics of estuarine suspended sediments. Mar. Geol. 40,1-14.

Owen, M. W. 1975. Erosion of Avonmouth mud. Hydraulics Research Station, Internal report 150.

Pak, H., Zaneveld, R. V., Beardsley, G. F. 1971. Mie scattering by suspended clay particles. J. Geophys. Res. 76,5065-5069.

Pantin, H. M. 1977. Quaternary sediments of the northern Irish Sea. in, Quaternary History of the Irish Sea, Ed. Kidson, C., Tooley, M.J. Seel House Press, Liverpool. Geological Journal Special Issue, 7.

Pantin, H. M. 1978. Quaternary sediments from the north east Irish Sea: Isle of Man to Cumbria. Bull. Geol. Survey of Great Britain. 64, 43 pp.

Parker, R. W., Kirby, R. 1981. The behaviour of cohesive sediment in the inner Bristol Channel and the Severn Estuary in relation to the construction of the Severn Barage. Inst. Oceanogr. Sci. Rep. No. 117.

Parker, R. W., Kirby, R. 1982. Time dependent properties of cohesive sediments relevant to sedimentation management-European Experience. in Estuarine Comparisons. ed. Kennedy, V. S., Academic Press.

Pejrup, M. 1986. Parameters affecting fine-grained suspended sediment in a micro-tidal estuary,Ho-Bugt, Denmark. Estuar. Coastal. Shelf Sci. 22,241-254.

Pingree, R. D., Pugh, P. R., Holligan, P. M., Forster, G. R. 1975. Summer phytoplankton blooms and red tides along tidal fronts in the approaches to the English channel. J. Mar. Biol. Ass. U.K. 56,845-873.

Pingree, R. D., Griffiths, D. K. 1979. Sand transport paths around the British Isles resulting from M2 and M4 tidal interaction. J. Mar. Biol. Ass. U.K. 59,497-513.

Postma, H. 1961. Suspended matter and secchi disc visibility in coastal waters. Neth. J. Sea. Res.1.359-390.

Priesendorfer, R. W. 1961. Radiant energy in the sea. Int. Union. Geophys. Monogr. 10, 11-29.

Prieur, L., Sathyendranath, S. 1981. An optical classification of coastal and oceanic waters based on the specific absorption curves of phytoplankton pigments, dissolved organic matter and other particulate materials. Limn. and Oceanol. 26, 671-685.

Probert, K. 1984. Disturbance,sediment stability and trophic structure of soft-bottomed communities. J. Mar. Res. 42,893-921.

Proctor, R. 1982. Tides and residual circulation in the Irish Sea, Ph.D. thesis, University of Liverpool.

Ritchie, J. C., Scheibe, F. R., McHenry,J.R. 1976. Remote sensing of suspended sediments in surface waters. Photogramm. Eng. Rem. Sens. 42,1539-1545.

Rhoads, D. C., Boyer, L. F. 1982. The effect of marine benthos on physical properties of sediments. In Animal-Sediment Relations. eds. McCall, P.L.,Tenez, M.J.S. Plenum Press.

Robinson, I. S. 1979. The tidal dynamics of the Irish and Celtic Sea. Geophys. J. Roy. Astr. Soc. 56,159-197.

Robinson, I.S., Srisaengthong.D. 1981. The use of Landsat MSS to observe sediment distribution and movement in the Solent coastal area. Proc.EARSel-ESA Symp., Voss, Norway, 19-20 May,1981. ESA-SP-167, 221-232.

Robinson, I .S. 1983. Satellite observations of ocean colour. Phil. Trans. R. Soc. Lond. A30, 415-432.

Round, F. E. 1973. The biology of the algae. Edward Arnold Ltd., London.

Saffman, P. G., Turner, J. S. 1956. On the collision of drops in turbulent clouds. J. Fluid. Mech. 1,16-30.

Schubel, J. R., Wilson, R. E., Okubo, A. 1978. Vertical transport of suspended sediment in Upper Chesapeake Bay. In Estuarine Transport Processes. ed. Kjerve.B. Columbia Univ.,South Carolina Press. 161-175.

Simpson, J. H, Hunter, J. 1974. Fronts in the Irish Sea. Nature. 250, 404-406.

Simpson, J. H., Hughes, D. G., Morris, N. G. 1977. The relation of seasonal stratification to tidal mixing on the continental shelf. In A Voyage of Discovery. ed. Angel.M. Pergamon Press, Oxford.

Simpson, J. H., Edelstein, D. J., Edwards, A., Morris, N. G., Tett, P. B. 1979. The Islay front: physical structure and phytoplankton distribution. Estuar. Coastal Mar.Sci. 9,713-726.

Simpson, J. H., Brown, J. 1987. The interpretation of visible band imagery of turbid shallow seas in terms of the distribution of suspended particulates. Cont. Shelf. Res. 7,1307-1313.

Smith, T. J. 1982. The response of elctro-optical turbidity meters to cohesive sediments. Inst. Oceanogr. Sci. Report. No.137.

Soulsby, R. 1977. Sensors for the measurement of sand in suspension. Inst. Oceanogr. Sci. Report No.27.

Spinrad, R. W., Zaneveld, J. R., Kitchen, J. 1983. The optical characteristics of suspended particles in the nepheloid layer of the Scotian Rise. J. Geophys. Res. 88, 7641-7645.

Spinrad, R. W. 1986. A calibration diagram of specific beam attenuation coefficients of natural suspensions. J. Geophys. Res. 89,8179-8203.

Stride, A. H. 1973. Sediment transport by the North Sea. In North Sea science, ed. Goldberg, E. D. The M.I.T. Press, Cambridge, MA. pp. 101-130

Strickland, J. H. D., Parsons, T. R. 1972. A practical handbook of sea water analysis. Bull. J. Fish. Res. Bd. Canada. 167, 311 pp.

Tett, P. B. 1987. Plankton. In Biological Surveys of estuaries and coasts. ed. Baker, J. M, Wolf, W. J, Cambridge Univ.Press.

Thorn, M. F. C. 1975. Monitoring silt movement in an estuary. Int. Assoc. for Hydraulics. Res., Proc. 16th Congress, Sao Paulo, C71.

Thompson. J. C. 1974. Short term fluctuations of transmittance in the Menai Straits. M.Sc.thesis, University of Wales.

Topliss,B.J.(1977) A study of optical irradiance in coastal waters. Ph.D. thesis, University of Wales.

Topliss, B. J. 1986. Spectral variations in upwelling radiant intensity in turbid coastal waters. Estuar. Coastal Shelf Sci. 22, 395-414.

Unesco 1981. 10th report of the joint panel on oceanographic tables and standards. Unesco Technical Papers on Marine Science, 36.

Van de Hulst, H. C. 1957. Light scattering by small particles. Wiley, New York. 75-76.

Webb, J. E., Dorges, D. J., Gray, J. S., Hessler, R. R., van Andel, T. H., Werner, F., Wolff, T. Z., Zijlstra, J. A., 1976. Working Group Report, Group E. Organism-sediment relationships. 273-295. in, The Benthic Boundary Layer. Ed. McCave, I. N., New York, Plenum Press.

Williams, S. J., Kirby, R., Smith, T. J., Parker, W. R. 1981. Sedimentation studies relevant to low level radioactive effluent dispersal in the Irish Sea. Inst. Oceanogr. Sci. Report No.120.